NASA/CP—1999-208526/SUPPL 1

Proceedings of the Fourth Microgravity Fluid Physics and Transport Phenomena Conference

March 1999

The NASA STI Program Office . . . in Profile

Since its founding, NASA has been dedicated to the advancement of aeronautics and space science. The NASA Scientific and Technical Information (STI) Program Office plays a key part in helping NASA maintain this important role.

The NASA STI Program Office is operated by Langley Research Center, the Lead Center for NASA's scientific and technical information. The NASA STI Program Office provides access to the NASA STI Database, the largest collection of aeronautical and space science STI in the world. The Program Office is also NASA's institutional mechanism for disseminating the results of its research and development activities. These results are published by NASA in the NASA STI Report Series, which includes the following report types:

- TECHNICAL PUBLICATION. Reports of completed research or a major significant phase of research that present the results of NASA programs and include extensive data or theoretical analysis. Includes compilations of significant scientific and technical data and information deemed to be of continuing reference value. NASA's counterpart of peer-reviewed formal professional papers but has less stringent limitations on manuscript length and extent of graphic presentations.

- TECHNICAL MEMORANDUM. Scientific and technical findings that are preliminary or of specialized interest, e.g., quick release reports, working papers, and bibliographies that contain minimal annotation. Does not contain extensive analysis.

- CONTRACTOR REPORT. Scientific and technical findings by NASA-sponsored contractors and grantees.

- CONFERENCE PUBLICATION. Collected papers from scientific and technical conferences, symposia, seminars, or other meetings sponsored or cosponsored by NASA.

- SPECIAL PUBLICATION. Scientific, technical, or historical information from NASA programs, projects, and missions, often concerned with subjects having substantial public interest.

- TECHNICAL TRANSLATION. English-language translations of foreign scientific and technical material pertinent to NASA's mission.

Specialized services that complement the STI Program Office's diverse offerings include creating custom thesauri, building customized data bases, organizing and publishing research results . . . even providing videos.

For more information about the NASA STI Program Office, see the following:

- Access the NASA STI Program Home Page at ***http://www.sti.nasa.gov***

- E-mail your question via the Internet to help@sti.nasa.gov

- Fax your question to the NASA Access Help Desk at (301) 621-0134

- Telephone the NASA Access Help Desk at (301) 621-0390

- Write to:
  NASA Access Help Desk
  NASA Center for AeroSpace Information
  7121 Standard Drive
  Hanover, MD 21076

Table of Contents

Session 2C: Interfacial Phenomena I

Session 3A: Phase Change I: Boiling

PREFACE AND ACKNOWLEDGMENTS

The Fourth Microgravity Fluid Physics and Transport Phenomena Conference provides us the opportunity to view the current scope of the microgravity Fluid Physics and Transport Phenomena Program and conjecture about its future. The program currently has a total of 106 ground-based and 20 candidate flight principal investigators. A look at the collection of papers in this document clearly shows both the high quality and the breadth of the ongoing research program. One can easily notice many established world class scientists as well as investigators who are early in their career poised to achieve that stature. We hope that many of the participants in this conference will perceive it as an exciting and rewarding area of research and choose to participate in the upcoming NASA Research Announcement expected to be released in Fall of 1998.

As we look to the future, we find ourselves amidst a sea of changes, most of them positive. The International Space Station (ISS) is about to be launched this year, providing the microgravity research community with a tremendous opportunity to conduct long-duration microgravity experiments which can be controlled and operated from their own laboratory. Frequent planned shuttle trips will provide opportunities to conduct many more experiments than were previously possible. NASA Lewis research Center is in the process of designing a Fluids and Combustion Facility (FCF) to be located in the Laboratory Module of the ISS that will not only accommodate multiple users but allow a broad range of fluid physics and transport phenomena experiments to be conducted in a cost effective manner.

NASA is in the process of defining strategy for exploring Mars and other planets in the "Better, Faster, Cheaper" framework. These missions pose considerable challenge in that they require humans and associated systems to be subjected to prolonged exposure to microgravity during the interplanetary transit phase and in reduced gravity while on the planet's surface. Knowledge of how these extraterrestrial gravitational environments affect various systems and processes is vital to the success of these missions. NASA's Microgravity Research Program and its participating research community have emerged as primary sources of expertise in this unique area of research. In order to fully utilize this expertise, the Microgravity Research Division of NASA's Office of Life and Microgravity Science organized a workshop in August 1997 to identify factors/issues critical to enabling research and technology development needs of the long-duration space explorations. The proceedings of this workshop have been published as NASA CP-1998-207431 and will be available at the conference.

As one might expect, fluid physics and transport phenomena play a major role in many of the research and technology development needs identified in the workshop. The Microgravity Research Division has developed specific performance goals that support these needs. The performance goals represent new opportunities for the Microgravity Fluid Physics and Transport Phenomena Community and are listed below:

1. Advance the state of knowledge sufficiently to enable dust control technologies and bulk material handling for extraterrestrial habitats and/or in situ resource utilization.
2. Advance the state of knowledge sufficiently to allow development of reliable and efficient heat transfer technologies for space and extraterrestrial operations.
3. Advance the state of knowledge sufficiently to allow development of effective fluid management technology for space and extraterrestrial and industrial applications.
4. Establish the knowledge base required to design chemical process systems for exploration missions.

This conference itself has undergone a number of changes and innovations. In consultation with the Fluid Physics and Transport Phenomena Discipline Working Group chaired by Professor Paul Neitzel, we decided to produce a prepublication of the conference proceedings using an electronic medium. The abstracts are already on the World Wide Web at the website http://www.ncmr.org and we plan to post the complete papers on the web shortly after the conference. In this regard we acknowledge the support of our principal investigators who have provided us timely inputs of their papers and abstracts and accommodated our format requirements. This cooperation was necessary to accomplish this and is much appreciated.

The Discipline Working Group has provided the much needed guidance in planning the content and the format of this conference. Their advice and guidance were essential for the success of this conference.

The establishment of the National Center for Microgravity Research on Fluids and Combustion represents another significant milestone for the program. The mission of the Center is to lead a national effort to increase the number of microgravity researchers and quality of research. The Center's primary role is to support the principal investigators in the program and promote not only dialogue but also working interactions among diverse groups and communities that are essential for continued success and growth of the program.

This conference has been organized and hosted by the National Center under the leadership of its Director, Professor Simon Ostrach. I would like to acknowledge the extensive efforts of members of the Center in planning, organizing, and hosting the conference and in preparing the proceedings and Conference materials. The first electronic publication and web based registration were major challenges that the Center staff handled skillfully. Sincere appreciation is offered to the authors for providing the papers in a timely manner and to the members of the Microgravity Fluids Physics Branch of NASA Lewis Research Center for their many contributions.

Finally I would like to express my gratitude to all of the Conference participants for their contributions to the success of this Conference.

Dr. Bhim S. Singh,
Fluid Physics Discipline Lead Scientist
Mail Stop 500-102
NASA Research Center
21000 Brookpark Road
Cleveland, OH 44135
Phone (216) 433-5396 or fax (216) 433-8660
E-mail: bhim.s.singh@lerc.nasa.gov

This conference was made possible by the efforts of many people. We acknowledge the contributions of the following individuals:

Fluid Physics and Transport Phenomena Discipline Working Group
G. Paul Neitzel (chair), Georgia Institute of Technology
Bhim Singh (vice-chair), NASA Lewis Research Center
Sanjoy Banerjee, University of California-Santa Barbara
S. George Bankoff, Northwestern University
Bradley Carpenter, NASA Headquarters
Stephen Davis, Northwestern University
Joe Goddard, University of California--San Diego
Joel Koplik, City College of the City University of New York
Michael Moldover, NIST
Harry Swinney, University of Texas at Austin
Matthew Tirrell, University of Minnesota

Session Chairs
Plenary Sessions:
Jack Salzman, Chief, Microgravity Science Division, NASA Lewis Research Center
Dr. David Weitz ,University of Pennsylvania
Dr. Iwan Alexander, National Center for Microgravity Research on Fluids and Combustion/Case Western Reserve University

Parallel Sessions (In Session Order):

Hasan Oguz, Johns Hopkins University
Robert Davis, University of Colorado at Boulder
Iwan Alexander, NCMR/Case Western Reserve University
Mark McCready, University of Notre Dame
Paul Chaikin, Princeton University
Dan Rosner, Yale University
Andrea Prosperetti, Johns Hopkins University
Joe Goddard, University of California at San Diego
Joel Koplik, City College of the City University of New York
Ain Sonin, Massachusetts Institute of Technology
Ashok Sangani, Syracuse University
Yasuhiro Kamotani, Case Western Reserve University
Peter Wayner, Rensselaer Polytechnic Institute
Alice Gast, Stanford University
Gareth McKinley, Massachusetts Institute of Technology
Vijay Dhir, University of California at Los Angeles
Eric Shaqfeh, Stanford University
Hossein Haj-Hariri, University of Virginia
Luis Bernal, University of Michigan
Mike Schatz, University of Texas at Austin
Kathleen Stebe, Johns Hopkins University

National Center for Microgravity Research on Fluids and Combustion

Dr. Simon Ostrach, Director
Thomas Cochran, Deputy Director
Ann Heyward, Outreach Programs Manager and Conference Lead
Iwan Alexander, Fluids Senior Scientist

Conference Team:	Ann Heyward, Chair	Iwan Alexander
	Judith Andersson	Tom Barkis
	Christine Gorecki	Annemarie Jones
	Beatrix Norton	Terri Rodgers
	Melissa Rogers	Norman Weinberg

The Logistics and Technical Information Division and its support service contractors, particularly Gregory Patt and Patricia Webb.

Jennifer Barovian and John Kizito of Case Western Reserve University.

Featured Presentation, Plenary Session:
Thursday, August 13, 1998

DYNAMICS OF DISORDER-ORDER TRANSITIONS IN HARD SPHERE COLLOIDAL DISPERSIONS

P.M. Chaikin[1], W.B. Russel[2], J. Zhu[1], Z. Cheng[1], S.-E. Eng[2] - [1]Department of Physics, Princeton University, Princeton NJ 08540, [2] Department of Chemical Engineering, Princeton University, Princeton, NJ 08540

ABSTRACT

The Physics of Hard Spheres Experiment (PHaSE) probes the structure, dynamics, and rheology associated with the entropically driven hard sphere phase transition in a colloidal dispersion. A sophisticated light scattering instrument, conceived and designed to detect low angle and Bragg scattering on a screen in the forward direction and static and dynamic scattering via a optical fibers at 20-160°, flew on board the Space Shuttle's Microgravity Science Laboratory in 1997 (STS-83 and STS-94). This flight and complementary ground based research with poly(methylmethacrylate) spheres dispersed in an (almost) index matching solvent reveal clearly several features of the system:

- an equation of state for the fluid and crystalline phases that conforms to expectations but demonstrates remarkable sensitivity to polydispersity for the crystal,
- a modulus for the crystalline solid that matches quantitatively predictions from computer simulations for the static modulus,
- a crystal structure that consists initially of randomly stacked hexagonal planes but moves toward face centered cubic under some conditions, and
- an instability in the crystal growth that produces long-lived dendritic structures.

In addition, evolution of the Bragg scattering with time offers substantial quantitative information on the nucleation and growth process. This talk will describe these results and put them in perspective with extensive ground based experiments reported in the literature.

Featured Presentation, Plenary Session:
Friday, August 14, 1998

MECHANICS OF GRANULAR MATERIALS AT LOW EFFECTIVE STRESSES

Stein Sture, Department of Civil & Arch Engineering, University of Colorado, Boulder, CO 80309-0428
sture@bechtel.colorado.edu

ABSTRACT

Six displacement controlled, drained and cyclic axisymmetric compression triaxial experiments on cohesionless granular soil specimens were conducted at very low effective confining stresses in a micro-gravity environment in the SpaceHab module of the Space Shuttle, STS-79 in September, 1996 and STS-89, January, 1998. The confining stresses in the six experiments were in the ranges 0.05, 0.52 and 1.30 kPa, with two tests conducted in each category. The specimens measured 75 mm in diameter by 150 mm long. The average grain size of the subangular to subrounded Ottawa quartz sand was 0.2 mm, and the specimens' relative densities were 86.5 % (STS-79) (±0.8 %; maximum porosity: 0.446 and minimum porosity: 0.327) and 65% (STS-89)(+/- 0.4%). The moisture content in the experiments was less than 0.2%, which resulted in insignificant capillary forces, and electrostatic effects were also found to be insignificant.

The results for the (a) 0.05 kPa (confining stress) experiments were a friction angle at peak strength equal to 70.1 degrees (max.); dilatancy angle of 31 degrees; and a friction angle at residual or constant volume strength level equal to 34.0 degrees, for the (b) 0.52 kPa experiment the results were friction angles at peak strength equal to 58.5 degrees; dilatancy angle of 30.0 degrees; and a friction angle at residual strength equal to 35.0 degrees, and for the (c) 1.30 kPa experiments the results were friction angles at peak strength equal to 56.4 degrees, dilatancy angle of 30.0 degrees; and a friction angle at residual strength also equal to 34.0 degrees. Terrestrial experiments on the same material at the same density shows peak friction angles of 41.0 degrees; dilatancy angle of 10.5 degrees; and a friction angle at residual strength equal to 34.2 degrees. Five unloading and reloading cycles were conducted at regular intervals in all three experiments, which were conducted to axial strains of 25%. The unloading-reloading cycles show very similar stiffness modulus behavior and insignificant coupling to deformation level and effective confining pressure. In all six experiments the initial stiffness moduli are similar to the unloading-reloading moduli. A periodic instability phenomenon which appears to result from buckling of multiple internal arches and columnar systems, augmented by stick-slips was observed in the experiments. The period and magnitude appear to be independent of confining stress and loading rate. The very high dilatancy angles observed in all experiments are perhaps the most unusual finding, which lead to the very high peak friction angles. The mechanisms and properties resulting in the unusually high friction angles will be discussed in the presentation, together with x-ray computed tomographic results and numerical simulations.

The author acknowledges support from NASA, Marshall Space Flight Center and his collaborators N.C. Costes, K. AlShibli, S. Batiste, M. Lankton, R. Swanson and M. Frank.

Session 1A: Multiphase Flow I

MECHANISM OF ATOMIZATION IN A TWO-LAYER COUETTE FLOW.

R. M. Roberts, H. -C. Chang and M. J. McCready, Department of Chemical Engineering, University of Notre Dame, Notre Dame, IN, 46556,USA, mccready.1@nd.edu

ABSTRACT

Atomization is an important issue for both process scale fluid-fluid flows on earth and possible energy exchange devices in microgravity. Currently the fraction of entrained liquid in process flows (e.g., annular gas-liquid flow) is predicted with correlations based on data over limited ranges of parameters. These correlation are generally inaccurate and unreliable. It has been recognized that an entrainment correlations will never work as procedures that treat atomization and deposition separately. Further atomization will not be predicted accurately unless the mechanism can be understood quantitatively. Previous photographic studies in (turbulent) gas-liquid flows have shown that liquid is atomized when it is removed by the gas flow from the crest of large solitary or roll waves. There is, however, no further experimental information about the effect of fluid properties or flow rates on atomization and the wave formation process for solitary and roll waves is not known well enough to make quantitative predictions for arbitrary conditions.

Our work on this topic is intended to examine all aspects of the atomization process. Linear and nonlinear theory is applied to the two-layer base film with the intention of predicting wave formation. Evolution equations are applied to the finite amplitude waves to determine if they will grow to large amplitude. Experiments are used to verify the wave formation mechanism and to verify the scaling with system parameters. The mechanism of atomization is directly examined experimentally in our matched-density, two-fluid rotating Couette experiment.

This talk will report on our theoretical and experimental efforts characterize atomization. Wave formation in laminar and turbulent flows is predicted using linear theories. We have found that at least based on a k-ε turbulence model, wave formation is significantly affected by the shape of the velocity profile as well as interfacial shear. This contradicts previous conjectures. Wave evolution beyond the linear onset is described with weakly-nonlinear bifurcation theory. After examining a wide range of conditions, we find evidence of only supercritical bifurcations for the initial onset of waves. This includes conditions where the flow is unstable to long waves at any rotation rate. In this range periodic waves form first, then solitary waves and finally atomization occurs as the rotation rate is increased. We have observed atomization events where a roll wave forms, grows and then is stretched out many gap widths before the snap off occurs. It is not clear if this mechanism is similar to the one for gas-liquid flow atomization when appropriate changes in time and length scales are made.

STUDIES ON NORMAL AND MICROGRAVITY ANNULAR TWO-PHASE FLOWS.

V. Balakotaiah[1], S. S. Jayawardena[2] and L. T. Nguyen[3],

Department of Chemical Engineering, University of Houston, Houston, TX 77204-4792

[1]Bala@uh.edu, [2]Subash@uh.edu, [3]LJN96442@jetson.uh.edu

INTRODUCTION

Two-phase gas-liquid flows occur in a wide variety of situations. In addition to normal gravity applications, such flows also occur in space operations such as active thermal control systems, power cycles, and storage and transfer of cryogenic fluids.

FLOW PATTERN TRANSITION

Various flow patterns exhibiting characteristic spatial and temporal distribution of the two phases are observed in two-phase flows. The magnitude and orientation of gravity with respect to the flow has a strong impact on the flow patterns observed and on their boundaries. The identification of the flow pattern of a flow is somewhat subjective. The same two-phase flow (especially near a flow pattern transition boundary) may be categorized differently by different researchers.

Two-phase flow patterns are somewhat simplified in microgravity, where only three flow patterns (bubble, slug and annular) have been observed. Annular flow is obtained for a wide range of gas and liquid flow rates, and it is expected to occur in many situations under microgravity conditions. Slug flow needs to be avoided, because vibrations caused by the slugs result in unwanted accelerations. Therefore, it is important to be able to accurately predict the flow pattern which exists under given operating conditions.

The absence of gravity simplifies the flow patterns and it also reduces the number of dimensionless groups needed to characterize the two-phase flow. For microgravity two-phase flows, (using experimental data from various systems) we developed a pair of dimensionless flow pattern transition maps. These maps suggest the importance of Suratman number, Su, in determining the transitions between the flow patterns.

The bubble-slug flow pattern transition occurs at a particular value of the ratio $(Re_{GS}/Re_{LS})_t$, which depends on the Suratman number as follows:

$$(Re_{GS}/Re_{LS})_t = K_1\, Su^{-2/3}. \qquad (1)$$

It is found that when $Su < 10^6$, slug-annular flow pattern transition occurs at a particular value of the ratio $(Re_{GS}/Re_{LS})_t$, which was found to depend on the Suratman number as follows:

$$(Re_{GS}/Re_{LS})_t = K_2\, Su^{-2/3}. \qquad (2)$$

When $Su > 10^6$, slug-annular flow pattern transition was found to be a function of the gas Reynolds number, $(Re_{GS})_t$, which was found to depend on the Suratman number as follows:

$$(Re_{GS})_t = K_3\, Su^2. \qquad (3)$$

Experimental data were used to estimate the numerical values of K_1, K_2 and K_3. and it was found that $K_1 = 464.16$, $K_2 = 4641.6$ and $K_3 = 2\times10^{-9}$. The Suratman number is determined by the tube diameter and physical properties of the fluid. Thus, the proposed maps can be used to identify the flow pattern for any given two-phase system, even when there are no prior experimental microgravity flow pattern data.

We collected new flow pattern data on microgravity two-phase flows with different Suratman numbers, using water based solutions of various surface tension and viscosity values. These experiments confirmed that the slug-annular transition boundary given by Eq. (2) extends to low values of the Suratman number ($10^2 < Su < 10^4$). However, they did not verify the bubble-slug transition boundary. These experiments were planned to validate the slug-annular transition for various two-phase flows in microgravity and we could do that with flows having Suratman numbers as low as 770.

We used the above flow pattern boundaries to generate system specific flow pattern maps (for a given fluid in a selected tube size). These two-phase quality vs. mass flow rate maps are useful for single-component, two-phase systems.

For bubble-slug transition and for low Suratman number slug-annular transitions, the two-phase quality at transition, $x_{t,B-S}$, is independent of the total mass flow rate. For higher Suratman number systems, it is possible to obtain slug flow at higher values of quality, provided mass flow rate of the two-phase flow is low.

The bubble flow pattern is observed in an extremely small range of quality, and for most flow conditions in microgravity, annular flow is observed.

WAVY FILMS IN MICROGRAVITY

It is known that the wavy liquid film in annular flow has a profound influence on the transfer of momentum and heat between the phases. Thus, an understanding of the characteristics of the wavy film is essential for developing accurate correlations.

In this work, we review our recent results on the analysis wavy films in microgravity, using existing data. We used data on wavy film profiles in microgravity collected using air-water, air-water-glycerin and air-water-Zonyl systems.

When properly non-dimensionalized using the friction velocity calculated with the measured pressure gradient, the mean film thickness can be predicted using the liquid Reynolds number. The mean film thickness of normal and microgravity two-phase flows are not fundamentally different.

Since we expect the surface tension effects to dominate under microgravity conditions, we analyzed the rms values of the film thickness in microgravity conditions. (Note: The rms film thickness is actually the standard deviation since we subtract the mean film thickness. However, we are following here the literature terminology.)

The rms values of the film thickness fluctuations is normalized using the same length scale defined using the friction velocity u^* (and that was denoted as h^+_{rms}). A correlation was obtained to predict the h^+_{rms} for a given two-phase flow. Experimental observations show that the annular flow liquid film becomes smoother at higher gas flow rates. The predicted and experimental values are in good agreement.

Another quantity we analyzed was the enhancement in the friction factor. Here we compare the friction factor based on the interfacial stress with that of a corresponding single phase gas flow. The micro-gravity data where compared with the existing correlations for normal gravity annular flows. Though the data showed more scatter, it is clear that the enhancement in the interfacial friction factor is higher in microgravity than in normal gravity.

New correlations were obtained for the enhancement of the friction factor in microgravity annular flows. These indicate the surface tension dependence, unlike in normal gravity flows.

CONCLUSIONS AND DISCUSSION

The recently proposed flow pattern map was verified at low Suratman number systems. Experiments confirmed the applicability of the proposed slug-annular flow pattern transition boundary for two-phase flow systems with a low Suratman number. System specific, dimensional flow pattern boundaries can be obtained for microgravity two-phase flows. For a wide range of two-phase qualities, slug flow can be observed in such a system if the total mass flow rate is small, provided Suratman number is large. Bubbly flow exists in microgravity only at extremely low two-phase qualities.

When properly non-dimensionalized using the pressure gradient, the mean film thickness of an annular flow depends only on the liquid Reynolds number, irrespective of gravity. The differences between the normal and microgravity annular liquid films are apparent when we compare the interfacial friction factors. It is found that the friction factor enhancement is higher in microgravity conditions than in normal gravity downward annular flows. In microgravity annular flows, the enhancement to the friction factor is surface tension dependent.

ACKNOWLEDGMENTS

This work is supported by a grant from the NASA-Lewis Research Center (NAG3-1840), a NASA Lewis GSRP grant to Luan Nguyen and the UH-JSC aerospace post-doctoral fellowship program.

EXPERIMENTAL AND ANALYTICAL STUDY OF TWO-PHASE FLOW IN MICROGRAVITY

D. Abdollahian,[1] J. Howerton[2], F. Barez[2] and John McQuillen[3], [1]S. Levy, Inc., Campbell, CA, [2] San Jose State University, San Jose, CA, [3]NASA Lewis Research Center, Cleveland, Ohio

ABSTRACT

A two-phase test loop has been designed and constructed to generate the necessary data for two-phase pressure drop and Critical Heat Flux (CHF) under reduced gravity conditions. A series of airplane trajectory tests aboard NASA KC-135 were performed and the data was used to evaluate the applicability of the earth gravity models for prediction of the reduced gravity data. Several commonly used correlations for the two-phase friction multiplier and critical heat flux were used to predict the data. It was generally concluded that the two-phase pressure drop can be predicted by the earth gravity correlations. The critical heat flux under reduced gravity conditions did not show a strong dependence on mass flow rate and the measured CHF were generally lower than the equivalent 1g conditions. The earth gravity models need to be modified for application to reduced gravities.

MEASUREMENT OF TWO-PHASE FLOW CHARACTERISTICS UNDER MICROGRAVITY CONDITIONS

E. G. Keshock[1], C. S. Lin[2], M. E. Harrison [3], L. G. Edwards [2], J. Knapp[2], and X. Zhang [4]
[1] Cleveland State University, E. 24th and Euclid Ave., Cleveland, OH 44115, e.keshock@csuohio.edu,
[2] Analex Corporation, 3001 Aerospace Parkway, Brookpark, OH 44135, sclin@lerc.nasa.gov

This paper describes the technical approach and initial results of a test program for studying two-phase annular flow under the simulated microgravity conditions of KC-135 aircraft flights. A helical coil flow channel orientation was utilized in order to circumvent the restrictions normally associated with drop tower or aircraft flight tests with respect to two-phase flow, namely spatial restrictions preventing channel lengths of sufficient size to accurately measure pressure drops. Additionally, the helical coil geometry is of interest in itself, considering that operating in a microgravity environment vastly simplifies the two-phase flows occurring in coiled flow channels under 1-g conditions for virtually any orientation. Pressure drop measurements were made across four stainless steel coil test sections, having a range of inside tube diameters (0.95 to 1.9 cm), coil diameters (25 - 50 cm), and length-to-diameter ratios (380 - 720). High-speed video photographic flow observations were made in the transparent straight sections immediately preceding and following the coil test sections. A transparent coil of tygon tubing of 1.9 cm inside diameter was also used to obtain flow visualization information within the coil itself. Initial test data has been obtained from one set of KC-135 flight tests, along with benchmark ground tests. Preliminary results appear to indicate that accurate pressure drop data is obtainable using a helical coil geometry that may be related to straight channel flow behavior. Also, video photographic results appear to indicate that the observed slug-annular flow regime transitions agree quite reasonably with the Dukler microgravity map.

INDUSTRIAL PROCESSES INFLUENCED BY GRAVITY.

J. P. Kizito[1], F.B. Weng[2], Y. Kamotani[3] and S. Ostrach[4] [1,2,3,4](Department Of Mechanical and Aerospace Engineering, Case Western Reserve University, Cleveland, Ohio, 44106) [3]e-mail: yxk@po.cwru.edu.

PART I[2]: ROTATING ELECTROCHEMICAL SYSTEMS

ABSTRACT

It is known that a rotating Ni/Zn battery can provide very high energy and long life-cycle. The main objective of our effort is to obtain a better understanding of convection in a rotating battery in order to improve Ni/Zn battery performance and life-cycle. With superimposed rotating motion in the charging cell, solutal buoyancy induces a swirling secondary flow through the coupling of centrifugal, Coriolis, gravitational acceleration and density variations in the electrolyte solution.

In the present work, solutal convection in shallow vertical rotating electrochemical cells is studied analytically, experimentally and numerically. Scaling analysis for the boundary layer regime is performed to determine the flow and solutal boundary layer characteristics. The experiment studies the mass transfer rate in the rotating electrochemical systems by utilizing the limiting current method. The detailed flow and solutal fields as well as mass transfer rate are investigated numerically. The results from this study are discussed in terms of dendrite formation and shape change on the electrode and how these processes can be prevented and controlled by the rotation of the battery.

The scaling analysis finds two convection regimes and shows that the parameters Ek and $ScRo_S$ are important to determine the mass transfer rate. The parameter $ScRo_S$ determines the thickness ratio of the viscous layer to the solutal layer as well as the convection regimes. The experimental study on mass transfer rate in rotating cells is conducted by utilizing the limiting current measurements with a cupric sulfate-sulfuric acid system. The overall mass transfer rates measured in the experiment are shown to agree with the scaling analysis. In numerical study, typical cases show the Coriolis force affect the flow and solutal fields. It is found that the Coriolis force suppresses the centrifugal convection, reducing the mass transfer rate, especially at low $ScRo_S$. The present numerical results are shown to be in good agreement with experiment and scaling analysis.

PART II[1]: STABILITY OF COATING FLOWS

ABSTRACT

Productivity reasons in industrial coating processes strive for high-speed applications. Because of such demands, attempts to use a specific coating process for a given application frequently fail due to film instability leading to temporal or spatial growth of surface waves. Therefore, direct numerical simulation of the flow field subject to an initial disturbance is preformed to study the stability of a coating film on a moving substrate. In addition, the temporal film thickness measurements are made using an ultra high accurate laser proximity probe which displays a local sensitivity of about two hundredth of a micron.

The new aspects and phenomena of importance to coating flow found in the present work are the following. The numerical results show that the direction of spatial wave growth is the same as the flow direction, which agrees with our experimental observation. In addition, when Re_r (Relative Reynolds number) is larger than unity, and T_o (non-dimensional film thickness) larger than 0.67, then the coating film on a moving substrate becomes wavy. This situation is different from a falling film whose critical Re_r =0 and T_o greater than unity.

The temporal film thickness measured by the laser-proximity-probe results into power spectrums, which shows that below a critical Re_r, the dominant frequency is that due to natural noise inherent in the system. Conversely, above the critical Re_r, the natural wave formation on the interface dominates the coating substrate. When the probe is moved downstream at the same operating condition, the magnitude of the average film-thickness increases by 26% over a distance of 0.1m. Thus, these results are in agreement with the numerical ones, which demonstrate the convective nature of the instability. The prime cause of interfacial instability is the crinkling of the interface due to gravity induced shear, which is ever present in normal gravity environment.

Session 1B: Electric and Magnetic Effects

WAVES IN RADIAL GRAVITY USING MAGNETIC FLUID.

D. R. Ohlsen[1], J. E. Hart[2], and P. D. Weidman[3],

[1]Program in Atmospheric and Oceanic Sciences, University of Colorado, Boulder, CO 80309-0311, ohlsen@fluida.colorado.edu

[2]Program in Atmospheric and Oceanic Sciences, University of Colorado, Boulder, CO 80309-0311, hart@tack.colorado.edu

[3]Department of Mechanical Engineering, University of Colorado, Boulder, CO 80309-0427, Patrick.Weidman@colorado.edu

ABSTRACT

Terrestrial laboratory experiments studying various fluid dynamical processes are constrained, by being in an Earth laboratory, to have a gravitational body force which is uniform and unidirectional. Therefore fluid free-surfaces are horizontal and flat. Such free surfaces must have a vertical solid boundary to keep the fluid from spreading horizontally along a gravitational potential surface. In atmospheric, oceanic, or stellar fluid flows that have a horizontal scale of about one-tenth the body radius or larger, sphericity is important in the dynamics. Further, fluids in spherical geometry can cover an entire domain without any sidewall effects, i.e. have truly periodic boundary conditions. We describe spherical body-force laboratory experiments using ferrofluid. Ferrofluids are dilute suspensions of magnetic dipoles, for example magnetite particles of order 10 nm diameter, suspended in a carrier fluid. Ferrofluids are subject to an additional body force in the presence of an applied magnetic field gradient. We use this body force to conduct laboratory experiments in spherical geometry.

The present study improves on the laboratory technique introduced in [1]. The apparatus is cylindrically axisymmetric. A cylindrical ceramic magnet is embedded in a smooth, solid, spherical PVC ball. The geopotential field and its gradient, the body force, were made nearly spherical by careful choice of magnet height-to-diameter ratio and magnet size relative to the PVC ball size. Terrestrial gravity is eliminated from the dynamics by immersing the "planet" and its ferrofluid "ocean" in an immiscible silicone oil/freon mixture of the same density. Thus the earth gravity is removed from the dynamics of the ferrofluid/oil interface and the only dynamically active force there is the radial magnetic gravity. The entire apparatus can rotate, and waves are forced on the ferrofluid surface by exterior magnets.

The biggest improvement in technique over [1] is in the wave visualization. Fluorescing dye is added to the oil/freon mixture and an argon ion laser generates a horizontal light that can be scanned vertically. Viewed from above, the experiment is a black circle with wave deformations surrounded by a light background. A contour of the image intensity at any light sheet position gives the surface of the ferrofluid "ocean" at that "latitude". Radial displacements of the waves as a function of longitude are obtained by subtracting the contour line positions from a no-motion contour at that laser sheet latitude. The experiments are run by traversing the forcing magnet with the laser sheet height fixed and images are frame grabbed to obtain a time-series at one latitude. The experiment is then re-run with another laser-sheet height to generate a full picture of the three-dimensional wave structure in the upper hemisphere of the ball as a function of time

We concentrate here on results of laboratory studies of waves that are important in Earth's atmosphere and especially the ocean. To get oceanic scaling in the laboratory, the experiment must rotate rapidly (4-second rotation period) so that the wave speed is slow compared to the planetary rotation speed as in the ocean.

In the Pacific Ocean, eastward propagating Kelvin waves eventually run into the South American coast. Theory predicts that some of the wave energy should scatter into coastal-trapped Kelvin waves that propagate north and south along the coast. Some of this coastal wave energy might then scatter into mid-latitude Rossby waves that propagate back westward. Satellite observations of the Pacific Ocean sea-surface temperature and height seem to show signatures of westward propagating mid-latitude Rossby waves, 5 to 10 years after the 1982-83 El Niño. The observational data is difficult to interpret unambiguously owing to the large range of motions that fill the ocean at shorter timescales. This series of reflections giving eastward, northward, and then westward traveling waves is observed cleanly in the laboratory experiments, confirming the theoretical expectations.

REFERENCE

1. Ohlsen, D.R. and P.B. Rhines: *J. Fluid Mech.*, **338**, 35-58, 1997.

Control Of Flowing Liquid Films By Electrostatic Fields In Space

E. M. Griffing[1], S. G. Bankoff[1], [1]Chemical Engineering, Northwestern University, Evanston IL, 60208-3120, USA, e-griffing@nwu.edu, R. A. Schluter[2], [2]Physics and Astronomy, Northwestern University, Evanston IL, 60208-3120, USA , M. J. Miksis[3], [3]Engineering Science and Applied Mathematics, Northwestern University, Evanston IL, 60208-3120, USA

ABSTRACT

The interaction of a spacially varying electric field and a flowing thin liquid film is investigated experimentally for the design of a proposed light weight space radiator . Electrodes are utilized to create a negative pressure at the bottom of a fluid film and suppress leaks if a micrometeorite punctures the radiator surface. Experimental pressure profiles under a vertical falling film, which passes under a finite electrode, show that fields of sufficient strength can be used safely in such a device. Leak stopping experiments demonstrate that leaks can be stopped with an electric field in earth gravity. A new type of electrohydrodynamic instability causes waves in the fluid film to develop into $3D$ cones and touch the electrode at a critical voltage. Methods previously used to calculate critical voltages for non moving films are shown to be inappropriate for this situation. The instability determines a maximum field which may be utilized in design, so the possible dependence of critical voltage on electrode length, height above the film, and fluid Reynolds number is discussed.

CELL AND PARTICLE INTERACTIONS AND AGGREGATION DURING ELECTROPHORETIC MOTION

Robert H. Davis, Shulin Zeng and Paul Todd, Department of Chemical Engineering,
University of Colorado, Boulder, Colorado 80309-0424

ABSTRACT

The stability and pairwise aggregation rates of small particles undergoing electrophoretic migration are predicted in the presence of gravitational motion for large particles and Brownian motion for small particles. The particle aggregation rates may be enhanced or reduced by appropriate alignment and strength of the electric field. Density gradient zone electrophoresis experiments to quantify particle aggregation are also described.

Magnetic control of convection in electrically nonconducting fluids

Jie Huang[1], Donald D. Gray[1], [1]*Department of Civil and Environmental Engineering, West Virginia University, Morgantown, WV 26506-6103, USA, un072134@wvnvms.wvnet.edu*, Boyd F. Edwards[2], [1]*Department of Physics, West Virginia University, Morgantown, WV 26506-6315, USA, bedwards@wvu.edu*

Abstract

Inhomogeneous magnetic fields exert a body force on electrically nonconducting, magnetically permeable fluids. This force can be used to compensate for gravity and to control convection. The effects of uniform and nonuniform magnetic fields on a laterally unbounded fluid layer heated from below or above are studied using a linear stability analysis of the Navier-Stokes equations supplemented by Maxwell's equations and the appropriate magnetic body force. For a uniform oblique field, the analysis shows that longitudinal rolls with axes parallel to the horizontal component of the field are the rolls most unstable to convection. The corresponding critical Rayleigh number and critical wavelength for the onset of such rolls are less than the well-known Rayleigh-Bénard values in the absence of magnetic fields. Vertical fields maximize these deviations, which vanish for horizontal fields. Horizontal fields increase the critical Rayleigh number and the critical wavelength for all rolls except longitudinal rolls. For a nonuniform field, our analysis shows that the magnetic effect on convection is represented by a dimensionless vector parameter which measures the relative strength of the induced magnetic buoyancy force due to the applied field gradient. The vertical component of this parameter competes with the gravitational buoyancy effect, and a critical relationship between this component and the Rayleigh number is identified for the onset of convection. Therefore, Rayleigh-Bénard convection in such fluids can be enhanced or suppressed by the field. It also shows that magnetothermal convection is possible in both paramagnetic and diamagnetic fluids. Our theoretical predictions for paramagnetic fluids agree with experiments. Magnetically driven convection in diamagnetic fluids should be observable even in pure water using current technology.

ELECTRIC FIELD INDUCED INTERFACIAL INSTABILITIES

Robert E. Kusner[1], Kyung Yang Min[2], [1,2]NASA Lewis Research Center, [1]rkusner@lerc.nasa.gov, [2]kym0270@lerc.nasa.gov, Xiao-lun Wu[3], [3]University of Pittsburgh, wu@vms.cis.pitt.edu, Akira Onuki[4], [4]Kyoto University, Kyoto, Japan

1 ABSTRACT

The study of the interface in a charge-free, critical and near-critical binary fluid in the presence of an externally applied electric field is presented. At sufficiently large fields, the interface between the two phases of the binary fluid should become unstable and exhibit an undulation with a predefined wavelength on the order of the capillary length. As the critical point is approached, this wavelength is reduced, potentially approaching length-scales such as the correlation length or critical nucleation radius. At this point the critical properties of the system may be affected.

In this paper, the flat interface of a marginally polar binary fluid mixture is stressed by a perpendicular alternating electric field and the resulting instability is characterized by the critical electric field E_c and the pattern observed. The character of the surface dynamics at the onset of instability is found to be strongly dependent on the frequency f of the field applied. The plot of E_c vs. f for a fixed temperature shows a sigmoidal shape, whose low and high frequency limits are well described by a power-law relationship, $E_c \sim \epsilon^{\zeta}$, with $\zeta \sim 0.35$ and $\zeta \sim 0.08$, respectively. The low-limit exponent compares well with the value $\zeta \sim 0.4$ for a system of conducting and non-conducting fluids. On the other hand, the high-limit exponent coincides with what was first predicted by Onuki.

The instability manifests itself as the conducting phase penetrates the non-conducting phase. As the frequency increases, the shape of the pattern changes from an array of bifurcating strings to an array of column-like (or rod-like) protrusions, each of which spans the space between the plane interface and one of the electrodes. For an extremely high frequency, the disturbance quickly grows into a parabolic cone pointing toward the upper plate. As a result, the interface itself changes its shape from that of a plane to that of a high sloping pyramid.

Session 1C: G-Jitter and Stochastic Flow

FLUID PHYSICS IN A FLUCTUATING ACCELERATION ENVIRONMENT

François Drolet, Supercomputer Computations Research Institute, Florida State University, Tallahassee, Florida 32306-4130, drolet@scri.fsu.edu, Jorge Viñals, Supercomputer Computations Research Institute, Florida State University, Tallahassee, Florida 32306-4130, and Department of Chemical Engineering, FAMU-FSU College of Engineering, Tallahassee, Florida 32310-6046, vinals@scri.fsu.edu

1 Abstract

Our program of research aims at developing a stochastic description of the residual acceleration field onboard spacecraft (g-jitter) to describe in quantitative detail its effect on fluid motion. Our main premise is that such a statistical description is necessary in those cases in which the characteristic time scales of the process under investigation are long compared with the correlation time of g-jitter. Although a clear separation between time scales makes this approach feasible, there remain several difficulties of practical nature: (i), g-jitter time series are not statistically stationary but rather show definite dependences on factors such as active or rest crew periods; (ii), it is very difficult to extract reliably the low frequency range of the power spectrum of the acceleration field. This range controls the magnitude of diffusive processes; and (iii), models used to date are Gaussian, but there is evidence that large amplitude disturbances occur much more frequently than a Gaussian distribution would predict. The lack of stationarity does not constitute a severe limitation in practice, since the intensity of the stochastic components changes very slowly during space missions (perhaps over times of the order of hours). A separate analysis of large amplitude disturbances has not been undertaken yet, but it does not seem difficult a priori to devise models that may describe this range better than a Gaussian distribution. The effect of low frequency components, on the other hand, is more difficult to ascertain, partly due to the difficulty associated with measuring them, and partly because they may be indistinguishable from slowly changing averages. This latter effect is further complicated by the lack of statistical stationarity of the time series.

Recent work has focused on the effect of stochastic modulation on the onset of oscillatory instabilities as an example of resonant interaction between the driving acceleration and normal modes of the system, and on cavity flow as an example of how an oscillatory response under periodic driving becomes diffusive if the forcing is random instead. This paper describes three different topics that illustrate behavior that is peculiar to a stochastic acceleration field. In the first case, we show that g-jitter can induce effective attractive or repulsive forces between a pair of spherical particles that are suspended in an incompressible fluid of different density provided that the momentum diffusion length is larger than the interparticle separation (as in the case in most colloidal suspensions). Second, a stochastic modulation of the control parameter in the vicinity of a pitchfork or supercritical bifurcation is known not to affect the location of the threshold. We show, however, that resonance between the modulation and linearly stable modes close to onset can lead to a shift in threshold. Finally, we discuss the classical problem of vorticity diffusion away from a plane boundary that is being vibrated along its own plane. Periodic motion with zero average vorticity production results in an exponential decay of the vorticity away from the boundary. Random vibration, on the other hand, results in power law decay away from the boundary even if vorticity production averages to zero.

THERMOCAPILLARY FLOWS WITH LOW FREQUENCY g-JITTER

P. Grassia, G. M. Homsy, *Department of Chemical Engineering, Stanford CA 94305-5025, USA.*
bud@chemeng.stanford.edu

ABSTRACT

A thermocapillary parallel return flow is established in a fluid filled slot of finite depth but infinite horizontal extent with a lengthwise applied temperature gradient. A vertically varying advected temperature field arises, which matches streamwise heat convection to vertical heat conduction. Low frequency jitter is imposed in arbitrary directions.

Vertical jitter proves to be relatively uninteresting, because the vorticity that it generates advects temperature in a way that has no further interaction with the jitter. Flows are produced which alternately augment or oppose the basic thermocapillary flow, and have a strength proportional to a dynamic Bond number.

Streamwise jitter proves more interesting because it is able to interact with thermocapillarity. This still produces parallel return flows, but these now exhibit a nonlinear dependence on the jitter amplitude, measured by a streamwise Rayleigh number. The flow profiles exhibit either boundary layers or layered cellular structures for large Rayleigh number as the applied stratification alternates between stable and unstable. Runaways are possible for unstable stratification and these correspond to resonant excitation of stationary long wave Rayleigh-Bénard modes.

Spanwise jitter produces fully three dimensional motion. A perturbation expansion is performed for weak jitter, and at first order, a purely buoyant spanwise-streamwise circulation results. Translational invariance properties, which follow from the simple slot geometry, are exploited to obtain the solutions. The circulations are necessarily non-return flows, but distant inpenetrable sidewalls present in a true shallow cavity are modelled by demanding that no net flux may enter any quadrant of the infinite slot. The spanwise-streamwise aspect ratio must be retained as a parameter here. The streamwise circulation advects heat and rotates the isotherms. Net depth averaged heat convection occurs, and interfacial heat transfer is effected by altering the surface temperature. This establishes a subsidiary spanwise thermocapillary flow. This flow is strong at large Marangoni number (when thermocapillarity is inherently strong) and also at small Biot number (when advected heat is trapped in the slot). The spanwise subsidiary flow has in addition, a counterintuitive dependence on the spanwise-streamwise aspect ratio, being favoured when the isotherm rotation and hence the streamwise circulation is largest.

Ground-Based Experiments on Vibrational Thermal Convection

Michael F. Schatz, Jeffrey L. Rogers, School of Physics, Georgia Institute of Technology, Atlanta, GA 30332-0430, USA, mike.schatz@physics.gatech.edu

Ground-based experiments on g-jitter effects in fluid flow provide insight that complements both theoretical studies and space-based experiments on this problem. We report preliminary results for experiments on Rayleigh-Benard convection subjected to time-dependent accelerations on a shaker table. For sinusoidal modulation, two qualitatively different pattern forming mechanisms come into play: geometry induced wavenumber selection (as in the standard ''no-shake'' Rayleigh-Benard problem) and dispersion induced wavenumber selection due to parametric instability (as in the Faraday surface-wave problem). We discuss preliminary results on the competition and coexistence of patterns due to these different instability mechanisms. We also discuss the implications of this work on the general question of pattern formation in the presence of noise.

DIFFUSING LIGHT PHOTOGRAPHY OF CONTAINERLESS RIPPLE TURBULENCE

William B. Wright and Seth J. Putterman,
Physics Department, University of California, Los Angeles, CA 90095

Extended Abstract

The key issue that has intrigued scientists about the turbulent motion of fluids is: How does fully developed turbulence differ from thermal noise with the same energy? To address this issue we have used diffusing light to quantitatively resolve the instantaneous spatial structure of a turbulently rippled surface. Our measurements indicate that the turbulent state is characterized by random motion at many different frequencies and wavelengths. Energy which enters the fluid at a long wavelength cascades to shorter and shorter wavelengths as a result of the nonlinear interaction of ripples so as to generate a turbulent energy spectrum. But in contrast with thermal equilibrium we find that this steady state is characterized by the intermittent appearance of large coherent structures with a probability that is far greater than would apply in thermal equilibrium at the same average energy. These diffusing light images quantify the competition between structure formation and randomization of energy in far off equilibrium fluid motion that must be contained in a unified theory of turbulence.

From a practical point of view thermal equilibrium differs from turbulence in that thermal equilibrium is global whereas the spectrum of turbulence has endpoints. Turbulence is driven by an external source of energy which enters at a long wavelength and then via nonlinear interactions cascades through an 'inertial' region of shorter wavelengths until the energy reaches a wavelength that is so small that viscosity damps out the motion .

In the steady state the spectrum of energy in the inertial range of turbulence and thermal equilibrium are both power laws in the wavelength. However, the challenges posed by turbulence are much deeper than the need to explain the different values for the exponent that apply to equilibrium and turbulence. The unique physical aspects of turbulence are to be found in the fluctuations around the steady state. Since motion is characterized by phase as well as amplitude the power spectra do not uniquely determine the state of fluid motion to which they apply. In thermal equilibrium the phases randomize so precisely that fluctuations are exponentially suppressed. The probability that a measurement of energy finds a power different from the average is proportional to the exponent of the difference and so follows a gaussian distribution (in amplitude) with the result that large fluctuations are highly improbable. In turbulence, large fluctuations are not exponentially suppressed and in fact the broad band power spectrum masks the spontaneous intermittent appearance of large coherent structures.

We have used diffusing light photography of surface capillary waves as a means of generating quantitative data regarding this key unexplained aspect of turbulence. While experiments on the ground have demonstrated the value of studying turbulent ripples, proposed experiments in microgravity will probe turbulence in a closed system for the first time and also make it possible to increase the measured turbulent range of motion by one decade.

DROP BREAKUP IN FIXED BED FLOWS AS MODEL STOCHASTIC FLOW FIELDS

Eric S. G. Shaqfeh, Alisa B. Mosler, and Prateek Patel, Department of Chemical Engineering , Stanford University
Stanford, CA 94305-5025 (email: eric@chemeng. stanford.edu)

ABSTRACT

We examine drop breakup in a class of stochastic flow fields as a model for the flow through fixed fiber beds and to elucidate the general mechanisms whereby drops breakup in disordered, Lagrangian unsteady flows. Our study consists of two parallel streams of investigation. First large scale numerical simulations of drop breakup in a class of anisotropic Gaussian fields will be presented. These fields are generated spectrally and have been shown in a previous publication to be exact representations of the flow in a dilute disordered bed of fibers if close interactions between the fibers and the drops are dynamically unimportant. In these simulations the drop shape is represented by second and third order small deformation theories which have been shown to be excellent for the prediction of drop breakup in steady strong flows. We show via these simulations that the mechanisms of drop breakup in these flows are quite different than in steady flows. The predominant mechanism of breakup appears to be very short lived twist breakups. Moreover the occurrence of breakup events is poorly predicted by either the strength of the local flow in which the drop finds itself at breakup, or the degree of deformation that the drop achieves prior to breakup. It is suggested that a correlation function of both is necessary to be predictive of breakup events.

In the second part of our research experiments are presented where the drop deformation and breakup in PDMS/polyisobutylene emulsions is considered. We consider very dilute emulsions such that coalescence is unimportant. The flows considered are simple shear and the flow through fixed fiber beds. Turbidity, small angle light scattering, dichroism and microscopy are used to interrogate the drop deformation process in both flows. It is demonstrated that breakup at very low Capillary numbers occurs in both flows but larger drop deformation occurs in the fixed bed flow. Moreover it is witnessed that breakup in the bed occurs continuously during flow and apparently with uniform probability through the bed length. The drop deformations witnessed in our experiments are larger than those predicted by the numerical simulations, and future plans to investigate these differences are discussed.

Session 2A: Multiphase Flow II

BUBBLE GENERATION IN A FLOWING LIQUID MEDIUM AND RESULTING TWO-PHASE FLOW IN MICROGRAVITY

S. C. Pais[1], Y. Kamotani[2], A. Bhunia[3] and S. Ostrach[4], [1,2,3,4] Department of Mechanical & Aerospace Engineering, Glennan Building, Case Western Reserve University, 10900 Euclid Avenue, Cleveland, OH 44106, [2] Corresponding Author, e-mail: yxk@po.cwru.edu,

ABSTRACT

The present investigation reports a study of bubble generation under reduced gravity conditions, using both a co-flow and a cross-flow configuration. This study may be used in the conceptual design of a space-based thermal management system. Ensuing two-phase flow void fraction can be accurately monitored using a single nozzle gas injection system within a continuous liquid flow conduit, as utilized in the present investigation. Accurate monitoring of void fraction leads to precise control of heat and mass transfer coefficients related to a thermal management system; hence providing an efficient and highly effective means of removing heat aboard spacecraft or space stations.

Our experiments are performed in parabolic flight aboard the modified DC-9 Reduced Gravity Research Aircraft at NASA Lewis Research Center, using an air-water system. For the purpose of bubble dispersion in a flowing liquid, we use both a co-flow and a cross-flow configuration. In the co-flow geometry, air is introduced through a nozzle in the same direction with the liquid flow. On the other hand, in the cross-flow configuration, air is injected perpendicular to the direction of water flow, via a nozzle protruding inside the two-phase flow conduit. Three different flow conduit (pipe) diameters are used, namely, 1.27 cm, 1.9 cm and 2.54 cm. Two different ratios of nozzle to pipe diameter (D_N^*) are considered, namely $D_N^* = 0.1$ and 0.2, while superficial liquid velocities are varied from 8 to 70 cm/s depending on flow conduit diameter.

It is experimentally observed that by holding all other flow conditions and geometry constant, generated bubbles decrease in size with increase in superficial liquid velocity. Detached bubble diameter is shown to increase with air injection nozzle diameter. Likewise, generated bubbles grow in size with increasing pipe diameter. Along the same lines, it is shown that bubble frequency of formation increases and hence the time to detachment of a forming bubble decreases, as the superficial liquid velocity is increased. Furthermore, it is shown that the void fraction of the resulting two-phase flow increases with volumetric gas flow rate (Q_d), pipe diameter and gas injection nozzle diameter, while they decrease with surrounding liquid flow. The important role played by flowing liquid in detaching bubbles in a reduced gravity environment is thus emphasized. We observe that the void fraction can be accurately controlled by using single nozzle gas injection, rather than by employing multiple port injection, since the later system gives rise to unpredictable coalescence of adjacent bubbles. It is of interest to note that empirical bubble size and corresponding void fraction are somewhat smaller for the co-flow geometry than the cross-flow configuration at similar flow conditions with similar pipe and nozzle diameters.

In order to supplement the empirical data, a theoretical model is employed to study single bubble generation in the dynamic (Q_d = 1 – 1000 cm^3/s) and bubbly flow regime within the framework of the co-flow configuration. This theoretical model is based on an overall force balance acting on the bubble during the two stages of generation, namely the expansion and the detachment stage. Two sets of forces, one aiding and the other inhibiting bubble detachment are identified. Under conditions of reduced gravity, gas momentum flux enhances, while the surface tension force at the air injection nozzle tip inhibits bubble detachment. In parallel, liquid drag and inertia can act as both attaching and detaching forces, depending on the relative velocity of the bubble with respect to the surrounding liquid. Predictions of the theoretical model compare well with our experimental results. However, at higher superficial liquid velocities, as the bubble loses its spherical form, empirical bubble size no longer matches the theoretical predictions.

In summary, we have developed a combined experimental and theoretical work, which describes the complex process of bubble generation and resulting two-phase flow in a microgravity environment. Results of the present study can be used in a wide range of space-based applications, such as thermal energy and power generation, propulsion, cryogenic storage and long duration life support systems, necessary for programs such as NASA's Human Exploration for the Development of Space (HEDS).

PRODUCTION OF GAS BUBBLES IN REDUCED-G ENVIRONMENTS

Hasan N. Oğuz, Jun Zeng, Department of Mechanical Engineering, The Johns Hopkins University, Baltimore, MD 21218, oguz@jhu.edu

In this paper, we have investigated the effect of an imposed flow on the bubble formation and detachment from underwater orifices for various cases. Experiments have been performed under normal gravity conditions and the working fluid was water. The process is modeled by axisymmetric and 3-D boundary integral techniques. The simplest situation is when the flow is parallel to the gas injection direction. The usefulness of this idea in terms of reducing bubble size has been recognized some time ago. The efficiency of this scheme is much better if the flow is bounded by a tube.

A remarkable characteristic of this flow is that bubble formation is quite regular with little or no variation from one bubble to another provided that water flow rate is sufficiently low. This regime is ideal for reliable production of bubbles of specified size. The agreement between experiment and simulations is very good despite the appreciable differences between the real and simulated bubble shapes at high water flow rates.

We have found that bubble size is solely determined by the liquid velocity and is relatively insensitive to the gas flow rate at low water flow rates. When the needle size is not too small, the primary factor is the high sensitivity of the added mass force to the bubble radius. As the bubble size becomes comparable to the tube size, it is forced to follow the liquid in the tube. For the smaller needles where the tube diameter is much larger than the needle diameter, the effect of the added mass is less significant. As a result, bubble size depends on the gas flow rate as well as the water flow rate. A substantial reduction in bubble size is observed as the water flow rate is increased while the gas flow rate is kept constant. At some point, the pinch-off process which is governed by the surface tension cannot keep up with the flow and the reduction in bubble size stops, limiting the bubble production frequency. This process is altered when the stabilizing effect of the tube prolongs the pinch-off process when the needle size is comparable to the tube size. As a consequence, the neck of the bubble gets longer with increasing water flow rates. The tube has little effect, on the other hand, when the needle is much smaller than the tube.

When the water velocity is further increased the bubble deforms substantially and becomes elongated while remaining coaxial in the tube. In this regime bubbles are shed from the tip of the bubble. Even when the gas injection is stopped a stable gas cavity is observed to persist at the tip of the needle (fig 1). The flow field in this limit is reminiscent of the velocity profile adjustment of a viscous free jet after it exits a nozzle. We have developed a new semi-analytical method to deal with a class of problems of this nature (Oğuz 1998). The free surface flow in the tube can be considered as an annular jet where the outer boundary remains in contact with the tube's inner wall while the inner boundary is a free surface defining an elongated bubble. Because of the high aspect ratio of the bubble shape it can be approximated as a cylindrical gaseous region of constant pressure. Computed bubble shapes for parabolic and uniform initial velocity profiles are compared with the experimental shapes. The profile is straighter and therefore more stable for the parabolic case than for the uniform velocity case. The experimental profile matches the uniform-case more closely but the real bubble is much shorter than the computed one. Temporal fluctuations that are ignored by the theory may be present in the flow and destabilize the downstream end of the cylindrical bubble. A stability analysis in which the steady state is given by the present theory is required to resolve this issue.

It has been shown that a precise control of the bubble size can be achieved at constant water flow rates. Since this arrangement may not be practical in some applications, an oscillatory flow in which the net water flux is zero is a better alternative. A series of experiments in which the flow is actuated by a rubber membrane driven by a solenoid show that it is possible to phase lock the bubble formation frequency to the forcing frequency under certain conditions. In the inflow phase of the oscillation, the growing bubble that is attached to the needle tip assumes an oblate shape. As a result, when the flow is reversed, the added mass force pushes the bubble away from the needle in a very efficient manner. Axisymmetric boundary integral simulations have been carried out to simulate this process. A very good agreement is found between experiment and the simulations (fig 2).

In several practical situations the process of bubble formation becomes three-dimensional. For instance, the orientation of the tube with respect to the gravitational field may cause the bubble to move off-center, towards the tube wall. The needle location with respect to the tube is another factor that renders the problem three-

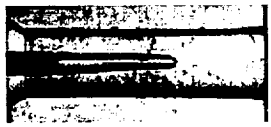

Figure 1: Steady bubble at U=2 m/s and the gas flow rate is zero. The tube diameter is 3.2 mm and the needle O.D. and I.D. are 1.27 mm and 0.84 mm respectively. This configuration can be used to create a steady gas-liquid interface in micro-gravity.

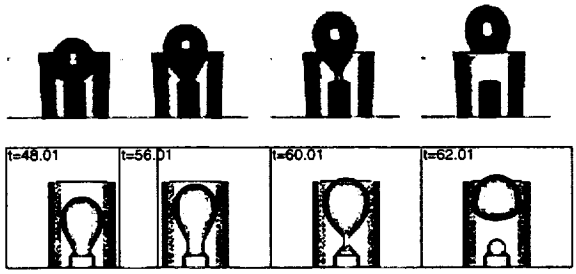

Figure 2: CCD images of of a bubble that is subject to an oscillatory flow field at 48, 56, 60 and 62 ms together with boundary integral simulations. Forcing frequency and amplitude of U are 15Hz and 13 cm/s. The tube diameter is 3.2 mm and the needle O.D. and I.D. are 1.27 mm and 0.84 mm respectively.

Figure 3: Comparison between experiment and boundary integral simulations for horizontal tube and eccentric needle cases. The gas flow rate is 0.22 ml/s. The tube diameter is 3.2 mm and the needle O.D. and I.D. are 1.27 mm and 0.84 mm respectively.

Figure 4: Cross-flow bubble formation in a tube: simulations and experiment. The average water velocity is 0.21 m/s. The tube diameter is 3.2 mm and the needle O.D. and I.D. are 1.27 mm and 0.84 mm respectively.

dimensional. The off-center placement of the needle is a typical situation of practical importance even in the absence of gravity and is considered in the present study.

We have developed a three dimensional potential-flow boundary-integral method that is applied to the cases mentioned above. For details of the problem formulation and the numerical procedure see Oğuz & Zeng (1997). We have tested the model for several cases and a good agreement is found between experiment and simulations. In fig. 3 we show the last computed shapes of bubbles for the case of a horizontal tube gravity pointing downward and an off- center needle. The match between experiment and simulation is remarkable considering the complexity of the 3-D system. One problem with these cases is that the bubble tend to move towards the tube wall or to the needle surface during the simulation and the boundary integral system becomes singular. We have adopted a scheme in which an artificial force is applied to the relevant portion of the bubble surface when it gets too close to solid walls. We have found that the necessary force is comparable in magnitude to the lubrication force that would be present if we take into account the effect of viscosity.

Gas injection from a needle embedded in the tube wall is also investigated. As bubbles grow they are forced to deform in the direction of the flow due to the added mass force just as in the case of the coaxial formation of bubbles. When the shape becomes unstable the bubble neck pinches off. This case which is inherently three-dimensional and much more difficult to model than the previous ones has also relevance in micro-gravity boiling in tubes. In fig. 4 we show a comparison of the computed bubble shapes with experiment. The agreement is again remarkably good.

We plan to employ the 3-D code for problems involving multiple injection ports in various geometrical arrangements. The effect of the neighboring bubble on the growth process will be investigated. Our initial results show that simultaneous growth of several bubbles can lead to strong interaction that is independent of the

inter-bubble distance. We also plan to study cases involving bubble removal by suction orifices.

Work supported by the Microgravity Science Program of NASA.

References

[1] H.N. Oguz. on the relaxation of laminar jets at high reynolds numbers. *Phys. Fluids*, 10:361–367, 1998.

[2] H.N. Oguz and J. Zeng. Axisymmetric and three-dimensional boundary integral simulations of bubble growth from an underwater orifice. *Engineering Analysis with Boundary Elements J.*, pages 319–330, 1997.

VORTEX DROPLET FORMATION BY A VORTEX RING IN MICROGRAVITY

Luis P. Bernal, Pepi Maksimovic, Choongil Kim, Department of Aerospace Engineering,
University of Michigan, Ann Arbor, MI 48109-2140, USA

ABSTRACT

The results of an experimental investigation of the interaction of a vortex ring with the interface between immiscible fluids are discussed. The experiments were conducted at high Weber number and Froude number resulting in interface breakup and drop formation. This flow is of interest as a prototype of liquid atomization by turbulent eddies. In addition to the Weber and Froude number, other important parameters of the interaction are the Ohnesorge number and the Bond number. Experimental observations include flow visualization results and velocity field measurements obtained using Particle Image Velocimetry (PIV). Using immiscible liquids of matched densities in 1g, flow visualization results have been obtained covering a wide range of Weber number and Froude number. These data show a change of the critical Weber number for droplet formation with Ohnesorge number. The velocity field measurements are used to determine the vorticity dynamics at the interface. It is shown that at low Weber number vorticity generated at the interface is very strong and cancels the vorticity in the vortex ring. At high Weber number the vortex ring propagates through the interface and forms a vortex droplet. The circulation of the vortex droplet was measured using PIV and found to be significantly lower than the circulation of the initial vortex ring. Experiments are being conducted in the 2.2 second Drop Tower facility at NASA Lewis Research Center to study the case of zero Bond number. Initial results show significant differences in the interaction process compared to the non-zero Bond number case.

DECOUPLING THE ROLES OF INERTIA AND GRAVITY ON PARTICLE DISPERSION

D. E. Groszmann, J. H. Thompson, S. W. Coppen, and C. B. Rogers,
Tufts University, Department of Mechanical Engineering, Medford, MA 02155

ABSTRACT

Inertial and gravitational forces determine a particle's motion in a turbulent flow field. Gravity plays the dominant role in this motion by pulling the particles through adjacent regions of fluid turbulence. To better understand and model how a particle's inertia effects its displacement, one must examine the dispersion in a turbulent flow in the absence of gravity. In this paper we present the particle experiments planned for NASA's KC-135 Reduced-Gravity Aircraft, which generates microgravity conditions for about 20 seconds. We also predict the particle behavior using simulation and ground-based experiments. We will release particles with Stokes numbers of 0.1, 1, and 10 into an enclosed tank of near-isotropic, stationary, and homogenous turbulence. These particle Stoke numbers cover a broad range of flow regimes of interest. Two opposed grids oscillating back and forth generate the turbulent field in the tank with a range of turbulence scales that covers about three orders of magnitude and with turbulence intensities of about ten times the mean velocity. The motion of the particles will be tracked using a stereo image velocimetry technique.

BUBBLE DYNAMICS ON A HEATED SURFACE

M. Kassemi[1], N. Rashidnia[2], [1,2]NCMR, NASA LeRC, Cleveland OH 44135, Mohammad.Kassemi@lerc.nasa.gov, Nasser.Rashidnia@lerc.nasa.gov

ABSTRACT

In this work, we study steady and oscillatory thermocapillary and natural convective flows generated by a bubble on a heated solid surface. The interaction between gas and vapor bubbles with the surrounding fluid is of interest for both space and ground-based processing. A combined numerical-experimental approach is adopted here.The temperature field is visualized using Mach-Zehnder and/or Wollaston Prism Interferometry and the flow field is observed by a laser sheet flow visualization technique. A finite element numerical model is developed which solves the transient two-dimensional continuity, momentum, and energy equations and includes the effects of temperature-dependent surface tension and bubble surface deformation. Below the critical Marangoni number, the steady state low-g and 1-g temperature and velocity fields predicted by the finite element model are in excellent agreement with both the visualization experiments in our laboratory and recently published experimental results in the literature. Above the critical Marangoni number, the model predicts an oscillatory flow which is also closely confirmed by experiments. It is shown that the dynamics of the oscillatory flow are directly controlled by the thermal and hydrodynamic interactions brought about by combined natural and thermocapillary convection. Therefore, as numerical simulations show, there are considerable differences between the 1-g and low-g temperature and flow fields at both low and high Marangoni numbers. This has serious implications for both materials processing and fluid management in space.

A Three-Dimensional Level Set Method for Direct Simulation of Two-Phase Flows in Variable Gravity Environments

F. Beux[1], B.A. Knowlton[1] and S. Banerjee[1]
[1]Chemical Engineering Department, University of California, Santa Barbara, CA 93106

ABSTRACT

A numerical method for the simulation of two-phase flows based on the level set formulation has been developed and applied to three-dimensional flows in a variety of situations. The ultimate objective is to directly simulate boiling, condensation, and electrochemical gas generation in microgravity environments. In the level set method, the two-phase fluid is treated as one domain with the fluid-fluid interface implicitly tracked by embedding the interface of the zero contour of a continuous function [called the level set function]. Away from the interface, the level set function is initialized to be the signed normal distance from the interface, i.e., to a distance function. In the absence of mass transfer, a simple hyperbolic equation can then written for the evolution of the levels set function and is incorporated into the solution of the Navier-Stokes equations. In comparison with other methods, the advantage is that the 'distance function equation' is continuous everywhere and exists in the whole field. The density and viscosity of the fluids then are made a function of the distance function and go through sharp changes where it is zero, i.e., at the interface. The sharpness of the change that can be tolerated depends on the robustness of the numerical scheme. Surface tension effects can also be incorporated at the interface by applying it to a delta function centered about the zero contour of the distance function. There are no smoothing requirements as the curvature of the interface is readily computed.

While the technique has been used for two dimensional and axisymmetric flows previously, the current work extends it to three dimensional problems, e.g., bubbles rising through a liquid and bursting at the interface. Note that there is no difficulty in handling interface breakup and coalescence. In addition we have extended the level set method to include interfacial mass transfer, i.e., vaporization, condensation, or species generation due to reaction and electrochemical effects

Tests have been done with a model problem in which a single vapor bubble collapses in a subcooled liquid, the heat transfer between the phases being prescribed as a constant value to simulate low levels of turbulence in the liquid. The problem can be solved analytically and the results compare well with the numerical simulations. The bubble is seen to maintain symmetry during the collapse process. However, there is some jitter in the bubble position due to numerical inaccuracies in the velocity field calculation close to the interface. While this does not affect the volume of the bubble, it does give rise to small convective effects that do not arise in the analytical situation.

The work is now being extended to examining bubble detachment from a solid wall, both under normal gravity and microgravity conditions in a laminar plane Couette flow. Microgravity experiments are available to compare with the simulations.

Session 2B: Colloids

SHEAR-INDUCED MELTING OF AQUEOUS FOAMS.

A. D. Gopal and D. J. Durian, UCLA Dept. of Physics and Astronomy.

ABSTRACT

Aqueous foam is a nonequilibrium collection of polydisperse gas bubbles packed in a smaller amount of water containing surfactants, or other surface-active macromolecules. As a form of matter, it is neither solid, liquid, nor vapor, yet can exhibit the hallmark features of all three. The ability of foam to support static shear arises from the tight packing of gas bubbles, while the ability to flow and deform arbitrarily without breaking arises from the rearrangement of bubbles from one tight-packing configuration to another. Experimental study of the packing structure and its dynamics is thus crucial for achieving fundamental understanding of the macroscopic behavior; however, it is hampered by the unavoidable fact that foams scatter light strongly and unavoidably, and hence have an opaque appearance that prevents direct imaging. Here, we review recent progress in the development of multiple light scattering techniques that take advantage of this generic property, and focus on their use as noninvasive probes of bubble dynamics in flowing foams. We also introduce a useful new rheological diagnostic. In particular, we investigate the crossover to a "melted" state which occurs with increasing strain rate. This can be seen microscopically via the functional form of the diffusing-wave spectroscopy correlation function, and macroscopically via the relaxation of stress following a step-strain imposed during steady shear flow. Besides intrinsic interest, these constitute a prelude to the ultimate flight experiments in which these same diagnostics will reveal the nature of the melting transition which occurs with increasing liquid content.

DYNAMICS OF SINGLE CHAINS OF SUSPENDED FERROFLUID PARTICLES.

S. Cutillas and J. Liu, California State University Long Beach, Department of Physics and Astronomy, 1250 Bellflower Boulevard, 90840 CA, Long Beach.

Abstract

We present an experimental study of the dynamics of isolated chains made of super-paramagnetic particles under the influence of a magnetic field. The motivation of this work is to understand if the chain fluctuations exist and, if it does, how does the fluctuation affect chain aggregation. *We find that single chains strongly fluctuate and that the characteristic frequency of their fluctuations is inversely proportional to the magnetic field strength. The higher the field the lower the characteristic frequency of the chain fluctuations. In the high magnetic field limit, chains behave like rigid rods without any internal motions.*

In this work, we used ferrofluid particles suspended in water. These particles do not have any intrinsic magnetization. Once a magnetic field is applied, a dipole moment is induced in each particle, proportional to the magnetic field. A dipolar magnetic interaction then occurs between particles. If dipole-dipole magnetic energy is higher than the thermal energy, the result is a structure change inside the dipolar fluid. The ratio of these two energies is expressed by a coupling constant λ [1] as:

$$\lambda = \frac{\pi a^3 \chi^2 \mu_0 H_0^2}{18kT}$$

Where a is the particle radius, μ_0 is the vacuum magnetic permeability, H_0 the applied magnetic field, k the Boltzmann constant and T the absolute temperature. If $\lambda>1$, magnetic particles form chains along the field direction. The lateral coalescence of several chains may form bigger aggregates especially if the particle volume fraction is high [2-4].

While many studies and applications deal with the rheological properties [5] and the structural changes [6] of these dipolar fluids, this work focuses on the understanding of the chain dynamics. In order to probe the chain dynamics, we used dynamic light scattering (DLS) in self-beating mode as our experimental technique [7]. The experimental geometry is such that the scattering plane is perpendicular to the magnetic field. Therefore, only motions in this plane are probed. A very dilute sample of a ferrofluid emulsion [3] with a particle volume fraction of 10^{-5} is used in this experiment. We chose such a low volume fraction to avoid multiply light scattering as well as lateral chain-chain aggregation. DLS measures the dynamic structure factor $S(q,t)$ of the sample (q is the scattering wave vector, t is the time). In the absence of the magnetic field, identical particles of ferrofluid droplets are randomly distributed and $S(q,t)$ reduces to $exp(-q^2 D_0 t)$. $D_0=(kT/6\pi\ \eta\ a)$ is the diffusion coefficient of Brownian particles (where $\xi=6\pi\ \eta\ a$ is the Stokes frictional coefficient of a spherical particle in a fluid of viscosity η). If interactions or polydispersity can not be ignored, an effective diffusion coefficient is introduced. Formally, D_{eff} is defined as:

$$D_{eff} = -\frac{1}{q^2}\frac{\partial}{\partial t}\ln(S(q,t))\Big|_{t\to 0}$$

D_{eff} reduces to D_0 if no interactions and only a few particles size are present. Therefore, we can use DLS to measure particle size. The particle radius was found to be $a=0.23\mu\ m$ with 7% of polydispersity. In this case, if we vary the scattering angle θ (and so q) we do not have any change in the measured diffusion coefficient: it is q-independent.

When a magnetic field is applied, particles aggregate into chains if $\lambda>1$. We first studied the kinetics of the chain formation when $\lambda=406$. At a fixed scattering angle, we measured diffusion coefficient D_{eff} as a function of time.

Experimentally, we find that D_{eff} decreases monotonously with time. Physically, this means that chains are becoming longer and longer. Since we are only sensitive to motions in the scattering plane and since chains have their main axis perpendicular to this plane, the measured diffusion coefficient is the transverse diffusion coefficient. We can relate D_{eff} to the mean number of particles per chain $N(t)$ at a given time and to the diffusion coefficient of an isolated particle D_0 as $D_{eff}=f(N(t))D_0$. Since $f(N)$ is known from other recent work [8], N can be expressed as a function of the time. We found a square root dependency: $N(t)\propto \sqrt{t}$. As expected for very low volume fraction, this behavior is characteristic of a diffusion-limited aggregation as suggested by several authors [9] and by our previous work [10].

In this study, we focus on the dependence of the effective diffusion coefficient on the scattering angle and the magnetic field strength. After the magnetic field is applied ($\lambda=406$) for a long time, typically 6 hours, kinetics of chain formation becomes very slow. Chain size does not vary much over the next hour period. Thus, we can perform different interesting experiments. First, at a fixed magnetic field, we measure the effective diffusion coefficient as a function of the scattering angle (from 5° to 130°). Our results show that the measured diffusion coefficient increases line-

arly with the scattering angle: $D_{eff} \propto q$. If we do the same experiment for different λ values, D_{eff} depends on λ as $D_{eff} \propto \lambda^{-1/2}$. We also find for different λ values that the same asymptotic D_{eff} value is obtained when q approaches zero.

The angle dependency of D_{eff} suggests that an additional motion exists besides chain drifting. Chain size is constant during experiment, which was verified by measuring the same diffusion coefficient at the beginning and at the end of the angle switching. If chains are rigid, D_{eff} is independent of q. Therefore, we found that D_{eff} not only measures the motion of the entire chain but also its internal fluctuations. These internal motions are the fluctuations of the particles in the chain.

To understand the q dependency of D_{eff}, let us look at the probing length used. In our study, the characteristic length scale probed is $l=2\pi/q$ which is in the range of $0.9<l/a<20$. When l is much larger than the particle radius ($l/a \rightarrow \infty$) we are mainly sensitive to the center of mass diffusion of the chain. D_{eff} is then the diffusion of the entire chain and depends only on N but not on q and λ. The value D_{eff} allows us to obtain the number of particles per chain N. In the opposite limit (i.e. $l/a<1$), we are sensitive to motions on the size of individual particles. The main contributions to the measured diffusion coefficient come from internal motions of the chains (i.e. particles' fluctuations inside the chain).

We investigated also the effect of the chain size on D_{eff}. For the same value of the magnetic interaction λ and different chain sizes, we found that the slope of D_{eff} versus q decreases when N increases as a power law $D_{eff} \propto N^{0.7}$. This is an important behavior because this means that the longer the chain the slower its internal fluctuations besides the whole chain motion.

In summary, we found that the effective diffusion coefficient takes the form:

$$D_{eff} = \left(\frac{2}{\sqrt{\lambda}} qa + 1\right) f(N) D_0$$

Where $f(N)$ is the inverse friction coefficient of a rigid chain of N spherical particles. D_{eff} has two contributions: the one coming from particle fluctuations and the one from the center of mass diffusion. This above relation is valid for the range of our measurements ($0.3 \leq qa \leq 2\pi$). When qa becomes larger than 2π, (the characteristic wavelength becomes shorter than the particle radius), we expect a different behavior of D_{eff}.

By analogy to the physics of crystals or polymers [11], when the characteristic length scale becomes shorter than the smaller moving object (atom or monomer), the diffusion coefficient reaches a constant value. This value defines the highest frequency probed. The frequency probed by DLS is $\Omega(q)=D_{eff}q^2$. Since the saturation frequency is reached when qa is roughly equal to 2π, we can obtain this highest characteristic frequency by replacing qa by 2π in the above relation. There, we expect the saturation frequency as:

$$\Omega(q) = \left(\frac{4\pi}{\sqrt{\lambda}} + 1\right) f(N) D_0 q^2$$

Thus, we found that $D_{eff}=D_{int}+D_{chain}$, where D_{int} is the apparent diffusion coefficient coming from fluctuations and D_{chain} is the diffusion coefficient of the whole chain. In our experiments, even at our highest magnetic field value (λ=406, D_{int}/D_{chain}=62%). From this we can see that chain fluctuations can not be neglected. Unfortunately, our experimental conditions are such that we did not reach this saturation region. Further experiments can be done with bigger particles to reach a smaller ratio l/a. However, the chain size may be more difficult to measure accurately.

Acknowledgements

We gratefully acknowledge M. Hagenbuechle for the experimental setup and earlier work [10] on which this work is based and the NASA for the grant NAG 3-1830 supporting this work.

References

[1.] de Gennes P.G. & Pincus P.A. (1970), *Phys Kondens Mat.*, **11**, 189.

[2.] G. A. Flores, J. Liu, M. Mohebi & N. Jamasbi, *proceeding of the 6th international conference on E.R.F. & M.R.S &A.T.* Japan (1997) To be published.

[3.] J. Liu and al, Field-Induced Structures in ferrofluid Emulsions, *Phys. Rev. Letters*, **74** (14), p. 2828 (1995).

[4.] S. Cutillas, G. Bossis, E. Lemaire, A. Meunier and A. Cebers, *proceeding of the 6th international conference on E.R.F. & M.R.S &A.T.* Japan (1997) To be published.

[5.] E. Lemaire, A. Meunier, G. Bossis, J. Liu, D. Felt, P. Bashtovoi, N. Matoussevitch, "Influence of the particle size on the rheology of magnetic suspensions", *J of Rheology*, **39**(5), (1995).

[6.] S. Cutillas, G. Bossis and A. Cebers, "Flow-Induced transition from cylindrical to layered patterns in MR fluids" *Phys Rev E*, **57** (1), 804, (1998).

[7.] B. J. Berne & R. Pecora, Dynamic Light Scattering, Wiley and Sons, New York, (1966).

[8.] K. Zhan, R. Lenke and G. Maret, *J. Phys. II France*, **4**, p. 555, (1994).

[9.] M. Fermigier & A. P. Gast, Structure Evolution in a Paramagnetic Latex Suspension, *J. Coll. Int. Sci.*, **154**, 522, (1992).

[10.] M. Hagenbuechle and J. Liu, *Applied Optics*, **36**, p. 7664, (1997) and *proceeding of the 6th international conference on E.R.F. & M.R.S &A.T.* Japan (1997) To be published.

[11.] de Gennes, Scaling concepts in polymer physics, Cornell University Press (1979).

CHAIN DYNAMICS IN MAGNETORHEOLOGICAL SUSPENSIONS

A.P. Gast[1] and E. M. Furst[2], [1,2] Chemical Engineering, Stanford University, Stanford CA 94305-5025, USA
alice@chemeng.standord.edu

ABSTRACT

Magnetorheological (MR) suspensions are composed of colloidal particles which acquire dipole moments when subjected to an external magnetic field. At sufficient field strengths and concentrations, the dipolar particles rapidly aggregate to form long chains. Subsequent lateral cross-linking of the dipolar chains is responsible for a rapid liquid-to-solid-like rheological transition. The unique, magnetically-activated rheological properties of MR suspensions make them ideal for interfacing mechanical systems to electronic controls. Additionally, the ability to experimentally probe colloidal suspensions interacting through tunable anisotropic potentials is of fundamental interest.

Our current experimental work has focused on understanding the fluctuations of dipolar chains. It has been proposed by Halsey and Toor (HT) that the strong Landau-Peierls thermal fluctuations of dipolar chains could be responsible for long-range attractions between chains. Such interactions will govern the long-time relaxation of MR suspensions. We have synthesized monodisperse neutrally buoyant MR suspensions by density matching stabilized ferrofluid emulsion droplets with D2O. This allows us to probe the dynamics of the dipolar chains using light scattering without gravitational, interfacial, and polydispersity effects to resolve the short- wavelength dynamics of the dipolar chains. We used diffusing wave spectroscopy to measurethese dynamics. The particle displacements at short times that show an independence to the field strength, but at long times exhibit a constrained, sub-diffusive motion that slows as the dipole strength is increased. The experiments are in good qualitative agreement with Brownian dynamics simulations of dipolar chains.

Although there have been several important and detailed studies of the structure and interactions in MR suspensions, there has not been conclusive evidence that supports or contradicts the HT model prediction that long-range interactions exist between fluctuating chains of dipolar particles [1]. Resolving this issue would contribute greatly to the understanding of these interesting and important materials.

We have begun to test the predictions of the HT model by both examining the dynamics of individual chains and by measuring the forces between dipolar chains directly to accurately and quantitatively assess the interactions that they experience. To do so, we employ optical trapping techniques and video-microscopy to manipulate and observe our samples on the microscopic level. With these techniques, it is possible to observe chains that are fluctuating freely in three-dimensions, independent of interfacial effects. More importantly, we are able to controllably observe the interactions of two chains at various separations to measure the force-distance profile. The techniques also allow us to study the mechanical properties of individual chains and chain clusters.

Our work to this point has focused on reversibly-formed dipolar chains due to field induced dipoles where the combination of this chaining, the dipolar forces, and the hydrodynamic interactions that dictate the rheology of the suspensions. One can envision, however, many situations where optical, electronic, or rheological behavior may be optimized with magneto-responsive anisotropic particles. Chains of polarizable particles may have the best properties as they can coil and flex in the absence of a field and stiffen and orient when a field is applied. We have recently demonstrated a synthesis of stable, permanent paramagnetic chains by both covalently and physically linking paramagnetic colloidal particles. The method employed allows us to create monodisperse chains of controlled length. We observed the stability, field-alignment, and rigidity of this new class of materials. The chains may exhibit unique rheological properties in an applied magnetic field over isotropic suspensions of paramagnetic particles. They are also useful rheological models as bead-spring systems [2]. These chains form the basis for our current experiments with optical traps.

[1] T.C. Halsey and W. Toor, J. Stat. Phys. 61, 1257 (1990).
[2] R. Byron Bird, Charles F. Curtiss, Robert C. Armstrong, and Ole Hassager. Dynamics of Polymeric Liquids, volume 2. Wiley, New York, 1987.

PHYSICS OF COLLOIDS IN SPACE.

P. N. Segre,[1] L. Cipelletti,[1] P. N. Pusey,[2] W. C. K. Poon,[2] A. B. Schofield[2] and D. A. Weitz,[1] [1]Dept. of Physics and Astronomy, University of Pennsylvania, 209 S 33rd St., Philadelphia, PA, 19104, [2]Dept. of Physics, University of Edinburgh, James Clerk Maxwell Building, King's Buildings, Mayfield Rd., Edinburgh, EH9 3JZ, UK.

The Physics of Colloids in Space project is an experiment that will be carried out in the International Space Station. It is designed to test several fundamental questions in colloid physics for which microgravity is essential. In addition, it is designed to test new concepts in the production of novel materials using colloidal particles as precursors in the materials synthesis.

The materials that will be studied include binary alloys of colloidal particles that form crystal structures, mixtures of colloids and polymers where the addition of the polymer induces an attractive interaction between the colloidal particles due to depletion, and very tenuous gels made of aggregating colloidal particles, where the internal structure on short range is fractal. Both the growth of the materials and the resultant structures will be studied. The majority of the studies will be performed with laser light scattering, and an apparatus that was flown in the PHaSE experiment is being modified to perform these experiments. This apparatus will allow Bragg scattering with laser excitation from a large volume of sample, thereby providing an effective powder average over the Bragg peaks, and allowing the crystal structures to be determined. In addition, dynamic light will be performed on smaller volumes allowing the dynamics to be probed. A new detector will also be added that will allow precise scattering at very low angles, and will be able to measure dynamic light scattering at extremely small angles, down to 0.1°. Some visualization will also be possible. The apparatus is being constructed by NASA LeRC.

In addition to the PCS experiment, this project has also flown a series of gloveblox experiments on MIR. These include BCAT1 and BCAT2, which were designed to take photographs of 10 samples twice a day over a 3 month period, and CGel, which was designed to do some simple light scattering, both static and dynamic, using an apparatus that was also originally flown by the PHaSE team. A main goal of these glovebox experiments is to address some of the more basic questions of PCS, and to help identify the optimum samples that will be flown on PCS.

This talk will report on the project of these flights. It will discuss some of the novel features of the PCS apparatus, particularly the very low angle static and dynamic light scattering camera. It will also review some of the results, and what was learned, by the glovebox experiments.

Analogies between colloidal sedimentation and turbulent convection at high Prandtl numbers

P. Tong , B. J. Ackerson, Department of Physics, Oklahoma State University, Stillwater, Oklahoma 74078, USA,
ptong@osuunx.ucc.okstate.edu

A new set of coarse-grained equations of motion is proposed to describe concentration and velocity fluctuations in a dilute sedimenting suspension of non-Brownian particles. With these equations, colloidal sedimentation is found to be analogous to turbulent convection at high Prandtl numbers. Using Kraichnan's mixing-length theory, we obtain scaling relations for the diffusive dissipation length δ_d, the velocity variance $\widetilde{\delta u}$, and the concentration variance $\widetilde{\delta\phi}$. The obtained scaling laws over varying particle radius a and volume fraction ϕ_0 are in excellent agreement with the recent experiment by Segrè, Herbolzheimer, and Chaikin [Phys. Rev. Lett. **79**, 2574 (1997)]. The analogy between colloidal sedimentation and turbulent convection gives a simple interpretation for the existence of a velocity cut-off length, which prevents hydrodynamic dispersion coefficients from being divergent. It also provides a coherent framework for the study of sedimentation dynamics in different colloidal systems.

Session 2C: Interfacial Phenomena I

THE EFFECTS OF THIN FILMS ON THE HYDRODYNAMICS NEAR MOVING CONTACT LINES

K.Stoev [1], E. Ramé [2], T. Leonhardt [3], S. Garoff [4]
[1,3,4] Physics Department, Carnegie Mellon University, Pittsburgh, PA
[2] National Center for Microgravity Research in Fluids and Combustion,
c/o NASA Lewis Research Center, Cleveland, OH 44135

We have studied the effects of films of various thicknesses on the hydrodynamics of macroscopic fluid bodies spreading over solid surfaces by measuring the interface shape within microns of moving contact lines and comparing those measurements to two asymptotic models valid at low capillary number *Ca*. In one model the film contains mobile fluid whose motion is modeled as fluid moves into or out of the film during spreading. In the other model, the films affect the hydrodynamics only in a submicroscopic region near the contact line and the macroscopic meniscus exhibits a non-zero effective contact angle. We examine fluids advancing and receding on wetting and nonwetting surfaces with spontaneously forming (molecular scale) and preexisting (micron scale) films. Our results stress the role of the mobility of molecules in these films in determining the hydrodynamics governing the moving contact line.

The first model, based on Landau & Levich's theory for a solid dragging a thin mobile liquid layer as it pulls out of a fluid, accounts for the hydrodynamics in the limit of small *Ca* both in recession. This theory requires that the macroscopic meniscus make an apparent 0-degree contact angle at the solid. Here the film thickness is uniquely determined by Ca and the geometry of the system. In contrast, when a fluid advances over a predeposited mobile film of the same fluid, we can independently fix Ca and the film thickness. This extra degree of freedom gives rise to two possible behaviors Landau & Levich's theory at distances from the contact line which are large compared to the film thickness; we conjecture that the appearance of each behavior is controlled by the grouping $F\equiv(d/a)Ca^{-2/3}$. The first behavior is the same as the one in recession, and corresponds to when F=O(1) as $Ca\rightarrow 0$. The second behavior arises when $F\rightarrow 0$ as $Ca\rightarrow 0$ and has the same logarithmic behavior as the classical contact line singularity.

The second model, which describes fluids advancing over dry surfaces, also accounts for the hydrodynamics of liquids advancing over very thin, immobile films. Surprisingly, the same model fails when fluid recedes on a non-wetting surface and no film is present in the same range of Ca where the same model is appropriate in advance, even though all the assumptions of the model seem to be satisfied.

We have used Poly(dimethylsiloxane) to examine the detailed interface shape of fluids advancing ad receding on wetting and nonwetting surfaces with spontaneously formed (molecular scale thickness) and deposited (micron scale thickness) films, and without films present. By comparing the measurements to the two models referred to above, we draw conclusions about the role films play in the hydrodynamics near moving contact lines. We find that films of molecular scale thickness which are tightly bound to the solid behave no different than "dry" surfaces without films when fluids advance over such surfaces; but fluids advancing in the presence of micron thick films are described by Landau & Levich's theory which assumes Newtonian behavior in the film. This suggests that film fluid mobility as allowed by the time scales of contact line passage might play a role in determining the behavior which the film exhibits.

We also examined receding motions on wetting and nonwetting surfaces. On the wetting surface, a thick film is pulled at the lowest receding speeds achievable (~1μm/sec) and the fluid motion is well described by Landau & Levich's theory as expected. However, on the nonwetting surface, fluid receding below a critical speed does not leave any trace on the solid (not even a monolayer); but above this critical speed it deposits a thick film in agreement with Landau & Levich. So it appears that on the nonwetting surface a receding fluid deposits either a thick, mobile film or no material whatsoever.

Finally we examined to what extent films spontaneously formed ahead of advancing fluid bodies may influence the hydrodynamics near moving contact lines. These films grow very slowly by surface diffusivity. Thus, they may play a role only if they grow fast enough and over a sufficiently long spatial range to allow the contact line to move over them. We find that, for contact lines advancing faster than ~5μm/s, spontaneously formed films longer than ~2μm may not exist ahead of the spreading body. Thus, either a film shorter than ~2μm exists and possibly removes the contact line singularity, or some other mechanism removes the singularity. Films formed ahead of an advancing fluid by fast Marangoni-driven flow, or via vapor deposition, may be entirely appropriate as mechanisms for removing the singularity.

Direct Numerical Simulation of Wetting and Spreading Behavior on Heterogeneous and Roughened Substrates

Leonard W. Schwartz, Departments of Mechanical Enginering and Mathematical Sciences, University of Delaware, Newark, DE 19716, USA, schwartz@me.udel.edu

A method of calculation is presented that allows the simulation of the time-dependent three-dimensional motion of thin liquid layers on solid substrates for systems with finite equilibrium contact angles. The contact angle is a prescribed function of position on the substrate. Similar mathematical models are constructed for substrates with a pattern of roughness. Evolution equations are given, using the lubrication approximation, that include viscous, capillary and disjoining forces. Motion to and from dry substrate regions is made possible by use of a thin energetically-stable wetting layer. We simulate motion on heterogeneous substrates with periodic arrays of high contact-angle patches. Two different problems are treated for heterogenous substrates. The first is spontaneous motion driven only by wetting forces. If the contact-angle difference is sufficiently high, the droplet can find several different stable positions, depending on the previous history of the motion. A second simulation treats a forced cyclical motion. Energy dissipation per cycle for a heterogeneous substrate is found to be larger than for a uniform substrate with the same total energy. The Landau-Levich solution for plate removal from a liquid bath is extended to account for a pattern of roughness on the plate.

On the Boundary Conditions at an Oscillating Contact Line

L. Jiang[1], Z. Liu[2], M. Perlin[2], and W.W. Schultz[1]

[1]Mechanical Engineering and Applied Mechanics
[2]Naval Architecture and Marine Engineering
University of Michigan, Ann Arbor, MI 48109

Abstract

We investigate principally the pinned contact line and the associated flow field, adjacent surface elevation, and contact angle. A limited discussion and results for partial slip, oscillating contact lines are included also. Previous experimental results are compared to the theories of Hocking and Miles. It is shown that at low frequencies, the pinned contact line experiments agree reasonably with Hocking; however, at higher frequencies, there is a significant difference. A discussion of the present experimental setup is included; the magnification, Brewster angle, and view camera techniques used are presented. New experimental results of the flow fields and surface elevations in the pinned contact line regime are presented. Finally, the partially-pinned contact-line problem is addressed. Results from standing (Faraday) wave experiments are presented and the need for an improved contact-line model is discussed. Additionally, a comparison is presented of a modified Tanner's law with the data of Ting and Perlin.

THE MICROMECHANICS OF THE MOVING CONTACT LINE

Seth Lichter, Department of Mechanical Engineering, Northwestern University, Evanston, IL 60208-3111
s-lichter@nwu.edu

ABSTRACT

A transient moving contact line is investigated experimentally. The dynamic interface shape between 20μm and 800μm from the contact line is compared with theory. A novel experiment is devised, in which the contact line is set into motion by electrically altering the solid-liquid surface tension γ_{SL}. The contact line motion simulates that of spontaneous wetting along a vertical plate with a maximum capillary number $Ca \sim 4 \cdot 10^{-2}$. The images of the dynamic meniscus are analyzed as a function of Ca. For comparison, the steady-state hydrodynamic equation based on the creeping flow model in a wedge geometry and the three-region uniform perturbation expansion of Cox (1986) is adopted. The interface shape is well depicted by the uniform solution for $Ca \leq 10^{-3}$. However, for $Ca > 10^{-3}$, the uniform solution over-predicts the viscous bending. This over-prediction can be accounted for by modifying the slip coefficient within the intermediate solution. With this correction, the measured interface shape is seen to match the theoretical prediction for all capillary numbers. The amount of slip needed to fit the measurements does not scale with the capillary number.

DYNAMICS OF THE MOLTEN CONTACT LINE

Ain A. Sonin[1] (speaker), Gregg Duthaler[2], Michael Liu[2], Javier Torresola[2] and Taiqing Qiu[3]

ABSTRACT

The purpose of this program is to develop a basic understanding of how a molten material front spreads over a solid that is below its melting point, arrests, and freezes. Our hope is that the work will contribute toward a scientific knowledge base for certain new applications involving molten droplet deposition, including the "printing" of arbitrary three-dimensional objects by precise deposition of individual molten microdrops that solidify after impact. Little information is available at this time on the capillarity-driven motion and arrest of molten contact line regions.

Schiaffino and Sonin (1997a) investigated the arrest of the contact line of a molten microcrystalline wax spreading over a subcooled solid "target" of the same material. They found that contact line arrest takes place at an apparent liquid contact angle that depends primarily on the Stefan number $S=c(T_f-T_t)/L$ based on the temperature difference between the fusion point and the target temperature, and proposed that contact line arrest occurs when the liquid's dynamic contact angle approaches the angle of attack of the solidification front just behind the contact line. They also showed, however, that the conventional continuum equations and boundary conditions have no meaningful solution for this angle (Schiaffino and Sonin, 1997b). The solidification front angle is determined by the heat flux just behind the contact line, and the heat flux is singular at that point. By comparing experiments with numerical computations, Schiaffino and Sonin estimated that the conventional solidification model must break down within a distance of order 0.1-1 μm of the contact line. The physical mechanism for this breakdown is as yet undetermined, and no first-principles theory exists for the contact angle at arrest.

Schiaffino and Sonin (1997c) also presented a framework for understanding low to moderate Weber number molten droplet deposition in terms of similarity laws and experimentation. The study is based on experiments with three molten materials—molten wax on solid wax, water on ice, and mercury on frozen mercury—which between them span a considerable range of the deposition/solidification similarity parameters. Correlations are obtained for the spreading velocity, spreading time scales, the spreading factor (i.e. ratio of deposited drop's final footprint radius and the drop's initial radius), post-spreading liquid oscillation amplitudes and time scales, and bulk solidification time scales.

Duthaler (1998) carried out an experimental and theoretical investigation of the relationship between the liquid's apparent contact angle and the Capillary number $Ca=\mu U/\sigma$ based on contact line speed, for molten materials spreading over subcooled solids. This relationship is required for modeling of melt spreading. We have adapted Voinov's (1976) methodology to the molten contact line and formulated a theoretical model for the Ca vs. contact angle relationship, based Schiaffino and Sonin's (1997a,b) wedge-like solidification front model. With the solidification front angle taken from Schiaffino and Sonin, the model is in good agreement with the experimental results for Ca vs. contact angle. Duthaler also extended the experimental investigation of droplet deposition and contact line freezing to more materials, including solder on glass, solder on solder, water on ice, and molten microcrystalline wax on wax. The latter also included tests on inclined targets. Deposition tests have also been done with molten octacosane ($C_{28}H_{58}$) on various targets.

An important objective of our program has been the development of micron-scale sensors for measuring the transient temperature at a point on the substrate surface as a molten contact line moves over it. The expectation is that this temperature history will yield a better understanding of the thermal process in the contact line region. The sensors are of the thermistor type, either 2.5 μm or 1.5 μm square, microfabricated with silicon-based technology on either pure silicon or amorphous silicon dioxide chips (Liu, 1998). Each chip has 32 sensors distributed on its surface in arrays. The time response is better than 10 μs. At the time of writing, sensor calibration is in progress. Results on thermal transients during contact line passage will be discussed at the conference. While we expect that the data will provide information on the near-contact-line heat transfer process, we also foresee possible problems. First, the spatial resolution of the sensors may be insufficient to resolve the near-contact-line region. Second, the sensors protrude about 0.5 μm above the substrate surface, and may affect the contact line motion. Third, a sensor's temperature history depends on both the heat flux distribution into it from the fusion front and the thermal properties of the substrate below it and the solidified melt between it and the fusion front. The heat flux distribution in the contact line region must therefore be unfolded from computations of the overall system's transient thermal response.

---

[1] Professor, Department of Mechanical Engineering, Room 3-256, MIT, Cambridge, MA 02139; sonin@mit.edu

[2] Graduate Research Assistant, Department of Mechanical Engineering, Room 3-243, MIT

[3] Assistant Professor, Department of Mechanical Engineering, Room 3-158, MIT

EFFECTIVE FORCES BETWEEN COLLOIDAL PARTICLES

Riina Tehver[1], Jayanth R. Banavar[1], [1]Department of Physics and Center for Materials Physics, Pennsylvania State University, University Park, Pennsylvania 16802, Joel Koplik[2], [2]Benjamin Levich Institute and Department of Physics, City College of the City University of New York, New York, New York 10031

Colloidal suspensions have proven to be excellent model systems for the study of condensed matter and its phase behavior. Many of the properties of colloidal suspensions can be investigated with a systematic variation of the characteristics of the systems and, in addition, the energy, length and time scales associated with them allow for experimental probing of otherwise inaccessible regimes. The latter property also makes colloidal systems vulnerable to external influences such as gravity. Experiments performed in micro-gravity by Chaikin and Russell have been invaluable in extracting the true behavior of the systems without an external field. Weitz and Pusey intend to use mixtures of colloidal particles with additives such as polymers to induce aggregation and form weak, tenuous, highly disordered fractal structures that would be stable in the absence of gravitational forces.

When dispersed in a polarizable medium, colloidal particles can ionize, emitting counterions into the solution. The standard interaction potential in these charged colloidal suspensions was first obtained by Derjaguin, Landau, Verwey and Overbeek. The DLVO potential is obtained in the mean-field linearized Poisson-Boltzmann approximation and thus has limited applicability. For more precise calculations, we have used *ab initio* density functional theory. In our model, colloidal particles are charged hard spheres, the counterions are described by a continuum density field and the solvent is treated as a homogeneous medium with a specified dielectric constant. We calculate the effective forces between charged colloidal particles by integrating over the solvent and counterion degrees of freedom, taking into account the direct interactions between the particles as well as particle-counterion, counterion-counterion Coulomb, counterion entropic and correlation contributions. We obtain the effective interaction potential between charged colloidal particles in different configurations. We evaluate two- and three-body forces in the bulk as well as study the influence of soft walls. We qualitatively explain the effects of the walls on the forces and demonstrate that many-body effects are negligible in our system. With adjustments in the parameters, the DLVO pair-potential can describe the results quantitatively.

Besides electrostatic interactions, entropic depletion effects that arise from (hard-core) exclusion play an important role in determining the behavior of multicomponent colloidal suspensions. A standard theory for depletion forces is due to Asakura and Oosawa and is based on the ideal gas approximation. To go beyond this approximation, we have studied entropic forces in molecular dynamics simulations of systems of hard spheres (the effects of the solvent have been ignored). The effective depletion forces for these systems can be found either from equilibrium distribution functions or from direct momentum transfer calculations. Our results obtained by either method show qualitative differences from the Asakura-Oosawa forces, indicating a longer range, higher value at contact and most importantly a more complicated structure, comprising of several maxima and minima. Our calculations include the determination of effective forces between two spheres, a hard sphere and a wall, and the behavior of a hard sphere near a step-edge and a corner. We also demonstrate that such entropic forces do not necessarily satisfy pairwise additivity.

Session 3A: Phase Change I: Boiling

CONSTRAINED VAPOR BUBBLE

J. Huang, M. Karthikeyan, J. Plawsky, P. C. Wayner, Jr., The Isermann Department of Chemical Engineering, Rensselaer Polytechnic Institute, Troy NY12180, USA, wayner@rpi.edu

ABSTRACT

The nonisothermal Constrained Vapor Bubble, CVB, is being studied to enhance the understanding of passive systems controlled by interfacial phenomena. The study is multi-faceted: 1) it is a basic scientific study in interfacial phenomena, fluid physics and thermodynamics; 2) it is a basic study in thermal transport; and 3) it is a study of a heat exchanger. The research is synergistic in that CVB research requires a microgravity environment and the space program needs thermal control systems like the CVB.

Ground based studies are being done as a precursor to flight experiment. The results demonstrate that experimental techniques for the direct measurement of the fundamental operating parameters (temperature, pressure, and interfacial curvature fields) have been developed. Fluid flow and change-of-phase heat transfer are a function of the temperature field and the vapor bubble shape, which can be measured using an Image Analyzing Interferometer.

The CVB, which is presented in Fig. 1 for a microgravity environment, has various thin film regions that are of both basic and applied interest. Generically, a CVB is formed by underfilling an evacuated enclosure with a liquid. Classification depends on shape and Bond number. The specific CVB discussed herein was formed in a fused silica cell with inside dimensions of 3x3x40 mm and, therefore, can be viewed as a large version of a micro heat pipe. Since the dimensions are relatively large for a passive system, most of the liquid flow occurs under a small capillary pressure difference. Therefore, we can classify the discussed system as a low capillary pressure system. The studies discussed herein were done in a 1*g* environment (Bond Number = 3.6) to obtain experience to design a microgravity experiment for a future NASA flight where low capillary pressure systems should prove more useful. The flight experiment is tentatively scheduled for the year 2000. The SCR was passed on September 16, 1997. The RDR is tentatively scheduled for October, 1998.

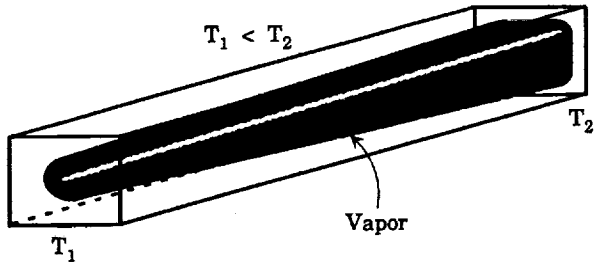

Figure 1: Vapor bubble constrained in glass cell.

COMMENTS ON THE OPERATION OF CAPILLARY PUMPED LOOP DEVICES IN LOW GRAVITY

K. P. Hallinan[1] and J. S. Allen[2]
[1]University of Dayton, Dayton, Ohio, 45469-0210, khallina@engr.udayton.edu
[2]MS500-102,NASA-LeRC, 2100 Brookpark Rd., Cleveland, OH, 44135, jeff.allen@lerc.nasa.gov

ABSTRACT

The operation of Capillary Pumped Loops (CPL's) in low gravity has generally been unable to match ground-based performance. The reason for this poorer performance has been elusive. In order to investigate the behavior of a CPL in low-gravity, an idealized, glass CPL experiment was constructed. This experiment, known as the Capillary-driven Heat Transfer (CHT) experiment, was flown on board the Space Shuttle Columbia in July 1997 during the Microgravity Science Laboratory mission.

During the conduct of the CHT experiment an unexpected failure mode was observed. This failure mode was a result of liquid collecting and then eventually bridging the vapor return line. With the vapor return line blocked, the condensate was unable to return to the evaporator and dry-out subsequently followed. The mechanism for this collection and bridging has been associated with long wavelength instabilities of the liquid film forming in the vapor return line. Analysis has shown that vapor line blockage in present generation CPL devices is inevitable.

Additionally, previous low-gravity CPL tests have reported the presence of relatively low frequency pressure oscillations during erratic system performance. Analysis reveals that these pressure oscillations are in part a result of long wavelength instabilities present in the evaporator pores, which likewise lead to liquid bridging and vapor entrapment in the porous media. Subsequent evaporation to the trapped vapor increases the vapor pressure. Eventually the vapor pressure causes ejection of the bridged liquid. Recoil stresses depress the meniscus, the vapor pressure rapidly increases, and the heated surface cools. The process then repeats with regularity.

A Study of Nucleate Boiling with Forced Convection in Microgravity

Herman Merte, Jr., The University of Michigan, Department of Mechanical Engineering and Applied Mechanics, 2148 G.G. Brown, Ann Arbor, Michigan 48109-2125, e-mail: merte@umich.edu

ABSTRACT

The ultimate objective of basic studies of flow boiling in microgravity is to improve the understanding of the processes involved, as manifested by the ability to predict its behavior. This is not yet the case for boiling heat transfer even in earth gravity, despite the considerable research activity over the past 30 years

The elements that constitute the nucleate boiling process – nucleation, growth, motion, and collapse of the vapor bubbles (if the bulk liquid is subcooled) – are common to both pool and flow boiling. It is well known that the imposition of bulk liquid motion affects the vapor bubble behavior relative to pool boiling, but does not appear to significantly influence the heat transfer. Indeed, it has been recommended in the past that empirical correlations or experimental data of pool boiling be used for design purposes with forced convection nucleate boiling. It is anticipated that such will most certainly not be possible for boiling in microgravity, based on observations made with pool boiling in microgravity. In earth gravity buoyancy will act to remove the vapor bubbles from the vicinity of the heater surface regardless of how much the imposed bulk velocity is reduced, depending, of course, on the geometry of the system. Vapor bubbles have been observed to dramatically increase in size in pool boiling in microgravity, and the heat flux at which dryout took place was reduced considerably below what is generally termed the critical heat flux (CHF) in earth gravity, depending on the bulk liquid subcooling. However, at heat flux levels below dryout, the nucleate pool boiling process was enhanced considerably over that in earth gravity, in spite of the large vapor bubbles formed in microgravity and perhaps as a consequence. These large vapor bubbles tended to remain in the vicinity of the heater surface, and the enhanced heat transfer appeared to be associated with the presence of what variously has been referred to as a liquid microlayer between the bubble and the heater surface.

The enhancement of the boiling process with low velocities in earth gravity for those orientations producing the formation of a liquid macrolayer described above, accompanied by "sliding" vapor bubbles, has been demonstrated. The enhancement was presented as a function of orientation, subcooling, and heated length, while a criterion for the heat transfer for mixed natural/forced convection nucleate boiling was given previously.

A major unknown in the prediction and application of flow boiling heat transfer in microgravity is the upper limit of the heat flux for the onset of dryout (or critical heat flux – CHF), for given conditions of fluid-heater surfaces, including geometry, system pressure and bulk liquid subcooling. It is clearly understood that the behavior in microgravity will be no different than on earth with sufficiently high flow velocities, and would require no space experimentation. However, the boundary at which this takes place is still an unknown. Previous results of CHF measurements were presented for low velocity flow boiling at various orientations in earth gravity as a function of flow velocity and bulk liquid subcooling, along with preliminary measurements of bubble residence times on a flat heater surface. This showed promise as a parameter to be used in modeling the CHF, both in earth gravity and in microgravity. The objective of the work here is to draw attention to and show results of current modeling efforts for the CHF, with low velocities in earth gravity at different orientations and subcoolings.

Many geometrical possibilities for a heater surface exist in flowing boiling, with boiling on the inner and outer surfaces of tubes perhaps being the most common. If the vapor bubble residence time on and departure size from the heater surface bear a relationship to the CHF, as results to be given indicate, it is important that visualization of and access to vapor bubble growth be conveniently available for research purposes. In addition, it is desirable to reduce the number of variables as much as possible in a fundamental study. These considerations dictated the use of a flat heater surface, which is rectangular in shape, 1.91 cm by 3.81 cm (0.75 x 1.5 inches), consisting either of a 400 Angstrom thick semi-transparent gold film sputtered on a quartz substrate which serves simultaneously as a heater and a resistance thermometer, or a copper substrate of the same size. The heater substrate is a disc which can be rotated so that the heated length in the flow direction can be changed from 1.91 to 3.81 cm (0.75 to 1.5 inches). The fluid is R-113, and the velocities can be varied between 0.5 cm/s and 60 cm/s.

For a sufficiently low velocity the CHF can be modeled reasonably well at various orientations by the correlation for pool boiling corrected for the influence of bulk liquid subcooling, multiplied by the square root of θ, the angle relative to horizontal. This arises from equating buoyancy and drag forces in the inverted positions where the vapor bubbles are held against the heater surface as they slide. A distortion of the measurements relative to pool boiling occurs as the flow velocity increases. In modeling this effect at different levels of subcooling it appeared appropriate to estimate the volumetric rate of vapor generation, using measurements of bubble frequency (or residence time), void fraction and average bubble boundary layer thickness. These were determined with the use of a platinum hot wire probe 0.025 mm in diameter by 1.3 mm long, applying a constant current to distinguish between contact with liquid or vapor. Two-dimensional spatial variations are obtained with a special mechanism to resolve displacements in increments of 0.025 mm. From such measurements it was determined that the fraction of the surface heat transfer resulting in evaporation varies inversely with the subcooling correction factor for the CHF.

The measured inverse bubble residence time is normalized relative to that predicted for an infinite horizontal flat plate at the CHF, and is correlated well with the CHF normalized relative to that for pool boiling, for various orientation angles and subcooling levels. This correspondence is then combined with a normalizing factor for the energy flux leaving the heater surface at the CHF and the computed bubble radius at departure, determined from the balance between the outward velocity of the interface due to evaporation and the buoyance induced velocity of the center of mass of the bubble. The product of the CHF and the corresponding residence time was determined to be a constant for all orientations at a given bulk flow velocity and liquid subcooling, and must be determined empirically for each velocity and subcooling at present.

It then becomes possible to predict the CHF for the different orientations, velocities, and subcoolings. These are compared with normalized measurements of the CHF for velocities ranging from 4 cm/s to 55 cm/s, subcoolings from 2.8 to 22.2°K, over orientations angles of 360 degrees.

EXPERIMENTAL INVESTIGATION OF POOL BOILING HEAT TRANSFER ENHANCEMENT IN MICROGRAVITY IN THE PRESENCE OF ELECTRIC FIELDS

Cila Herman, Department of Mechanical Engineering, The Johns Hopkins University
3400 N. Charles St., Baltimore, MD 21218, herman@titan.me.jhu.edu

EXTENDED ABSTRACT

In boiling high heat fluxes are possible driven by relatively small temperature differences, which make its use increasingly attractive in aerospace applications. The objective of the research is to develop ways to overcome specific problems associated with boiling in the low gravity environment by substituting the buoyancy force with the electric force to enhance bubble removal from the heated surface. Previous studies indicate that in terrestrial applications nucleate boiling heat transfer can be increased by a factor of 50, as compared to values obtained for the same system without electric fields. The goal of our research is to experimentally explore the mechanisms responsible for EHD heat transfer enhancement in boiling in low gravity conditions, by visualizing the temperature distributions in the vicinity of the heated surface and around the bubble during boiling using real-time holographic interferometry (HI) combined with high-speed cinematography.

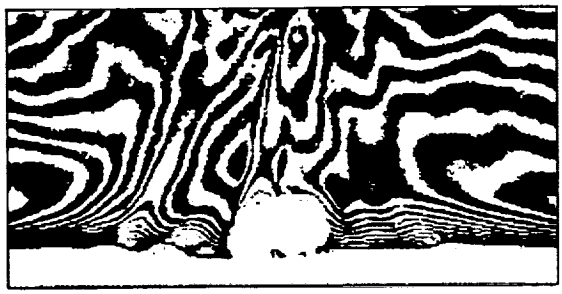

Figure 1. Temperature fields in the liquid phase in the vicinity of the bubble visualized by HI

Method of study

In the first phase of the project the influence of the electric field on a single bubble is investigated. Pool boiling is simulated by injecting a single bubble through a nozzle into the subcooled liquid or into the thermal boundary layer developed along the flat heater surface. Since the exact location of bubble formation is known, the optical equipment can be aligned and focused accurately, which is an essential requirement for precision measurements of bubble shape, size and deformation, as well as the visualization of temperature fields by HI. The size of the bubble and the frequency of bubble departure can be controlled by suitable selection of nozzle diameter and mass flow rate of vapor. In this approach effects due to the presence of the electric field can be separated from effects caused by the temperature gradients in the thermal boundary layer. The influence of the thermal boundary layer can be investigated after activating the heater at a later stage of the research.

Experimental setup

For the visualization experiments a test cell was developed. All four vertical walls of the test cell are transparent, and they allow transillumination with laser light for visualization experiments by HI. The bottom electrode is a copper cylinder, which is electrically grounded. The copper block is heated with a resistive heater and it is equipped with 6 thermocouples that provide reference temperatures for the measurements with HI. The top electrode is a mesh electrode. Bubbles are injected with a syringe into the test cell through the bottom electrode. The working fluids presently used in the interferometric visualization experiments, water and PF 5052, satisfy requirements

Figure 2. Three-dimensional thermal plume above the heated surface

regarding thermophysical, optical and electrical properties. A 30kV power supply equipped with a voltmeter allows to apply the electric field to the electrodes during the experiments. The magnitude of the applied voltage can be adjusted either manually or through the LabVIEW data acquisition and control system connected to a PC. Temperatures of the heated block are recorded using type-T thermocouples, whose output is read by a data acquisition system. Images of the bubbles are recorded with 35mm photographic and 16mm high-speed cameras, scanned and analyzed using various software packages.

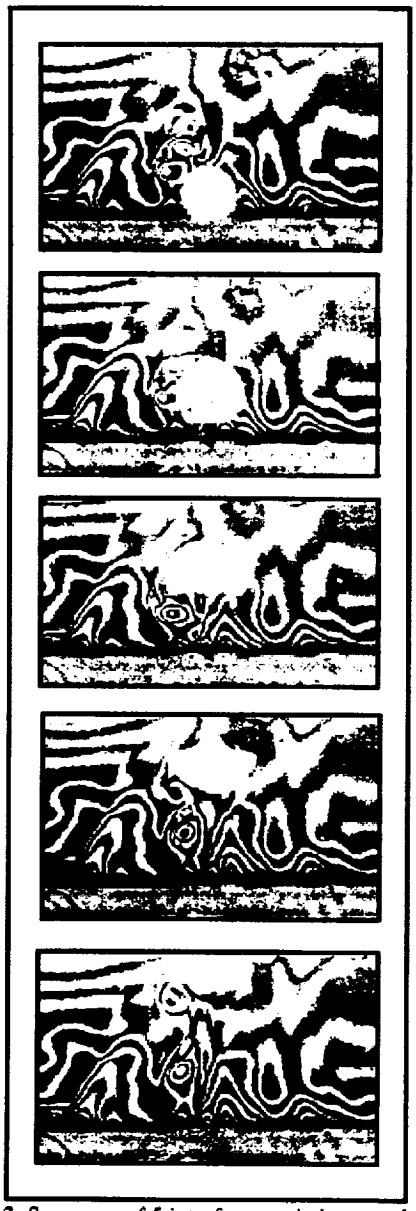

Figure 3. Sequence of 5 interferometric images showing rising bubbles injected into the thermal boundary layer through a nozzle

Visualized temperature fields

HI allows the visualization of temperature fields in the vicinity of bubbles during boiling in the form of fringes. Typical visualized temperature distributions around the air bubbles injected into the thermal boundary layer in PF5052 are shown in Figure 1. The temperature of the heated surface is 35 °C. The temperature difference for a pair of fringes is approximately 0.05 °C. The heat flux applied to the bottom surface is moderate, and the fringe patterns are regular. In the image a bubble penetrating the thermal boundary layer is visible. Because of the axial symmetry of the problem, simplified reconstruction techniques can be applied to recover the temperature field. In Figure 2 the thermal plume developing above the heated surface for more intensive heating is shown. The temperature distribution in the liquid is clearly 3D, and tomographic techniques have to be applied to recover the temperature distribution in such a physical situation. A sequence of interferometric images showing the temperature distribution around the rising bubble, recorded with a high-speed camera is shown in Figure 3. Again, the temperature distribution is 3D, and a more complex approach to the evaluation, the tomographic reconstruction has to be taken.

Measurement of the temperature distribution

From the fringe pattern temperature distributions that yield important information regarding heat transfer are determined. Two algorithms that allow the quantitative evaluation of interferometric fringe patterns and the reconstruction of temperature fields during boiling have been developed at the Heat Transfer Laboratory of the Johns Hopkins University.

In the first algorithm the bubble is assumed to be axially symmetrical, which significantly reduces the computational effort for quantifying the temperature distribution around the bubble. For this purpose the thermal boundary layer around the bubble is divided into equidistant concentric shells, and the refractive index is assumed to be constant in each of the shells. Since large temperature gradients are expected in the vicinity of the bubble during boiling, the deflection of the light beam cannot be neglected in boiling experiments. Since the exit angle of the light beam is known, this allows to account for the deflections and phase shifts outside the boundary layer (in the bulk fluid and in the windows of the test cell).

Three dimensional temperature distributions in the vicinity of the bubble are reconstructed using tomographic techniques. In tomography, the measurement volume is sliced into 2D planes. In the present study these planes are parallel to the heated surface. The objective is to determine the values of the field parameter of interest in form of the field function in these 2D planes. The field parameter is the change of the refractive index of the liquid in the measurement volume caused by temperature changes. By superimposing data for many 2D planes recorded at the same time instant, the 3D temperature distribution in the measurement volume is recovered.

Session 3B: Near Critical Point Flows

CRITICAL VISCOSITY OF XENON: SURPRISES AND SCIENTIFIC RESULTS

R. F. Berg[1], M. R. Moldover[1], and G. A. Zimmerli[2]

[1]Physical and Chemical Properties Div., National Institute of Standards and Technology, Gaithersburg, MD 20899,
[2]NYMA Incorporated, 2001 Aerospace Parkway, Brook Park, Ohio 44142; present address: National Center for Microgravity Research, c/o MS 110-3, NASA Lewis Research Center, Cleveland, OH 44135

ABSTRACT

CVX, which flew on board Space Shuttle flight STS-85 in August 1997, measured the viscosity of xenon near the liquid-vapor critical point. Very close to the critical temperature (T_c = 290 K), the viscosity η of a pure fluid is expected to diverge as a power law, $\eta \propto [(T-T_c)/T_c]^{-y}$. Microgravity allowed CVX to make the first direct observation of this divergence. This talk will summarize the scientific results and the unexpected behavior of CVX in orbit.

The scientific results are measurements of the complex viscosity at frequencies f from 2 Hz to 12 Hz and at temperatures as close as 0.3 mK to T_c. The observed divergence of the viscosity is a factor of two larger than the best ground measurements. It is characterized by the exponent y = 0.0429 ± 0.0003, in agreement with the value y = 0.0416 ± 0.0013 from a recent two-loop perturbation expansion. Viscoelastic behavior was evident at T_c + 3 mK, further from T_c than predicted. Viscoelastic behavior scaled as $Af\tau$, where τ is the decay time of the critical fluctuations. The measured value of A is 1.90 ± 0.33 times the result of a one-loop calculation. The uncertainty of A is dominated by the uncertainty of the correlation length amplitude measured by others.

The orbital environment affected CVX in surprising ways. These effects, which were absent in preflight and postflight tests, included greatly increased noise below 0.1 Hz and spurious viscosity signals related to the Shuttle's orbit. There were several large excursions per day that were superposed on a smaller 45-minute oscillation. The excursions usually occurred when the orbiter was near the South Atlantic Anomaly, a region of minimum magnetic field near Argentina. This timing and the phase of the 45-minute oscillations suggest that the effect could have been caused by charged particles.

GROWTH AND MORPHOLOGY OF PHASE SEPARATING SUPERCRITICAL FLUIDS (GMSF), BOILING IN SUBCRITICAL FLUIDS, AND CRITICAL FLUCTUATIONS

John Hegseth[1], Vadym Nikolayev [1], Daniel Beysens[2], Yves Garrabos[3], and Carole Chabot[3], [1]Department of Physics, University of New Orleans, New Orleans, Louisiana 70148, U.S.A., [2] Commissariat à l'Energie Atomique, Département de Rechereche Fondamentale sur la Matière Condensée, CEA-Grenoble, 17, Avenue des Martyrs, 38054 Grenoble Cedex 9, France, [3] Institut de Chimie de la Matière Condensée de Bordeaux, CNRS-Université Bordeaux I, Château Brivazac, Avenue du Docteur A. Schweitzer, 33608 Pessac Cedex, France

The GMSF flight experiment will study the properties of a fluid near the liquid-gas critical point. The first set of experiments will study the relation between the morphology and the growth kinetics of domains during phase separation. The second set of experiments will study the gas-liquid interfacial behavior as the critical point is approached from the two-phase region. The final set of experiments will visualize density fluctuations in a pure fluid to study their spatial-temporal evolution and statistics.

This project uses the ALICE II instrument on the MIR space station to perform the three types of experiments. Each experiment requires as ALICE II computer program stored on PCMCIA cards that are prepared on the ground. The phase separation experiments are performed by temperature quenching from the one-phase state to the two-phase state. After quenching is performed, the growth of bubbles in a liquid is observed and recorded. The fluctuation experiments are very similar with the temperature quenched to the critical point in a cell with the density accurately and precisely at the critical density. The cell and thermostat for the critical fluctuations experiment has been specially modified to boost the ALICE II microscopy to the diffraction limited resolution. The supercritical boiling experiments increase the temperature from the two-phase state to the one-phase state. The interfacial behavior of a large gas bubble is observed and recorded as the temperature is increase toward the critical point.

Three new cells and thermostat systems will be used that have the capability of changing the sample density by varying the cell volume. This new degree of freedom is a significant improvement in the state of the art. In addition to the three new variable volume cells, we plan to use two constant density cells of SF_6 (0.2% off-critical and 0.7% off critical) that have been precisely characterized in previous experiments.

All the data and visualizations that result from these experiments are stored on DAT digital videotapes and PCMCIA cards. The cards and tapes are later returned to earth. Hardware for the GMSF experiment will be transported to the MIR station on the Space Shuttle mission STS-91 in June 1998. The operation of the ALICE II apparatus may commence in summer 1998 depending on crew training.

A COMPRESSIBLE GEOPHYSICAL FLOW EXPERIMENT (CGFE)

John Hegseth, Laudelino Garcia, and M. Kamel Amara, Department of Physics, University of New Orleans, New Orleans, Louisiana 70148, jjhph@uno.edu

ABSTRACT

We report recent progress in developing a prototype experimental system that studies large-scale planetary flows. The unique characteristic of this experiment is that a density gradient is established in a compressible fluid in spherical geometry. This is accomplished by working with a fluid near the critical point where the compressibility of the fluid is greatly increased. We report results from an experimental system in which a compressible fluid in spherical geometry becomes stratified in density when an AC electric field is applied. The apparatus consists of a spherical capacitor filled with fluid in a controlled temperature environment. To generate the density gradient we use a small system (~1" diameter) and we operate the system near the fluid's (SF_6) critical density and critical temperature.

We use holographic interferometry to detect density variations in the system. The expected density profile and interferometric data are calculated. The interferometric data is compared with these calculations.

Our new cell with many improvements is discussed and the expected density profiles presented. Very recent results are also presented.

PHASE SEPARATION KINETICS IN ISOPYCNIC MIXTURES OF H_2O/CO_2/ETHOXYLATED ALCOHOL SURFACTANTS

Markus Lesemann[1], Michael E. Paulaitis[1], and Eric W. Kaler[2], [1]Department of Chemical Engineering Johns Hopkins University, Baltimore, MD 21218, email: michaelp@jhunix.hcf.jhu.edu, [2]Department of Chemical Engineering, University of Delaware, Newark, Delaware 19716.

Abstract

Ternary mixtures of H_2O and CO_2 with ethoxylated alcohol (C_iE_j) surfactants form three coexisting liquid phases at conditions where two of the phases have equal densities (isopycnic phases). Isopycnic phase behavior has been observed for mixtures containing C_8E_5, $C_{10}E_6$, and $C_{12}E_6$ surfactants, but not for those mixtures containing either C_4E_1 or C_8E_3 surfactants. Pressure-temperature (PT) projections for this three-phase equilibrium were determined for $H_2O/CO_2/C_8E_5$ and $H_2O/CO_2/C_{10}E_6$ mixtures at temperatures from approximately 25 to 33 °C and pressures between 90 and 350 bar. Measurements of the microstructure in $H_2O/CO_2/C_{12}E_6$ mixtures as a function of temperature (25-31 °C), pressure (63.1-90.7 bar), and CO_2 composition (0-3.9 wt%) have also been carried out to show that while micellar structure remains essentially unchanged, critical concentration fluctuations increase as the phase boundary and plait point are approached. In this report, we present our first measurements of the kinetics of isopycnic phase separation for ternary mixtures of $H_2O/CO_2/C_8E_5$.

Session 3C: Interfacial Phenomena II

THE DISSOLUTION OF AN INTERFACE BETWEEN MISCIBLE LIQUIDS

D. H. Vlad[1], J. V. Maher[1], [1]Department of Physics and Astronomy, University of Pittsburgh, Pittsburgh, PA 15217

The dissapearance of the surface tension of the interface of a binary mixture, measured using the dynamic surface light scattering technique, is slower for a binary mixture of higher density contrast. A comparison with a naive diffusion model, expected to provide a lower limit for the speed of dissolution in the absence of gravity shows that the the interfacial surface tension dissapears much slower than even by diffusion with the effect becoming much more pronounced when density contrast between the liquid phases is increased. Thus, the factor most likely to be responsible for this anomalously slow dissolution is gravity. A mechanism could be based on the competition between diffusive relaxation and sedimentation at the dissolving interface.

This work was supported by NASA under Grant No. NAG3-1833.

INVESTIGATION OF THERMAL STRESS CONVECTION IN NONISOTHERMAL GASES UNDER MICROGRAVITY CONDITIONS

Daniel W. Mackowski, Mechanical Engineering Department
Auburn University, AL 36849, dmckwski@eng.auburn.edu

The continuum description of momentum and energy transport in gases, based upon Newton–Stokes–Fourier constitutive relations, can become inaccurate in rarefied or highly nonequilbrium regimes, i.e., regimes in which the Knudsen number Kn ($= \lambda/L$, where λ is the gas mean free path and L is the characteristic system or gradient length) is no longer small. The Burnett equations, which represent the order–Kn^2 solution to the Boltzmann equation, ostensibly provide a means of extending continuum formulations into the transitional Knudsen regimes ($\sim Kn < 0.1$). The accuracy and validity of the Burnett equations, however, have not been firmly established. As has been noted by several authors, the asymptotic series expansion of the molecular distribution function – from which the Burnett equations are derived – has unknown convergence properties for finite Kn. The Burnett equations can also lead to Second–law impossibilities, such as heat flux in an isothermal gas. Furthermore, the Burnett equations increase the order of the differential equations that govern momentum and heat transport in the gas. Additional boundary condition information is required to fully close the problem – yet such information is generally not available from physical principles alone.

Because of these issues, it is generally held that the Burnett equations are valid only in regimes in which the Navier-Stokes-Fourier level of approximation already provides an adequate description of transport, i.e., regimes in which the Burnett contributions represent a small perturbation to heat and momentum transport. Such conditions can be representative of high–Mach number flows, for which application of the Burnett equations appears to have been the most successful. On the other hand, there is not a broad understanding of the accuracy of the Burnett equations when applied to slow–moving, nonisothermal flow conditions. In principle, 'thermal stresses' (fluid stresses resulting from temperature gradients – which are predicted by the Burnett equations) could become a significant convection mechanism in buoyancy–free, nonisothermal gases. Indeed, it has been recently suggested that thermal stress convection could affect the growth of crystals in microgravity physical vapor transport experiments.

The work presented here consists of a theoretical and numerical examination of thermally–induced stresses and flows in enclosed, highly nonisothermal gases under buoyancy–free conditions. A central objective has been to identify a strategy in which stress and/or convection effects, as predicted by the Burnett equations, could be isolated and measured in microgravity–based experiments. Because of the questionable veracity of the Burnett equations, a second objective has been to test Burnett predictions of nonisothermal gas stress and convection with the exact description provided by the direct simulation Monte Carlo (DSMC) method.

The initial phase of the project was aimed at calculation, using continuum and DSMC methods, of gas convection in two dimensional nonuniformly heated rectangular enclosures. Typically, two adjacent surfaces of the enclosure were modeled as adiabatic, zero–stress surfaces (i.e., planes of symmetry), and the other two adjacent surfaces were maintained at specified temperature distributions with one surface transferring a net amount of heat to the gas, and the other transferring the heat from the gas. According to continuum theory, convection in the enclosure would result from thermal stress in the bulk gas and thermal creep along the side walls – the latter mechanism being the slip flow of gas over a solid surface that is driven by a gas temperature gradient tangential to the surface.

Our continuum and DSMC calculations to date have not identified conditions in the enclosure that lead to measurable thermal stress flows that are comparable to or larger than thermal creep flows, and simultaneously maintain the $Kn < 0.1$ regime required of the Burnett equations. With the exception of the pure continuum limit ($Kn \to 0$, under which thermal stress vanishes), elimination of thermal creep cannot be accomplished by maintaining the heated/cooled walls at uniform temperatures. Rather, the discontinuity (or jump) between the surface and adjacent gas temperatures – which will be proportional to Kn and the local normal temperature gradient – will lead to nonuniform gas temperatures along the nonuniformly heated surfaces. For all realistic values of Kn, thermal creep flows generated by the temperature jump effects were substantially larger than those resulting from thermal stress.

To minimize the effects of creep, we performed additional simulations in which the temperature distributions along the heated/cooled surfaces were assigned to provide, for a given Kn, nearly uniform gas temperature adjacent to the surface. Surface temperature distributions were determined from solution of the gas conduction equation with uniform gas temperature boundary conditions along the adjacent heated/cooled surfaces, and subsequent application of the solution into

the order–Kn temperature jump relations. This approach imposed a surface temperature variation along the heated wall which increased towards the junction with the cooled wall, with an opposite trend along the cooled wall. The effect of this strategy largely eliminated thermal creep from continuum–based models, and left a computed flow field which was driven almost entirely by thermal stress. However, this strategy would also lead to highly nonequilibrium conditions in the vicinity of the hot/cold surface junction, for which the Burnett equations are not expected to hold. DSMC calculations on the same system showed convective flows that were qualitatively similar yet substantially larger than those predicted by the continuum model – even though the DSMC and continuum–calculated temperature fields were in significant agreement.

A more direct method of examining thermal stress effects would be to directly measure the normal stress in a gas that is contained between two parallel surfaces at different yet uniform temperature – which will eliminate convection from thermal creep. We have investigated the effects of thermal stress, as predicted by the Burnett equation, on the pressure distributions and normal stress in a stationary, buoyancy–free, hard–sphere gas for the case of one–dimensional heat transfer. Using First–Law principles and the Burnett equation, it can be shown that thermal stress results in a reduction in normal stress in the nonisothermal gas relative to that in the equilibrium state. The normal stress, in turn, can be obtained as an eigenvalue to a second–order ordinary differential equation, representing the Burnett equation, for the pressure distribution in the gas. The Burnett and DSMC predictions of pressure are in close agreement for effective Knudsen numbers (based on the temperature gradient in the gas) less than 0.1. In particular, the Burnett equations can accurately describe the shape of the Knudsen (or rarefaction) layers adjacent to the heated and cooled surfaces that bound the gas, and can also describe the variation in pressure in the 'bulk' gas (i.e., outside the Knudsen layers). In addition, theoretical predictions of the reduction in normal stress correspond well to DSMC–derived values. The effect of buoyancy on the predictions, and the potential for μg experiments of thermal stress, are discussed.

PHORETIC FORCE MEASUREMENT FOR MICROPARTICLES UNDER MICROGRAVITY CONDITIONS.

E. J. Davis and R. Zheng, University of Washington, Department of Chemical Engineering, Box 351750, Seattle, WA, 98195-1750, davis@cheme.washington.edu.

ABSTRACT

This theoretical and experimental investigation of the collisional interactions between gas molecules and solid and liquid surfaces of microparticles involves fundamental studies of the transfer of energy, mass and momentum between gas molecules and surfaces. The numerous applications include particle deposition on semiconductor surfaces and on surfaces in combustion processes, containerless processing, the production of nanophase materials, pigments and ceramic precursors, and pollution abatement technologies such as desulfurization of gaseous effluents from combustion processes. Of particular emphasis are the forces exerted on microparticles present in a nonuniform gas, that is, in gaseous surroundings involving temperature and concentration gradients. These so-called phoretic forces become the dominant forces when the gravitational force is diminished, and they are strongly dependent on the momentum transfer between gas molecules and the surface. The momentum transfer, in turn, depends on the gas and particle properties and the mean free path and kinetic energy of the gas molecules.

The experimental program involves the particle levitation system shown in Figure 1. A micrometer size particle is held between two heat exchangers enclosed in a vacuum chamber by means of ac and dc electric fields. The ac field keeps the particle centered on the vertical axis of the chamber, and the dc field balances the gravitational force and the thermophoretic force. Some measurements of the thermophoretic force are presented in this paper.

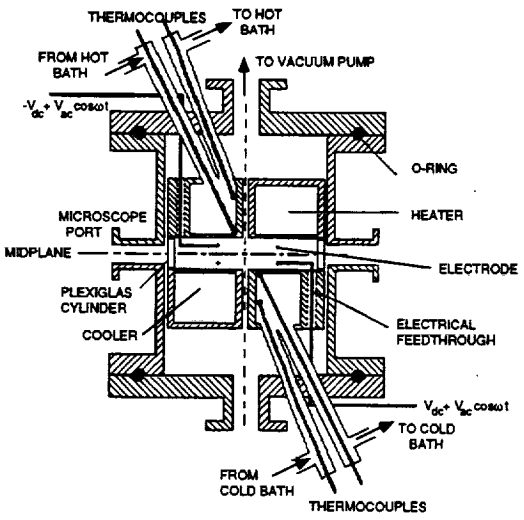

Figure 1. Cross section of the EDB used for thermophoretic force measurement.

Theoretical interpretation of thermophoretic force data requires knowledge of the thermal properties of the microparticle. One way to determine the required thermal properties is to measure the surface temperature variations of a particle when it is electromagnetically heated by means of a pulsed IR laser. Such measurements were carried out by Monazam *et al.* [1,2] at the Morgantown Energy Technology Center (METC) using high thermal conductivity carbonaceous particles, and they performed a numerical analysis of the relevant unsteady state heat transfer problem assuming uniform heating. The experiments involved heating the levitated particle from two sides. Comparison of theory and experiment permitted them to determine the thermal properties (thermal diffusivity, thermal conductivity, and heat capacity). Their assumption of uniform heating and uniform surface temperature is not likely to be valid for the lower thermal conductivity particles of interest in this research, so we extended the analysis to nonuniform heating, taking into account the internal variations in the heat generation function computed from Mie Theory [3].

Our analytical solution for the conditions of Monazam and his coworkers is compared with their data in Figure 2. There is excellent agreement between theory and experiment for the "best fit" parameters selected by Monazam *et al.* For lower thermal conductivity particles (lower by a factor of only 10) the simplified analysis is inadquate, so we extended the analysis of unsteady state microsphere heating to take into account two-sided heating rigorously. Large angular variations in surface temperature are predicted for lower conductivity particles. A paper based on the analysis is in press [4].

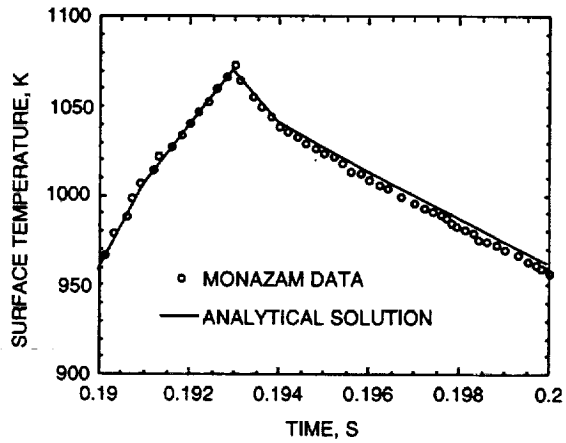

Figure 2. A comparison between theory and experiment for one asymptotic cycle.

For microparticles with thermal conductivities lower than carbonaceous materials (a factor of only ten lower) the simplified analysis of Monazam and Maloney is not adequate because large surface temperature variations occur in the angular direction. More rigorous analysis of the problem yields results presented in Figure 3. The analysis of two-dimensional (r,θ) unsteady state pulsed heating is based on computations of the electromagnetic heat source using Mie theory. The heat source is highly nonuniform. For high thermal conductivity media, angular variations in temperature are minimized by conduction, but for lower conductivity microparticles large angular variations occur.

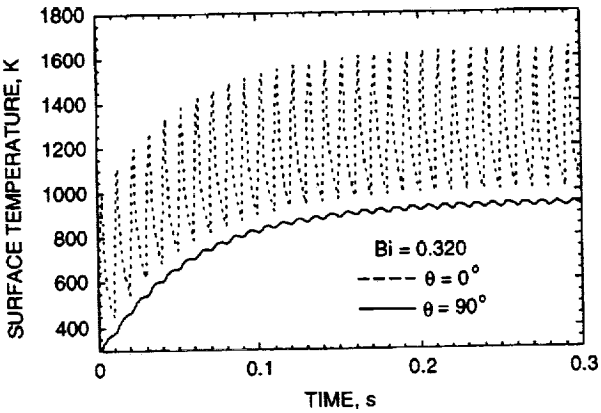

Figure 3. Surface temperature histories predicted for lower conductivity particles (lower Biot numbers, Bi).

The figure shows that very large fluctuations in the surface temperature occur at the illuminated side of the particle. At right angles to that point the temperatures are substantially lower, and the fluctuations are small. These results must be taken into account when determining the thermal properties of the particle from surface temperature measurements.

In addition to the analyses of microparticle heating, we have studied the effects of natural convection on the force measurement using the chamber shown in Figure 1. Figure 4 presents raw data consisting of the levitation voltage as a function of chamber pressure. The ratio of other external forces, F, on the particle to the gravitational force, mg, is determined from the levitation voltage by recording the dc levitation voltage with no applied temperature gradient then measuring the voltage after the heat transfer system has come to steady state. If V_0 is the dc voltage required to balance the gravitational force at thermal equilibrium and V is the voltage when the particle exists in the thermally nonuniform gas, the force ratio is given by

$$F / mg = (V_0 - V)/ V_0. \qquad (1)$$

When natural convection occurs, the external force includes the thermophoretic force and aerodynamic drag associated with the convective motion of the gas. The figure indicates that for pressures greater than 20 torr natural convection arising at the edge of the heat exchangers within the vacuum chamber led to an aerodynamic drag force larger than the thermophoretic force, but the aerodynamic drag force was negligible at lower pressures. One way to eliminate the undesirable convective effects is to operate the chamber under microgravity conditions.

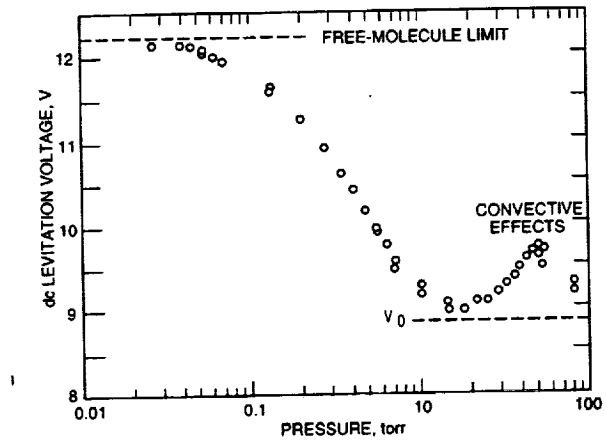

Figure 4. The levitation voltage as a function of chamber pressure for a polystyrene latex particle in air.

ACKNOWLDEGMENT

The authors are grateful to NASA for the support of this research through Grant NAG3-1837.

REFERENCES

1. E. R. Monazam, D. J. Maloney and L. O. Lawson, Measurements of Heat Capacities, Temperatures, and Absorptivities of Single Particles in an Electrodynamic Balance, *Rev. Sci. Instrum.* **60**, 3460-3465 (1989).
2. E. R. Monazam and D. J. Maloney, Temperature Transients Associated with Pulsed Heating of Single Particles, *J. Appl. Phys.* **71**, 2552-2559 (1992).
3. C. F. Bohren and D. R. Huffman, *Absorption and Scattering of Light by Small Particles*, Wiley-Interscience, New York, 1983.
4. E. J. Davis and J. F. Widmann, Pulsed Electromagnetic Heating of Microparticles, *Intl. J. Heat Mass Transfer*, in press (1998).

SURFACTANTS ON DEFORMING INTERFACES: STRESSES CREATED BY MONOLAYER-FORMING SURFACTANTS

C. E. Eggleton[1], Van Nguyen[2], and K. J. Stebe[3], [1]Department of Mechanical Engineering , UMBC, 1000 Hilltop Circle, Baltimore, MD 21250, eggleton@umbc7.umbc.edu; [2,3]Department of Chemical Engineering, The Johns Hopkins University, 3400 North Charles Street, Baltimore, MD 21218, kjs@jhu.edu

ABSTRACT

Surfactants adsorb on interfaces of moving drops or bubbles and reduce the surface tension γ. Surface convection redistributes adsorbed surfactant, creating Marangoni stresses.

Such phenomena have been extensively studied in the context of a simple model in which γ is assumed to depend linearly on the surface concentration Γ, and Γ to be linearly related to the bulk concentration C. These assumptions are limited to trace surfactant concentrations. They are of limited utility even when dilute amounts of surfactant are present, since locally elevated surface concentrations can be created by the surface convective flux, and the assumed linear relationship between the surface tension and the local surface concentration breaks down. This linear relationship neglects the finite dimensions of the surfactant molecules at the interface. The surface pressure Π is defined:

$$\Pi = \gamma_o - \gamma(\Gamma)$$

where γ_o is the surface tension in the absence of surfactant. The surface pressure is the work per unit area to compress a surfactant monolayer; Π increases strongly when the limiting area/surfactant molecule is approached. In this limit, contraction of the interface is strongly resisted, whereas expansion is not. That is, the interface behaves as if it were incompressible, but not inextensible.

In this work, a drop in an extensional flow is studied in the limit where the internal and external fluid viscosities μ are equal. The aim is to understand surfactant effects on strongly deforming interfaces. For example, consider a non-deforming spherical droplet with a surfactant-laden interface. It is understood that the interface can be rendered partially immobile if the surfactant is insoluble (the stagnant cap regime) or completely immobile if such surfactant is present in sufficient quantity. This same interface can be made tangentially mobile if a surfactant is introduced with mass transfer rates that are sufficiently rapid, again at high surfactant concentration. The question of how a deforming droplet interface behaves in such limits is the focus of this work.

The response of a spherical droplet of radius a to an applied flow with strain rate G is studied. Initially, the surfactant is uniformly distributed on the interface, with initial surface concentration Γ_{eq} and surface tension γ_{eq}. The ratio of the characteristic viscous stresses that deform the drop to the Laplace pressures that resist deformation defines the capillary number Ca:

$$Ca = \frac{\mu G a}{\gamma_{eq}}$$

The drop is studied as a function of the strain rate (Ca) and the fraction of interface initially covered by surfactant :

$$x = \frac{\Gamma_{eq}}{\Gamma_\infty}$$

where Γ_∞ is the upper bound to the surface concentration that can be accommodated in a monolayer. The coverage x is varied from 0.01-0.996. (Such coverages can be realized for surfactants in experiment.)

Three issues are addressed:

(i) *The physical chemical mechanism which causes stagnant regions to occur at steady state on the interface for finite Ca is described.* For insoluble surfactants, the stagnant cap limit is shown to apply to any axisymmetric fluid particle at steady state when surface diffusion is negligible. In particular, at low surface coverages ($x<<1$) stagnant tips are shown to occur at the drop poles. At elevated coverages, (e.g. x=0.99) the entire interface is rendered immobile in this limit. This is caused at finite Ca by the Marangoni stress which strongly opposes the surface velocity to prevent Γ from reaching Γ_∞ anywhere on the interface. At high initial coverages, any surface concentration gradient causes Γ to approach Γ_∞ near the poles. Therefore, a strong Marangoni stress resisting the accumulation occurs for an infinitesimal surface concentration gradient. As a result, Γ remains nearly spatially uniform, not only at steady state, but throughout the deformation process.

(ii) *A new paradigm is proposed to describe the (unsteady) mechanical behavior of surfactant-laden interfaces at elevated concentration.* The observation that Γ remains spatially uniform for x near unity for an insoluble surfactant is used to pose a new manner for describing the interface at high surfactant concentration. Throughout the deformation, Marangoni stresses regulate the tangential velocity to force Γ to remain spatially uniform. The surface mass balance is simplified assuming that no gradients in Γ develop. This balance then constrains the global area dilatation to balance local dilatation. This approach is shown to agree with the full solution.

(iii) *These results are extended to soluble surfactants with adsorption/desorption controlled mass transfer.* For soluble surfactants, the adsorption-desorption controlled limit is studied. For high initial surface concentrations in the insoluble limit, the Marangoni stress alone regulates the surface velocity to force Γ to remain everywhere less than Γ_∞. However, soluble surfactants can adsorb/desorb to enforce the limiting area/surfactant molecule constraint. Surfactants swept by surface convection can be replenished near the equator by adsorption, and removed from the pole by desorption. This allows the tangential velocity to remain finite while Γ remains everywhere less than Γ_∞. The tangential velocity increases to the clean interface limit as the adsorption-desorption rates increase relative to the surface convection rate. In the high coverage limit, Γ again remains spatially uniform, and increases with the mass transfer rate to its equilibrium value. A simplified approach neglecting Γ gradients in the mass balance agrees with the full solution.

FUTURE WORK

Future work will address the control of drop spreading on hydrophilic interfaces pre-wet with aqueous thin films. Surfactant adsorption on the liquid-gas interface and on the solid-aqueous surface has been observed to influence drop spreading. For example, Marmur and Lelah observed that drops containing Triton X-100 spread with a circular periphery at concentrations well below the CMC. At concentrations about the CMC, the drops do not spread. Concentrations much greater than the CMC exhibit a fingering instability, leaving dry patches.

Our premise is that the stresses exerted at the liquid-gas interfaces vary strongly with concentration. As the drop spreads, surface convection dilutes the surface concentration at the apex region and collects surfactants in the three phase contact line. The presence of concentration gradients at the drop's surface causes Marangoni stresses. This causes a stress to develop that pulls toward the drop center, stabilizing against the driving stress which pulls out toward the thin film. This stress stabilizes the circular periphery by pulling any extensions back into the parent drop. However, at concentrations much greater than the CMC, micelles act as reservoirs, replenishing the liquid-gas interface with surfactants. In this case, developing fingers will progress without the stabilizing Marangoni stress.

Surfactant adsorption on the solid-aqueous interface may play an equally important role in drop spreading. In the vicinity of the CMC, surfactants adsorbing head groups down and alkyl tails up create a hydrophobic surface that stops the drop from spreading. This phenomenon is termed autophobing. It is believed this stopping mechanism is driven by the interactions between the head group and the substrate. Experiments are currently being developed to directly visualized the surfactant distribution of a spreading droplet. The aims are as follows:

i. Develop a protocol to make reproducible adsorbed water film on silicon wafers

Aqueous films form in a controlled humidity environment on SiO_2 wafers. The thickness and uniformity of the film will be characterized by ellipsometry.

ii. Perform Drop Spreading Experiments

Once a film formation protocol is developed, the drop spreading and fluorescence microscopy experiments will be conducted in a humidity-controlled environment. Drop spreading will be studied at various concentrations below, about, and above the CMC. The evolving drop periphery will be recorded with a CCD camera.

iii. Directly image the surfactant distribution using fluorescence microscopy

The fluorescence microscopy experiments will be conducted in similar fashion. Direct observations are made with an Axiotech Vario Zeiss epi-fluorescence microscope. Using a fluorescently tagged surfactant, the distribution of surfactant at both the vapor-liquid interface and the solid-liquid interface will be recorded and digitized with a Hamamatsu intensified CCD camera, frame grabber, and imaging software.

Session 4A: Phase Change II: Solidification

INTERFACE MORPHOLOGY DURING CRYSTAL GROWTH: EFFECTS OF ANISOTROPY AND FLUID FLOW

S.R. Coriell[1], B.T. Murray[2], A.A. Chernov[3], and G.B. McFadden[4], [1]Metallurgy Division, National Institute of Standards and Technology, Gaithersburg, MD 20899, USA, coriell@nist.gov, [2] Department of Mechanical Engineering, Binghamton University, Binghamton, NY 13902, USA, bmurray@binghamton.edu, [3]Universities Space Research Association and NASA Marshall Space Flight Center, 4950 Corporate Drive, Suite 100, Huntsville, AL 35806, USA, alex.chernov@msfc.nasa.gov, [4]Mathematical and Computational Sciences Division, National Institute of Standards and Technology, Gaithersburg, MD 20899, USA, mcfadden@nist.gov

During alloy solidification, a smooth crystal-fluid interface may become unstable, leading to cellular or dendritic growth. Linear morphological stability theory describes the conditions under which the interface becomes unstable. The original treatment of morphological stability by Mullins and Sekerka assumed local equilibrium at the crystal-melt interface and isotropy of the crystal-melt surface tension; this is an excellent approximation for many metals at low growth velocities. However, many materials, including semiconductors and metals such as gallium and bismuth, grow with facets indicating strong anisotropy and deviations from local equilibrium. Kinetic anisotropy causes traveling waves along the crystal-melt interface. Yuferev has shown that for growth in which the interface is near a singular orientation (an atomically smooth orientation), there is an enhancement of morphological stability; we have carried out more detailed calculations for a binary alloy and for growth into a supersaturated solution and supercooled melt. The effect of shear flows and anisotropic interface kinetics on the morphological stability of a binary alloy growing from the melt and a crystal growing from supersaturated solution have also been considered [1-6].

The motion of elementary steps is the essence of layerwise growth. If the step motion occurs by regular step trains with a constant interstep distance, homogeneous crystals are produced. However, under a wide range of conditions the elementary steps can cluster into step bunches, i.e., the interface is morphologically unstable with respect to step bunching. The step bunches trap impurities in amounts that depend on the local step densities, and therefore the impurity distribution differs from that formed by regular step trains. Step bunches themselves may, in turn, lose their stability and trap inclusions of solvent.

In order to treat anisotropic kinetics phenomenologically, we assume that growth is by the motion of elementary steps, which leads to a macroscopic anisotropic kinetic law. The interface kinetic coefficient is assumed to depend on the step density p. In general, the kinetic coefficient may be a nonlinear function of the step density and may depend on the interface concentration as well. A singular interface becomes macroscopically or locally vicinal due to a screw dislocation or a two-dimensional nucleation growth mechanism, which generates steps. A locally finite value of p at any macroscopic area of the interface results.

We have chosen a sign convention such that positive p corresponds to step motion to the left (negative x direction). If we consider a small sinusoidal perturbation of a planar interface characterized by a constant positive value of $p = \bar{p}$, then regions of the perturbed interface with positive slopes will have larger values of p and therefore larger kinetic coefficients and larger step densities. Thus for the same supersaturation, regions of the interface with positive slopes will grow faster than regions with negative slope; this leads to a translation of the sinusoidal perturbed interface in the direction of the step motion. Both this lateral translation of the sinusoidal interface perturbation and the lateral flow of liquid can move a depression in the interface to a solute-enriched region of solution where it can grow faster and thus provide a stabilizing mechanism.

Recently we have extended the analysis of growth from a supersaturated solution to allow for a kinetic coefficient that is a nonlinear function of supersaturation and crystallographic orientation. Experimental measurements on the (100) face of ammonium dihydrogen phosphate (ADP) and potassium dihydrogen phosphate (KDP) have shown that the kinetic coefficient is strongly nonlinear in supersaturation and that the nonlinearity may cause step bunching. If the kinetic coefficient depends on supersaturation, an additional mechanism affecting interface stability is present. If the kinetic coefficient increases with supersaturation, then a protuberance on the interface sees a higher supersaturation and will grow faster than a depression, which sees a lower supersaturation, and hence there is enhanced instability.

Experiments and theory indicate that a solution flowing above a vicinal face of a crystal can either

enhance or prevent the development of step bunches. For growth on a prismatic face of ADP, experiments by Chernov et al. showed that macrosteps develop on the portion of the growth hillock where the flow was down the hillock (in the direction of step motion). On reversing the direction of flow, the original macrosteps disappeared, but new macrosteps developed on the other side of the growth hillock. This indicated that flow in the direction of step motion is destabilizing and that flow opposite to direction of step motion is stabilizing.

Growth hillocks arise when growth is by a dislocation mechanism. Since a shear flow along the interface will be in the direction of step motion on one side of the hillock and opposite to the direction of step motion on the other side of the hillock, it is unclear that enhanced stability will result from the shear flow. Maximum stability might be obtained when there is no flow since the step motion provides a stabilizing influence. However, an oscillating flow of a given frequency might also provide enhanced stabilization.

We have carried-out a linear stability analysis for growth at constant velocity $\overline{V}$ in the z –direction into a supersaturated solution. We solve the incompressible Navier-Stokes equations for the fluid velocity $\boldsymbol{u}$ and the convection-diffusion equation for solute concentration $C(x, z, t)$ in the absence of gravity. We consider a two-dimensional problem and assume all quantities are independent of the coordinate y. We present results on the effect of shear flows (including those that are oscillatory in time) on the morphological stability of a crystal growing from solution by a step mechanism.

References

[1] S. R. Coriell, B. T. Murray, and A. A. Chernov, Kinetic Self-Stabilization of a Stepped Interface: Binary Alloy Solidification, J. Crystal Growth, Vol. 141, 1994, pp. 219-233.

[2] A. A. Chernov, S. R. Coriell, and B.T. Murray, Morphological Stability of a Vicinal Face Induced by Step Flow, J. Crystal Growth, Vol. 132, 1993, pp. 405-413.

[3] A. A. Chernov, S. R. Coriell, and B. T. Murray, Kinetic Self-Stabilization of a Stepped Interface: Growth into a Supercooled Melt, J. Crystal Growth, Vol. 149, 1995, pp. 120-130.

[4] S. R. Coriell, B. T. Murray, A. A. Chernov, and G. B. McFadden, Effects of Shear Flow and Anisotropic Kinetics on the Morphological Stability of a Binary Alloy, Metallurgical and Materials Trans., Vol. 27A, 1996, pp. 687-694.

[5] S. R. Coriell, B. T. Murray, A. A. Chernov, and G. B. McFadden, Step Bunching on a Vicinal Face of a Crystal in a Flowing Solution, J. Crystal Growth, Vol. 169, 1996, pp. 773-785.

[6] S. R. Coriell, A. A. Chernov, B. T. Murray, and G. B. McFadden, Step Bunching: Generalized Kinetics, J. Crystal Growth, Vol. 183, 1998, pp. 669-682.

DIRECTIONAL SOLIDIFICATION OF A BINARY ALLOY INTO A CELLULAR CONVECTIVE FLOW: LOCALIZED MORPHOLOGIES

Y.-J. Chen and S. H. Davis, Department of Engineering Sciences and Applied Mathematics, Northwestern University, Evanston, IL60208

ABSTRACT

A steady, two dimensional cellular convection modifies the morphological instability of a binary alloy that undergoes directional solidification. When the convection wavelength is far longer than that of the morphological cells, the behavior of the moving front is described by a slow, spatial-temporal dynamics obtained through a multiple-scale analysis. The resulting system has a 'parametric-excitation' structure in space, with complex parameters characterizing the interactions between flow, solute diffusion, and rejection. The convection stabilizes two dimensional disturbances oriented with the flow, but destabilizes three dimensional disturbances in general. When the flow is weak, the morphological instability behaves incommensurably to the flow wavelength, but becomes quantized and forced to fit into the flow-box as the flow gets stronger. At large flow magnitudes the instability is localized, confined in narrow envelopes with cells traveling with the flow. In this case the solutions are discrete eigenstates in an unbounded space. Their stability boundary and asymptotics are obtained by the WKB analysis.

FLUID DYNAMICS AND SOLIDIFICATION OF MOLTEN SOLDER DROPLETS IMPACTING ON A SUBSTRATE IN MICROGRAVITY

C. M. Megaridis[1], D. Poulikakos [2], G. Diversiev[1], K. Boomsma[1], B. Xiong[1] and V. Nayagam[3]
[1]Department of Mechanical Engineering, University of Illinois at Chicago, Chicago IL 60607, cmm@uic.edu
[2]Institute of Energy Technology, Swiss Federal Institute of Technology, CH-8092 Zurich, Switzerland
[3]National Center for Microgravity Research, Cleveland, Ohio 44135.

ABSTRACT

This program investigates the fluid dynamics and simultaneous solidification of molten solder droplets impacting on a flat smooth substrate. The problem of interest is directly relevant to the printing of microscopic solder droplets in surface mounting of microelectronic devices. The study consists of a theoretical and an experimental component. The theoretical work uses axisymmetric Navier-Stokes models based on finite element techniques. The experimental work will be ultimately performed in microgravity in order to allow for the use of larger solder droplets which make feasible the performance of accurate measurements, while maintaining similitude of the relevant fluid dynamics groups (Re, We).

The primary application of interest (solder microdroplet dispensing) employs solder droplets approximately 50 to 100 μm in diameter, which collide, spread, recoil and eventually solidify on the substrate. Due to the small size of the droplets and the relatively high surface tension coefficient of solder, gravity effects are negligible. This solder application technology has shown great promise in microelectronic packaging and assembly, therefore, the development of a good understanding of the pertinent fluid dynamics and solidification phenomena is essential for its successful commercial implementation. However, progress in this area has been hindered by the small length scales of the problem (50 to 100 μm), which have made experimental measurements of the relevant fundamental transport phenomena difficult. Alternative approaches, which employed much larger (mm-size) droplets, yielded results that were affected by the masking effects of gravity. Hence, even though mm-size droplets yield significantly improved resolution, the applicability of the obtained results for much smaller droplets remains suspect. Conducting experiments in a microgravity environment eliminates the unwanted influence of gravity and makes the experimental investigation of large droplet dispension directly relevant.

The study aims to create a science base and identify the influence of the dominant process parameters in solder droplet dispensing. These process parameters are: droplet size and velocity; droplet, substrate and ambient gas temperatures; and contact angle between solder and substrate before and after solidification. The sensitivity of the solidified-droplet (bump) shape and size to variations in the above parameters is critical because solder bump volume, position, and height variation are key metrics for solder jet technology. Through a combination of experiments and numerical modeling, the effect of the dimensionless groups *Re, We, Fr* and the physics they represent are systematically documented.

The numerical model simulates the axisymmetric impact and subsequent solidification of an initially spherical, molten solder droplet on a flat multi-layer composite substrate. The Navier-Stokes equations combined with heat transfer and solidification are solved in the liquid phase using a Lagrangian approach. The heat conduction equation is solved in the solid phase, i.e., substrate and solidified sector of the droplet. The mathematical model formulation has been described elsewhere in detail (see Waldvogel et al., 1996; Waldvogel and Poulikakos, 1997).

Two separate jetting apparati are employed in the experimental work. The first is capable of jetting 50-80μm solder droplets with velocities ~1m/s, while the other generates mm-sized droplets at injection speeds of ~0.1m/s. Both devices create droplets on demand, and feature heated reservoirs, in which high-purity 63%Sn–37%Pb eutectic solder is maintained at temperatures ~210°C (melting point of solder is 183° C). The droplet flight occurs in a nitrogen atmosphere to avoid oxygen adsorption on the solder surface. The presence of oxygen is avoided because it is known to degrade the surface properties of the liquid metal.

The experimental results reported in this paper were obtained in normal gravity, in order to test the

effectiveness of the instrumentation to be used in the upcoming microgravity tests.

The thermal contact resistance between a typical electronic substrate and impacting solder microdroplets was examined first. The chosen conditions correspond to a 63%Sn–37%Pb solder droplet with pre-impact diameter 53μm, velocity 1.6 m/s and temperature 210°C. The two-layered substrate (consisting of a 2μm-thick nickel layer on a 212μm layer of silicon) had an initial temperature of 35°C. The dimensionless numbers corresponding to these conditions are Re=266, We=3.23 and Fr=4930. These operating conditions are characteristic of practical situations, and have been chosen primarily because of the availability of experimental data in terms of solder bump morphology; see Waldvogel and Poulikakos (1997), as well as Xiong et al. (1998). Model simulations showed that the computed solder bump shape is very sensitive to the contact resistance between droplet and substrate; see Xiong et al. (1998). A detailed comparison of several computed bump shapes with those determined experimentally was conducted, in order to determine the value(s) of thermal contact resistance which provided the best match between the two shapes. A phase-dependent value of contact resistance allowed the best agreement between experiment and modeling. It was concluded that the thermal contact between solder and the Ni/Si substrate is reduced nearly by twenty-fold with the appearance of the solid phase. More specifically, the value 235 kW/m^2 K was identified for liquid solder/substrate contact, and the value 13 kW/m^2 K for solid solder/substrate contact.

Experiments involving large (mm-size) droplets were conducted in normal gravity with the setup that will be used at the 2.2s drop tower of the NASA Lewis Research Center. A 63%Sn–37%Pb solder droplet with pre-impact diameter 0.9mm, velocity 0.6m/s and temperature 210°C was visualized using high-speed video (1000 fps) during its collision with a smooth stainless steel substrate at a temperature of 20°C. The dimensionless numbers corresponding to these conditions are Re=1676, We=7.4 and Fr=37. The oscillatory nature of the impact event was clearly captured in these experiments. Quantitative image analysis was performed to resolve the temporal character of several shape parameters of the deforming droplet during its collision with the flat substrate. An additional test was performed with a 0.9mm-diameter solder droplet impacting on a smooth copper substrate of temperature 25°C. The initial droplet temperature was 210°C, and the impact velocity was 1.14m/s. The nondimensional numbers corresponding to these conditions are Re = 3200, We = 27.7 and Fr = 147.5. Under the above conditions, breakup of the droplet was revealed at the end of the first recoiling cycle after impact. The smaller droplet created by this breakup was subsequently reattached to the main mass (due to gravity), eventually creating a solid bump showing no apparent signs of the earlier separation event.

In conclusion, the capabilities of the numerical model have been demonstrated, while the experimental apparatus that will be used in the pending microgravity experiments has been successfully implemented in droplet dispensing in normal gravity.

REFERENCES

Waldvogel, J. M., Poulikakos, D., Wallace, D. B., and Marusak, R., 1996, "Transport Phenomena in Picoliter Size Solder Droplet Dispension," *Transactions of the ASME, J. Heat Transfer*, Vol. 118, pp. 148-156.

Waldvogel, J. M. and Poulikakos, D., 1997, "Solidification Phenomena in Picoliter Size Solder Droplet Deposition on a Composite Substrate," *Int. J. Heat Mass Transfer*, Vol. 40, pp. 295-309.

Xiong, B., Megaridis, C. M., Poulikakos, D. and Hoang, H., 1998, "An Investigation of Key Factors Affecting Solder Microdroplet Deposition," *ASME, J. Heat Transfer*, Vol. 120, pp. 259-270.

TWO DIMENSIONAL DENDRITIC CRYSTAL GROWTH FOR WEAK UNDERCOOLING

S. Tanveer, M.D. Kunka and M.R. Foster, The Ohio State University, Columbus OH 43210.
tanveer@math.ohio-state.edu

ABSTRACT

We discuss the framework and issues brought forth in the recent work of Kunka, Foster & Tanveer, which incorporates small but nonzero surface energy effects in the nonlinear dynamics of a conformal mapping function $z(\zeta, t)$ that maps the upper-half ζ plane into the exterior of a dendrite. In this paper, surface energy effects on the singularities of $z(\zeta, t)$ in the lower-half ζ plane were examined, as they move toward the real axis from below. In particular, the dynamics of complex singularities manifests itself in predictions on nature and growth rate of disturbances, as well as of coarsening.

Session 4B: Granular Media

PARTICLE SEGREGATION IN COLLISIONAL SHEARING FLOWS.

J. T. Jenkins[1] and M. Y. Louge[2], [1]Department of Theoretical and Applied Mechanics, [2]Sibley School of Mechanical and Aerospace Engineering, Cornell University, Ithaca, NY 14853·

ABSTRACT

The size segregation of flowing or shaken grains is a commonly observed phenomenon in industrial processes and in nature. In systems that do not involve much agitation of the grains, several mechanisms that involve gravity have been identified as leading to such segregation. In highly agitated flows, there is a mechanism independent of gravity that is available to drive separation of different grains. This is associated with spatial gradients in the energy of their velocity fluctuations.

Because collisions between grains inevitably dissipate energy, collisional granular shear flows are usually of limited extent in the direction transverse to the flow. One consequence of this is that shear flows are strongly influenced by their boundaries. Because grains, on average, slip relative to boundaries, a bumpy or frictional boundary can convert slip energy into fluctuation energy. However, because each collision between a grain and the boundary dissipates fluctuation energy, there is a competition between production and dissipation.

In principle, it is possible to design the geometry of the boundary - for example, the size and spacing of the bumps - so that the boundary either produces or dissipates fluctuation energy. This permits the control of the component of the spatial gradient of the fluctuation energy that is normal to the boundary. The gradients in fluctuation energy established by such boundaries may be exploited to drive the separation by size or other properties in a binary mixture of spherical grains.

Microgravity makes the visual observations possible by permitting us to employ moderate rates of shear. On earth, the effects of gravity can be minimized by shearing so rapidly that the particle pressure overwhelms gravity. However, in this event, separation takes place too rapidly for visual observation, buoyancy and/or condensation associated with the centripetal acceleration must be accounted for, and the particles can be severely damaged. Because, in the absence of gravity, the only available time scale is proportional to the speed of the moving boundary, this speed can be made arbitrarily slow to permit observations and to avoid particle damage, without altering the phenomenon under study.

The primary goal of this research is to carry out a physical experiment in which particle segregation is induced and maintained in a collisional flow of a binary mixture of two different types of spheres. The segregation will be driven in the absence of gravity by a spatial gradient in the kinetic energy of the velocity fluctuations of the mixture. The flow is to take place in a shear cell in the form of a race track in which the grains are sheared by the motion of the inner boundary relative to the outer. The gradient of the kinetic energy is to be maintained using boundaries with different geometric features that result in different rates of conversion of the mean slip velocity into fluctuation energy at their surfaces.

In the experiment, a steady shearing flow will be maintained in shear cell by the relative motion of parallel, bumpy boundaries. The resulting profiles of mean velocity, fluctuation velocity, and concentration will be measured in a region of fully-developed flow. They will be compared with those predicted by theory and those measured in computer simulations. We will also test simple analytical results for the mean velocity and fluctuation energy, obtained in a dense limit of the kinetic theory, against the experiment. The extent of agreement between the experiments, the theory, and the computer simulations will provide a test of the assumptions upon which the theory and the computer simulations are based.

Computer simulations play an important role in the research. They have guided the design of the shear cell shown in Fig. 1, and they have assisted us in determining the strategy for flow visualization and in establishing our requirements for microgravity.

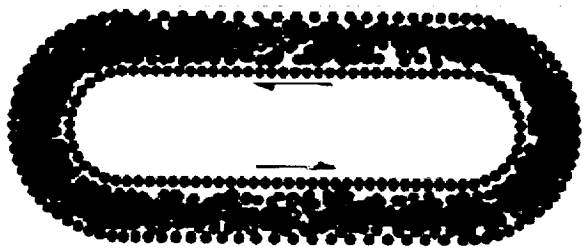

Figure 1 A shear cell of modest size. The outer boundary is fixed. The inner boundary moves with speed U in the direction shown.

The link between the computer simulations, the theory, and the physical experiments is provided by our ability to measure the collision parameters in an accurate and reproducible experiment. Our hope is to provide a demonstration of the power and utility of computer simulations and to establish them as an equal partner to physical experiment and theory.

ACKNOWLEDGMENT

This research is supported by the Microgravity Fluid Physics Program of the National Aeronautics and Space Administration.

MATERIAL INSTABILITIES IN PARTICULATE SYSTEMS

J.D. Goddard, Department of Applied Mechanics and Engineering Sciences, University of California, San Diego, La Jolla, CA 92093-0411, USA, jgoddard@ucsd.edu

Abstract

Following is a brief summary of a theoretical investigation of material (or constitutive) instability associated with shear induced particle migration in dense particulate suspensions or granular media. It is shown that that one can obtain a fairly general linear-stability analysis, including the effects of shear-induced anisotropy in the base flow as well as Reynolds dilatancy. A criterion is presented here for simple shearing instability in the absence of inertia and dilatancy.

Introduction

This is an extension of previous work on migrational instabilities in sheared particle suspensions. That work [2-3] employs as constitutive prototype a slight variant of the neutrally-buoyant "Stokesian" suspension model of Leighton and Acrivos [5] in which the stress and the particle flux relative to the mixture are given, respectively, by

$$\left.\begin{array}{l} \mathbf{T} = 2\eta(\phi,\dot\gamma)\mathbf{D} - p\mathbf{1} \\ \mathbf{j} = -\{\kappa(\phi,\dot\gamma)\nabla\phi + \nu(\phi,\dot\gamma)\nabla\dot\gamma\} \end{array}\right\} \quad (1)$$

where ϕ denotes particle volume fraction,

$$\mathbf{D} := \frac{1}{2}\{\nabla\mathbf{v} + (\nabla\mathbf{v})^T\}, \quad \dot\gamma := \left\{2\mathrm{tr}\left(\mathbf{D}^2\right)\right\}^{\frac{1}{2}} \quad (2)$$

and $\mathbf{v}$ is mixture velocity. This model and certain variants have been employed to explain particle migration effects in suspensions of rigid particles.

In the present work, we allow for the possibility of more complex rheology, such as yield stress arising from particle contact, and anisotropic response to perturbations on a uniform steadily sheared base state. Also, we include a "source" term $G(\phi,\dot\gamma)$, say, in the balance equation for ϕ, intended to represent Reynolds dilatancy in dense suspensions or dry granular media, whereby shearing may lead to a change in local particle density.

Linear Stability

In the standard balance equations for infinitesimal perturbations $\mathbf{v}^{(1)}, \phi^{(1)}, p^{(1)}$ on a uniform base state $\mathbf{v}^{(0)} = \mathbf{Lx}$, with $\mathbf{L} = (\nabla\mathbf{v}^{(0)})^T$ and $\phi^{(0)}$ independent of spatial position $\mathbf{x}$, we assume a general linear constitutive response, with

$$\left.\begin{array}{l} \tau_{ij}^{(1)} = \mathcal{H}_{ijkl}\nabla_k v_l^{(1)} + M_{ij}\phi^{(1)} - p^{(1)}\delta_{ij} \\ j_i^{(1)} = -\mathcal{N}_{ijkl}\nabla_j\nabla_k v_l^{(1)} - K_{ij}\nabla_j\phi^{(1)} \\ G^{(1)} = G_{ij}\nabla_i v_j^{(1)} + F\phi^{(1)} \end{array}\right\} \quad (3)$$

The representation (3) can be justified as a "short-memory" approximation [1] to functional derivatives for memory fluids, e.g. viscoelastic models such as

$$\mathbf{T} + \lambda\{\mathcal{D}_t\mathbf{T} - \mathbf{DT} - \mathbf{TD}\} = 2\eta\mathbf{D} \quad (4)$$

with

$$\lambda \to 0, \quad \text{with} \quad \lambda|\mathcal{D}_t(\,)| \to 0 \quad \text{and} \quad \lambda|\nabla\mathbf{v}| \ \text{fixed} \quad (5)$$

where $\mathcal{D}_t$ denotes the Jaumann derivative.

Linear stability is then determined by the constitutive equations (3) and the balance equations, together with suitable boundary conditions. We summarize here a recent analysis [4] for the unbounded, uniform simple shear:

$$v_x^{(0)} = \dot\gamma^{(0)}y \quad \text{and} \quad \{v_y^{(0)}, v_z^{(0)}, \nabla\dot\gamma^{(0)}, \nabla\phi^{(0)}\} = 0, \quad (6)$$

In the absence of inertia ($\rho = 0$) and dilatancy ($G = 0$), the asymptotic growth of perturbations is governed by wave-vector shearing [2-3], with the growth rate of the Fourier amplitude $\Phi(\mathbf{k},t)$ of $\phi^{(1)}(\mathbf{x},t)$ determined by the diffusion equation

$$\hat d_t \log\Phi = (K_{22} - \mathcal{N}_{2221}\mathcal{H}_{1221}^{-1}M_{12})k^2(t) \quad (7)$$

Here, the time-dependent wave number $k(t) = |\mathbf{k}(t)|$ is given in terms of the initial wave vector $\hat{\mathbf{k}}$ by

$$k_x \equiv \hat k_x \quad \text{and} \quad k_y = \hat k_y - \hat k_x t \quad (8)$$

and $\hat d_t$ denotes partial time derivative at constant $\hat{\mathbf{k}}$ [2-3]. Thus, instability corresponds to positivity of the right-hand side of (7) and is determined by only four material parameters, with (7) encompassing the isotropic model (1) [2,3] . Furthermore, as with (1), this short-wavelength "shear-band" instability corresponds to loss

of static ellipticity in the field equations.

As a continuation of the present work, an investigation is underway into the effects of the terms $G^{(1)}$ in (3), which lead to different dependence on disturbance wave length than the terms considered here.

Acknowledgement

Partial support from the U.S. National Aeronautics and Space Administration (Grant NAG 3-1888) and the U.S. National Science Foundation (Grant CTS 9510121) is gratefully acknowledged.

References

[1] Akbay, U., Becker, E. and Sponagel, S. (1985) Instability of Plane Couette Flow of Viscoelastic Liquids, *J. Non-Newtonian Fluid Mech.*,**18**, 123.

[2] Goddard, J.D.(1998) Migrational Instabilities in Particle Suspensions, in *The Dynamics of Complex Fluids*, M.J. Adams *et al.*, eds., Imperial College Press - The Royal Society, 281.

[3] Goddard, J.D.(1998) Migrational Instabilities in Shear-Thinning Suspension, in *IUTAM Symposium on Lubricated Transport of Viscous Materials*, H. Ramkisson, ed., Kluwer Academic Publishers, 193.

[4] Goddard, J.D. (1997) Migrational Instabilities in Particle Suspensions, Paper 119j, Annual AIChE Meeting, Los Angeles,CA, November 16-21.

[5] Leighton, D. T. & Acrivos, A. (1987) The shear-induced migration of particles in concentrated suspensions, *J. Fluid Mech.*, **181**, 415.

ABSTRACT: GRAVITY AND GRANULAR MATERIALS

R.P. Behringer[1], Daniel Howell[1], Lou Kondic[1], Sarath Tennakoon[1], Christian Veje[2]
[1]*Department of Physics and Center for Nonlinear and Complex Systems, Duke University, Durham NC, 27708-0305*
bob@phy.duke.edu
[2]*Center for Chaos and Turbulence Studies, Niels Bhor Institute, Blegdamsvej 17, DK-2100 Copenhagen ø, Denmark*

Granular flows exhibit a rich phenomenology that is still only partially understood [1]. On the Earth, granular materials show dynamics that is often dominated by the effects of gravity. For instance, they are typically random densely packed at rest; if they initially have a large kinetic energy so that they are in a gas-like state, inelastic effects quickly dissipate that energy, leading back to the dense state. In a reduced gravity environment, the dynamics of granular materials is almost certainly different. The dense packed state is much less likely to occur, and other interesting phenomena are likely to be unmasked. In the present work, we have identified a second-order-like phase transition that is always masked by gravity for ordinary materials; this transition would be accessible in low gravity. Goldhirsch et al. have predicted that as a granular gas cools, it will undergo another dynamical transition that will lead to spatial inhomogeneity, although gravity makes the study and interpretation of this effect on earth difficult.

Understanding these phenomena would be scientifically interesting, and quite possibly technically important. Such understanding would be crucial in any effort to mine in a reduced gravity environment, such as the Moon.

In the experiments described below, we have probed the effects of gravity in two ways. In the first, we have modulated gravity through shaking. This shaking includes motion in both the vertical and horizontal directions simultaneously, as well as pure horizontal shaking. In the second probe, we have studied a 2D granular system in which the grains are supported on a smooth slippery sheet. Thus, we can control the density independently. With this probe, we have shown that there is a kind of second order phase transition at the packing fraction for which the system can just sustain shear. The remainder of this abstract highlights results from these two systems.

Shaken Granular Materials. For the shaking experiments, we have developed a novel apparatus that allows us to provide independent two-axis shaking (a third axis could be added). One of the directions is vertical and the other horizontal. Effectively, this shaking allows us to modulate g. An additional feature of the apparatus is that is allows us to fluidize the grains by gas flow through a porous bottom plate. This fluidization is intended to reduce the contact forces between grains, and also reduces the effect of gravity

For purely horizontal shaking [2], we have studied the onset of flow as the dimensionless acceleration,

$$\Gamma h = A_h \omega_h^2 / g, \qquad (1)$$

is increased from 0. Here, the horizontal displacement is

$$x = A_h \sin \omega_h t. \qquad (2)$$

The initial transition to flow is hysteretic, i.e. once flow has begun, it can be sustained at lower Γh, as shown in Fig. 1. The hysteresis is lifted, however, if the layer is dilated about 2% by gas fluidization. The overall flow pattern consists of sloshing motion which drives convection in the direction of shaking, plus a novel wall shearing effect that drives a weaker flow in the cross direction to shaking. We have probed the latter effect through soft-particle MD simulations. This motion occurs because of dilation near the outer wall.

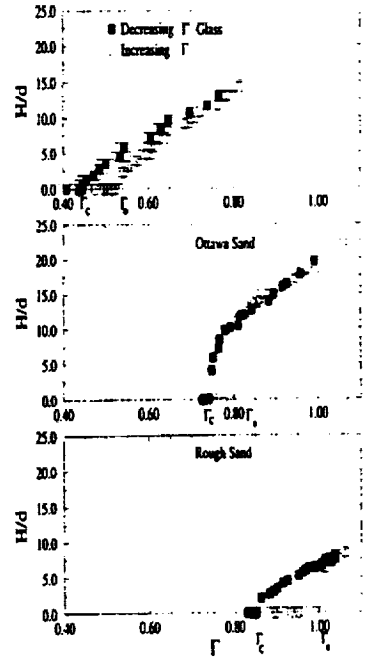

Figure 1: Examples showing the hysteresis near onset of flow under horizontal shaking for several different materials.

For mixed vertical and horizontal shaking [3], a number of interesting effects occur, including the spontaneous formation of static heaps and at higher horizontal accelerations, the onset of sloshing flow. To describe these experiments, we define a corresponding dimensionless acceleration,

$$\Gamma v = A_v \omega_v^2 / g, \quad (3)$$

for shaking in the vertical direction,

$$y = A_v \sin(\omega_v t + \phi). \quad (4)$$

As seen in Fig. 2, static heaps form spontaneously when $\Gamma_v < 1\Gamma$ and Γ_h is gradually increased from 0. We understand the formation of these heaps as the point at which grains become unstable to the horizontal acceleration under the reduced effective gravity $g(1-\Gamma_v)$. Sloshing flow occurs when Coulomb friction can no longer sustain grains from sloshing up and down in the inclined slope of the spontaneously formed heap. Standard Coulomb friction predicts all of these features qualitatively. but not quantitatively. An interesting application of the shaking technique used here is the mixing of dissimilar granular materials.

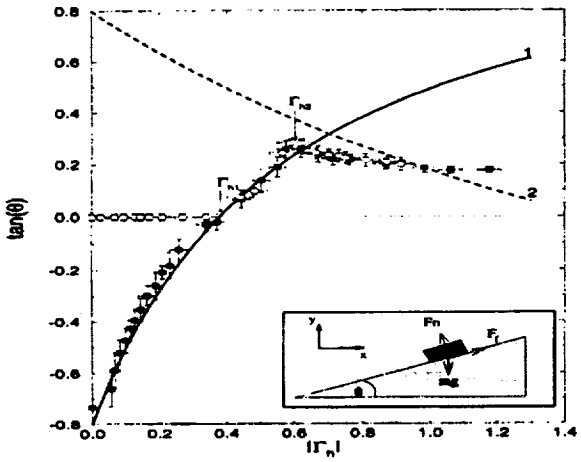

Figure 2: Data for the heap angle vs. Γ_h at fixed Γ_v, showing the onset of spontaneous static heap formation from an initially flat state (open symbols) at Γ_{h1}, and the heap inclination angle starting from the angle of repose (solid symbols).

Slowly Sheared Granular Materials. The final experiment [4] consists of disks, a 2D granular material, that slide on a smooth slippery plane, and that are sheared in an annular geometry. Specifically, the disks can be sheared from an inner rough wheel or by a surrounding rough ring. A key feature in these experiments is the absence of gravity, so that we can independently control the density. The disks are photoelastic, i.e. birefringent in proportion to the local shear deformation of the disks. We view them using a circular polariscope and use a novel technique to relate the photoelastic measurement to the applied force. In addition, each disk is marked with a dark bar so that we can track individual particle positions and orientations using video. From these measurements we deduce particle velocities, V and rotation rates (spins), S. Here, we will focus on the velocity in the axial direction, V_ϕ. In addition, we measure the local packing fraction, Υ, which is effectively the density of disks. Shearing by the inner wheel creates a shear band with an exponential variation of V_ϕ with distance from the wheel. We observe approximate but not perfect rate invariance, and we attribute the small departures from rate invariance to small long time restructuring of the grains well away from the wheel. Distributions for V and S near the wheel show complex structures that indicate a combination of slip and noslip motion at the boundary. A particularly interesting feature of these experiments is the observation of a transition that has some of the hallmarks of a second order phase transition. At a critical packing fraction, $\Upsilon_c \simeq 0.77$, the grains can just sustain shear; at this point the system is highly compressible. Also, there is critical slowing down; for instance the mean speed of the grains vanishes. The distribution of forces changes qualitatively near Υ_c. Well above Υ_c, the distribution is qualitatively like the predictions of the q-model of Coppersmith et al [5]. Time series for the stress and corresponding spectra are similar the these that we found for sheared 3D materials [6]. Nearer the transition, the distribution is qualitatively different. We observe an interesting and apparently smooth change from slip to nonslip behavior as we pass beyond Υ_c. Finally, we define a slip event to be a continuous decrease in the measured stress. Distributions of the size, M of slip events are exponentially distributed well above Υ_c but appear to vary as M-1 close to Υ_c.

Acknowledgments. This work was supported by NASA grant NAG3-1917. We appreciate the hospitality of the P.M.M.H. of the Ecole Superieure de Physique et Chemie Industrielle de Paris, where parts of this work were carried out.

[1] For reviews see H.M. Jaeger, S.R. Nagel and R.P. Behringer, Rev. Mod. Phys. **68**, 1259 (1996); R.P. Behringer and J.T. Jenkins, ed.*Powders and Grains '97*, Balkema, Rotterdam (1997); H.J. Herrmann, S. Luding, and J.P. Hovi, eds.*Dry Granular Media*, NATO ASI series, Kluver, Amsterdam (1998).

[2] S. Tennakoon, L. Kondic, and R.P. Behringer, submitted to Phys. Rev. Lett. (1998).

[3] S. Tennakoon and R.P. Behringer, to appear, Phys. Rev. Lett. (1998).

[4] D. Howell, B. Miller, C. O'Hern, and R.P. Behringer, in *Friction, Arching, Contact Dynamics*, p. 133-148, World Scientific (1997); C.T. Veje,' D.W. Howell, and R.P. Behringer, to be published.

[5] C.-h. Liu et al. *Science* **269**, 513 (1995); S.N. Coppersmith et al. Phys. Rev. E **53**, 4673 (1996).

[6] B. Miller, C. O'Hern, and R.P. Behringer, Phys. Rev. Lett. **77**, 3110 (1996).

MRI MEASUREMENTS AND GRANULAR DYNAMICS SIMULATION OF SEGREGATION OF GRANULAR MIXTURE

M. Nakagawa[1], Jamie L. Moss[1] and Stephen A. Altobelli[2]
[1] Particulate Science and Technology Group, Division of Engineering, Golden. Colorado 80401;
mnakagaw@mines.edu, jmoss@mines.edu,
[2] The New Mexico Resonance, 2425, Ridgecrest Dr. SE, Albuquerque, New Mexico 87108; salto@nmr.org.

ABSTRACT

A counter intuitive axial segregation phenomenon in a rotating horizontal cylinder has recently captured attention of many researchers in different disciplines. There is a growing consensus that the interplay between the particle dynamics and the evolution of the internal structure during the segregation process must be carefully investigated. Magnetic resonance imaging (MRI) has been used to non-invasively obtain much needed dynamic/static information such as velocity and concentration profiles, and it has proven to be capable of depicting the evolution of segregation processes [1-4]. Segregation in a rotating cylinder involves two processes: the first is to transport small particles in the radial direction to form a radial core, and the second is to transform the radial core into axially segregated bands. Percolation and/or "stopping" have been proposed as mechanisms for the radial segregation. As to mechanisms for axial band formation, much less is known.

The difference in the dynamic angle of repose has been proposed to segregate different components in the axial direction. Recently, Hill and Kakalios [3] have reported that particles mix or demix depending upon the competition between diffusion and preferential drift whose order can be determined by the dynamic angle of repose through the adjustment of the rotation rate. We claim that the dynamic angle of repose could be one of the causes, however, it fails to offer reasonable explanations for certain aspects of the axial migration. For example, we always observe that the radial segregation precedes the axial segregation and small particles migrate in the radial direction to form an axially extended radial core. It then transforms into axially segregated bands. By definition, the effects of the dynamic angle of repose are restricted near the free surface where the flowing layer is present. However, during the process of transforming from the radially segregated core to axially segregated bands, small particles located in the deep core region, which is untouched by the flowing layer, also completely disappear. Usually, the dynamics angle of repose are uniquely defined for individual species to characterize particle properties, and the dynamic angle of repose thus defined provides little information for the dynamic angle of repose of the mixture since the concentration ratio and the internal packing structure do not remain the same during the segregation processes.

Under microgravity environment, the dynamics angle of repose argument does not hold since there is simply no flowing layer to influence/determine the preferred directions of segregation. We have thus designed an experiment so that the effects of the dynamic angle of repose can be minimized by filling the cylinder almost completely full. Small particles still formed a radial core and also migrated to form axial bands. As ground based experiments we have designed and conducted both 2D and 3D segregation experiments. The 2D experiments are performed using a thin cylinder (the gap between two end caps is about 5 mm) filled with different combinations of particles. The 3D experiments are conducted with a long cylinder of its length and diameter of 27cm and 7cm, respectively. Results of 2D experiments indicate that different mechanisms govern particle motion in regions near and far from the axis of rotation. Results of 3D experiments indicate that a series of collapses of microstructures of particle packing (micro-collapses) may be responsible for the creation of voids for small particles to migrate through in the axial direction. We have successfully eliminated the dynamic angle of repose as a cause for segregation, however, by almost completely filling the cylinder with the particles, we have lost an opportunity to investigate a possibility of particle "mobility" being a cause for segregation which requires a flowing surface but not the difference in the angle of repose. This is currently being investigated.

REFERENCES

1. Nakagawa, M., Altobelli, S.A., Caprihan, C., Fukushima, E., and Jeong, E.,-K., "Non-invasive measurements of garnular flows by magnertic resonance imaging," Experiments in Fluids, 16, 54-60, 1993.
2. Nakagawa, M., Altobelli, S.A., Caprihan, S., and Fukushima, E., " NMRI study: axial migration of radially segregated core of granular mixtures in a horizontal cylinder," Chem. Eng. Sci., Vol. 52, No.23, 4423, 1997.
3. Hill, K.M. and Kakalios, J., " Reversible axial segregation of binary mixtures of granular materials," Phys. Rev. E., 49, 3610, 1994.
4. Hill, K.M. and Kakalios, J., " Reversible axial segregation of rotating granular media," Phys. Rev. E., 52, 4393, 1995.

Session 4C: Thermocapillary Flows I

SURFACE TENSION DRIVEN CONVECTION EXPERIMENT-2 (STDCE-2)

Y. Kamotani[1], S. Ostrach[2] and J. Masud[3] [1,2,3] Department of Mechanical and Aerospace Engineering
Case Western Reserve University, Cleveland, Ohio 44106

ABSTRACT

Thermocapillary flows are known to become oscillatory (time-periodic), but how and when they become oscillatory in containers of unit-order aspect ratio are not yet fully understood. The present work is a part of our continuous effort to obtain a better understanding of the phenomenon. Thermocapillary flow experiments in normal gravity are limited to a narrow parametric range in order to minimize gravity and buoyancy effects, which is an important reason for our lack of full understanding of the oscillation phenomenon. One important unanswered question is what role, if any, free surface deformation plays in the oscillation mechanism. For that reason we performed thermocapillary flow experiments, called the Surface Tension Driven Convection Experiment-2 (STDCE-2), aboard the USML-2 Spacelab in 1995. The main objectives of the experiments were to investigate oscillatory thermocapillary flows in microgravity and to clarify the importance of free surface deformation in such flows.

Conditions for the onset of oscillations and nature of oscillatory flows were investigated under a variety of test conditions and configurations, including a study of the effect of heating mode, heating rate, surface heat flux distribution, container size and static free surface shape on the oscillations.

Cylindrical test cells of various sizes (1.2, 2.0 and 3.0 cm diameter test cells), each with a nominal aspect ratio of one (radius=depth), were used. Silicone oil with kinematic viscosity of two centistokes was selected for use in STDCE-2. The static free surface shape of the test fluid was a variable in the STDCE-2 test matrix. Each test module contained an oil delivery system, which allowed the oil in the module's test cell to be filled to various levels.

Steady and oscillatory thermocapillary flows were generated by employing two heating modes. A CO_2 laser was used in the Constant Flux (CF) configuration to heat the free surface. In the CF heating mode the laser power level and laser spot size could be varied to study the effects of heat input and surface heat flux distribution on the flow field. The laser heated the fluid surface at powers from 0.2 to 5.0 Watts, in 0.01 Watt increments, with all the energy absorbed within 0.2 mm of the surface. The optics were designed to produce heating zone sizes between 0.6-6 mm at the free surface for both curved and flat surface shapes. The other configuration investigated in STDCE-2 was the Constant Temperature (CT) configuration in which a submerged cylindrical cartridge heater placed at the symmetry (axial) axis of the test container heated the fluid. These cartridge heaters were one-tenth the diameter (1.2, 2.0 and 3.0 mm) of the test chamber and extended the depth of the test cell from the pinning edge plane

The flow field was investigated by flow visualization, and the temperature field was measured by thermistors and an infrared imager. The free surface shape and motion were measured by a Ronchi system.

The important dimensionless parameters for steady thermocapillary flows in the present experimental configuration with a flat free surface are: Marangoni number (Ma), Prandtl number (Pr), aspect ratio (Ar), and heater ratio (Hr). In addition, the relative fluid volume (Vr) is important in the curved surface tests.

Forty two tests were performed in the CF mode. The parametric ranges of those CF tests were: $Ma < 6\times10^4$, Pr = 22-32, and Hr = 0.05, 0.1, and 0.2. 32 tests were conducted with Ar = 1. In the other 10 tests a cylindrical plastic disc was inserted at the bottom of each test chamber to reduce its aspect ratio to 0.5. Ar and Hr in the thirteen CT tests were fixed at 1.0 and 0.1, respectively. The values of Pr and Ma in the CT tests were Pr=26-31 and $Ma \le 1.7\times10^5$.

All the tests were completed successfully and oscillations were found in most of the tests. The observed oscillatory motion in all the tests in STDCE-2 was similar in nature. In the oscillatory flow, the fluid particles moved back and forth in the azimuthal direction with the frequency of oscillations as they circulated in the flow cell. In a fixed radial plane, the flow was observed to go through periods of strong and weak motion during one oscillatory cycle.

In the CT tests the onset of oscillatory flow is signified by a critical temperature difference (ΔT_{cr}). For the test containers with diameter around 1.2 cm, the onset of oscillations in 1-g and microgravity occurred at a similar ΔT_{cr}. For the test containers with 1.2 cm diameter, in addition to the similarity in the observed oscillatory flow field, the oscillation frequency and the IR image of the free surface were also similar in the 1-g and microgravity tests. Therefore, one can conclude that the onset of oscillations in test containers with diameter smaller than 1.2 cm is not affected by buoyancy in normal gravity.

If the free surface is assumed to be nondeformable, then the conditions of the experiment are determined by Pr, Ar, Hr and Ma. In the present experiments Ar

and Hr are fixed and Pr is nearly constant in all the tests, therefore, the only variable parameter is Ma. Consequently, the onset of oscillations should be characterized by a critical Marangoni number (Ma_{cr}). However, it is shown that for different tests with similar Pr, Ar and Hr, the value of Ma_{cr} changes almost fourfold over the range of the experiments. This shows that Ma_{cr} is not a sufficient parameter to characterize the onset of oscillations in the CT configuration.

It is clear then that some other factor needs to be included in the analysis. Since buoyancy and heat loss from the free surface are insignificant, the only important factor is the deformability of the free surface. Our extensive experimental and theoretical work on the oscillation phenomenon in the past has shown that the additional aspect is free surface deformation. Our physical model of oscillations is summarized as follows. It is convenient to divide the flow field into two: surface flow along the free surface toward the cold wall and return flow in the interior toward the heated region. The surface flow is driven by thermocapillarity and the return flow is due to the pressure field caused by the surface flow. Consider a transient situation where the surface flow is somewhat changed for some reason. The return flow does not respond to that change immediately, because the surface flow must deform the free surface shape first to modify the pressure field. Such a small delay could cause a large change in the flow field, if the free surface deformation alters the thermal boundary layer thickness along the free surface significantly.

Based on the model, the amount of transient free surface deformation relative to the thermal boundary layer thickness in the hot corner (the region next to the heater where the surface temperature gradient is large), called S-parameter, is derived by scaling analysis. According to our oscillation model, the oscillation process could start when the S-parameter becomes larger than a certain finite number. It is shown that all the data can be correlated well by S: the flow becomes oscillatory when S is larger than about 15. The oscillation period is shown to scale with the time of convection along the heater surface.

Similarly, the STDCE-2 data and our ground-based data with small containers show that a critical Maragoni number does not exist in the CF tests: Ma_{cr} increases with increasing container diameter. A surface deformation parameter (S-parameter) is then introduced, which represents the thickness of thermal boundary layer relative to free surface deformation as in the CT configuration. It is shown that the S-parameter correlates all the data well: the flow becomes oscillatory when S is larger than about 70. The oscillation period scales with the overall time of convection.

The main conclusion from the STDCE-2 tests is that the Marangoni number cannot specify the onset of oscillations in both CT and CF configurations but the S-parameter, which represents the ratio of free surface deformation to thermal boundary layer thickness, can specify the onset in both configurations.

THERMALLY-DRIVEN INTERFACIAL FLOW IN MULTILAYERED FLUID STRUCTURES

H. Haj-Hariri[1], [1]Mechanical and Aerospace Enginering, University of Virginia, Charlottesville VA 22903, USA, hh2b@virginia.edu, A. Borhan[2], [2]Chemical Engineering, The Pennsylvania State University, University Park PA 16801, borhan@psu.edu

Abstract

Thermocapillary flows are of considerable technological importance in materials processing applications such as crystal growth from the melt, particularly under microgravity conditions where the influence of buoyancy is minimized. The structure and stability of thermocapillary convection has been a subject of active research during the past decade in an effort to better understand, and eventually control, thermally-induced motions in the melt and optimize the quality of the resulting product. In this study, thermally-driven convection within a differentially-heated rectangular box containing two immiscible liquid layers is considered in the absence of gravity. The effects of fluid-fluid interface deformations on the structure of the basic flow state in these systems is examined. Such deformations are shown to be small when the contact line of the interface is pinned on the solid boundaries.

Results comparing two-layer thermocapillary flow with a single-layer one are presented and discussed. These results clearly confirm previous observations of a reduction in the intensity of the thermocapillary flow upon the introduction of a more viscous 'encapsulant' layer. The higher viscosity of the encapsulant layer gives rise to a higher pressure gradient in that layer in order to satisfy the no-net flux condition through cross sections. This pressure distribution causes the surface deformation to have the reverse sense to what it would be in the absence of the encapsulant layer: the interface will bulge out of the encapsulated layer near the low-surface-tension boundary and depress into the layer near the high-surface tension boundary; the free surface of an unencapsulated layer does the opposite.

Finally, it is shown that the flow within the encapsulated layer may be closely approximated by simply considering the single-layer problem, but with a *modified* shear-stress condition even for non-small aspect ratios.

STUDIES IN THERMOCAPILLARY CONVECTION OF THE MARANGONI-BENARD TYPE

R.E. Kelly[1] and A.C. Or[1]

[1]Mechanical & Aerospace Enginering, University of California, Los Angeles, CA 90095-1597, USA, rekelly@seas.ucla.edu

A nonlinear feedback control strategy for delaying the onset and eliminating the subcritical nature of long-wavelength Marangoni-Bénard convection is investigated based on an evolution equation. A control temperature is applied to the lower wall in a gas-liquid layer otherwise heated uniformly from below. It is shown that, if the interface deflection is assumed to be known via sensing as a function of both horizontal coordinates and time, a control temperature with a cubic-order polynomial dependence on the deflection is capable of delaying the onset as well as eliminating the subcritical instability altogether, at least on the basis of a weakly nonlinear analysis. The control coefficients required for stabilization are $O(1)$ for both delaying onset indefinitely and eliminating subcritical instability.

Thermocapillary Convection in a low-Pr Material under Simulated Reduced Gravity

Mingtao Cheng and Sindo Kou
Department of Materials Science and Engineering
University of Wisconsin
Madison, WI 53706

Abstract

A liquid bridge of molten Si (Pr = 0.027) was established by having the bottom of a Si rod in contact with the top of a resistance heated BN rod, both rods being 13 mm in diameter. The height of the liquid bridge was 10 mm and the temperature difference was 50 °C, corresponding to a high Marangoni number of 6200. Temperature oscillations were detected on the free surface with an optical pyrometer. Oscillation about 0.07 Hz in frequency and 4 °C in amplitude was observed. The rapid response of the optical pyrometer helped revealed the faster and weaker waves superimposed on the oscillation, e.g., about 1.5 Hz and 1.5 °C, and 10 Hz and 0.5 °C.

Exposition

PHASE DIAGRAMS OF ELECTRIC-FIELD-INDUCED AGGREGATION IN CONDUCTING COLLOIDS.

B. Khusid[1] and A. Acrivos[2], The Levich Institute, City College of the City University of New York, Steinman Hall T-1M, 140th Street and Convent Avenue, New York, NY 10031,
[1]boris@levdec.engr.ccny.cuny.edu, [2]acrivos@scisun.sci.ccny.cuny.edu.

1. INTRODUCTION

Under the application of a sufficiently strong electric field, a suspension may undergo reversible phase transitions from a homogeneous random arrangement of particles into a variety of ordered aggregation patterns. The surprising fact about electric-field driven phase transitions is that the aggregation patterns, that are observed in very diverse systems of colloids, display a number of common structural features and modes of evolution thereby implying that a universal mechanism may exist to account for these phenomena. It is now generally believed that this mechanism emanates from the presence of the long-range anisotropic interactions between colloidal particles due to their polarization in an applied field. But, in spite of numerous applications of the electric-field-driven phenomena in biotechnology, separation, materials engineering, chemical analysis, etc. our understanding of these phenomena is far from complete. Thus, it is the purpose of the proposed research to develop a theory and then test experimentally, under normal- and low-gravity conditions, the accuracy of the theoretical predictions regarding the effect of the synergism of the interparticle electric and hydrodynamic interactions on the phase diagram of a suspension.

The main results from our theoretical studies performed to-date enable one to trace how the variations of the electrical properties of the constituent materials influence the topology of the suspension phase diagram "the particle concentration-the electric field strength" and then, by using an appropriate phase diagram, to evaluate how the electric-field-induced transformations will depend on the frequency and the strength of the applied field.

2. ELECTRIC-FIELD-INDUCED PHASE TRANSITIONS

The first step in the development of a theory for the electric-field-induced phase transitions in a suspension of electrically uncharged conducting particles dispersed in a conducting fluid was taken in Ref. [1]. The main difficulty which was encountered in constructing a theory of electric-field-induced phase transitions was that, for materials such as conducting suspensions whose complex dielectric permittivity $\varepsilon_s^* = \varepsilon_s' - i\varepsilon_s''$ varies strongly with the frequency of an applied electric field, it is not possible to construct an expression for the electric energy using macroscopic electrodynamics [2]. The reason for this difficulty is that the frequency dependence of the dielectric permittivity implies that such a material contains mobile charges and electric dipoles capable of orientation, so that the stored electric energy will depend on the time-history of how the electric field was established [2]. To be sure, an expression for the electric energy of a conducting material, namely, Brillouin's formula, can be derived from macroscopic electrodynamics, but only when the energy dissipation in this material is negligibly small and the time-variations of the applied electric field are very slow compared to the rate of relaxation phenomena.

To overcome the limitations of Brillouin's formula, we developed [1] a microscopic theory for the electric energy W as a function of the concentration c of conducting spheres dispersed in a conducting fluid when the particles were arranged randomly and provided that the particles and the suspending fluid can be described by the model of a leaky dielectric. This model corresponds to the classical mechanism of the so-called Maxwell-Wagner interfacial polarization typical of colloids [3].

The main objective of the present work is to extend our previous studies [1] beyond the dilute regime and to develop a microscopic theory for phase diagrams of concentrated conducting suspensions subject to strong dc and ac electric fields.

3. CLASSIFICATION SCHEME OF DC- AND AC-FIELD PHASE DIAGRAMS

The topology of the suspension phase diagram is determined by the sign and the magnitude of $\partial^2 W/\partial c^2$ which characterizes the contribution of the electric-field-induced long-range interparticle interactions to the suspension free energy. A thorough analysis of the associated equations for the spinodal and coexistence curves yields a complete set of phase diagrams as a function of the mismatch of the dielectric constants and of the conductivities of the particles to those of the fluid as well as of the frequency and the strength of the applied field.

For the case when $\partial^2 W/\partial c^2 > 0$ over the entire concentration range, increasing the strength of an electric field applied to this suspension will eventually

cause electric-field-induced transition. Thus, the phase diagram of such a suspension consists of the low-field one-phase region which includes the random spatial arrangement of the particles in the absence of an electric field and the high-field two-phase region corresponding to the appearance of aggregates caused by the action of an applied field. This phase diagram appears to be similar to the phase diagram concentration vs. temperature of a binary fluid or a binary alloy with a miscibility gap [4], so that these species exist in solution at high temperature but their mixture eventually separates into coexisting phases below the critical point of miscibility. In this regard, the application of an electric field to a conducting suspension is equivalent to a quench of an atomic system from its high-temperature one-phase state. Although such a similarity between the structural ordering in colloids and the structural behavior in conventional atomic systems- gas, liquid, crystal, and glasses- under suitable conditions has already been well recorded [3, 5], electric-field driven phase transitions in colloids have not been treated from this point of view thus far.

On the other hand, if $\partial^2 W/\partial c^2 < 0$ over the entire concentration range, the random arrangement of the particles appears to be stable, so that the phase diagram of such a suspension reduces to the one-phase domain. We found that the sign of $\partial^2 W/\partial c^2$ may become negative for dc and relatively low-frequency ac fields depending on the particle-to-fluid ratios of the conductivities and of the dielectric constants. A peculiarity of concentrated suspensions is that the sign of $\partial^2 W/\partial c^2$ may change at some value of the concentration. As a result of this feature, the ability or inabilty of the particles to aggregate in the presence of applied electric fields depends on the particle concentration as well.

We also showed, however, that the sign of $\partial^2 W/\partial c^2$ always becomes positive when the frequency of the applied ac field becomes sufficiently high. Hence it follows that there always exists a threshold value of the frequency, above which the particles having a dielectric constant different from that of the suspending fluid (regardless of the mismatch of their conductivities) will aggregate as the strength of an applied electric field becomes sufficiently large.

As in the case of conventional atomic systems [4], the use of a phase diagram provides a convenient way to distinguish "metastable" and "unstable" states of a suspension subject to an electric field, where we refer to the domain between the coexistence curve and the spinodal curve in its phase diagram as metastable, and the domain beyond the spinodal line as unstable. The free energy of a suspension, being considered as a function of the particle concentration, is convex in the metastable region of the phase diagram "the particle concentration-the electric field strength", so that the free energy will increase with a spontaneous concentration fluctuation, giving rise to an energetic barrier that will stabilize the suspension. The free energy, however, turns into a concave function of the particle concentration in the unstable region of the phase diagram, so that no energetic barrier to phase separation will exist in this state. This distinction can correspond to two different mechanisms of electric-field-induced transformations in a suspension: spinodal decomposition and nucleation, as occurs in atomic systems. For atomic systems, the former (in the unstable domain) corresponds to the growth of long-wavelength spontaneous concentration fluctuations with time whereas the nucleation of microdomains of the other phase starts the transformation for the latter (in the metastable domain).

In any event, we can expect that there exists some similarity between how spinodal and nucleation transformations operate in a suspension subject to an electric field and how they operate in quenched atomic systems, even though the electric-field-induced interparticle interactions are anisotropic. In this connection, a complete set of phase diagrams of suspensions, which we have constructed, can predict how the topology of the suspension phase diagram depends on the particle and fluid dielectric constants and conductivities and on the frequency of applied field.

4. ACKNOWLEDGEMENT

This work was supported in part by grants from NASA (NCC3-607) and the NSF (CTS-9318820).

5. REFERENCES

1. B. Khusid and A. Acrivos, Phys. Rev. E, **52**, 1669 (1995); **54**, 5428 (1996)
2. L.D. Landau, L.P. Lifshitz, and L.P. Pitaevskii, *Electrodynamics of Continuous Media*, (Pergamon Press Oxford, 1984); L. Brillouin, *Wave Propagation and Group Velocity*, (Academic Press, New York 1960)
3. W.B. Russel, D.A. Saville, and W.R. Schowalter, *Colloidal Dispersions*, (Cambridge University Press, Cambridge, 1989)
4. L.D. Landau and L.P. Lifshitz, *Statistical Physics, Pt. 1* (Pergamon Press Oxford, 1980)
5. A. K. Sood, in *Solid State Physics*, v.45, edited by H. Ehrenreich and D. Turnbull, pp. 2-73 (Academic Press, San Diego, CA, 1991)

Ultrasound Thermal Field Imaging of Opaque Fluids[1]

C. David Andereck, Department of Physics, The Ohio State University, 174 W. 18th Ave., Columbus, OH 43210
E-mail: andereck@mps.ohio-state.edu.

ABSTRACT

We have initiated an experimental program to develop an ultrasound system for non-intrusively imaging the thermal field in opaque fluids under an externally imposed temperature gradient. Many industrial processes involve opaque fluids, such as molten metals, semiconductors, and polymers, often in situations in which thermal gradients are important. For example, one may wish to understand semiconductor crystal growth dynamics in a Bridgman apparatus. Destructive testing of the crystal after the process is completed gives only indirect information about the fluid dynamics of the formation process. Knowledge of the coupled thermal and velocity fields during the growth process is then essential.

Most techniques for non-intrusive velocity and temperature measurement in fluids are optical in nature, and hence the fluids studied must be transparent. In some cases (for example, LDV (laser Doppler velocimetry) and PIV (particle imaging velocimetry)) the velocities of small neutrally buoyant seed particles suspended in the fluid, are measured. Without particle seeding one can use the variation of the index of refraction of the fluid with temperature to visualize, through interferometric, Schlieren or shadowgraph techniques, the thermal field. The thermal field in turn gives a picture of the pattern existing in the fluid. If the object of study is opaque, non-optical techniques must be used. In this project we focus on the use of ultrasound, which propagates easily through opaque liquids and solids. To date ultrasound measurements have almost exclusively relied on the detection of sound scattered from density discontinuities inside the opaque material of interest. In most cases it has been used to visualize structural properties, but more recently the ultrasound Doppler velocimeter has become available. As in the optical case, it relies on seed particles that scatter Doppler shifted sound back to the detector. Doppler ultrasound techniques are, however, not useful for studying convective fluid flow in crystal growth, because particle seeding is unacceptable and flow velocities are typically too low to be resolved, and may be even lower in microgravity conditions where buoyancy forces are negligible.

We will investigate a different use of ultrasound to probe the flows of opaque fluids non-intrusively and without the use of seed particles: our goal is to ultrasonically visualize the thermal field of opaque fluids with relatively high spatial resolution. The proposed technique relies upon the variation of sound speed with temperature of the fluid. A high frequency ultrasound pulse passing through a fluid-filled chamber will traverse the chamber in a time determined by the relevant chamber dimension and the temperature of the fluid through which the pulse passes. With high time-resolution instrumentation that compares the excitation signal with the received pulse we can detect the influence of the fluid temperature on the pulse travel time. This is effectively an interferometric system, which in its optical form is an extremely sensitive approach to measuring thermal fields in fluids. Moreover, the temperature dependence of sound velocity in liquid metals is comparable to the temperature dependence of the speed of light required for accurate interferometric thermal images in transparent fluids. With an array of transducers scanned electronically a map of the thermal field over the chamber could be produced. An alternative approach would be to use the ultrasound analog of the shadowgraph technique. In the optical version, collimated light passes through the fluid, where it is focused or defocused locally by temperature field induced variations of the index of refraction. The resulting image reveals the thermal field through the spatial pattern of light intensity variations. By analogy, an ultrasound plane wave traversing an opaque fluid sample would be also locally focused or defocused depending on the speed of sound variations, giving rise to spatial variations in sound intensity that will reveal the thermal field pattern.

These approaches could be applied to any situation in which temperature differences are expected to occur, and will rapidly provide information about the flow that simply cannot be obtained by any current intrusive or non-intrusive diagnostic technique. As materials processing in microgravity matures it will become increasingly important to have available simple and versatile diagnostic tools, such as we will develop, for studying the flows of opaque fluids under thermal forcing.

[1] Work supported by NASA Grant NAG3-2138.

A NOVEL ACOUSTO-ELECTRIC LEVITATOR FOR STUDIES OF DROP AND PARTICLE CLUSTERS AND ARRAYS

Robert E. Apfel, Yibing Zheng, and Yuren Tian, Department of Mechanical Engineering, Yale University, New Haven, CT 0511, robert.apfel@yale.edu

ABSTRACT

A novel and compact instrumentation for studying the behavior of drop sprays and of clusters of drops now permits fundamental research into the behavior of reacting and non-reacting fluid and solid species. The new capability is made possible by simultaneous acousto-electric levitation and charging of "seed" droplets (10-30 μm in diameter) which come together in 2-D clusters (with up to 300 droplets). These clusters are interesting in their own right because of their crystalline and quasi-crystalline forms, which depend on the acoustic and electric field parameters. By varying the electric and acoustic field intensities, one can cause a cluster of droplets to condense into larger drops (e.g. 50-300 μm) which, because of their charge, form uniformly spaced 2-D arrays of monodispersed drops (e.g. 30-40 array drops in preliminary experiments). One or more layers of these 2-D arrays can form in the acoustic standing wave. Such a configuration permits a wide range of fundamental studies of drop evaporation, combustion, and nucleation. The drops can be single or multicomponent. Therefore, fundamental materials studies can also be performed. Using this same Cluster and Array Generation (CAG) instrumentation, it has been also possible in preliminary experiments to demonstrate the clustering and arraying of solid particles, both coated with an electrically conducting layer and uncoated, and both charged and uncharged.

Fluid Physics of Foam Evolution and Flow

H. Aref[1], S. T. Thoroddsen[1], [1]Dept. of Theoretical and Applied Mechanics, University of Illinois, Urbana, IL 61801,
J. M. Sullivan[2], [2]Dept. of Mathematics, University of Illinois, Urbana, IL 61801

When the influence of gravity on fluid behavior is diminished or removed, other forces, such as capillary forces, can assume paramount roles. We are particularly interested in the physics of foams under low-gravity conditions. A foam may be thought of as a two-phase substance that has many of the attributes of a fluid but carries relatively little liquid per unit volume. The consistency of a foam, its ability to transport a large amount of gas, and the elastic and acoustic damping properties of foams are all useful in applications. Due to the dominance of capillary forces, foams may also be extremely useful in low-gravity environments. The mechanical properties of foams and related cellular materials are known to be quite versatile and interesting, and since they are generally very light-weight, one can expect considerable use of them in space technology, including low-gravity environments.

In our work we will pursue the topic of foam evolution and flow through a series of numerical and laboratory experiments. In the numerical experiments a zero-gravity assumption is typically made. In an Earth-based laboratory one must deal with the issues of film drainage due to gravitational forces on the fluid in the bubble interfaces, and the relative magnitudes of gravitational forces to capillary forces. Our objectives are to identify interesting phenomena and mechanisms using this hybrid form of numerical/physical experimentation, and to refine and automate the experimental component with a view to implementation in a zero-gravity environment in the future. We are particularly interested in phenomena that are masked by gravitational effects.

The research builds on a body of work conducted some years ago by Aref and then graduate student Thomas Herdtle on two-dimensional foams, where in the dry foam limit there exists a very elegant algorithm for following foam evolution. On the numerical side the main thrust of the proposed research is to extend this earlier work to more complex foam flow situations, and to establish the numerical technology to explore three-dimensional foams at the same level of detail as is possible today for two-dimensional foams. The Surface Evolver package of Brakke provides a promising start on the 3D problem, but it may include too much geometrical detail to be useful in applications involving a large number of interacting bubbles. Sullivan, who is an expert on computational geometry and the Surface Evolver package, will apply this software to situations involving foam flow, and to situations where real gas effects are included in the internal state description of the bubbles.

Foam experiments, to be conducted and supervised by Thoroddsen, constitute a significant part of the work. The 3D structure and evolution of the foam will be studied using optical methods. A new video technique is being developed and optimized with eventual experiments in a zero-gravity environment in mind.

Preliminary experiments have shown that the 3D cell structure can be constructed from a set of video frames. For this work we use a small plexyglass container (about 3cm on a side) and use two regular CCD video-cameras, which are arranged at a 90-degree angle to each other. These cameras are equipped with narrow-focus lenses, which effectively look at a planar slice through the foam, each slice being about 2mm in depth.

The use of two cameras is mandated by the following considerations: First, due to the finite depth of focus of the lenses the exact depth of each node can not be determined using only one camera. Secondly, there is often an unavoidable overlap of nodes, which can lead to errors in node identification and connectiveness.

Manual micro-meter stages are currently used to accurately traverse the cameras with respect to the container, thus moving the focal plane into the foam. This imaging only works for rather dry foam. Using appropriate lighting, one can look at least 2cm into the foam. This corresponds to about 6 layers of foam cells. By observing the foam from both sides of the container one can therefore study foam up to twelve cells deep. Typical video frames from the two cameras are shown on our poster display.

Only the *Plateau* borders in focus show up as narrow lines. The various borders show up differently in the image, depending on their orientation with respect to the illuminating light. They can appear as either dark or light lines or a combination thereof. The most challenging aspect of reconstructing the 3D topology from these video images is constructing efficient computer algorithms for the image processing neccessary to identify the nodes and determine their interconnectedness. These programs are currently being constructed. They take advantage of the known geometry of the nodes. These rules were first postulated by Joseph Plateau in 1873 and state that four Plateau borders meet at each node and the angle between any two are the same about 109^o. As a proof of concept we have reconstructed manually, from 12 such video images, some of the Plateau borders and their connections. The reconstruction is not complete, as the perpendicular view has not been used to find connections hidden from this view.

Current experiments have dealt with a static or almost

static foam. As the research progresses we will improve our algorithms for reconstructing the foam geometry and topology from the images, and introduce new techniques for studying a dynamically evolving foam. The development of rapid detection and reconstruction algorithms, and the automation of all phases of the experiment, are crucial to the development of an experiment that can fly in space.

Foam dynamics may be expected to play a role in the manipulation of fluids in space (as it does on Earth), in materials processing of various kinds, and in applications such as bioreactors where it is desirable to have a large surface to volume ratio. Foams are used extensively in the food industry.

Apart from engineering applications, foams have played an important scientific role in communities where one might not have expected to see them at all. The role of soap films as models of the mathematics of minimal surfaces is well known. Detailed explorations of the topology and structure of foams have been carried out by botanists due to the obvious morphological similarities between foams and the cellular materials that pervade biology. Metallurgists and condensed matter physicists have been interested in the similarities between foams and the structure of polycrystalline materials. Foams seem to contain many of the scientific foci that have emerged in NASA's microgravity program, including examples of phase transitions. Our research is being conducted with an eye to this broader paradigm of scientific inquiry provided by foams.

Suggestions for further reading:

Almgren, F. J. & Taylor, J. E., 1976, "The geometry of soap films and soap bubbles", *Scient. Amer.* **235**(1), 82–93.

Durian, D. J., Weitz, D. A. & Pine, D. J., 1991, "Multiple light-scattering probes of foam structure dynamics", *Science* **252**, 686–688.

Gibson, L. J. & Ashby, M. F., 1988, *Cellular Solids — Structure & Properties*, Pergamon Press.

Herdtle, T. & Aref, H., 1992, "Numerical experiments on two-dimensional foam", *J. Fluid Mech.* **241**, 233–260.

Kraynik, A. M., 1988, "Foam flows", *Ann. Rev. Fluid Mech.* **20**, 325–357.

Smith, C. S., 1954, "The shape of things", *Scient. Amer.* **190**(1), 58–64.

Sullivan, J., 1991, "Generating and rendering four-dimensional polytopes", *Mathematica J.* **1**(3), 76.

Sullivan, J., 1998, "The Geometry of Bubbles and Foams", in *Foams, Emulsions, and Cellular Materials*, Kluwer (NATO ASI), to appear.

Weaire, D. & Rivier, N., 1984, "Soap, cells and statistics — Random patterns in two dimensions", *Contemp. Phys.* **25**, 59–99.

INERTIAL EFFECTS IN SUSPENSION DYNAMICS

J. F. Brady, Division of Chemistry and Chemical Engineering, 210-41, California Institute of Technology, Pasadena, CA 91125, USA, jfbrady@caltech.edu

Fluid-solid particle mixtures are encountered in a number of natural and man-made settings, ranging from sediment transport in coastal estuaries to the coating of photographic emulsions. Transporting and processing these multiphase materials requires a knowledge of their response to pressure and shearing forces, that is, their rheological constitutive behavior. The constitutive behavior of small sub-micron-sized particle suspensions is relatively well understood. In these colloidal dispersions, inertial effects are unimportant and viscous hydrodynamic and thermal forces compete to set the microstructure and determine properties. Macroscopic stresses scale viscously ($\eta\dot{\gamma}$) and depend on the volume fraction of solids and the relative importance of hydrodynamic and thermal forces, known as the Peclet number.

At the other extreme is a system of very large particles suspended in air (or vacuum). Here, the suspending fluid plays little role in the dynamics, and in these dry granular flows direct particle collisions transport momentum as in a dense gas. Stresses now scale inertially as the particle density times the particle velocity fluctuation squared ($\rho_p u'u'$). Granular flows differ from those of a molecular gas in that the particle collisions dissipate energy, and thus the rate of doing work by the flow directly influences the structure and the rheological response. This coupling is understood and has been modeled to give a reasonably successful picture of the rapid flow of granular materials.

Between these two extremes of small and large particles, dimensional arguments show that, in addition to the volume fraction, the stress depends on the Reynolds, $Re = \rho\dot{\gamma}a^2/\eta$, and Stokes, $St = \rho_p\dot{\gamma}a^2/\eta$, numbers. When the Reynolds and Stokes numbers are small, the stress reduces to the 'Stokesian' regime, and when the fluid is not important at all ($Re, St \to \infty$) we have dry granular flow. Apart from these limits, little is known fundamentally about the rheological behavior of these materials, despite the fact that many suspension flows fall in this regime, *eg.* fluidized beds, slurry transport, etc.

The proposed work is to investigate the role of inertia on constitutive behavior. In fluid-particle flows, both the fluid (Re) and particle (St) inertia need to be investigated and modeled. Ideally, one would like to vary separately the effects of fluid and particle inertia -- that is, vary separately Re and St -- in order to fundamentally understand the origin of the rheological response. On Earth, these two effects cannot be studied separately, however, because varying the particle to fluid density ratio results in sedimentation (or flotation), which introduces an additional parameter and alters the suspension structure and thus its rheology; only their combined effect can be studied and this limits our understanding of and ability to model fluid-particle flows. In microgravity, however, the role of particle inertia alone can be studied in rheological experiments at finite Stokes number and low Reynolds number by using particles that are much denser than the fluid. Parallel experiments on Earth with density matched particles and fluid can then be compared with the microgravity experiments to understand how fluid inertia alters the response. In this way, a more complete understanding of fluid-particle behavior can be achieved and constitutive equations capable of modeling fluid-particle flows under a wide range of conditions can be developed.

In this work the effect of finite Stokes number will be studied numerically by extending the Stokesian Dynamics simulation method to include particle inertia, thus covering the range $Re \ll 1$ for arbitrary St. Sangani *et al* (1996) have shown that the limit $Re \ll 1, St \gg 1$ connects nicely to that for granular flows, and we wish to consider all St and connect with the known behavior for $St \ll 1$.

MARANGONI EFFECTS ON NEAR-BUBBLE TRANSPORT DURING BOILING OF BINARY MIXTURES

Van P. Carey, Mechanical Engineering Department, University of California at Berkeley,
6123 Etcheverry Hall, Berkeley, CA 94720, vcarey@,me.berkeley.edu

ABSTRACT

Results of our recently-completed reduced gravity experimental studies indicate that Marangoni effects in some systems tend to draw liquid toward the surface during binary mixture boiling, resisting the tendency to create a blanketing vapor film over the heated surface. These experiments demonstrated that Marangoni effects can sustain nucleate boiling at reduced gravity (< O.Olg) in some systems, resulting in heat transfer coefficients that are virtually the same as those observed for the same conditions at lg. They also demonstrated that the resulting pool boiling critical heat flux condition was only slightly lower than that observed at 1 g for the same conditions. The results clearly indicate that Marangoni effects in these systems are at least equal in importance to gravity buoyancy under lg conditions, and they are the dominant mechanism at reduced gravity. These results suggest that it is possible to achieve enhanced boiling heat transfer and high critical heat flux even under reduced gravity conditions by properly selecting a binary mixture working fluid.

Work under this project will experimentally obtain more detailed information on how Marangoni forces affect microscale transport near bubbles growing at the heated surface during binary mixture boiling. To accomplish this objective, novel experiments will be conducted which will generate a stable bubble in a temperature gradient near the heated surface. The temperature field created in the liquid around the bubble will result in vaporization over the portion of its interface near the heated surface and condensation over portions of its interface away from the heated surface. This type of simultaneous vaporization and condensation scenario is characteristic of bubbles during boiling of binary mixtures. In the experiments we propose to document the shape of the bubble and the density field in the adjacent liquid by using schlieren and/or interferometer optical methods. We will simultaneously determine the surface temperature and heat flow transported by the bubble. A computational model of the microscale transport in the liquid near the bubble will be developed concurrently. The experimental data will be compared with the computational predictions of the temperature and concentration fields near the bubble and the overall transport. The proposed experiments will span conditions ranging from those that help move liquid toward the heated surface to those that tend to move liquid away from the heated surface. The proposed studies will be done using a modified version of the experimental system fabricated for our recently-completed study of Marangoni effects. By conducting the experiments under low gravity conditions, we will be able to directly observe the effect of the Marangoni forces on transport without the presence of buoyancy which tends to obscure the effects of these forces. These investigations will provide information vital to the more effective use of binary mixture working fluids in a variety of applications, including terrestrial heat pump systems, power cycles or spacecraft thermal control.

DYNAMICS OF DUST IN PHOTOELECTRON LAYERS NEAR SURFACES IN SPACE

J. E. Colwell[1], M. Horanyi[1], A. Sickafoose[1], [1]Laboratory for Atmospheric and Space Physics, University of Colorado, Boulder CO 80309-0392, USA, josh.colwell@lasp.colorado.edu, S. Robertson[2], [2]Department of Physics, University of Colorado, Boulder, CO 80309-0390, USA, R. Walch[3], [3]University of Northern Colorado, Greeley CO 80639, USA.

Electric fields are generated over a sunlit surface in space by the emission of photoelectrons. Small grains in the regolith of the surface acquire a charge and the Lorentz force can overcome gravity and surface adhesive forces to levitate these grains above the surface. This process may explain the lunar horizon glow observed by the Surveyor spacecraft (Figure 1, Rennilson and Criswell 1974), scattered light observed by Apollo astronauts, and more recently by the Clementine spacecraft (Zook et al. 1995). The levitation and near-surface dynamics of this dust has important implications for future manned and unmanned activity on the surfaces of solar system objects with low surface gravities, such as the Moon, the moons of Mars, the asteroids, and comets. Horizontal and vertical transport of dust in the photoelectron sheath could lead to contamination of landed instruments.

Figure 1. Surveyor image showing levitated layer of dust above the western lunar horizon shortly after sunset.

The space charge generated above a planetary surface by the emission of photoelectrons is called the photoelectron layer, or sheath, and has typical dimensions of tens of centimeters at 1 AU. Closer to the Sun the sheath is thicker due to the greater solar ultraviolet flux on the surface. In the asteroid belt, the sheath may be correspondingly thinner. In the initial phase of this program, we will modify an existing plasma chamber to perform ground-based experiments on dust dynamics in a photoelectron layer. We will study the plasma parameters in the photoelectron layer as a function of illumination geometry, surface material, and surface roughness, using terrestrial mineral analogs for lunar, asteroidal, and cometary surface materials.

Near the terminator of a rough surface, some regions are illuminated by solar UV radiation while neighboring regions are still in shadow. This can lead to strong horizontal electric fields capable of dust transport in addition to the vertical field which is present over the entire sunlit hemisphere. We will study the conditions under which surface dust, or regolith, can be mobilized by electrostatic forces, and the dynamics of that mobilized dust. We will vary the particle size distribution in the simulated regolith, the dust composition, and we will apply external forces to the surface to simulate natural and artificial activity on the planetary body, such as meteorite impacts and spacecraft or human activity.

As a first step, we have modified a small plasma chamber to accept ultraviolet photons from a 1000 Watt Mercury Xenon arc lamp through a quartz window. The lamp will illuminate metals with known work functions and photoelectric yields. A Langmuir probe will be used to verify the properties of the emitted photoelectron sheath. Then, dust particles will be dropped through this photoelectron layer at various distances from the illuminated plate. The charge on the dust particles will be measured as they fall into a Faraday cup. In this way the dust particles will act as a probe of the photoelectron layer, and we will determine the charging properties of various sizes and compositions of dust grains in a photoelectron layer. We will also measure the photoelectron current from individual grains by removing the photoelectron emitting plate and measuring the charge on grains as they fall through the ultraviolet beam.

The ground-based studies will provide a comprehensive database of experimental results which will enable us to define the appropriate experimental configuration and parameters for a future microgravity experiment. At the present time, there are too many unknowns to warrant running the experiment in a microgravity environment. Our ground-based experiment and associated theoretical studies will indicate the appropriate illumination and plasma conditions, dust properties, and external perturbations, if any, for subsequent microgravity experiments. Figures 2 and 3 illustrate one-dimensional test particle simulations of dust in the photoelectron layer at Mercury. The dust is stably levitated at an altitude of about 3 m above the surface. The laboratory work will be guided by contemporaneous theoretical modeling of the dynamics of dust in photoelectron layers.

Figure 2. Simulation of dust launched from the surface of Mercury stably levitated in the photoelectron sheath. The grain has a radius of 0.1 micrometers and was launched with an upward velocity of 200 cm/s.

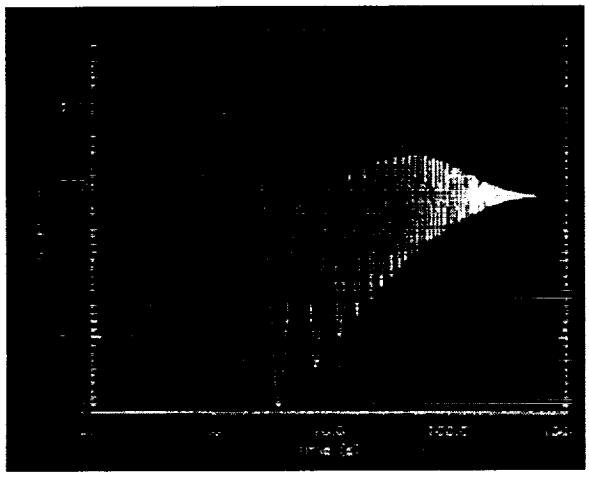

Figure 3. Simulation of dust launched from the surface of Mercury stably levitated in the photoelectron sheath. The grain has a radius of 0.1 micrometers and was launched with an upward velocity of 500 cm/s.

Subsequent laboratory work will use a larger plasma device with a horizontal photo-emitting surface coated with dust. The material properties of the surface and dust will be adjusted to investigate the effects of different photoelectron yields on the sheath and dust dynamics. Shadowing elements will be used to simulate the terminator region on asteroids or the Moon. We will carry out systematic measurements of a dusty surface using the dusty plasma device and vary the following parameters: (1) dust composition, (2) dust size distribution, (3) ultraviolet radiation field, including time-dependent illumination to simulate terminator passage, and small-scale surface roughness to produce shadowing, and (4) ambient plasma properties (ion mass, thermal velocity, density). The surface roughness will be created using simple geometrical forms to allow repetition of the experiment and simulation of the experimental conditions with numerical models. This phase of the experiment will guide us in choosing dust sizes and compositions for further experiments where we will study the effects of disturbing the surface to simulate external activity. This will include agitation of the dust layer to impart upward velocities like those that would be expected for impact ejecta, and also human and spacecraft activity on the surface.

SCALING OF MULTIPHASE FLOW REGIMES AND INTERFACIAL BEHAVIOR AT MICROGRAVITY.

C. J. Crowley, Creare Incorporated, P.O. Box 71, Hanover, NH 03755, cjc@creare.com.

Previous studies by NASA show that a two-phase approach reduces the mass of thermal management systems which range in size from small to large — a 100 W heat pump/radiator for a small satellite to a 25,000 W active thermal control system (ATCS) for a space station. To facilitate confident design of future two-phase systems, design data and methods for the flow regimes, fluid phase distributions, and the interfacial characteristics of each flow regime are critical. To address this need, NASA has initiated projects such as the Two-Phase Extended Evaluation in Microgravity (TEEM) space flight experiment, with pressure drop experiments at three pipe sizes and detailed void fraction and phase distribution measurements at one pipe size (19 mm). NASA has also funded complementary NRA grants.

The NRA research and the TEEM experiment are supported by NASA ground calibration and planned KC-135 aircraft facilities, where detailed measurements of the two-phase flow phenomena will be made. This scaling project will be coordinated with the test matrices in the ongoing NASA research to take advantage of data generated under those projects. We will supplement that research by providing unique instrumentation to enable void fraction and film thickness measurements at 12, 19, and 25 mm tube sizes. We can therefore examine the scaling of detailed multiphase behavior with tube size. With the refrigerants (R-134a and R-12) used as working fluids for these experiments, we can also explore the scaling of the multiphase data with a large variation in gas density compared with previous air-water experiments. Detailed void fraction and phase distribution measurements permit design data and analysis to validate the scaling relationships for the key multiphase phenomena. These relationships will be incorporated in easy-to-use steady-state and transient design tools (computer programs) which we are developing on separate projects.

Our project will address the following primary objective:

> To facilitate the confident design of two-phase thermal management systems for spacecraft, by enabling detailed measurement of flow characteristics over a range of pipe sizes and gas densities for scaling of two-phase flow behavior.

In Table 1 we summarize the main features of our research program to accomplish this objective. Our contribution to this project maximizes the use of existing facilities and research, yet provides new scientific research results of its own with respect to design data and methods for scaling. Our technical approach is to:

1. Obtain design data at other diameters (*e.g.* 12 and 25 mm) to complement ongoing low-gravity research at 19 mm diameter;
2. Obtain void fraction data for flow regime transitions (bubbly/slug, or slug/annular), detailed phase distributions (bubble lengths, slug lengths, and film thickness), and interfacial characteristics (wave heights in annular flow); and
3. Develop scaling methods for these phenomena.

The design data, tools and the two-phase theory that we develop on this project will be definitive for design and development of two-phase thermal management systems for spacecraft. We summarize our three-year plan to address this scaling issue in Table 2.

Table 1. The Proposed Project Features a Comprehensive Strategy

Feature	Activity	Comment
Coordinate with Existing NASA Facilities	LeRC Ground Test Loop for R-134a	Built in 1996 by LeRC to support void meter flight instrument
	LeRC Aircraft (KC-135) Test Loop for R-134a	Under construction by LeRC in 1998 to support NRA research
	JSC Aircraft (KC-135) Test Loop for R-12	Existing facility undergoing modification by Texas A&M in 1998
Use Unique Instrumentation Capability	Creare Capacitive Void Fraction Instruments at 12, 19 and 25 mm ID for – Average Void Fraction – Local Void Fraction	Developed under the SBIR program for NASA LeRC Delivered as space-qualified instruments at 19 mm ID for TEEM experiment
Coordinate with and Complement Existing NRA Research Grants	University of Houston (V. Balakotiah, *et al.*)	Study of Flow Pattern Transitions and Wavy Annular Films
	NASA LeRC/IMFT (J. McQuillen, J. Fabre, C. Colin)	Study of Physics in Bubbly and Slug Flow Regimes
Provide New Contributions to Microgravity Science	Scaling methods for key multiphase behavior	Design Data at 12 and 25 mm ID to complement 19 mm ID
Validate Design Methods and Tools	Validate transient code software	Use Creare MΦTRAN software being developed on NASA LeRC SBIR program
	Validate steady-state multiphase regime models	Use Creare MICROREG and MICROP software

Table 2. Summary of Research Plan by Year

Year 1	Obtain test data at 12 mm pipe diameter, using superficial velocities to match data at 19 mm pipe size from ongoing NASA research projects. Perform a preliminary assessment of scaling with pipe diameter.
Year 2	After a preliminary evaluation of the scaling, perform tests adjusting the flow rates to match the appropriate dimensionless groups in the flow regime transitions for the 12 , 19 , and 25 mm tubes. Complete and validate the modeling of flow regime transitions.
Year 3	Perform tests adjusting the flow rates to match the appropriate dimensionless groups to model multiphase flow characteristics to calculate void fraction and pressure drop for the 12 , 19, and 25 mm tubes. Complete the validation of pressure drop and void fraction models.

THERMOCAPILLARY-INDUCED PHASE SEPARATION WITH COALESCENCE

Robert H. Davis, Michael A. Rother and Alexander Z. Zinchenko
Department of Chemical Engineering, University of Colorado, Boulder, Colorado 80309-0424

ABSTRACT

Research has been initiated on interactions of two or more deformable drops (or bubbles) in a viscous fluid and subject to a temperature and/or gravitational field. An asymptotic theory for nearly spherical drops shows that small deformations reduce the coalescence and phase separation rates. Boundary-integral simulations for large deformations show that bubbles experience alignment and enhanced coalescence, whereas more viscous drops may break as a result of hydrodynamic interactions. Preliminary experiments for buoyancy motion confirm these observations. Simulations of many drops show clustering phenomena which lead to enhanced phase separation rates.

Fourth Microgravity Fluid Physics & Transport Phenomena Conference, Cleveland, OH, Aug. '98.

SIMULATION OF ROTATING THERMAL CONVECTION AND COMPARISON WITH SPACE-LABORATORY EXPERIMENTS

A.E. Deane (Institute for Physical Science and Technology, University of Maryland, College Park, MD 20742-2431, *deane@morphy.umd.edu*

ABSTRACT

The deep atmospheres of the planets such as Jupiter and Saturn and rotating stars such as our Sun are strongly influenced by buoyancy and Coriolis forces. In addition the giant planets also feel the effects of differential heating (North-South temperature gradients). The latitudinal variation of Coriolis forces is crucial to understanding large-scale motions (scales comparable to the curvature of the body) that are manifested in diverse phenomena such as the differential rotation of the Sun, and the cloud bands on Jupiter.

While important results have been obtained in terrestrial laboratory experiments, in an ambitious and novel experiment, Prof. John Hart has led an effort at the University of Colorado to move from a terrestrial laboratory situation to a space laboratory platform in order to study the effects of these forces on deep atmospheres. In the terrestrial laboratory gravity is aligned with the rotation vector unlike the geophysical case where these vectors move from being (anti-)parallel at the poles to orthogonal at the equator. In the Geophysical Fluid Flow Cell (GFFC) experiment which has been run twice in a microgravity environment (in 1985 and in 1995) radial gravity was achieved by charging a dielectric liquid with an ac voltage on the inner sphere (the outer sphere is ground). The inner and outer spheres were held at different temperatures and the whole apparatus rotated. Thus an analog of the geophysical environments was made. During its missions the GFFC obtained large quantities of data in a wide variety of parameter ranges. This data has shown many interesting flow features that are poorly understood.

The Spectral Element Method combines the geometric flexibility of finite element method with the exponential accuracy of spectral methods. The solution domain is broken up into quadrilateral elements each of which contains a representation as N^{th} order polynomials.

Using the Spectral-Element Method we are able to obtain highly accurate solutions corresponding to the geometry and parameter regime of the GFFC experiment. We present some preliminary results of surveys in Rayleigh number (corresponding to thermal driving) and Taylor number (corresponding to rotational driving). Also, in the GFFC experimental arrangement of obtaining radial gravity the force law is proportional to $1/r^5$ as opposed to the desired $1/r^2$. In our numerical simulations we are able to study the effects of this difference in the force laws and some results have been obtained.

ATTENUATION OF GAS TURBULENCE BY A NEARLY STATIONARY DISPERSION OF FINE PARTICLES

J.K. Eaton, [1] (Department of Mechanical Engineering, Stanford University, Stanford, CA 94305, eaton@vk.stanford.edu)

ABSTRACT

Turbulence attenuation by greater than a factor of two has been observed in many practical gas flows carrying volume fractions as small as 0.01% of dispersed particles. Particles which cause such attenuation usually are smaller than the smallest scales of the turbulence and have time constants 5 to 10 times greater than the time scale of a typical turbulent eddy. That is, strongly attenuating particles usually have Stokes numbers in the range of 5 to 10, indicating that they do not respond to the turbulent fluctuations, but instead just fall through the flow responding only to the mean flow.

There are two mechanisms by which free falling particles may attenuate turbulence. First, the unresponsive particles act as a drag on the turbulent eddies, passing energy from the turbulent eddies to the small scale wakes of the particles where it is quickly dissipated by viscosity. The second mechanism is more complicated. Particles falling under gravity convert gravitational potential energy to turbulent velocity fluctuations. If the particles are large, this mechanism increases the overall turbulence level. However, with moderate size particles, the small scale turbulence generated apparently distorts the turbulent eddies leading to more rapid dissipation. Unfortunately, this conclusion is supported only by circumstantial evidence to date.

The objectives of the experiment are to use microgravity to separate the two mechanisms. A region of nearly-isotropic decaying turbulence with zero mean flow will be formed in a box in the microgravity environment. Different sets of particles with Stokes numbers in the range of 2 to 20 will be dispersed in the flow. With zero gravity and no mean fluid velocity the particles will have zero mean velocity. With the large Stokes numbers, the fluctuating velocities will also be small. Therefore, the only attenuation mechanism will be the direct action of the particles on the turbulence. Control experiments will also be done in which the particles fall through the measurement volume.

Measurements will be acquired using a high resolution image velocimetry (PIV) system being developed specifically for work in particle-laden flows. The measurements will include the decay of the turbulence kinetic energy under various particle loadings. The spatial spectra of the turbulence will also be measured.

In a second set of experiments, the interaction of a single eddy with a collection of nearly stationary particles will be examined. The eddy will be a vortex ring emitted by a jet pulse through an orifice. The distortion of the vortex under the influence of the particles will be examined to gain a better understanding of how fine particles can cause such large reductions in turbulence levels. This experiment could not be conducted in terrestrial gravity because the high particle velocities would overwhelm the relatively low speed motion of the vortex ring.

This experimental program is just getting underway. The initial challenge is to build a closed facility containing reasonably homogeneous and isotropic turbulence with zero mean velocity. Our approach is to use a set of synthetic jets mounted on the periphery of a transparent plexiglass box to create the turbulence. A synthetic jet is a plenum chamber with an orifice open to the volume of interest. The volume of the chamber fluctuates periodically so alternately a jet is ejected from the volume or flow is drawn back in as a sink. The asymmetry of this situation results in a net transport of momentum and kinetic energy into the volume of interest. The present apparatus includes eight synthetic jets each powered independently by a six inch loudspeaker. The synthetic jets discharge through ejector tubes to increase the scale of the turbulence.

Construction of the apparatus is now complete and preliminary flow visualization studies have been conducted. The PIV system is also under development. A compact dual-pulse YAG laser has been acquired as the light source and special software is under development to allow simultaneous measurements of both the particle phase and the fluid phase (marked by fine tracers).

OVERVIEW OF THE DUST AGGREGATION AND CONCENTRATION SYSTEM (DACS) DEFINITION PROGRAM FOR THE MICROGRAVITY SPACE ENVIRONMENT

F.J. Giovane, Space Science Division, Naval Research Laboratory, Washington, DC 20375-5320,
giovane@nrl.navy.mil
J. Blum, Astrophysical Institute and University Observatory, University of Jena, Jena, Germany
blum@astro.uni-jena.de

ABSTRACT

The Dust Aggregation and Concentration System, DACS, Project is an international effort intended to complete the preliminary definition of a system for suspending and concentrating dust particles in a microgravity environment for extended periods of time. The DACS design concept is based on extensive ground, drop tower, and parabolic flight tests. During the present proposed work, the DACS design will be completed, and a Science Requirements Document generated. At the end of the proposed 2 year project, DACS will be positioned to enter the advanced definition phase.

The DACS will allow the morphology of a dust cloud to be studied as the individual particles aggregate and concentrate. The system represents a unique opportunity to study in situ astrophysical conditions similar to those experienced in the formation and evolution of the proto-solar nebula. The DACS project team, whose principal interests are in astrophysics will naturally pursue this interesting area. However, it is expected that the unique opportunity afforded by the DACS to hold dust particles and aerosols in suspension for extended periods, and the instruments ability to concentrate these particles during suspension will be of interest to scientist in other fields such as fluid dynamics, material and biological science.

The astrophysical importance of studying dust aggregation is evident when one considers that the formation of planetary systems is a multistage process. In this process initially fine dispersed dust grains accumulate into larger and larger bodies through frequent collisions between the dust grains due to Brownian motion, differential drift velocities, and decoupling from gas turbulence until their internal gravity becomes the dominant source for their further growth. An understanding of the changing morphologies and light scattering characteristics of aggregated dust under various growth conditions is needed to better interpret astronomical observations of dust in star forming regions. However, the direct simulation of the long-term behavior of a cloud of dust grains under thermal motion, as in the very early stages of the proto-solar nebula, is not possible in a terrestrial laboratory. Even in levitation-compensated experimental setups the relative velocity is determined by the Earth's gravity field, and a velocity field, which simulates the motion of astronomical dust grains, is not feasible.

It was with the goal of developing a system for observing the self-interaction of a cloud of dust grains due to Brownian motion that the present international team of investigators joined together in the Cosmic Dust Aggregation, (CODAG) Microgravity Experiment. CODAG, when it flies later this year, will for the first time undertake the study of light scattering from a cloud of astrophysical relevant dust aggregating under controlled conditions. Its observation time is however limited by the diffusion time of dust to the walls of the stationary chamber. The proposed DACS is intended to overcome this shortcoming and to dramatically extend the duration which dust particles can be suspended and concentrated. These improvements should result in the formation of larger aggregates. The DACS will build on the lessons learned from the CODAG, and from experience gained in drop tower tests, parabolic flights, and ground experiments conducted at the University of Jena (UJena), Germany.

DACS is based on the principal that a dilute gas is much stiffer than a gas at atmospheric pressure. Consequently a dilute gas of 1 mbar pressure injected into a rotating vacuum chamber thermalizes on a time scale of a few tenths of a second, and will quickly follow the motion of the chamber. Thus, if a rotating vacuum chamber is injected with a mixture of gas and dust particles, the gas will begin rotating at the velocity of the chamber almost immediately. The dust, baring outside forces, will stream with the gas. However, if a force is applied, the particles will circulate about an equilibrium point where the forces of the streaming gas and the external force balance. Such a rotating chamber has been build and tested at UJena where it has successfully demonstrated the validity of the concept over periods of several minutes. In DACS case we intend to explore the use of a light induced thermal phoresis force, in which a force is created on the particle by a low intensity light differentially heating the low-pressure gas around the particle. This phenomena, the photophoretic force, has been observed in parabolic microgravity flights and

has been explored by several investigators in earth laboratories. We intend to further investigate how best to use this force with the astronomically relevant dust particles proposed for our future investigations.

By aerodynamically levitating the particles with the aid of the photophoretic force the particles can be suspended about an equilibrium point, where they will describe closed orbits at the rotation frequency of the chamber. If the applied force has a sufficiently strong gradient over the chamber dimensions, their orbital radius will slowly decrease creating an even greater concentration of particles. It is our intention to carry out experiments that will validate a design that will be suitable for the microgravity environment, and that will allow particles to be suspended for several days. The system will be designed to allow the equilibrium point to be observed by zoom cameras or long reach stereo microscopes with high speed video cameras, and an array of photometers will be used to observe the light scattering from the cloud.

DACS investigation will be managed from the Naval Research Laboratory, NRL, which will also carry out the theoretical and numerical modeling, build most of the test and modeling apparatus, and perform the laboratory tests which will serve to validate and extend the numerical predictions. The numerical modeling and computer simulations will include fluid mechanical and photo induced thermophoresis mechanism calculations. In addition, theoretical modeling and laboratory analogue simulations of the light scattering of the dust and its effect on the photon induced thermo-phoresis process will be performed at the University of Florida working closely with NRL. While in Germany, using the existing rotating chamber, UJena and the Max Planck Institute (MPI) for Aeronomie, will conduct suspension tests and make observations to support the numerical and scattering modeling work. NRL will also work closely with UJena and MPI in evolving the DACS design so that it will be ready for the advance definition and development phase.

PLASMA DUST CRYSTALLIZATION

J. Goree,[1] R.A. Quinn,[1] G. Morfill,[2] H. Thomas,[2] T. Hagl,[2] U. Kopoka,[2] H. Rothermel,[2] and M. Zuzic[2],
[1]Dept. of Physics and Astronomy, The University of Iowa, Iowa City, IA 52246,
[2]Max-Planck-Institut fuer extraterrestrische Physik, 85740 Garching, Germany.

INTRODUCTION

A dusty plasma is an ionized gas containing small particles of solid matter, which become electrically charged. It behaves much like a colloidal suspension, exhibiting for example crystalline, liquid and gas phases, and a melting/freezing phase transition. The charged particles interact through a repulsive Coulomb potential that is screened by the Debye length of the electron-ion plasma in which they are immersed.

Unlike a colloidal suspension, the particles in a dusty plasma are widely spaced, so that the medium is optically thin, and the particles are immersed in a low-pressure gas rather than a liquid, so that they are not over-damped and they have no buoyancy.

The use of large (~5-10 micron) particles allows the use of direct imaging of all the particles in a sample volume, using laser illumination and video micrography. This permits the study of structure and dynamics, during the phase transition for example, at a microscopic level, which is not possible with three-dimensional colloidal suspensions.

In laboratory experiments, the lack of buoyancy of particles in a dusty plasma leads to sedimentation. In other words, gravity prevents the formation of extended three-dimensional particle clouds.

In 1998 are carrying out ground-based experiments at The University of Iowa led by P.I. John Goree under NASA funding, and microgravity experiments in Germany, primarily under DLR funding, with NASA funding for the participation of Prof. Goree. NASA funding for this project began in 1997.

GROUND-BASED EXPERIMENTS

Ground-based experiments in preparation at The University of Iowa will focus on the melting/freezing phase transition. The apparatus consists of a vacuum chamber filled to ~ 0.3 Torr pressure with Krypton gas. Inside the chamber a horizontal metal electrode is powered with capacitively-coupled 13.56 MHz radio-frequency high voltage to ionize the gas. Highly spherical particles of 9.4 micron diameter, and made of melamine-formaldehyde, are introduced into the plasma by shaking them from above. The particles then form a cloud levitated about a millimeter above the electrode. The cloud is imaged in horizontal and vertical cross sections using sheets of laser light and video cameras. Each particle is individually distinguishable in the video images, allowing their positions to be measured precisely.

The present series of ground-based experiments will focus on the microscopic structure and dynamics during a melting/freezing phase transition. In addition to analytical tools developed under a previous NASA-funded project, we will develop new tools including the computation of dynamic structure factors. We will work with the hypothesis that the melting/freezing transition in this quasi-two-dimensional medium occurs by a gradual change in the percentage of liquid-like phase that co-exists with solid-phase media.

MICROGRAVITY EXPERIMENTS

Microgravity experiments have been flown already aboard the Texus 35 and Texus 36 sounding rocket flights. A get-away-special (GAS) payload is presently in the design phase, intended for a shuttle launch sometime after mid-1999. These Texus and GAS missions are funded primarily by the DLR, in a group led by the German P.I., Gregor Morfill. The NASA-funded P.I., John Goree, is a participant in these missions. Moreover, the Russian government has recently offered a flight aboard the MIR space station, including 14 hours of experimental time. Funding from the DLR is presently being sought for flight hardware to be flown on MIR in early 1999.

In the Texus sounding rocket experiments, the apparatus was mainly similar to the laboratory hardware described above, except that the vacuum chamber was smaller, using a pair of parallel electrodes 4.2 cm diameter and 3 cm spacing. The rocket launches, carried out in Sweden, provided approximately 6 min. of microgravity. The experiment was monitored by telemetry of video and electrical measurements, and controlled by telecommand. The radio-frequency (rf) voltage was varied from 50 to 100 Volt peak-to-peak. Particles were 14.9 micron diameter in Texus 35, and 6.9 micron in Texus 36.

In both Texus missions, a particle cloud was successfully introduced into the plasma. The cloud filled the inter-electrode region in a way that is impossible in the laboratory. The absence of gravity as a perturbing force in the experiments revealed a lower-order perturbing force, termed the ion-drag force, exerted by ions flowing past the charged particles. Efforts are underway to minimize this ion-drag force in the planned GAS and MIR experiments.

In the Texus 36 mission, which flew 7 February 1998, the particle cloud filled the experimental volume between the electrodes. At low rf powers, the particle cloud exhibited a cyclical throbbing motion, which we termed the 'heartbeat instability.' This mode,

which had a frequency of about 1.5 Hz, was unexpected. It was stabilized at higher rf powers, when a centimeter-size void formed in the center of the particle cloud. The void is believed to be due to the ion drag force exerted by ions flowing from the center of the experimental volume outward. The particle structural order appeared to be liquid-like, with vortex shear motion apparent especially near the edges of the particle cloud. The vortices are thought to be driven by a gradient in the ion drag force, due to a spatial gradient in the ion density in the plasma. Away from the edges a more highly ordered structure was found.

The GAS apparatus is planned to be similar to the Texus apparatus, except that telemetry will not be used. Instead, the experiment will be controlled by an automated computer program, and data will be recorded by video recorders. A sequence of experiments lasting 6 hours is planned.

The MIR apparatus will be similar the Texus hardware, except that the telemetry will provide only low-resolution video signals, so that data recording will be supplemented by video recorders. Video tapes will then be returned to Earth.

DETERMINATION OF THE ACCOMMODATION COEFFICIENT USING VAPOR/GAS BUBBLE DYNAMICS IN AN ACOUSTIC FIELD.

N. A. Gumerov[1], [1]DYNAFLOW, Inc. 7210 Pindell School Road, Fulton, MD 20759, nail@dynaflow-inc.com.

INTRODUCTION

Non-equilibrium liquid/vapor phase transformations can occur in superheated or subcooled liquids in fast processes such as in evaporation in a vacuum, in processing of molten metals, and in vapor explosions. The rate at which such a phase transformation occurs, ξ, can be described by the Hertz-Knudsen-Langmuir formula (e.g. see Volmer, 1939)

$$\xi = \frac{\beta(T_a)}{\sqrt{2\pi R_v T_a}}[p_s(T_a) - p_v]$$

where p_s is the vapor saturation pressure which is a known function of the temperature, p_v the actual vapor pressure, T_a the temperature of the interface, R_v the gas constant of the vapor, and β the "condensation" or "accommodation" coefficient, and depends on the number of accommodated and reflected gas molecules colliding at the interface.

More than one century of the history of the accommodation coefficient measurements shows many problems with its determination. This coefficient depends on the temperature, is sensitive to the conditions at the interface, and is influenced by small amounts of impurities. Even recent measurements of the accommodation coefficient for water (Hagen *et al*, 1989) showed a huge variation in β from 1 for 1 μm droplets to 0.006 for 15 μm droplets. Moreover existing measurement techniques for the accommodation coefficient are complex and expensive. Thus development of a relatively inexpensive and reliable technique for measurement of the accommodation coefficient for a wide range of substances and temperatures is of great practical importance.

PROPOSED TECHNIQUE

We propose to use the observation of the oscillations of vapor bubbles in an ultrasonic field to achieve this measurement. It is known that at temperatures close to the saturation temperature small vapor bubbles grow in a liquid under the action of an acoustic field due to the non-linear effects of "rectified heat transfer", or "rectified heat diffusion", e.g. Akulichev, 1982. Our preliminary theoretical study of bubble growth due to rectified heat transfer, which included non-equilibrium kinetics of phase transformations (Gumerov, 1991), showed that the dynamics of the bubble in a high-frequency acoustic field strongly depends on the value of the accommodation coefficient. This is particularly true of its average radius at stable oscillations (Gumerov, 1995, see Figure 1). This finding can be used as the basis for an effective measurement technique of this coefficient.

The measurements can be performed only in a microgravity environment, where buoyancy forces are reduced by orders of magnitude for the following main reason. The accuracy of the proposed method depends strongly on the amplitude of the bubble oscillations. Accurate measurements require relatively long observation, whereas our evaluations of the parametric bubble shape instability (Gumerov, 1998) show that conventional methods of bubble stabilization using acoustic levitation in a gravity field produce relatively strong non-linear bubble radius and shape oscillations that are not acceptable.

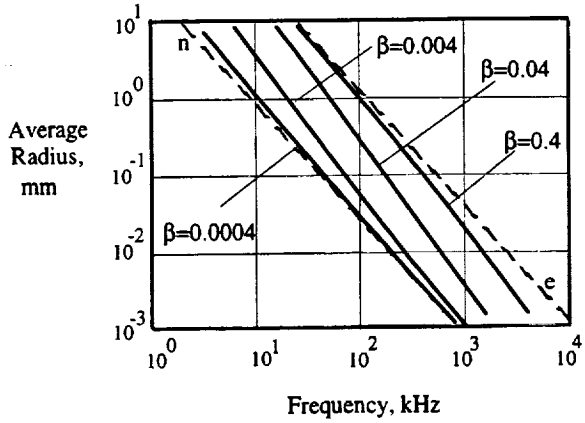

Figure 1. The stable average radius of a water vapor bubble in an acoustic field at various values of the accommodation coefficient. The dashed lines 'e' and 'n' correspond to the limiting cases of equilibrium phase transitions and $\beta \to 0$ (Taken from Gumerov, 1995).

MATHEMATICAL MODEL

Our previous studies ignored several physical effects that can influence dynamics of vapor bubbles and that are taken into account in the present study. These effects include mass diffusion of the dissolved gases in the liquid, liquid viscosity and compressibility, surface tension, the dependence of the transport coefficients on temperature, and effects of the two-component gaseous phase consisting of the vapor and inert gas. Also in the present model exact mass, momentum, and energy conservation equations at the interface are taken into account. The kinetic equation is modified according to Volmer (1939) for binary mixtures. This model covers the case of gas, and vapor/gas bubbles, and generalizes all present models for rectified diffusion.

The analysis starts using a spherically symmetric scheme of a vapor bubble in an isotropic pressure field that includes internal and external heat transfer. In the

second task we include the motion of the bubble in a standing acoustic wave (anisotropic pressure field).

The bubble motion and the position in a standing wave are tightly connected with the bubble size. Variation in the bubble position leads to variation of the sound intensity at the bubble location and corresponding change of the bubble growth rate. In the same time variation in the bubble size changes the hydrodynamic forces acting on the bubble in the acoustic wave which causes variations of the bubble position. Therefore the position of the bubble in a standing wave can also be used for the accommodation coefficient measurement.

Note that the bubble translatory motion also can effect the heat and mass transfer. This effect can be taken into account within the framework of the model of spherical bubble by averaging the heat an mass fluxes to the bubble over the bubble surface.

METHODS OF SOLUTION

To solve the closed system of the governing equations describing non-linear bubble dynamics in an acoustic wave we use approximate analytical and numerical techniques and their combination.

A multiscale asymptotic technique used for derivation of equations describing the evolution of the average bubble radius in an isotropic pressure field was developed in our preliminary investigation (Gumerov, 1991). In the present study the technique is modified to include the above-mentioned physical effects and effects of the bubble drift in a standing acoustic wave.

This leads to the system of type

$$\frac{\partial\langle a\rangle}{\partial t_2} = F(\langle a\rangle)\sin^2 k\langle x_b\rangle - G(\langle a\rangle), \quad \frac{\partial^2\langle x_b\rangle}{\partial t_2^2} = E\left(\langle a\rangle, \langle x_b\rangle, \frac{\partial\langle x_b\rangle}{\partial t_2}\right)$$

describing the evolution of the period-averaged bubble radius, $\langle a\rangle$, and position $\langle x_b\rangle$ in "slow" time, t_2, proportional to the energy of the acoustic wave. Functions F, G, and E can be found from the condition of solvability of the system in the second-order of approximation with respect to the amplitude of the acoustic field. Function F is complex and depends on the accommodation coefficient as well as on other physical properties of the system and parameters of the acoustic wave; k is the wavenumber. The case of isotropic pressure field is a particular case that corresponds to the first equation at $\langle x_b\rangle = const$.

Numerical study of the above system and additional analytical expressions for steady bubble size can be investigated to determine the effect of the accommodation coefficient on the bubble dynamics.

In parallel with the asymptotic approach a numerical algorithm solving the governing partial differential equations can be developed. These algorithms can be based on spectral methods, such as methods used for numerical studies of spherical bubbles in acoustic fields related to sonoluminescence (Kamath *et al*, 1993). Asymptotic results can be used for testing and validation of the direct numerical simulations. At the same time approximate analytical results that are especially valuable in the case of low amplitude acoustic fields can substantially save computation time when computing high frequency oscillations, because they allow us to use substantially larger time steps and solve systems of smaller dimension.

Due to the universality of the model covering cases of gas, vapor/gas, and vapor bubbles theoretical results obtained for various situations can be verified by comparison with known experiments on rectified diffusion and heat transfer in water, cryogenic liquids, and other substances. Previous published theoretical studies of particular cases also can be used for verification.

ANTICIPATED RESULTS

As a result of this research we anticipate to get understanding of the physics accompanying bubble dynamics with non-equilibrium phase transitions, determine the feasibility of the novel method of determination of the accommodation coefficient, and provide a basis for future flight experiments.

Once successfully implemented in microgravity conditions, the method may be further developed to account for strong non-linear oscillations in a ground-based laboratory.

ACKNOWLEDGMENTS

This work is being supported by NASA through Grant NAS3-98094 in Microgravity Fluid Physics.

REFERENCES

M. Volmer, *Kinetik der Phasebildung*, Dresden-Leipzig: Steinkopff, 1939.

D. E. Hagen, J. Schmitt, M. Trueblood, J. Carstens, D. R. White, and D. J. Alofs, Condensation coefficient measurement for water in the UMR cloud simulation chamber, *J. Atmospheric Sci.* 46(6), 803-816, 1989.

V. A. Akulichev, Acoustic cavitation in cryogenic and boiling liquids. In: *L. van Wijngaarden (ed.) Mechanics and Physics of Bubbles in Liquids*, Martinus Nijhoff, the Netherlands, 1982.

N. A. Gumerov, Weakly non-linear oscillations of the radius of a vapour bubble in an acoustic field, *J. Appl. Maths Mechs*, 55(2), 205-211, 1991.

N. A. Gumerov, On waves of the self-induced acoustic transparency in mixtures of liquid and vapor bubbles. In: *S. Morioka & L. van Wijngaarden (eds.), IUTAM Symposium on Waves in Liquid/Gas and Liquid/Vapour Two-Phase Systems*, Kluwer, the Netherlands, 77-86, 1995.

N. A. Gumerov, Effect of acoustic radiation on the stability of spherical bubble oscillations. *Physics of Fluids* 10(7), 1998.

V. Kamath, A. Prosperetti & F. N. Egolfopoulos, A theoretical study of sonoluminescence, *J. Acoust. Soc. Am.* 94(1), 248-260, 1993.

ENGINEERING OF NOVEL BIOCOLLOID SUSPENSIONS

D.A. Hammer, S. Rodgers, A. Hiddessen[1] and D.A. Weitz[2], [1]Department of Chemical Engineering, 311A Towne Building, 220 S. 33rd Street, University of Pennsylvania, Philadelphia, PA 19104, hammer@seas.upenn.edu, and [2]Department of Physics, University of Pennsylvania, Philadelphia, PA 19104, weitz@dept.physics.upenn.edu.

ABSTRACT

Colloidal suspensions are materials with a variety of uses from cleaners and lubricants to food, cosmetics, and coatings. In addition, they can be used as a tool for testing the fundamental tenets of statistical physics. Colloidal suspensions can be synthesized from a wide variety of materials, and in the form of monodisperse particles, which can self-assemble into highly ordered colloidal crystal structures. As such they can also be used as templates for the construction of highly ordered materials. Materials design of colloids has, to date, relied on entropic self-assembly, where crystals form as result of lower free energy due to a transition to order. Here, our goal is to develop a completely new method for materials fabrication using colloidal precursors, in which the self-assembly of the ordered colloidal structures is driven by a highly controllable, attractive interaction. This will greatly increase the range of potential structures that can be fabricated with colloidal particles.

In this work, we demonstrate that colloidal suspensions can be crosslinked through highly specific biological crosslinking reactions. In particular, the molecules we use are protein-carbohydrate interactions derived from the immune system. This different driving force for self-assembly will yield different and novel suspensions structures. Because the biological interactions are heterotypic (A binding to B), this chemical system can be used to make binary alloys in which the two colloid subpopulations vary in some property – size, density, volume fraction, magnetic susceptibility, etc. An additional feature of these molecules which is unique – even within the realm of biological recognition – is that the molecules bind reversibly on reasonable time-scales, which will enable the suspension to sample different configurations, and allow us to manipulate and measure the size of the suspension dynamically. Because of the wide variety of structures that can be made from these novel colloids, and because the suspension structure can be altered dynamically, we believe this biocolloid system will yield a novel set of materials with many technological applications, including sensors (both biological and non-biological), optical filters and separation media.

To demonstrate the feasibility of our approach, we have made aggregates of a two-component system of colloids, which we refer to as A and B, and observed the dynamics of aggregate formation and break-up in a Hele-Shaw chamber. The molecular interaction that mediates the aggregation in this study is the binding between E-selectin, an immune system adhesion molecule that selectively binds carbohydrates, and sialyl-Lewis^x (sLe^x), a tetrasaccharide carbohydrate that is a ligand for E-selectin. sLe^x and E-selectin recognize each other selectively as a key binds to a lock. Polystyrene spheres are used as the colloid. To make one type of colloid (A), polystyrene spheres coated with avidin are purchased, and modified by binding a biotinylated-sLe^x. Bonding between biotin and avidin is high affinity (energy about 25kT), and the time-scale for release is several days; thus, this interaction is irreversible on the time-scale of the experiment. To make the second type of colloid (B), polystrene spheres coated with protein A are coated with an E-selectin-IgG chimera, in which the antigen recognition domains of a human IgG are replaced with a truncated form of E-selectin. The lectin domain on this truncated form is retained, however, providing full functionality. Previous work from the Hammer laboratory (Brunk, D.K., D.J. Goetz, and D.A. Hammer *Biophysical Journal* 71:2902-2907 (1997)) demonstrates that colloidal immobilization of these molecules retains full functionality, and that the interaction between sLe^x and E-selectin is specific in this system.

To observe the dynamics of interaction of these colloids, a dilute suspension (total volume fraction of several percent) of A and B type beads was injected into a Hele-Shaw flow chamber. The chamber was made by cutting a Hele-Shaw profile out of a sialastic gasket whose thickness was approximately 200 microns. This gasket was placed between two Lexan blocks, the bottom of which was fitted with a microscope slide for observation with an inverted microscope. The Hele-Shaw profile ensures that the shear stress will vary linearly with the axial position in the chamber. Flow rate through the chamber was controlled using syringe pumps, and measured using a buret. Events are recorded with video microscopy and analyzed using digital image analysis. Ample calibrations have been performed of the hydrodynamics within the chamber. The spheres are 10 microns in diameter, the wall shear rate was below 50^{-s}, and the particle Reynolds number is less than 1.

Observation of dynamic events with these particles revealed several interesting characteristics. First, colloidal aggregates could be grown in this system analogously to how a snowball can be grown. Larger aggregates can be seen catching up to smaller monomers and dimers of aggregates, and in several instances, the smaller oligomer was captured by the larger aggregate. The mechanism of this snowballing growth is that as the aggregate grows, its center of mass is extended into higher streamlines, and thus its average velocity increases compared to the velocity of monomers which are nearer to the surface. Gravity is an important controlling mechanism in snowball growth, as monomers

sediment on the surface. These smaller monomers are in a slower moving streamline, and thus, the larger aggregates catch up to the smaller monomers. When they encounter each other, the large aggregate adheres to the smaller aggregates, carrying the oligomer along. This seems to be a technology for growing aggregates under well-defined shear conditions.

Additional observation of the aggregates demonstrates restructuring. In many cases, aggregates are seen to disassemble into smaller oligomers and Rouse-like chains. Such restructuring is facilitated by the flow kinematics. In some cases, aggregates break apart, then regrow by the snowball mechanism. This disassembly and regrowth should enable system annealing, which would necessary for crystallization.

It should be apparent that the disassembly is facilitated by the fast off rate of selectin-sLe^x bonds, and would not be possible with just any biological recognition system. These molecules are specialized, and their special properties enable the construction of novel materials. Additional work in the Hammer laboratory is directed at identifying additional biomacromolecular pairs that can recognize each other selectively with a wide range of energies and kinetic rate constants.

Future work on this system will involved observing the dynamics of aggregate assembly with different size A and B spheres, attempting shear or temperature induced cycling and annealing of binary crystals, and performing light scattering on forming or preformed colloidal aggregates.

ACKNOLEDGMENT

Work supported by NASA Fluid Physics 96-HEDS-01-168.

SONOLUMINESCENCE IN SPACE: THE CRITICAL ROLE OF BUOYANCY IN STABILITY AND EMISSION MECHANISMS

R. Glynn Holt (rgholt@bu.edu) and Ronald A. Roy (ronroy@bu.edu), Boston University, Dept. of Aerospace and Mechanical Engineering, 110 Cummington St, Boston, MA 02215

INTRODUCTION AND MOTIVATION

Sonoluminescence is the term used to describe the emission of light from a violently collapsing bubble. Sonoluminescence ("light from sound") is the result of extremely nonlinear pulsations of gas/vapor bubbles in liquids when subject to sufficiently high amplitude acoustic pressures. In a single collapse, a bubble's volume can be compressed more than a thousand-fold in the span of less than a microsecond. Even the simplest consideration of the thermodynamics yields pressures on the order of 10,000 ATM. and temperatures of at least 10,000K. On the face of things, it is not surprising that light should be emitted from such an extreme process. Since 1990 (the year that Gaitan discovered light from a single bubble) there has been a tremendous amount of experimental and theoretical research in stable, single-bubble sonoluminescence.

Yet there remain four fundamental mysteries associated with this phenomenon:

- *the light emission mechanism itself,*
- *the mechanism for anomalous mass flux stability,*
- *the disappearance of the bubble at some critical acoustic pressure, and*
- *the appearance of quasiperiodic and chaotic oscillations in the flash timing.*

Gravity, in the context of the buoyant force, is implicated in all four of these unexplained phenomena.

We are developing microgravity experiments probing the effect of gravity on single bubble sonoluminescence. By determining the stability boundaries experimentally in microgravity, and measuring not only light emission but mechanical bubble response, we will be able to directly test the unambiguous predictions of existing theories. By exploiting the microgravity environment we will gain new knowledge impossible to obtain in earth-based labs which will enable explanations for the above mysteries. We will also be in a position to make new discoveries about bubbles which emit light.

OBJECTIVES

The objectives of the planned investigation are:

(1) To test the validity of fractoluminescence as a mechanism for light emission in single bubble sonoluminescence by making careful of the light emission and mechanical oscillations of bubbles in 1g, mg, and μg where buoyancy-induced coupling of translation and oscillation motions is reduced or absent

(2) To develop an experimental apparatus to perform scientifically controlled experiments aboard parabolic flight aircraft and in drop towers to attempt to quantify the effect of gravity on light emission and the extinction threshold, to meet objectives 1, 3 and 4, and to investigate the possibility of μg experimentation.

(3) To measure (in 1g, mg and μg) the precise values of acoustic pressure and equilibrium radius that leads to the extinction of a light-emitting bubble, a phenomenon which occurs at a well defined critical acoustic pressure in 1g experiments. This will test theories which postulate either a nonlinear levitation instability, or a Rayleigh-Taylor instability mechanism for the bubble disappearance.

(4) To test the prediction that chaotic and quasiperiodic timing of the flashes observed in 1g is due to buoyancy-related effects, which could either be induced shape oscillations or a global levitator instability due to time-varying detuning of the levitation cell resonance resulting from the nonlinear bubble oscillations.

TECHNICAL PLAN

Single-bubble sonoluminescence experiments in water with dissolved gases will be designed for performance in a microgravity environment. Since many of the seminal experiments have already been performed in 1g, the initial phase of the proposed investigation will concentrate on using lessons learned from the 1g experiments to build and test designs for a mature apparatus which will measure the critical observables successfully in a space environment. Extensive testing of the preliminary designs will be performed on parabolic aircraft flights, which can also produce useful scientific data for short time periods.

MICROGRAVITY RELEVANCE

As we will show later, SBSL bubbles experience a time-varying buoyancy which reaches maximal excursions precisely where sonoluminescence is observed. This results in a strong nonlinear coupling between volume and translatory motions, which can induce mechanical and mass flux effects which result in light emission and anomalous stability. Removing the acceleration of gravity from the system will eliminate buoyancy-driven translatory oscillations of the bubble, providing a direct test of Prosperetti's theory of fractoluminescence. This will be a decisive test of this light emission mechanism, and will also shed light on the chemical reaction theory of mass flux for volume

stability as well as the resonance-controlled shape oscillation instability . Thus, a microgravity environment will change the geography of the parameter space, and the only hope for a clear understanding of the SBSL phenomenon is to perform careful experiments which locate light emission within the context of the instability boundaries that exist in the parameter space

SIGNIFICANCE

Acoustically-induced light emission from a single bubble (SBSL) has proven to be one of the most exciting and perplexing problems in physics in last decade. There have been many attempts at modeling the underlying physical processes governing SBSL behavior, both in terms of gross bubble dynamics and in terms of the details of the light emission process. The effort is exciting for, in most cases, the models suggest an physical environment within this minute collapsing bubble that is entirely unique in nature. Predictions of mega-Kelvin temperatures and mega-Bar pressures abound; however, it is important to point out that many of these model predictions possess little or no unambiguous experimental guidance. We believe that many of these models will remain untested and untestable unless a microgravity experiment is performed. It is also clear that only a carefully designed set of experiments proposing to measure more than just the light emission is necessary to answer unambiguously certain fundamental questions. The microgravity experiments proposed here could help solve the mysteries associated with sonoluminescence

RHEOLOGY OF FOAM NEAR THE ORDER-DISORDER PHASE TRANSITION.

R. Glynn Holt (rgholt@bu.edu) and J. Gregory McDaniel (jgm@bu.edu), Boston University, Dept. of Aerospace and Mechanical Engineering, 110 Cummington St, Boston, MA 02215

INTRODUCTION AND MOTIVATION

Foams are extremely important in a variety of industrial applications. Foams are widely used in fire-fighting applications, and are especially effective in fighting flammable liquid fires. In fact the Fire Suppression System aboard the Space Shuttle utilizes cylinders of Halon foam, which, when fired, force a rapidly expanding foam into the convoluted spaces behind instrument panels. Foams are critical in the process of enhanced oil recovery, due to their surface-active and highly viscous nature. They are also used as drilling fluids in underpressurized geologic formations. They are used as transport agents, and as trapping agents. They are also used as separation agents, where ore refinement is accomplished by froth flotation of the typically lighter and hydrophobic contaminants.

OBJECTIVES

The goal of the proposed investigation is the determination of the mechanical and rheological properties of foams, utilizing the microgravity environment to explore foam rheology for foams which cannot exist, or only exist for a short time, in 1g. The specific objectives of the proposed investigation are:

1) To develop a novel acoustic technique for experimentally measuring the stress-response of small samples of foam ("foam drops") subjected to both static and time-varying extensional shear and pure dilatational strain. Our efforts will concentrate on developing a shape-modal oscillation technique, and an ambient (hydrostatic) pressure variation technique to meet our goals, and we will investigate step-function, quasistatic and oscillatory temporal variations in the acoustic and ambient pressures. A reliable diagnostic for the volume fraction will be developed. A reliable foam drop production technique will be developed. A demonstration of capabilities and preliminary data will be obtained for publication and for support of a follow on proposal.

2) To model the response of foam drops to static and time-varying modulation of the acoustic field to extract two properties: the bulk elastic shear modulus and the effective bulk shear viscosity. We will treat the foam as a lumped-element continuum with a known imposed average velocity field. Expressions will be developed for frequency and damping of modal oscillations of foam drops, relating these measurables to the bulk shear modulus and the bulk shear viscosity. The quasi-static response will allow direct determination of the yield stress.

TECHNICAL PLAN

Foam drops will be levitated acoustically. The levitation pressure will be systematically varied quasi-statically to infer stress/strain relationships. The drops will then be subjected to slow ambient pressure and radiation pressure modulation to locate and study the simplest normal modes. Frequency and damping data for the monopole and quadrupole mode will be collected in detail for a variety of control parameters: drop size, number of components, average cell size, time of existence, and material parameters. The volume fraction will be varied from 1.0 (the dry limit) down to the minimum supportable in 1g. Capillary waves, their inception, interactions, and their effect on breakup and coarsening will be studied on levitated drops. Selected tests will be flown on KC-135 parabolic flights to help resolve technical issues related to designing long-term microgravity experiments.

Theoretical expressions for low-amplitude modal oscillations of foam drops will be derived, treating the foam as a lumped-element material in order to define rheological variables. These will be compared with measurements to allow the inference of modulus and viscosity as functions of volume fraction down to the minimum attainable in 1g.

MICROGRAVITY RELEVANCE

All but the driest foams drain in gravity. The liquid component will flow downward, and the bubbles will rise until a pool of liquid with a dry foam cap will form. Gravity will thus prevent the measurement of any properties as the gas volume fraction is decreased towards the order-disorder transition, because the foam will be destroyed. There is very little experimental data on the rheological properties of 3D foams, primarily because potential experiments are severely hindered by the requirement for contact containment, and draining and thinning due to gravity. Our technique can provide non-contact control and manipulation of foam drops to gather such data.

SIGNIFICANCE

Understanding the rheological behavior of foams is important as a basic problem in fluid physics, and as a practical problem in many industries. Foams are tremendously important in a variety of applications. The most important quality of a foam in many of these applications is its response to imposed strain, or its rheological behavior. Yet there exists almost no experimental data on the rheological properties of real

3D foams. This is due in large part to the earth-based requirements for contact containment, and to the fact that gravity-induced drainage quickly destroys all but the "driest" foams, those with a very high gas volume fraction ϕ . We will develop a unique method to provide non-contact control and manipulation of foam samples. The development of this technique, together with experimentation in 0g, will provide the ability to carry out a set of benchmark experiments which will allow determination of a foam's yield stress, effective bulk modulus and effective bulk viscosity as a continuous function of gas volume fraction from the dry limit ($\phi \approx 1$) through the order-disorder phase transition to the wet limit ($\phi \approx 0$) of a bubbly liquid. In addition to providing the first measurements of such quantities as functions of ϕ to compare with theory, the knowledge gained will have practical application to the myriad actual uses of foams on the earth, and to space-based systems.

Fluid Flow in An Evaporating Droplet

H. Hu and R. Larson, Department of Chem. Eng., University of Michigan,
2300 Hayward St., Ann Arbor, MI 48109.

ABSTRACT

Droplet evaporation is a common phenomenon in everyday life. For example, when a droplet of coffee or salt solution is dropped onto a surface and the droplet dries out, a ring of coffee or salt particles is left on the surface. This phenomenon exists not only in everyday life, but also in many practical industrial processes and scientific research and could also be used to assist in DNA sequence analysis, if the flow field in the droplet produced by the evaporation could be understood and predicted in detail.

In order to measure the fluid flow in a droplet, small particles can be suspended into the fluid as tracers. From the ratio of gravitational force to Brownian force $a^3\Delta\rho g / k_B T$, we find that particle's tendency to settle is proportional to a^4(a is particle radius). So, to keep the particles from settling, the droplet size should be chosen to be in a range 0.1 -1.0μm in experiments. For such small particles, the Brownian force will affect the motion of the particle preventing accurate measurement of the flow field. This problem could be overcome by using larger particles as tracers to measure fluid flow under microgravity since the gravitational acceleration g is then very small. For larger particles, Brownian force would hardly affect the motion of the particles. Therefore, accurate flow field could be determined from experiments in microgravity.

In this paper, we will investigate the fluid flow in an evaporating droplet under normal gravity, and compare experiments to theories. Then, we will present our ideas about the experimental measurement of fluid flow in an evaporating droplet under microgravity.

Deegan et al.(1997) measured the radial, height-averaged velocity distribution in an evaporating droplet and observed the formation of a ring. Their experimental results agreed well with the results of the theoretical analysis which they also carried out. Kantor(1997) also derived a velocity field using a different expression for the evaporation rate than that used by Deegan et al. Both expressions predict a height-averaged outward radial flow in an evaporating droplet. But both theories give only an expression for the radial height-averaged velocity. We therefore derive expressions for both the radial and vertical velocities as functions of local radius $\bar{r}$ (dimensionless radial position of a particle, $\bar{r} = r/R$), and height h. From the theory of Deegan et al, the local radial and vertical velocities v_r and v_z are:

$$v_r = \frac{3}{8}\frac{R}{t_f - t}\frac{1}{\bar{r}}\left[\left(1-\bar{r}^2\right)^{\lambda} - \left(1-\bar{r}^2\right)\right]\left[2\left(\frac{z}{h}\right) - \left(\frac{z}{h}\right)^2\right]$$

$$v_z = \frac{3}{8}\frac{R}{t_f - t}\frac{1}{\bar{r}}\left[\lambda\left(1-\bar{r}^2\right)^{\lambda-1} + 1\right]\left[3\left(\frac{z}{h}\right)^2 - \left(\frac{z}{h}\right)^3\right]$$

where t_f is the drying time of droplet evaporation.

From the theory of Kantor, the local radial and vertical velocities v_r and v_z are also derived:

$$v_r = \frac{3A\sqrt{1-\delta^2}}{4R^2\alpha\delta}\frac{1}{\bar{r}(1-\bar{r}^2)}\left[\frac{1+\delta^2}{1-\delta^2}\left(\sqrt{1-\bar{r}^2(1-\delta^2)}-1\right)+\frac{1}{6\delta^4}\left(\frac{\left((1-\delta^2)^2-2\delta^2(1-\bar{r}^2)\right)\sqrt{(1+\delta^2)^2-4\delta^2\bar{r}^2}-}{(1+\delta^2)\left((1-\delta^2)^2-2\delta^2\right)}\right)\right]\left(\frac{2z}{h}-\frac{z^2}{h^2}\right)$$

$$v_z = -\frac{3A\sqrt{1-\delta^2}}{4R^2\alpha\delta}\frac{1}{(1-\bar{r}^2)^2}\left[\frac{1+\delta^2}{1-\delta^2}\left(\frac{2-(1-\delta^2)(1+\bar{r}^2)}{\sqrt{1-\bar{r}^2(1-\delta^2)}}-2\right)+\frac{1}{6\delta^4}\left(\frac{2(1-\delta^2)^2\sqrt{(1+\delta^2)^2-4\delta^2\bar{r}^2}-}{\frac{4\delta^2\left((1-\delta^2)^2-2\delta^2(1-\bar{r}^2)\right)(1-\bar{r}^2)}{\sqrt{(1+\delta^2)^2-4\delta^2\bar{r}^2}}-}{2(1+\delta^2)\left((1-\delta^2)^2-2\delta^2\right)}\right)\right]\left(\frac{z^2}{h}-\frac{z^3}{3h^2}\right)$$

where $A = 17.28(1-H)\sqrt{T}\exp\left(\frac{-5283}{T}\right)$, H is the ambient humidity, $\alpha = \arctan\left(\sqrt{\frac{1-\delta}{1+\delta}}\right)$, $\delta \equiv \tan\left(\frac{\theta}{2}\right) \equiv \tanh(\lambda)$, θ is the contact angle, $\hat{n}$ is an outward-pointing normal vector at a point on the oblate surface, and λ' and μ are the parameters of an oblate spheroid, defined such that the r and z coordinates of the surface of the droplet satisfy:

$$\frac{r^2}{(\cosh\lambda \cos\mu)^2} + \frac{z^2}{(\sin sh\lambda \sin\mu)^2} = 1$$

A comparison for these two different expressions was made by numerical calculation. The calculated results show that near the end of the drying process, the theory of Deegan et al. predicts a much higher radial velocity than vertical velocity. For Kantor's theory, the vertical velocity is larger than the radial velocity near the end of drying.

In addition, the effect of evaporation heterogeneity of a droplet and ambient humidity on the flow field is discussed.

We experimentally investigated the overall evaporation rate. The experimental results show that the overall evaporation rate is constant during the droplet evaporation. This result is consistent with the results given by Rowan et al.(1995).

Tracking the particle motion in an evaporating droplet is providing experimental data from which the competing theories for the flow in an evaporating droplet can be distinguished.

Studies of Gas-Particle Interactions in a Microgravity Flow Cell

Michel Louge[1] and James Jenkins[2], [1]Sibley School of Mechanical and Aerospace Engineering, [2]Department of Theoretical and Applied Mechanics, Cornell University, Ithaca, NY 14853

Scope

We are developing a microgravity flow cell in which to study the interaction of a flowing gas with relatively massive particles that collide with each other and with the moving boundaries of the cell. The absence of gravity makes possible the independent control of the relative motion of the boundaries and the flow of the gas.

The cell will permit gas-particle interactions to be studied over the entire range of flow conditions over which the mixture is not turbulent. Within this range, we shall characterize the viscous dissipation of the energy of the particle fluctuations, measure the influence of particle-phase viscosity on the pressure drop along the cell, and observe the development of localized inhomogeneities that are likely to be associated with the onset of clusters. These measurements and observations should contribute to an understanding of the essential physics of pneumatic transport.

Background

The ability to transport particulate materials predictably and efficiently using a flowing gas is likely to play an important role in the development of Lunar and Martian environments that are hospitable to humans. Lunar soil contains significant amounts of oxygen, chemically bound in various minerals. Through appropriate processing, this oxygen may be recovered for use in propulsion and life support systems. Similarly, it is believed that Martian soil contains significant amounts of water which can be electrolyzed into oxygen and hydrogen, again for propellants and life support. The transport of such granular soils from where they are mined and between stages of their processing is likely to involve pneumatic transport carried out in systems of pipes using flows of the liberated gases.

The pneumatic transport of particulate solids is a relatively common but not very well understood process in many terrestrial manufacturing operations. In the dilute regime, a relatively homogeneous dispersion of particles is transported by the flowing gas through a pipe by the drag associated with the difference in the mean velocity of the two phases. The particles may also be supported against gravity by this drag and their suspension sustained by the turbulent velocity fluctuations of the flow. As long as the mixture of gas and particles is relatively uniform, transport is relatively stable and predictable; although because the particles are dilute, the mass transport is low. As the particle concentration increases, denser clusters begin to form, eventually leading to severe inhomogeneities in the flow and, finally, the collapse of transport, or choking, in vertical sections of the system.

Recently, an appreciation has developed for the influence of collisional interactions between relatively massive particles on pneumatic transport, particularly in the dilute regime, both in situations where the flow of the mixture is laminar (Sinclair & Jackson, 1989) and turbulent (e.g. Louge, Mastorakos & Jenkins, 1991; Dasgupta, Sundaresan & Jackson, 1994; Bolio, Yasuna & Sinclair, 1995). Collisions between such particles can transfer a significant amount of momentum within the flow and at the boundaries. This provides an additional resistance to the passage of the gas, but also introduces a mechanism that promotes more homogeneous flows and, at least in small diameter pipes, may forestall the development of clusters.

Relatively massive particles are those that are not influenced by the turbulent velocity fluctuations of the gas as they travel between collisions. As the concentration of particles increases, there is evidence that such particles suppress the gas turbulence (Tsuji, Morikawa & Shiomi, 1984). Collisions between particles, and the random component of the particle velocity that is associated with them, are driven by differences in mean particle velocity across the flow and by the mean slip of the particle phase with respect to the boundary.

Because collisions between particles inevitably dissipate energy, at a point within the flow there may be an excess or a deficiency of energy put into the particle velocity fluctuations through collisions. In this event, energy associated with the velocity fluctuations is transported to or from that point. Similarly, at a boundary there may be an excess or deficiency of the energy of the velocity fluctuations converted from the mean slip over that dissipated in collisions; in this case there is a flux of fluctuation energy from or to the boundary.

In recent years, an understanding has developed of how the balance of momentum tangential to the boundary determines the slip velocity there and how the conversion of the energy of the particle slip velocity into fluctuation energy is influenced by the boundary geometry and collisional dissipation. For example, Richman and Chou (1988) have characterized the exchange of momentum and the conversion of slip energy to fluctuation energy at a bumpy frictionless boundary with cylindrical features, and Jenkins and Louge (1997) have derived boundary conditions at a flat, frictional wall based on the three parameter model for frictional collisions introduced by Walton (1988). Using these, it is relatively easy to write down expressions for the particle slip velocity and flux of fluctuation energy at a boundary with frictional, cylindrical features that involve only the diameter and spacing of the cylinders and collision parameters that can be experimentally determined (Foerster, Louge, Chang, and Allia, 1994).

The same collision model may be used to characterize the dissipation due to collisional contact between two spheres of the flow in terms of measured parameters. When the contribution of the friction to the collisional dissipation is not too great, Jenkins and Zhang (1997) show how the kinetic theory for frictionless collisions can be adapted to

apply to frictional collisions by incorporating the translational energy lost to friction and the additional rotational degrees of freedom of the energy into an effective coefficient of restitution. This means that in a continuum description of the particle phase based on the kinetic theory for colliding particles, the additional balance equations for the mean particle spin and rotational fluctuation energy do not have to be considered.

In addition, Sangani, Mo, Tsao and Koch (1996) have recently determined the contribution to the dissipation of particle fluctuation energy of the viscous forces of the gas in random flights of particles between collisions. They do this over a range of concentrations for simple shearing flows in which the particle Reynolds number is small and the Stokes number is greater than one. In this work, they analyze the viscous dissipation of particle fluctuation energy for such particles when there is, on average, no velocity difference between the particles and the gas. It is, however, relatively clear how to extend their analysis to more general and less homogeneous shearing flows, provided that the average flow of the mixture is not turbulent.

Research in progress

We are modifying an existing shear cell, originally designed to investigate purely collisional flows of granular materials in microgravity, to permit the flow of a gas relative to the particles. We will then use the resulting cell in microgravity to study the relationship between the collisional transport of momentum in the grains and the mean drag of the gas. This will be done over the range of mean gas flow rate and particle concentrations where turbulence in the mixture is suppressed. The characterization of this range will be an important result of the proposed research. Careful visual observations through the side of the cell will permit measurement of the mean velocities, particle velocity fluctuations, and average particle concentrations over the width of the cell in sections where the flow of the mixture is steady and fully developed.

Because the particle phase viscosity is a function of the particle fluctuation energy, the energetics of the particle phase plays a crucial role in the balance between gas drag and particle momentum transport. To study the energetics, boundaries will be employed that either produce or dissipate fluctuation energy and the viscous contribution to the rate of dissipation of particle fluctuation energy will be measured.

We anticipate that increased particle agitation will promote more homogeneous flows and delay the onset of particle clusters. We will carefully monitor the development of inhomogeneities in the particle concentration as the strength of the gas flow is varied for more and less energetic particles interacting with boundaries that either produce or dissipate fluctuation energy.

Acknowledgments

This work is currently supported by NASA grant NAG3-2112. Computation resources are provided by the Cornell Theory Center and the National Partnership for Advanced Computational Infrastructure.

References

Bolio, E. J., Yasuna, J. A. and Sinclair, J. L. 1995 Dilute, turbulent gas-solid flow in risers with particle-particle interactions. *AIChE J.* 41, 1375-1388.

Dasgupta S., Jackson R. and Sundaresan S. 1994 Turbulent gas-particle flow in vertical risers. *AIChE J.* 40, 215-228.

Foerster .S, Louge M., Chang H. and Allia K. 1994 Measurements of the Collision Properties of Small Spheres. *Phys. Fluids* 6, 1108-15.

Jenkins, J.T. and Louge, M. 1997 "On the flux of fluctuation energy in a collisional grain flow at a flat, frictional wall," *Phys. Fluids* **9** (10), 2835-2840.

Jenkins, J. T. and Zhang, C. 1997 Kinetic theory for identical, slightly frictional, nearly elastic spheres. *Phys. Fluids* (under review).

Louge M.Y., Mastorakos M. & Jenkins J.T. 1991 "The Role of Particle Collisions in Pneumatic Transport", *J. of Fluid Mechanics* **231**, 345-59.

Richman M. and Chou 1988 Boundary effects on granular shear flows of smooth disks. *Journal of Applied Mathematics and Physics* (ZAMP) 39, 885-901.

Sangani A.S., Mo G., Tsao H.-K., and Koch D.L. 1996 Simple shear flows of dense gas-solid suspensions at finite Stokes number. *J. Fluid Mech.* 313, 309-41.

Sinclair, J. L. and Jackson, R. 1989 Gas-particle flow in a vertical pipe with particle-particle interactions. *AIChE J.* 39, 1473-1486.

Tsuji Y., Morikawa Y., and Shiomi H. 1984 LDV measurements of an air-solid two-phase flow in a vertical pipe. *J. Fluid Mech.* 139, 417-434.

Walton, O. R. 1988 Granular Solids Flow Project, Quarterly Report: Jan.-Mar. 1988, UCID-20297-88-1, Lawrence Livermore National Laboratory.

MICROGRAVITY EXPERIMENTS TO EVALUATE ELECTROSTATIC FORCES IN CONTROLLING COHESION AND ADHESION OF GRANULAR MATERIALS

J. Marshall[1], M. Weislogel [2], and T. Jacobson[2], [1]SETI Institute, NASA Ames Research Center, MS 239-12, Moffett Field, CA 94035-1000; jmarshall@mail.arc.nasa.gov, [2] NASA Lewis Research Center MS 500/102, Cleveland, OH 44135

The bulk behavior of dispersed, fluidized, or undispersed stationary granular systems cannot be fully understood in terms of adhesive/cohesive properties without understanding the role of electrostatic forces acting at the level of the grains themselves. When grains adhere to a surface, or come in contact with one another in a stationary bulk mass, it is difficult to measure the forces acting on the grains, and the forces themselves that induced the cohesion and adhesion are changed. Even if a single grain were to be scrutinized in the laboratory, it might be difficult, perhaps impossible, to define the distribution and character of surface charging and the three-dimensional relationship that charges (electrons, holes) have to one another.

The hypothesis that we propose to test in microgravity (for dielectric materials) is that adhesion and cohesion of granular matter are mediated primarily by dipole forces that do not require the presence of a net charge; in fact, nominally electrically neutral materials should express adhesive and cohesive behavior when the neutrality results from a balance of positive and negative charge carriers. Moreover, the use of net charge alone as a measure of the electrical nature of grain-to-grain relationships within a granular mass may be misleading. We believe that the dipole forces arise from the presence of randomly-distributed positive and negative fixed charge carriers on grains that give rise to a resultant dipole moment. These dipole forces have long-range attraction. Random charges are created whenever there is triboelectrical activity of a granular mass, that is, whenever the grains experience contact/separation sequences or friction.

Electrostatic forces are generally under-estimated for their role in causing agglomeration of dispersed grains in particulate clouds, or their role in affecting the internal frictional relationships in packed granular masses. We believe that electrostatic, in particular dipole-mediated processes, are pervasive and probably affect, at some level, everything from astrophysical-scale granular systems such as interstellar nebulae, protoplanetary dust and debris disks, planetary-scale systems such as debris palls from meteorite impact, volcanic eruptions, and aeolian dust storms, all the way to industrial-scale systems in mining, powder and grain processing, pharmaceuticals, and smoke-stack technologies. NASA must concern itself with the electrostatic behavior of dust and sand on Mars because of its potentially critical importance to human exploration. The motion and adhesion of martian surface materials will affect the design and performance of spacesuits, habitats, processing plants, solar panels, and any externally exposed equipment such as surface rovers or communication and weather stations. Additionally, the adhesion of dust and sand could greatly enhance contact with the potentially toxic components of the martian soil.

We have demonstrated /1,2/ in previous microgravity experiments (USML-1 & USML-2) that dipole forces give rise to the rapid conversion of particulate clouds into populations of aggregates (most commonly, filamentary in form). Because filaments appear to be recurring building structures for aggregates, and because of their probable ubiquity in particulate clouds, they are worthy of study for this reason alone. However, both the filaments themselves and the way they respond to electrical fields provide valuable clues to electrostatic forces acting in granular matter. We therefore propose that a very good method of probing the electrostatic character of granular material, in a non-intrusive way, is to allow grains and aggregates to express their interactions through unconstrained motions (acceleration/drift rates, repulsions, attractions) while they are freely suspended under microgravity conditions as part of a dispersed cloud. The motions would be induced by controlled electrical (homogeneous and inhomogeneous) fields and variable degrees of electrical neutralization of the grain cloud.

Thus, the dispersion and protracted suspension of grains is the "tool" of choice for interrogating individual grains regarding their electrostatic properties. In particular, filamentary aggregation of grains in a cloud is a powerful method for determining electrical polarization effects, and relationships between monopole and dipole forces, using growth rates, morphology, and especially the rotational and translational motions of aggregates as diagnostic expressions of the forces at work. Because different electrostatic forces cause different types of motion, this method enables each force to be isolated for study. Experimental investigations will be achieved by modifications to hardware that has already been successful deployment on two USML missions and laid much of the groundwork for the proposed research. Making relatively straightforward modifications to existing flight hardware provides a cost-effectiveness to the research effort.

Substantial progress has been made during the first year of the project; operations are proceeding through two parallel efforts -- scientific experiments and modeling are being studied by the PI (J. Marshall) at NASA Ames, while technical implementation of the project is being studied at LeRC, under the direction of M. Weislogel. At LeRC, an experiment development team has been formed to work with the PI for the identification of the "tall poles" in the design of the experiment. In concert with the PI, the team has worked to quantify the specific science requirements, and will conduct preliminary proof-of-concept tests as necessary. The team will establish the carrier options based on

an early assessment of the hardware necessary to meet the science requirements. Several concepts have already been proposed. These are being reviewed in light of the cost/benefit of an automated verses crew-interactive test apparatus.

The primary science data are obtained by measuring the rates of formation, drift, and rotation of aggregates which form during the experiment procedures. The three-dimensional orientation of the aggregates is also valuable information as are the orientation and density of adhered particles/aggregates to the solid surfaces of the test apparatus. A statistically meaningful population is necessary to draw connections between theory and experiment. Thus, the challenge to designing an experimental apparatus to accomplish the above measurements is to provide a well-characterized "electrostatically clean" test chamber within which an imaging system can record 3-D particle behavior.

Secondary design issues concern the initial dispersion of particles, the ability to control local particle density, variable voltage supply and measurement for the aggregate "manipulators", and the ability to neutralize charged particles. Although several of these issues have been addressed in previous tests by the PI, the cell size, electrostatic shielding techniques, voltage levels, and the particle dispersion-neutralization procedures need to be addressed in proof tests to be performed at NASA LeRC in the coming months. These tests can be performed in the low-g environment of the KC-135 aircraft without significant effort; particle dispersion tests can be performed in simple drop tower experiments. The tests will enable quantitative descriptions of the science requirements for the flight experiment hardware. They will also buttress the fundamental scientific arguments to be presented during NASA's Science Concept Review (SCR) of the experiment.

At Ames, advances have been made in four areas:

(1) Three new models for the behavior of granular materials have been developed by the PI [3,4,5], and were presented at the Lunar & Planetary Science Conference at LPI/NASA JSC in March of 1998: (i) As a direct implication of both microgravity aggregation experiments and ground-based slurry-flow experiments conducted previously by the PI, it is suggested that electrostatic interparticle forces impose a "Coulombic friction" in the motion of grains in clouds, fluidized beds, or granular slurries and flows. Neutralized materials flow faster and become more sluggish" as triboelectric charging occurs. Ionized grain populations where grains may repel one another from acquiring like charges, could result in even lower resistance to motion than even a neutralized grain population, (ii) A densely-populated, triboelectrically charged monodispersed cloud of particulates cannot exist in a steady state unless it is in dynamic equilibrium with continuous mechanical disturbance (kinetic energy input). Inherently, the cloud collapses to an aggregated state, and then collapses further if the aggregates are disturbed. These changes of state have almost exact parallels with phase changes in gas-liquid-solid transitions because they occur precipitously, and they involve densification and energy release. The term "electrostructural phase changes" has been coined to describe the phenomenon, (iii) A model for planetary aeolian transport has been proposed which suggests that flux of wind-blown material is a function of both aerodynamic and bed-dilatancy thresholds; the latter is controlled by elastic energy release and confinement by electrostatic interparticle forces.

(2) Computer modeling efforts have been initiated by the PI to expand upon previous computer replication of filamentary aggregates using the dipole model. In the new work, the number of charge carriers on a grain will be varied so that dipole and monopole interactions become increasingly competitive; sudden behavioral transitions are expected. Once the algorithms have been developed (by T. Sauke of the SETI Institute), they will form the template for modeling the behavior of aggregates in any proposed engineering design for the microgravity experiment. Computer modeling (by D. Stratton of the SETI Institute) has also been initiated to test the cascading flux effect caused by the reptation grain population in the aeolian model just noted.

(3) A sand circulating device has been constructed in the laboratory at Ames to induce triboelectrification of an energetic grain population. This is intended to corroborate the future microgravity work by testing the limits of the dipolarization. At peak triboelectric charge saturation, the Coulombic viscosity of the population might decrease because the dipole moments becomes weakened by the "washing-out" effect of so many charge carriers on the grain surfaces.

(4) Experiments with the same device will be conducted in partnership with W. Farrell at NASA Goddard to determine the exchange of charge carriers between grains using RF signals as indicators of nanoscale electrical discharging.

References:

(1) Marshall, J. Particle Dispersion Experiment (PDE). NASA Conf. Publ. 3272 (II) (Ramachandran et al., eds.) 717732 (1994).

(2) Marshall, J., Freund, F., & Sauke, T. Catastrophic collapse in particulate clouds: Implications from aggregation experiments in the USML-1 and USML-2 Glovebox. USML-2/USMP-3 Launch Plus-One-Year Conf., NASA CP, in press (1998).

(3) Marshall, J. "Coulombic viscosity" in granular materials: Planetary and astrophysical implications. LPSC XXIX, 1135 (1998).

(4) "Electrostructural phase changes" in charged particulate clouds: Planetary and astrophysical implications. LPSC XXIX, 1132 (1998).

(5) Marshall, J., Borucki, J. & Sagan, C. Aeolian sand transport in the planetary context: Respective roles of aerodynamic and bed-dilatancy thresholds. LPSC XXIX, 1131 (1998).

SINGLE BUBBLE SONOLUMINESCENCE IN LOW GRAVITY AND OPTICAL RADIATION PRESSURE POSITIONING OF THE BUBBLE

D. B. Thiessen, J. E. Young, M. J. Marr-Lyon, S. L. Richardson, C. D. Breckon, S. G. Douthit, P. S. Jian, W. E. Torruellas, P. L. Marston, Department of Physics, Washington State University, Pullman, WA 99164-2814; marston@wsu.edu

ABSTRACT

Several groups of researchers have demonstrated that high frequency sound in water may be used to cause the regular repeated compression and luminescence of a small bubble of gas in a flask. The phenomenon is known as single bubble sonoluminescence (SBSL). It is potentially important because light emitted by the bubble appears to be associated with a significant concentration of energy within the volume of the bubble. Unfortunately, the detailed physical mechanisms causing the radiation of light by oscillating bubbles are poorly understood and there is some evidence that carrying out experiments in a weightless environment may provide helpful clues. In addition, the radiation pressure of laser beams on the bubble may provide a way of simulating weightless experiments in the laboratory.

The standard model of SBSL attributes the light emission to heating within the bubble by a spherically imploding shock wave to achieve temperatures of 50,000 K or greater. In an alternative model [A. Prosperetti, J. Acoust. Soc. Am. **101**, 2003–2007 (1997)] the emission is attributed to the impact of a jet of water which is required to span the bubble and the formation of the jet is linked to the buoyancy of the bubble. The coupling between buoyancy and jet formation is a consequence of the displacement of the bubble from a velocity node (pressure antinode) of the standing acoustic wave that drives the radial bubble oscillations. One objective of this grant is to understand SBSL emission in reduced buoyancy on KC-135 parabolic flights. To optimize the design of those experiments and for other reasons which will help resolve the role of buoyancy, laboratory experiments are planned in simulated low gravity in which the radiation pressure of laser light [B. T. Unger and P. L. Marston, J. Acoust. Soc. Am. **83**, 970–975 (1988)] will be used to position the bubble at the acoustic velocity node of the ultrasonic standing wave. Laser light will also be used to push the bubble away from the velocity node, increasing the effective buoyancy.

The original experiments on the optical levitation and radiation pressure on bubbles in water by Unger and Marston noted above were carried out using a continuous wave (CW) beam of an Ar-ion laser. For lateral stability the beam had a intensity minimum along its axis. Calculations [D. B. Thiessen and P. L. Marston, J. Acoust. Soc. Am. **102**, 3185 (1997)] of the optical radiation force on an SBSL bubble indicate that ion laser technology is a poor choice for providing the magnitude of the average optical radiation force required. Consequently (as explained in our proposal) it is necessary to examine various diode-pumped solid state laser technologies. The approach for this part of the research will be to achieve optical levitation of a quiescent bubble based on contemporary laser technology and then to strobe the laser synchronously with the SBSL bubble oscillations.

Progress: The grant started early in 1998. With assistance from a group of undergraduate physics majors (J. Young, S. Richardson, C. Breckon, and S. Douthit), preliminary measurements were made in March 1998 of the SBSL average intensity as the effective gravitational acceleration g was varied on NASA's KC-135 aircraft. The effective g levels were varied between a hypergravity condition ($g \approx 2$) and low gravity ($g \approx 0$). This used an improved procedure over our earlier experiments [J. E. Young et al., in Proceedings of the 16th International Congress on Acoustics (at press)]. The effective g was monitored and recorded along with the average current output from a photomultiplier tube (PMT) which monitored the SBSL emission. The experiments demonstrate conclusively that the SBSL emission is maintained during the reduced gravity available on the KC-135. During the typical cycling of g between hyper gravity and low gravity conditions the SBSL intensity grew steadily during the first 10 seconds of low g. It is appropriate to note, however, that it was not possible to regulate certain environmental conditions such as the ambient pressure in this preliminary experiment. Consequently it will be necessary to improve the apparatus prior to concluding that low gravity is the cause of the increased SBSL intensity. In addition, there was some background drift of the SBSL intensity during a typical 15 minute long set of parabolas and that drift may also have been environmentally caused.

There has also been progress in the development of a suitable solid state laser. P. S. Jian and W. E. Torruellas have constructed a laser-diode pumped Nd:YVO_4 laser with a CW output of 8.5 watts at a wavelength of

1.06 μm. A frequency doubler placed within the laser cavity produces an output of 3.5 watts in the visible. While these power levels are sufficient for the planned experiments, it will be necessary to alter the transverse modal structure to produce a beam pattern similar to the one used by Unger and Marston and then to Q-switch the laser.

This work is supported by NASA grant NAG3-2114.

AN INTERFEROMETRIC INVESTIGATION OF CONTACT LINE DYNAMICS IN SPREADING POLYMER MELTS AND SOLUTIONS

G. H. McKinley[1] and B. Ovryn[2], [1]Mechanical Engineering, M.I.T. Room 3 –250, 77 Massachusetts Avenue, Cambridge, MA 02139 (gareth@mit.edu) [2]Mechanical and Aerospace Engineering, Case Western Reserve University and NCMR, NASA Lewis, MS-110-3, 21000 Brookpark Road, Cleveland, Ohio, 44135 (ovryn@wave.lerc.nasa.gov)

INTRODUCTION

Moving contact-line problems in polymeric materials are encountered in many coating flows, gravity-driven drainage and in spin-coating operations where spreading arises from the combined action of gravitational and/or centrifugal body forces on a deposited droplet. Examples of industrial processes where spreading of a viscous liquid over a flat dry substrate is important include: dip-coating of sheet metal; gravity drainage of paints; spin-coating of surface layers on silicon substrates and coating of inks on paper. Typically, the polymeric material is dissolved in a low-vapor pressure solvent that evaporates increasingly rapidly as the surface area of the film increases. Achieving a spatially uniform coating requires careful control and understanding of the mechanisms that influence the radial spreading dynamics of a fluid droplet. As the mass fraction of solvent progressively decreases, the viscoelastic properties become increasingly important. The interface profile is therefore governed by an ever-changing balance between surface tension, viscous stresses and elastic stresses, and pronounced differences in the shape of the interface between Newtonian and non-Newtonian droplets have been predicted and observed experimentally.

The theoretical and experimental literature associated with the dynamics and stability of the slow {~*O*(seconds)} spreading of a viscous liquid over a flat dry substrate is extremely extensive and several excellent reviews are available (Padday, 1978; Dussan V, 1979, de Gennes, 1985). These reviews show that in addition to the bulk properties of the coating fluid (the viscosity μ and density ρ) and the equilibrium surface properties (the surface tension σ and the equilibrium contact angle θ_e) it is also important to understand the local dynamics of the motion of the contact line (or 'common line') between the liquid, the vapor and the solid substrate, typically characterized by a dynamic advancing contact angle θ_a. Application of the no-slip boundary condition of continuum fluid mechanics at the advancing contact line leads to a well-known singularity in the fluid stresses (cf. Dussan V, 1979) and it is necessary to relax this condition. Numerous methods have been proposed to deal with this singularity including (but not limited to) the possibility of local fluid slip in a microscopic region at the contact line or the existence of a thin 'precursor film' in advance of the macroscopically observable contact line (de Gennes 1985). A number of theoretical studies have shown how it is possible to systematically decompose the full spreading and wetting problem into a number of simpler sub-problems that are connected by matched asymptotic expansions (e.g. Goodwin & Homsy, 1991).

- In the bulk of the fluid (denoted *Region I* by Homsy & coworkers), on length scales of (typically) greater than a few microns, the slow motion of the spreading fluid film is described globally by a lubrication analysis appropriate to the geometry of interest and capillary effects are, in general, negligible since the surface is almost flat.
- In a smaller 'inner region;' (*Region II*) capillary effects become important and, in conjunction with the viscous stresses in the film, balance the imposed body force driving the spreading (e.g. the gravitational body force or angular rotation) and govern the shape of this region.
- In *Region III*, (on length scales of 100 Å and smaller) 'long range' forces (in a molecular sense) become important in the wetting of the substrate and there exists the possibility of the formation of a precursor film or local slip between the fluid and solid molecules.

We have begun the preliminary phase of a four year investigation to systematically measure the spatial and temporal evolution of surface profiles of Newtonian liquids, weakly elastic dilute polymer solutions, inelastic shear thinning fluids and oligomeric polymer melts that develop in the inner and outer regions (I, II) of the flow down an inclined plane using a recently developed phase shifted laser feedback interference microscope (Ovryn B and Andrews J H 1998). This instrument is capable of measuring changes in the optical path–length (film thickness) with high axial precision {~*O*(nm)}, high transverse spatial resolution {~*O*(300μm)} and short temporal resolution {~*O*(ms)}. An important attribute of this interferometer is that the previous operating parameters can be achieved with minimal power deposited on a thermally sensitive liquid film {~*O*(μW/cm^2)}.

To elucidate the possible rheological behavior near the contact line, experiments will focus on a single solid substrate (polished silicon wafers) and four distinct classes of fluids; a simple viscous Newtonian reference standard, a dilute polymer solution, an inelastic shear-thinning fluid and a weakly entangled oligomeric melt. Access to a microgravity environment will ultimately be important for two reasons: (1) in the absence of centrifugal forces arising from droplet rotation, the experimental spreading rate can be systematically controlled by varying the gravitational body force imposed on the drop and (2) the 'inner scale' region over which elastic, viscous and capillary effects are all important will be physically enlarged as the gravitational driving force is reduced.

NON-NEWTONIAN RHEOLOGY

In many commercially important operations the rheology of the fluid coating may be non-Newtonian (*i.e.* it may exhibit shear-thinning in the viscosity or the presence of additional viscoelastic normal stresses; Bird *et al.* 1987) which can have a very important effect in the region of high shear rate and on the complex two-dimensional flow near the advancing contact line. The review by de Gennes (1985) discusses the few quantitative measurements of the film profiles in Region II, and the connection to the first two suggested boundary conditions in Region III, however he points out that because of the experimental difficulties involved *"we do not yet have a quantitative experimental law for the simplest (steady state) film profile"* as the rate of spreading is varied (e.g. by changing the bulk viscosity, the temperature or the angle of the inclined plane) even in a simple liquid.

EXPERIMENTAL PLAN

In order to focus on the wide range of possible rheological behavior near the contact line, the proposed experiments focus on a single solid substrate (polished silicon wafers) and four distinct classes of fluids; a simple viscous Newtonian reference standard, a dilute polymer solution, an inelastic shear-thinning fluid and a weakly entangled oligomeric melt. A phase shifted laser feedback interference microscope will be used to probe *both* the outer and inner (Regions I & II) fluid dynamics of an advancing sheet of fluid.

An inclined plane geometry will be employed with individual polished silicon wafers (surface roughness typically $\leq$ 10 nm) and which can be coated to vary the surface wetting characteristics. The wafers will be mounted on Peltier heating elements providing both an isothermal boundary condition and allowing uniform elevation of the experimental test temperature; the latter will be especially useful when highly entangled high molecular weight polymer melts are employed.

The measured profiles of surface height will be compared with the predictions of the similarity solutions. To explore the influence of fluid rheology on the possible 'core region' mechanisms that might relieve the stress singularity at the contact line, four distinct classes of fluid will be examined:

(i) A Newtonian fluid of moderate viscosity and low molecular weight (e.g. glycerol, oligomeric melts of PIB, PS or polydimethylsiloxane (PDMS)) will first be examined as a control. More viscous PDMS oils with higher molecular weights are deliberately excluded from consideration here, because of their possibly anomalous melt-like behavior (de Gennes, 1985);

(ii) A high-viscosity dilute polymer solution (referred to generically as a 'Boger fluid'; Boger 1977/78) will be studied to investigate the first effects of elasticity. A Boger fluid consisting of 0.05 wt% monodisperse polystyrene dissolved in a Newtonian oligomeric styrene can readily be prepared (Spiegelberg & McKinley, 1997). Studies of the spreading characteristics of such fluids in Region I have shown that at least macroscopically (in length scales $x >$ 1mm) the fluids behave similarly to Newtonian fluids (Fraysse & Homsy 1994) after initial viscoelastic transients have decayed, however, the local surface profile in region II is unknown.

(iii) An inelastic shear-thinning fluid will be studied in order to investigate if shear-thinning near the contact line can eliminate the singular stresses and obviate the need for a core region. Aqueous solutions prepared from moderate concentrations (2 wt% – 5 wt%) of Xanthan gum exhibit almost immeasurable elasticity and shear-thinning across a wide range of shear rates.

(iv) The effects of polymeric entanglements will be examined by focusing on a homologous series of progressively higher molecular weight PDMS oils and 'gums'. To facilitate the flow of these materials, the spreading experiments will be performed at elevated temperatures using the Peltier hot stage.

CONCLUSIONS

We have begun a four-year investigation to measure the dynamics in a small inner region of a fluid near an advancing contact line. For non-Newtonian fluids, the resulting film profile is predicted to be markedly different to that expected in simple Newtonian liquids and this leads to changes in the stability of the advancing fluid film. When the gravitational body force on the film is lowered the extent of the 'inner' region near the contact line singularity is expanded, and can be imaged using interferometry. Phase shifted laser feedback interferometry has both sufficient lateral and vertical spatial resolution to accurately resolve systematic variations in the film profiles as the bulk rheology of the fluid is modified.

REFERENCES

Boger, D.V., A Highly Elastic Constant-Viscosity Fluid, *J. Non-Newtonian Fluid Mech.*, **3**, (1977/78), 87-91.

de Gennes, P.-G., Wetting: Statics and Dynamics, *Rev. Mod. Phys.*, **57**, (1985), 827.

Dussan V, E.B., On the Spreading of Liquids on Solid Surfaces: Static and Dynamic Contact Lines, *Ann. Rev. Fluid Mech.*, **11**, (1979), 371.

Fraysse, N. and Homsy, G.M., An experimental Study of Rivulet Instabilities in Centrifugal Spin-Coating of Viscous Newtonian and non-Newtonian Fluids, *Phys. Fluids*, **6**(4), (1994), 1491-1504.

Goodwin, R. and Homsy, G.M., Viscous flow down a slope in the vicinity of a contact line, *Phys. Fluids A*, **3**(4), (1991), 515-528.

Ovryn, B. and Andrews, J.H., Phase-Shifted Laser Feedback Interferometry, *Opt. Let.*, **23(14)**, (1998), In press.

Padday, J.F., *Wetting, Spreading & Adhesion*, Academic Press, New York, 1978.

Spiegelberg, S.H. and McKinley, G.H., Stress Relaxation and Elastic Decohesion of Viscoelastic Polymer Solutions in Extensional Flow, *J. Non-Newtonian Fluid Mech.*, **67**, (1997), 49-76.

NUMERICAL SIMULATION OF PARAMETRIC INSTABILITY IN TWO AND THREE-DIMENSIONAL FLUID INTERFACES.

C. Pozrikidis[1] and S. A. Yon[1], [1]Dept. of Applied Mechanics and Engineering Sciences, University of California, La Jolla, California 92093 syon@ames.ucsd.edu.

Fluid interfaces are susceptible to an instability induced by harmonic oscillation of the imposed body force. Faraday's original observations in 1831, and numerous subsequent experimental investigations have indicated that when the acceleration is perpendicular to the undisturbed surface, the interface may develop standing waves which generally exhibit a square unit cell while oscillating with half the frequency of the imposed acceleration. A large number of experimental studies have shown that the harmonically forced interface may sustain large but finite amplitude waves over a broad range of frequencies and amplitudes of the forcing vibration. One striking feature of the motion is that, as the amplitude of the oscillation is increased, spatially periodic waves with square, hexagonal, or triangular unit cells yield disordered or fluctuating states which may have a profound effect on the rate of mixing at the interface as well as the motion of drifting fluid parcels and suspended particles, and bubble generation and entrainment by interfacial structures. In addition, as the fluids become more viscous, doubly-periodic three-dimensional waves are replaced by linear two-dimensional waves. Further, under certain conditions, the interface may develop soliton-like structures.

In the absence of viscous forces, linearization of the governing equations yields a Mathieu equation, the solutions of which reveal the existence of regimes in which the amplitude of the standing interfacial waves is periodic or non-periodic but bounded, and other regimes in which the amplitude grows exponentially and the flow is unstable. When viscous forces cannot be neglected, the linearized evolution equations yield an eigen-value problem involving partial differential equations. Most previous investigators have emulated the effects of viscosity by inclusion of a damping term in the Mathieu equation or a dissipation term in the boundary integral formulation.

We study the fully non-linear behavior of forced standing waves at the interface between two generally viscous fluids with different densities in the presence of surface tension, considering both two-dimensional and three-dimensional doubly-periodic waves. We concentrate on large amplitude waves with steep interfacial deformations, study the characteristics of non-periodic and disordered states, and establish conditions for interfacial breakup.

Considering the interface between two stably stratified, effectively inviscid fluids of finite depth with non-vanishing interfacial tension, dimensional analysis indicates the behavior of the interface depends on the depth ratio, the density ratio, two reduced wave numbers, the reduced amplitude of the oscillation, the Bond number and the effective Froude number. When the density of the upper fluid is negligible, application of standard boundary integral techniques yields an integral equation relating the potential on the interface to the normal component of interfacial velocity. Careful selection of the Green's function, considering periodicity of the interface and the presence of vertical and lateral boundaries greatly simplifies the domain of the integral operators. Given the distribution of potential on the interface at some initial time, we obtain a Fredholm integral equation of the first kind for the normal velocity on the interface, while the evolution of the potential is governed by the unsteady Bernoulli equation. Alternately, confining our attention to two-dimensional waves, we may regard the motion as being induced by a vortex sheet coincident with the interface. Describing the interface in terms of a Lagrangian coordinate, we express the evolution of the interface in terms of the Biot-Savart law, while the strength of the sheet obeys a more complicated evolution equation.

The effects of viscosity on the morphology of interfacial waves have been studied only in the context of Floquet theory for linearized disturbances. We plan to conduct an extensive numerical study of the viscous problem using two classes of numerical techniques: (a) The immersed boundary method of flows with non-vanishing Reynolds number, and (b) the boundary integral method for Stokes flow when the effects of inertia are negligible. In the limit of vanishing Reynolds number, the governing equations become linear with respect to velocity and pressure, and the oscillations of the interface are in phase with the imposed acceleration. In the limit as Reynolds number increases without bound, and for small disturbances, we obtain behavior similar to that described by Mathieu's equation. In our investigation of the viscous problem, our objectives are: 1) Describe changes in the frequency of oscillation as the effects of inertia become more important; 2) Describe the associated changes in the shapes of the standing waves; 3) Describe the mechanisms of unsteady vorticity generation at the interface.

COMPLEX DYNAMICS IN MARANGONI CONVECTION WITH ROTATION

H. Riecke, F. Sain, Engineering Sciences and Applied Mathematics, Northwestern University, Evanston, IL 60208, h-riecke@nwu.edu

Under conditions of reduced gravity surface-tension gradients become increasingly important in driving convection with free surfaces. In contrast to Boussinesq buoyancy-driven convection the typical planform of the convection pattern is hexagonal. While complex dynamics have been studied in great detail in systems that lead to roll- or stripe-like patterns, this is not the case for hexagonal structures. Due to their increased bending rigidity spatio-temporal chaos in hexagonal structures may be qualitatively different from that observed in Rayleigh-Bénard convection. The goal of this project is to investigate various instabilities of hexagonal structures, focussing on those that are due to the effect of rotation and on the complex dynamics that are expected to arise from them. These questions are of fundamental and of applied interest. For instance, the results may be relevant, for instance, to crystal growth from the melt, which is often performed in the presence of rotation, where convection affects the impurity distribution in the growing solid.

In buoyancy-driven convection the effect of rotation on the stability of the roll structures has been studied extensively. One of the striking features is the fact that even directly at the onset of convection the usually stable stripe pattern can become unstable if the rotation rate is large enough. This Küppers-Lortz instability is due to the Coriolis force. It renders rolls of one orientation unstable to rolls of a different orientation leading to a persisting switching of orientations. In systems with large aspect ratio this switching occurs incoherently in space in the form of fronts propagating through the system.

So far, the effect of rotation on hexagonal structures has been studied mainly within the context of three coupled amplitude equations describing the three sets of rolls that make up the hexagons. It is found that the steady transition from hexagons to rolls that typically occurs as the amplitude of the pattern is increase is replaced by a Hopf bifurcation. It leads to a periodic oscillation of the individual roll amplitudes that make up the hexagonal pattern. The oscillations are phase-shifted such that at different times a different set of rolls dominates.

The project will involve a number of main aspects. The stability investigations will be based on amplitude equations, Ginzburg-Landau equations, and long-wave equations. These will be derived in suitable limits from the fluid equations. The stability analyses will be largely done analytically, to be followed by extensive numerical simulations to study the complex dynamics that are expected to arise.

We will focus on a single convecting layer bounded on one side by a plate and having a free surface on the other side. The heating will be applied from the side of the plate. The rotation will be assumed to be small enough to ignore the centrifugal force, and the surface tension will be assumed to be large enough to keep the surface flat. A weak residual gravity field is assumed which affects the layer mainly through the hydrostatic pressure. Under these conditions we will be able to perform a weakly nonlinear analysis leading to amplitude and Ginzburg-Landau equations for the three sets of rolls that are rotated with respect to each other by 120°. For poorly conducting plates we will be able to perform also a strongly nonlinear analysis based on the long wavelength of the instability. With respect to the investigation of the expected complex dynamics the long-wave equation will have the great advantage over Ginzburg-Landau equations in that it preserves the isotropy of the system.

We will first perform a weakly nonlinear analysis and derive the three coupled Ginzburg-Landau equations describing hexagons of a fixed orientation from the fluid equations. This will allow predictions for the Hopf bifurcation identified previously by Swift. Then we will investigate side-band instabilities within this framework, both of the steady hexagons and of the oscillating hexagons. The latter will require the derivation of three coupled equations for the amplitude of oscillation and two phases, which arise from the two translational symmetries of the system. Of interest is in particular whether the side-band instabilities can lead to persistent complex dynamics. This will be investigated by detailed numerical investigations of the coupled Ginzburg-Landau equations.

In order to obtain equations that preserve the isotropy of the system we will derive long-wave equations. This is possible for poorly conducting boundaries. The long-wave equation will be considerably simpler than the full fluid equations and will allow a full stability analysis for small amplitudes. Of particular interest will be perturbations that are rotated with respect to the original hexagons. Our preliminary calculations show that the straightforward perturbation calculation is of limited use since it leads to singularities when the wave vector of the perturbing modes approaches one of the wave vectors of the hexagonal pattern. To remove these resonances a considerably more involved perturbation calculation is necessary. The main result from that calculation will be the determination of the stability limits for hexagons as a function of the heating and the wave number of the hexagons. It will also show in which regime the Hopf bifurcation of Swift will be relevant and where it will be preempted by a Hopf bifurcation at a finite angle between the hexagon and the perturbation. In addition, the usual side-band instabilities will arise.

In both regimes, the weakly nonlinear and the long-wave one, the derivation of the reduced equations will be used to identify regimes in which the theoretically obtained results are accessible in experiments. Since in buoyancy-driven convection the effect of rotation has been studied experimentally in great detail it is to be expected that such experiments can also be performed for surface-tension driven convection.

Further extensions within this project may address instabilities of Marangoni convection with free-slip boundary conditions at the top and at the bottom. This is relevant for freely suspended films. In buoyancy-driven convection it has been found that for these boundary conditions even arbitrarily slow rotation can destabilize the roll pattern. Whether this is also the case for the hexagonal structures in surface-tension driven convection is not known.

The Effect of Surface Induced Flows on Bubble and Particle Aggregation

Scott A. Guelcher, Yuri E. Solomentsev, Marcel Böhmer*, John L. Anderson, and Paul J. Sides**

Department of Chemical Engineering
Carnegie Mellon University
Pittsburgh, PA 15213

*Philips Research Laboratories
Eindhoven, Prof. Holstlaan 4
5656 AA Eindhoven, The Netherlands

**Corresponding author: ps7r@andrew.cmu.edu

ABSTRACT

Almost 20 years have elapsed since a phenomenon called "radial specific coalescence" was identified. During studies of electrolytic oxygen evolution from the back side of a vertically oriented, transparent tin oxide electrode in alkaline electrolyte, one of the authors (Sides) observed that large "collector" bubbles appeared to attract smaller bubbles. The bubbles moved parallel to the surface of the electrode, while the electric field was normal to the electrode surface. The phenomenon was reported but not explained. More recently self ordering of latex particles was observed during electrophoretic deposition at low DC voltages likewise on a transparent tin oxide electrode. As in the bubble work, the field was normal to the electrode while the particles moved parallel to it. Fluid convection caused by surface induced flows (SIF) can explain these two apparently different experimental observations: the aggregation of particles on an electrode during electrophoretic deposition, and a radial bubble coalescence pattern on an electrode during electrolytic gas evolution. An externally imposed driving force (the gradient of electrical potential or temperature), interacting with the surface of particles or bubbles very near a planar conducting surface, drives the convection of fluid that causes particles and bubbles to approach each other on the electrode.

Modeling of Transport Processes in a Solid Oxide Electrolyzer Generating Oxygen on Mars

K. R. Sridhar

The University of Arizona

Tucson, Arizona

The objective of this work is to obtain a better understanding of the transport processes that occur in a solid oxide electrolyzer that generates oxygen from carbon dioxide for life support and propulsion needs. A solid oxide electrolyzer is an electrochemical device that uses a d.c. electric potential to separate oxygen from oxygen bearing gases. The device is made of a solid nonporous electrolyte that is sandwiched between porous electrodes to form an electrochemical cell. Oxygen separation occurs by virtue of the fact that oxygen is ionically transported, selectively, across the nonporous electrolyte when an electric potential is applied. The work is in the area of In Situ Resource Utilization (ISRU), specifically transport processes associated with the generation of oxygen from the predominantly carbon dioxide atmosphere of Mars. It should be noted that ISRU has been identified as one of the key areas that needs to be developed to facilitate human missions to Mars. This work will seek to establish a scientific understanding for one of the key technologies required for future human missions to Mars.

All the major studies conducted by NASA in the recent past have identified the need for utilizing space resources, i.e., "living off the land," as a key technology for future space exploration. Several studies have shown that producing oxygen from the Martian atmosphere for propulsion needs could reduce the cost of both robotic and human return missions. In addition, the generation of oxygen by this means and maintaining an emergency cache for life support could considerably reduce the risks.

There are several transport processes that occur in a solid oxide electrolyzer that generates oxygen from carbon dioxide. Transport processes include the mass transfer of the reactants and products, heat transfer due to the chemical reactions, external heating to supply energy for the endothermic reaction, and charge transfer reactions that accompany the electrochemical transport of oxygen. The electrolyzer operates at temperatures in the range of 850 to 1000 Celsius since the oxygen ion conductivity and the chemical kinetics of carbon dioxide dissociation favor high temperature operation. While the d.c. current associated with the process is determined by the number of oxygen ions transported, the applied potential is made up of reversible and irreversible components. The energy efficiency of the electrolyzers can be substantially increased if the irreversible portion of the d.c.potential, associated with the concentration gradients and charge transfer barri-

ers, can be minimized. The overpotentials associated with the two irreversibilities are called concentration and surface polarizations, respectively. The concentration polarization is a function of the geometry of the electrolyzer, the gas flow paths and flow rates, the temperature profile of the electrolyzer surfaces, and the mass flux of oxygen generated. The surface overpotential will depend on the electrode materials, surface morphology, and the nature of the interface at the electrode/ electrolyte boundary. In an electrolyzer stack, the arrangement of the interconnects and the paths of electron flow will also have a big effect on the mass flux density of oxygen generated. An understanding of the potential field in a stacked electrolyzer is essential to the development of efficient devices. A thorough understanding of the different transport processes that occur in the electrolyzer is critical to designing efficient electrolyzers for space applications.

Currently, an experimental program is underway and simple proof-of-concept electrolyzer cells are being used to obtain data that will help characterize the performance of the electrolyzer. The electrode materials, porosity and tortuosity of the electrodes, grain size, and the nature of the three phase boundary will be varied systematically. performance data will be obtained in each case to quantify the effect of electrode morphology on cell performance. To understand the effect of three phase boundary on cell performance fractal shaped electrodes, and pitting and/or cladding of the electrolyte to increase effective surface area will be attempted. A mathematical model based on transport equations and material properties obtained from the experimental program will be developed to completely characterize the transport processes that occur in the electrolyzer.

A solver for mixed convection heat transfer (both forced and free convection based on the reduced gravity environment of Mars) using the penalty-based finite element method will be developed. A second transport equation will also be included in the solution routine to solve for mass transfer simultaneously with the mass flux boundary condition. The mass flux boundary condition will simulate the production of oxygen at the electrode. Faraday's law and Fick's law will be used to equate the molar flux to the current density per unit-active area of the electrochemical cell. The experimental data obtained from laboratory experiments will quantify the porosity and tortuosity of the porous electrodes that are used in the electrolyzer. The modeling will include the diffusion of gases through the porous electrodes. The following equations will be used to model the flow: (1) balances for energy and each chemical species, (2) rate equations for the transports and for chemical kinetics, (3) relevant constants and properties from the experimental investigations, and (4) appropriate boundary conditions.

Unlike solid oxide fuel cells and terrestrial oxygen generators (from air), the environment, operating conditions, and figures of merit for the Mars oxygen generator are quite different. This necessitates a dedicated study of this problem for NASA applications. The endothermic nature of the carbon dioxide dissociation reaction, the advantage of operating the electrolyzer at pressures well below one bar and the diurnal thermal cycling of the electrolyzer due to power constraints, all make this application unique.

The P.I. is also building an "Oxygen Generator System (OGS)" that will be the principal experiment on the Mars In-situ Propellant Production Precursor (MIP) payload that will fly aboard the 2001 Mars Lander. OGS will demonstrate production of oxygen from the Mars atmosphere.

COMPUTATIONS OF BOILING IN MICROGRAVITY

G. Tryggvason[1] and D. Jacqmin[2], [1]The University of Michigan, Department of Mechanical Engineering and Applied Mechanics, 2031 Automotive Laboratory, Ann Arbor, MI 48109-2121 (gretar@engin.umich.edu), [2] NASA Lewis Research Center, 2100 Brook Park Road, Cleveland, OH 44135 (fsdavid@lerc.nasa.gov).

The absence (or reduction) of gravity, can lead to major changes in boiling heat transfer. On Earth, convection has a major effect on the heat distribution ahead of an evaporation front, and buoyancy determines the motion of the growing bubbles. In microgravity, convection and buoyancy are absent or greatly reduced and the dynamics of the growing vapor bubbles can change in a fundamental way. In particular, the lack of redistribution of heat can lead to a large superheat and explosive growth of bubbles once they form. While considerable efforts have been devoted to examining boiling experimentally, including the effect of microgravity, theoretical and computational work is limited to very simple models.

In this project, the growth of boiling bubbles is studied by direct numerical simulations where the flow field is fully resolved and the effects of inertia, viscosity, surface deformation, heat conduction and convection, as well as the phase change, are fully accounted for. The proposed work is based on previously funded NASA work that allowed us to develop a two-dimensional numerical method for boiling flows and to demonstrate the ability of the method to simulate film boiling. While numerical simulations of multi-fluid flows have been advanced in a major way during the last five years, or so, similar capability for flows with phase change are still in their infancy. Although the feasibility of the proposed approached has been demonstrated, it has yet to be extended and applied to fully three-dimensional simulations. Here, a fully three-dimensional, parallel, grid adaptive code will be developed.

The numerical method will be used to study nucleate boiling in microgravity, with particular emphasis on two aspects of the problem:

- Examination of the growth of bubbles at a wall nucleation site and the instabilities of rapidly growing bubbles. Particular emphasis will be put on accurately capturing the thin wall layer left behind as a bubble expands along a wall, on computing instabilities on bubble surfaces as bubbles grow, and on quantifying the effects of both these phenomena on heat transfer.
- Examination of the effect of shear flow on bubble growth and heat transfer. Experimentally it is well known that boiling in a forced flow can be fundamentally different from boiling in a quiescent liquid. A fully three-dimensional code will allow shear to be introduced.

In addition to fundamental scientific knowledge, this research will provide critical knowledge for the use of two-phase systems for transport of material and energy in space. The proposed work will also have a major methodological component since considerable numerical development is required. The key steps are:

- Extension of the current two-dimensional methodology to three-dimensional flows. For validation purposes, the method will first be implemented for film boiling and growth of bubbles in pipes. The code will be built on an already existing fully parallel code for isothermal problems.
- Development of adaptive gridding capabilities. Initially, nonunifom stretched grids will be used to concentrate grid points near the growing bubble, later fully dynamic adaptive gridding will be incorporated.

The goal of this project is to advance the state-of-the-art in simulations of multiphase flows to the point at which fully three-dimensional simulations of large boiling systems and use direct simulations to obtain fundamental insight into the dynamics of nucleate boiling in microgravity are possible. The development will have a major impact on the current understanding of boiling and allow investigations that are currently not possible. Although this project does not contain an experimental component, it fits in with a number of ongoing NASA projects on boiling in microgravity. As such, this study will both aid in the analysis of available and forthcoming data as well as produce tools that will aid in the design of future experiments.

Boiling involves both fluid flow and heat transfer and thus requires the solution of the Navier-Stokes and energy equations. We write one set of governing transport equations which is valid in both the liquid and vapor phases. This local, single-field formulation incorporates the effect of the interface in the governing equations as source terms which act only at the interface. These sources account for surface tension and latent heat in the equations for conservation of momentum and energy as well as mass transfer across the interface due to phase change. It is important to recognize that the single-field formulation naturally incorporates the correct mass, momentum and energy balances across the interface. Integration of the conservation equations across the interface directly yields the jump

conditions derived in the local instant formulation for two-phase systems

The numerical implementation of these equations combines ideas from the front-tracking methods developed originally for isothermal multifluid flows (Unverdi and Tryggvason, 1992) and solidification without fluid flow (Juric and Tryggvason, 1996). The fundamental idea is that the equations are solved on a fixed grid by a finite difference method but the interface is represented by separate, non-stationary computational points connected to form a two-dimensional front which lies within the three-dimensional stationary mesh. The interface points are used to calculate geometric information. We find the curvature, and the normal and the tangent vector at each interface point by fitting polynomials through the points. The front is advected in a Lagrangian fashion by the normal velocity. Computations of surface tension, curvature, and the construction of the various material fields, given the location of the interface, and regridding of the front follows Unverdi and Tryggvason (1992). The key addition when in simulating boiling is the energy equation which is solved by an iterative scheme to adjust the propagation velocity of the phase boundary in such a way that the correct interface temperature is obtained at the end of each time step and the right expansion of at the phase boundary takes place. The solution algorithm used here has been implemented for two-dimensional flow as described in Juric and Tryggvason (1997). The method has been validated by comparison with analytical solutions for simple one-dimensional problems, by comparisons with results from stability analysis of nearly flat phase boundaries, and by extensive grid refinement studies. The method has been used to examine film boiling and even though the simulations are only two-dimensional, the predicted heat fluxes agree reasonably well with experimental correlations.

The original method with no phase change has been applied to a number of multifluid problems, and these developments form the background for the current work. Extensive simulations of the motion of many two- and three-dimensional bubbles (Esmaeeli and Tryggvason, 1996, 1997) have been used to obtain detailed insight into the effect of void fraction as well as deformability of the collective bubble interactions as well as the interactions of the bubbles with the surrounding fluid. A fully parallelized version of the method has been used to simulate 64 bubbles is on a 128^3 grid using eight processors on the IBM-SP2 machine at the Center for Parallel Computing at the University of Michigan (Bunner and Tryggvason, 1997).

Similar studies have been done for suspensions of drops in a channel and the collision of drops (Nobari, Jan, and Tryggvason, 1996: Nobari and Tryggvason, 1996). The method has been extended to include various physical effects such as surfactants and theromcapillary migration Nas and Tryggvason, 1993). As a preliminary for the development of a method for phase change, a method has been developed to examine the solidification of pure materials, including the formation of dendrites, in the absence of flow (Juric and Tryggvason, 1996).

The physical problem addressed in this study is of fundamental importance for thermal/fluid management in microgravity. Since flow regimes are usually very different than on earth, design data obtained on earth is generally not applicable to microgravity conditions. This study will result in both a greatly improved understanding of boiling multiphase as well as tools that can be used to address other situations. This should greatly reduce the need for experiments for relatively simple situations and help plan experiments for more complex flows.

REFERENCES

B. Bunner and G. Tryggvason, "Direct Simulations of Multi-Phase Flow," Proceedings of ISAC '97 JAPAN

A. Esmaeeli and G. Tryggvason, "An Inverse Energy Cascade in Two-Dimensional, Low Reynolds Number Bubbly Flows." *J. Fluid Mech.* 314 (1996), 315-330.

A. Esmaeeli and G. Tryggvason, "Direct Numerical Simulations of Bubbly Flows. Part II—Moderate Reynolds Number Arrays" Submitted to *J. Fluid Mech.*

D. Juric and G. Tryggvason. Computations of Boiling Flows. To appear in *Int'l. J. Multiphase Flow.*

D. Juric and G. Tryggvason, "A Front Tracking Method for Dentritic Solidification." *J. Comput. Phys.* 123, 127-148, (1996).

S. Nas and G. Tryggvason. Computational investigation of the thermal migration of bubbles and drops, Proc. ASME Winter Annual Meeting, 1993, FED-175, pp. 71-83.

M.R. Nobari and G. Tryggvason. Numerical Simulations of Three-Dimensional Drop Collisions. *AIAA Journal* 34 (1996), 750-755.

M.R. Nobari, Y.-J. Jan and G. Tryggvason. "Head-on Collision of Drops--A Numerical Investigation." *Phys. Fluids* 8, 29-42 (1996).

S.O. Unverdi and G. Tryggvason. A front-tracking method for viscous, incompressible, multi-fluid flows, J. Comput Phys. 100 (1992), 25-37.

ENTROPIC SURFACE CRYSTALS AND CRYSTAL GROWTH IN BINARY HARD-SPHERE COLLOIDS

A. G. Yodh, Department of Physics and Astronomy, University of Pennsylvania , Philadelphia, PA 19104-6396
yodh@dept.physics.upenn.edu

EXTENDED ABSTRACT

In this paper we will describe experiments to crystalize large particle arrays in low volume fraction binary particle suspensions. Crystallization is achieved using the attractive interactions brought about by the depletion effect. By using attractive interactions for colloidal assembly we create conditions for growth that are qualitatively different from the space-filling mode of colloidal crystal growth that is driven by packing constraints.

The suspensions we are studying are well approximated as a mixture of hard spheres. Hard sphere colloids lack the attractive and long range interactions which typically compete with entropic effects to produce ordered phases. Nonetheless as Asakara and Oosawa first noted [1], in mixtures of different size spherical particles and ordered arrangement of large spheres can increase the total entropy of the system by increasing the entropy of the small spheres. In the simplest version of the theory the attraction between two large spheres in the bulk is proportional to the ratio of the particle diameters times the volume fraction of the small spheres; the attraction is initiated when the large sphere surfaces move to within one small ball diameter of one another.

We have mapped out the bulk phase diagrams of some of these systems [2], and we have discovered that a surface phase first grows on the walls of our containers at volume fractions below those required for bulk crystallization [3]. Thus it is possible to nucleate and grow large crystals on the walls of our containers without interference from bulk effects. These experiments will be described.

In addition we have begun making surface templates in order to bias the growth of particular colloidal crystal structures, and we have directly measured the depletion potential between two large particles moving in a sea of small particles [4]. In these latter studies we have observed depletion repulsion as well as depletion attraction. Ongoing work will be presented.

References:

[1] S. Asakura and F. Oosawa, J. of Chem. Phys. 22, 1255 (1954).

[2] A.D. Dinsmore, A.G. Yodh, and D.J. Pine, Phys. Rev. E 52, 4045-57 (1995).

[3] P.D. Kaplan, J.L. Rouke, A.G. Yodh, and D.J. Pine, Phys. Rev. Lett. 72, 582-85 (1994).

[4] J.C. Crocker, J. Matteo, A.D. Dinsmore, and A.G. Yodh, manuscript under review.

ENHANCED BOILING ON MICRO-CONFIGURED COMPOSITE SURFACES UNDER MICROGRAVITY CONDITIONS

Nengli Zhang and An-Ti Chai, NASA/Lewis Research Center, Cleveland, OH 44135

ABSTRACT

In order to accommodate the growing thermal management needs of future space platforms, several two-phase active thermal control systems (ATCSs) have evolved and were included in the designs of space stations. Compared to the pumped single-phase liquid loops used in the conventional Space Transportation System and Spacelab, ATCSs offer significant benefits that may be realized by adopting a two-phase fluid-loop system. Alternately, dynamic power systems (DPSs), based on the Rankine cycle, seem inevitably to be required to supply the electrical power requirements of expanding space activities.

Boiling heat transfer is one of the key technologies for both ATCSs and DPSs. Nucleate boiling near critical heat flux (CHF) can transport very large thermal loads with much smaller device size and much lower pumping power. However, boiling performance deteriorates in a reduced gravity environment and operation in the CHF regime is precarious because any slight overload will cause the heat transfer to suddenly move to the film boiling regime, which in turn, will result in burnout of the heat transfer surfaces.

New materials, such as micro-configured metal-graphite composites, can provide a solution for boiling enhancement. It has been shown experimentally that this type of material manifests outstanding boiling heat transfer performance and their CHF is also extended to higher values. Due to the high thermal conductivity of graphite fiber (up to 1,200 W/m-K in the fiber direction), the composite surfaces are non-isothermal during the boiling process. The composite surfaces are believed to have a much wider safe operating region (a more uniform boiling curve in the CHF regime) because non-isothermal surfaces have been found to be less sensitive to variations of wall superheat in the CHF regime. The thermocapillary forces formed by the temperature difference between the fiber tips and the metal matrix play a more important role than the buoyancy in the bubble detachment, for the bubble detachment manifests itself by a necking process which should not be weakened by reduced gravity. In addition, the composite surfaces introduce no extra pressure drop, no fouling and do not impose significant primary or maintenance costs. All of these suggest that this type of composite is an ideal material for the challenge of accounting for both reliability and economy of the relevant components applied in the ATCSs, the DPSs and other devices in future space missions.

The aim of the proposed work is to experimentally investigate high nucleate pool boiling performance on a micro-configured metal-graphite composite surface and to determine the mechanisms of the nucleate boiling heat transfer both experimentally and theoretically. Freon-113 and water will be used as the test liquids to investigate wettability effects on boiling characteristics. The Cu-Gr and Al-Gr composites with various volume fractions of graphite fibers will be te
sted to obtain the heat transfer characteristic data in the nucleate boiling region and in the CHF regime. In the experiments, the bubble emission and coalescence processes will be recorded by a video camera with a magnifying borescope probe immersed in the working fluid. The temperature profile in the thermal boundary layer on the composite surfaces will be measured by a group of micro thermocouples consisting of four ultra fine micro thermocouples. This instrument was developed and successfully used to measure the temperature profile of evaporating liquid thin layers by the proposers in a study performed at the NASA/Lewis Research Center. A two tier model to explain the nucleate boiling process and the performance enhancement on the composite surfaces has been suggested by the authors. According to the model, the thicknesses of the microlayer and the macrolayer underneath the bubbles and mushrooms, can be estimated by the geometry of the composite surface. The experimental results will be compared to the predictions from the model, and in turn, to revise and improve it.

THE SMALL-SCALE STRUCTURE OF TURBULENCE

G. Zimmerli[1] and W. I. Goldburg[2]. [1]The National Center for Microgravity Research, NASA Lewis Research Center, 21000 Brookpark Road, MS 110-3, Cleveland, OH 44135, [2]Department of Physics and Astronomy, University of Pittsburgh, Pittsburgh, PA 15260

SUMMARY

The objective of this research is to experimentally investigate the statistical properties of turbulent flow at small length scales using the technique of homodyne correlation spectroscopy. By applying this technique to a wider range of Reynolds number flows, we will also test the range of validity of the frozen turbulence assumption.

Our approach is based on the non-intrusive light scattering technique known as homodyne correlation spectroscopy (HCS), which is sensitive to a quantity of fundamental interest in turbulent flow: the velocity difference $u(l,t)$ between two points separated by a distance l. Using HCS in turbulent flows, we will obtain direct information regarding the probability density function (p.d.f.) of velocity differences, with no need to use Taylor's hypothesis (the "frozen turbulence" assumption). These results will be compared with local fluid velocity measurements, $V(r,t)$, using Laser Doppler Velocimetry (LDV), from which the p.d.f. is calculated by invoking the frozen turbulence assumption. By using the wind tunnel facilities at NASA Lewis Research Center, we will be able to cover a large range of Reynolds number flows.

By applying the HCS technique to higher Reynolds number flows, we will be able to investigate turbulent structures down to smaller length scales. The experimental data will provide a useful check of theories, especially scaling relations and intermittency phenomena. Moreover, a direct comparison of measurements made with HCS and LDV systems will provide a test of how the frozen turbulence assumption affects the shape of the probability density function.

The investigation of turbulent flow is of practical significance, and has a long history. Notable examples of active research in fluid physics and combustion supported by the NASA Microgravity program which involve turbulent phenomena include: enhanced heat and mass transfer of turbulent flow, transition from laminar to turbulent flow, convective flow, buoyant plumes and instabilities, evaporation from a meniscus, thermocapillary convection, capillary wave turbulence, turbulent gas jet combustion, premixed turbulent flames, and flame-vortex interactions. The aeronautics and transportation industries are also interested in turbulence, particularly in boundary layers and in the wake behind a moving craft. The HCS technique may prove to be a valuable tool in industries where turbulence is of interest, particularly in aeronautics, propulsion, and transportation. The apparatus required for the HCS technique is of modest size and cost, and is amenable to miniaturization through fiber optics, making it an excellent candidate as a diagnostic instrument aboard the planned International Space Station Fluids and Combustion Facility. We believe that the HCS technique will make a significant contribution to the study of turbulent flows.

In the study of turbulent flows, a quantity of fundamental interest is the velocity difference $u(l)$ between two points separated by some distance l. More generally, one is interested in measuring the moments $<(u(l))^p>$ of the probability density of $u(l)$ as a function of the spatial variable l. Here, the bracket notation indicates an ensemble average, and p is an integer which represents the p^{th} moment.

In 1970, Bourke et al. [J. Phys. A , Vol 3, p. 216, 1970] demonstrated that the probability density function $P(u(l))$ was accessible by the technique of homodyne correlation spectroscopy. In the HCS technique, one measures the intensity correlation function $g(t) = <I(t')I(t'+t)>$ of scattered light from a seeded flow. Here, the measured intensity $I(t)$ is proportional to the beating of Doppler shifts coming from particle pairs moving at different relative velocities. The output of the photodetector is modulated at frequencies equal to the difference of Doppler shifts of all particle pairs in the scattering volume. For a pair of particles separated by distance l, the difference frequency is $\mathbf{q}\cdot[\mathbf{v}(r(t)-\mathbf{v}(r(t)+l)] = \mathbf{q}\cdot\mathbf{u}(l,t)$ and the amplitude of the scattering vector $\mathbf{q}$ is $(4\pi n/\lambda)\sin(\theta/2)$. Here,

n is the index of refraction of the fluid, λ the wavelength of light, and θ the scattering angle.

The research group at the University of Pittsburgh has been using the HCS technique for several years to study turbulent flows. They use a lens to image the scattered light onto a slit of width L which, together with the incident beam diameter, defines the scattering volume. Tong et al. [Phys. Rev. A, Vol 37, p.2125, 1988] showed that the intensity correlation function is an incoherent sum of time averaged phase factors $\cos[\mathbf{q}\cdot\mathbf{u}(l)t]$ over all particle pairs in the scattering volume. Then, the correlation function is given by

$$g(t) = 1 + \int_0^L dl\, h(l) \int_{-\infty}^{\infty} du(l)\, P(u(l)) \cos[qu(l)t]$$

where $u(l)$ is the component of $\mathbf{u}(l)$ along $\mathbf{q}$, and $h(l)$ is the number distribution of particle pairs separated by distance l in the quasi one-dimensional scattering volume. When the particles are evenly distributed, $h(l) = (2/L)(1-l/L)$. If a pair of points is imaged instead of a line, then $h(l)$ is simply a delta function. Herein lies the power of a design using fiber optics. In the usual method of imaging (using a slit), the extra integral makes it impossible to accurately unfold the p.d.f. from the measured correlation function. With point-like detection using fibers, the extra integral drops out and one can determine $P(u(l))$. Thus, $g(t)$-1 is the Fourier cosine transform of the probability density function of velocity differences at scale l (along the scattering vector $\mathbf{q}$). Because $g(t)$ is a cosine transform, it can only measure the even components of the p.d.f. Not much is lost however, since the even components contain a wealth of information.

The characteristic decay time of the correlation function is $1/qu(l)_{rms}$ where $u(l)_{rms}$ is the rms value of the velocity-difference fluctuations on a scale l. For a typical q value of 10^5 cm^{-1}, we find that the decay time is 10 nsec for $u(l)_{rms} = 10^3$ cm/s. This is too fast to measure accurately, since the fastest correlators are limited to about a 10 nsec sampling time. Thus, there is an upper limit to the velocity differences which can be measured. However, it is also important to consider the length scale l under study: at small length scales the velocity fluctuations are correspondingly less. Another fundamental limitation of HCS is the requirement that the transit time of the particle in the scattering volume be much greater than the decay time of the correlation function. The ratio of transit time to decay time is approximately given by Iqw, where w is the beam width. Thus, at a turbulence intensity $I = 0.1$ and $q = 10^5$ cm^{-1}, we find that this condition is still satisfied at length scales down to 10 μ m, where the ratio equals ten. Therefore, the fundamental limitations of the HCS technique do not prevent us from studying the small scales of turbulence at moderate intensities.

We are planning to apply the HCS technique to higher Reynolds number flows using a small wind tunnel facility available at NASA Lewis Research Center. The small wind tunnel is made of plexiglass walls for easy optical access, has a cross section of 45x50 cm^2, and is capable of wind speeds from 0 to 75 m/s. This facility is available for small scale research projects, and would be ideal for our purposes.

A distinct advantage of the HCS technique is that there is no need to invoke the frozen turbulence assumption in the data analysis. An important consequence of this is that HCS is also applicable to flows where the mean flow velocity $U = 0$. For example, in a combustion chamber with an oscillating element for turbulent mixing the mean flow is zero. Another important example is boundary layer flows; the turbulence is anisotropic and the mean flow normal to the boundary is zero. The HCS technique also has advantages over a two-component LDV system. First, HCS senses the instantaneous velocity difference from pairs of particles. In the two-component LDV technique, such a measurement would only be possible if two particles simultaneously crossed the respective patch areas. Thus, one must interpolate between signal "bursts" to determine $u(l,t)$. Additional advantages of the HCS technique include the fact that it has the potential to be a compact instrument, and the data analysis is less intensive.

Session 5A: Phase Change III: Boiling

INVESTIGATION OF NUCLEATE BOILING MECHANISMS UNDER MICROGRAVITY CONDITIONS

V.K. Dhir[1], D.M. Qiu[1], N. Ramanujapu[1] and M.M. Hasan[2], [1]Mechanical and Aerospace Engineering Department, University of California, Los Angeles, CA 90095, U.S.A, [2]NASA Lewis Research Center, 2100 Brookpark Road, Cleveland, OH 44135, U.S.A., e-mail: Vdhir@seas.ucla.edu

ABSTRACT

The present work is aimed at the experimental studies and numerical modeling of the bubble growth mechanisms of a single bubble attached to a heating surface and of a bubble sliding along an inclined heated plate. Single artificial cavity of 10 μm in diameter was made on the polished Silicon wafer which was electrically heated at the back side in order to control the surface nucleation superheat. Experiments with a sliding bubble were conducted at different inclination angles of the downward facing heated surface for the purpose of studying the effect of magnitude of components of gravity acting parallel to and normal to the heat transfer surface. Information on the bubble shape and size, the bubble induced liquid velocities as well as the surface temperature were obtained using the high speed imaging and hydrogen bubble techniques. Analytical/numerical models were developed to describe the heat transfer through the micro-macro layer underneath and around a bubble formed at a nucleation site. In the micro layer model the capillary and disjoining pressures were included. Evolution of the bubble-liquid interface along with induced liquid motion was modeled. As a follow-up to the studies at normal gravity, experiments are being conducted in the KC-135 aircraft to understand the bubble growth/detachment under low gravity conditions. Experiments have been defined to be performed under long duration of microgravity conditions in the space shuttle. The experiment in the space shuttle will provide bubble growth and detachment data at microgravity and will lead to validation of the nucleate boiling heat transfer model developed from the preceding studies conducted at normal and low gravity (KC-135) conditions.

BOILING HEAT TRANSFER MEASUREMENTS ON HIGHLY CONDUCTIVE SURFACES USING MICROSCALE HEATER AND TEMPERATURE ARRAYS

J. Kim[1], S.W. Bae[2], M.W. Whitten[1], J.D. Mullen[1], R.W. Quine[1], and T.S. Kalkur[3]
[1]University of Denver, Department of Engineering, Denver, CO 80208, jkim@du..edu, [2]Pohang University of Science and Technology, Department of Mechanical Engineering, Pohang, Kyungbuk, 790-784, Korea, bswon@postech.ac.kr, [3]University of Colorado, Department of Electrical Engineering, Colorado Springs, CO 80933, kalkur@vlsie.uccs.edu.

The vast majority of experimental work performed to date regarding boiling has utilized single heaters that were large compared to individual bubble sizes, making it difficult to look at details of the boiling process. These experiments usually used a heating element operated in a constant heat flux mode, making it difficult to study transition boiling effects beyond critical heat flux. Other experiments have utilized surfaces held at constant temperature, but the *local* heat flux and temperature were not measurable. Even when local measurements were obtained, this was done at only a few locations on the heater surface. The work described in this paper investigates at boiling on a small heated areas with high spatial and temporal resolution.

It must be remembered that boiling behavior on small heated areas can differ from that on large heated areas. First, the total number of nucleation sites is much smaller, and can result in heaters smaller than the corresponding average distance between nucleation sites on large heaters. Boiling can be delayed to higher wall superheats as a result, or the number of nucleation sites may not be statistically representative. Second, the Taylor wavelength, which is significant at CHF and transition and film boiling, can be larger than the heater size. Third, edge-effects can become significant.

Two systems have been developed to study boiling heat transfer on the microscale. Each of these is discussed below.

Diode array. This technique uses a 32 x 32 array of silicon diodes constructed on a silicon substrate to obtain the surface temperature distribution during boiling by measuring the forward voltage drop across each diode as the substrate is heated from below. Silicon diodes typically have a forward voltage drop of 0.7 V that decreases by 2 mV for every 1 °C increase in temperature near room temperature. The voltage drop across a diode is approximately proportional to the inverse of the absolute temperature of the diode for a wide range of temperatures.

The advantages of using a diode array to measure temperature rather than microthermocouples or liquid crystals are that 1). the temperature can be measured at many more points than is possible using microthermocouples, 2). temperature fluctuations over a much wider range can be measured compared to liquid crystals, 3). the resolution of the temperature measurements is much better than is possible using liquid crystals. The main limitation on the current technique is that the measurements are confined to relatively small areas.

An example of how the diodes would be connected together is shown on Figure 1 for a 3 x 3 array of diodes. If the voltage drop across diode A-2 is desired, a current (typically 1 mA) is sent into row A while the other rows are grounded. Simultaneously, column 2 is grounded while the other columns are set to 5 V. All of the diodes in the array with the exception of A-2 are now either reverse biased or have no voltage drop across them. The voltage at A is then measured to obtain the forward voltage drop across diode A-2. The voltage drop across the other diodes in the array are obtained by scanning across the array. Preliminary data from a 32 x 32 diode array is currently being taken.

Constant temperature heater array. The local wall heat flux variations in boiling of FC-72 on a small heated area was examined using an array of microscale heaters each maintained at constant surface temperature. The scale of the individual heaters was approximately the same as that of the departing bubbles in nucleate boiling. The information contained in this paper is unique in that data was taken at many points simultaneously instead of at a single point, enabling a much more detailed picture of the heat transfer process to be obtained.

Local surface heat flux and temperature measurements are provided by an array of platinum resistance heater elements deposited on a quartz wafer in a serpentine pattern. Each of these elements is 0.26 mm x 0.26 mm in size, and have a nominal resistance of 1000 Ω and a nominal temperature coefficient of resistance of 0.002 $°C^{-1}$. Ninety six individual heaters are arranged in a square array about 2.7 mm on a side, as shown in Figure 2.

The temperature of each heater in the array is kept constant by a feedback circuit similar to that used in constant temperature hot-wire anemometry. The instantaneous power required to keep each heater at a constant temperature is measured and used to determine the heat flux from each heater element.

Visualization of the bubble behavior on the surface along with heat transfer measurements has

recently been performed. The semi-transparent nature of the heater array enabled high speed digital videos to be made of the bubbles from below. Heat flux data was obtained under the condition shown in Figure 2 at 2500 Hz along with high-speed videos. The heat flux traces for the heaters underneath the bubble growing on the upper left corner of the heater array (the bubble growing on heaters 44 and 72-74) is shown on Figure 3. Between 14 and 15 ms, the shadow from the bubble that departed previously was seen. Nucleation of a new bubble occurred between 16 ms and 18 ms– this corresponded to a sharp increase in the wall heat flux. The formation of what appeared to be a dry spot underneath the growing bubble occurred soon after nucleation. This dry spot decreased in size starting from 18 ms and seemed to disappear around 21 ms, which corresponded to a sharp drop in wall heat transfer. The detached bubble moved away from the surface after 21 ms and a new bubble was observed to nucleate at 35 ms. It is interesting to note that there is a large amount of heat transfer associated with nucleation, but also a large amount of heat transfer as the dry spot shrinks and liquid re-wets the wall. The magnitude of heat transfer during re-wetting of the wall is smaller than during nucleation, but is of longer duration, resulting in comparable overall heat transfer rates. The heat transfer after bubble departure is very low in comparison.

The large heat transfer associated with nucleation could be due to evaporation of the microlayer, as postulated. The numerical models, however, do not seem to predict the large amounts of heat that are transferred just before the bubble departs the surface. The heat transfer mechanism seen is different from the widely accepted view that microlayer evaporation is the dominant heat transfer mechanism in saturated pool boiling. It is important to note that this data is preliminary–data from other bubbles on the surface suggest different heat transfer mechanisms.

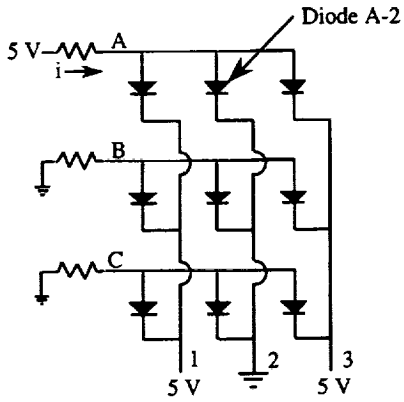

Figure 1: Example of a 3 x 3 diode array.

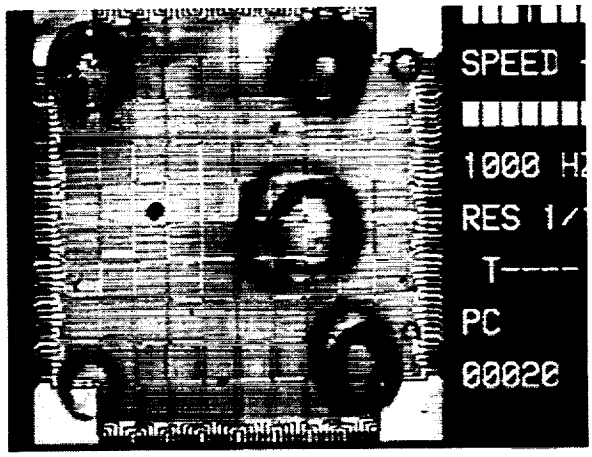

Figure 2: Photograph of boiling on the heater array– isolated bubble regime (ΔTsat=29 °C). Each heater in the array is 0.27 mm x 0.27 mm in size.

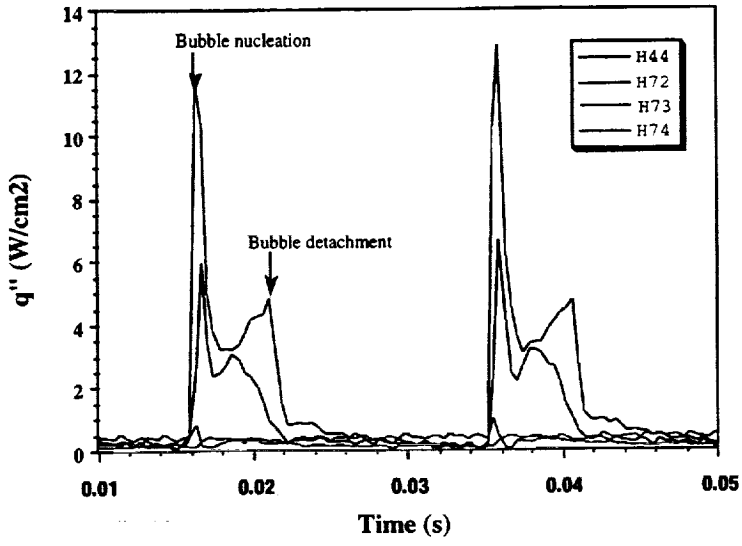

Figure 3: Wall heat flux vs. time for selected heaters. The times correspond to those on Figure 2.

VIBRATION-INDUCED DROPLET ATOMIZATION

M. K. Smith, A. James, B. Vukasinovic, and A. Glezer
The George W. Woodruff School of Mechanical Engineering
Georgia Institute of Technology, Atlanta, GA 30332-0405
marc.smith@me.gatech

ABSTRACT

Thermal management is critical to a number of technologies used in a microgravity environment and in Earth-based systems. Examples include electronic cooling, power generation systems, metal forming and extrusion, and HVAC (heating, venting, and air conditioning) systems. One technique that can deliver the large heat fluxes required for many of these technologies is two-phase heat transfer. This type of heat transfer is seen in the boiling or evaporation of a liquid and in the condensation of a vapor. Such processes provide very large heat fluxes with small temperature differences.

Our research program is directed toward the development of a new, two-phase heat transfer cell for use in a microgravity environment. In this paper, we consider the main technology used in this cell, a novel technique for the atomization of a liquid called vibration-induced droplet atomization. In this process, a small liquid droplet is place on a thin metal diaphragm that is made to vibrate by an attached piezoelectric transducer. The vibration induces capillary waves on the free surface of the droplet that grow in amplitude and then begin to eject small secondary droplets from the wave crests. In some situations, this ejection process develops so rapidly that the entire droplet seems to burst into a small cloud of atomized droplets that move away from the diaphragm at speeds of up to 50 cm/s. By incorporating this process into a heat transfer cell, the active atomization and transport of the small liquid droplets could provide a large heat flux capability for the device.

Experimental results are presented that document the behavior of the diaphragm and the droplet during the course of a typical bursting event. In addition, a simple mathematical model is presented that qualitatively reproduces all of the essential features we have seen in a burst event. From these two investigations, we have shown that delayed droplet bursting results when the system passes through a resonance condition. This occurs when the initial acceleration of the diaphragm is higher than the critical acceleration and the driving frequency is larger than the initial resonance frequency of the diaphragm-droplet system.

We have incorporated this droplet atomization device into a design for a new heat transfer cell for use in a microgravity environment. The cell is essentially a cylindrical container with a hot surface on one end and a cold surface on the other. The vibrating diaphragm is mounted in the center of the cold surface. Heat transfer occurs through droplet evaporation and condensation on the hot and cold ends of the cell. A prototype of this heat transfer cell has been built and tested. It can operate continuously and provides a modest level of heat transfer, about 20 W/cm^2. Our work during the next few years will be to optimize the design of this cell to see if we can produce a device that has significantly better performance than conventional heat exchangers and heat pipes.

Session 5B: Suspensions

EFFECTS OF GRAVITY ON SHEARED TURBULENCE LADEN WITH BUBBLES OR DROPLETS

Said Elghobashi[1], [1]Mechanical and Aerospace Engineering Department, University of California, Irvine, California 92697, USA, selghoba@uci.edu, Juan Lasheras[2], [2] Applied Mechanics and Engineering Sciences Department, University of California, La Jolla, California 92093, USA, lasheras@ames.ucsd.edu

Abstract

The objective of this numerical/experimental study is to improve the understanding of the effects of gravity on the two-way interaction between dispersed particles (bubbles or liquid droplets) and the carrier turbulent flow. The first phase of the project considers isotropic turbulence. Turbulent homogeneous shear flows laden with droplets/bubbles will be studied in the next phase.

The experiments reported here are concerned with the dispersion of liquid droplets by homogeneous turbulence under various gravitational conditions and the effect of these droplets on the evolution of the turbulence of the carrier fluid (air).

Direct numerical simulations (DNS) of bubble - laden isotropic decaying turbulence are performed using the two-fluid approach (TF) instead of the Eulerian - Lagrangian approach (EL). The motivation for using the TF formulation is that EL requires considerable computational resources especially for the case of two-way coupling where the instantaneous trajectories of a large number of individual bubbles need to be computed. The TF formulation is developed by spatially averaging the instantaneous equations of the carrier flow and bubble phase over a scale of the order of the Kolmogorov length scale which, in our case, is much larger than the bubble diameter. On that scale, the bubbles are treated as a continuum (without molecular diffusivity) characterized by the bubble phase velocity field and concentration (volume fraction). The bubble concentration, C, is assumed small enough ($C \leq 10^{-3}$) to neglect the bubble-bubble interactions.

DNS of the bubble - laden decaying turbulence is performed for both cases of one-way and two-way coupling. Here, the bubble diameter and response time are much smaller than the Kolmogorov length and time scales respectively. In this case, as expected, the effects of the preferential accumulation of the bubbles are not pronounced. The results also show that the bubble - laden flow is analogous to a stratified flow with an effective density = $(1 - C)\rho_f$. Thus, due to the two-way interaction between the bubbles and carrier flow, the turbulence decay is enhanced with stable stratification, and reduced with unstable stratification.

Two sets of experiments were conducted to systematically studied the role of gravity. In all cases, only half of the wind tunnel entrance cross section was laden with a uniform-concentration spray of droplets of a given polydispersed size distribution. In the first set, the uniform-concentration droplet spray initially occupied the lower half portion of the entrance cross section (stable stratified case), while in the second set of experiments the spray occupied initially the upper half portion of the wind tunnel cross section (unstable stratified case).

The cross stream dispersion of the particles of varying sizes was measured at each downstream distance using a Phase Doppler Particle Analyzer (PDPA). A dilute concentration of submicron-size smoke particles can also be added to the air to allow for simultaneous characterization of the carrier flow (air). The PDPA allowed for measurement of the size as well as the two components of the velocity of the water particles and carrier gas (axial and cross stream components). In all the measurements the droplet distribution was discretized into 8 size bins. The carrier fluid (air) was characterized by the measurements corresponding to the smoke particles which always populate the smaller size bin (particle diameters less than 2 microns).

It is shown that the evolution of the droplet size PDFs along the cross stream coordinate is strongly affected by the sense and orientation of the gravity vector. This marked differences can not be explained with a simple linear addition of the settling velocity of the droplets. In the stable stratified case, the measured PDFs along the cross stream direction (diffusion) are shown to be nearly identical, indicating an uniform diffusion coefficient independent of the droplet size. However, in the unstable stratified case the evolution of the PDFs indicated marked differences in the diffusion coefficients depending on the droplet size.

BUOYANCY DRIVEN SHEAR FLOWS OF BUBBLE SUSPENSIONS.

D. L. Koch[1], R. J. Hill[1], T. Chellppannair[1], R. Zenit[1], [1]Chemical Engineering, Cornell University, Ithaca NY 14853, USA, don@cheme.cornell.edu, A. Sangani[2], P. D. M. Spelt[2], [2]Chemical Engineering and Materials Science, Syracuse University, Syracuse, NY 13244, USA, asangani@syr.edu

In this work the gas volume fraction and the root-mean-squared fluid velocity are measured in buoyancy driven shear flows of bubble suspensions in a tall, inclined, rectangular channel. The experiments are performed under conditions where $We \ll 1$ and $Re \gg 1$, for which comparisons are made with kinetic theory and numerical simulations [1]. Here $Re = \gamma a^2/\nu$ is the Reynolds number and $We = \rho\gamma^2 a^3/\sigma$ is the Weber number; γ is the shear rate, a is the bubble radius, ν is the kinematic viscosity of the liquid, ρ is the density of the liquid, and σ is the surface tension of the gas/liquid interface.

Kang et al. [1] calculated the bubble phase pressure and velocity variance of sheared bubble suspensions under conditions where the bubbles are spherical and the liquid phase velocity field can be approximated using potential flow theory, i.e. $We = 0$ and $Re \gg 1$. Such conditions can be achieved in an experiment using gas bubbles, with a radius of O(0.5mm), in water. The theory requires that there be no average relative motion of the gas and liquid phases, hence the motivation for an experimental program in micro-gravity.

The necessity of performing preliminary, Earth based experiments, however, requires performing experiments where the gas phase rises in the liquid, which significantly complicates the comparison of experiments with theory. Rather than comparing experimental results with theory for a uniform, homogeneous shear flow, experiments can be compared directly with solutions of the averaged equations of motion for bubble suspensions. This requires accounting for the significant lift force acting on the gas phase when the bubbles rise parallel to the average velocity of the sheared suspension.

Shear flows can be produced in which the bubble phase pressure gradient, arising from shear induced collisions amongst the bubbles, balances a body force (centrifugal or gravitational) on the gas phase. A steady, non-uniform gas volume fraction can be measured, from which the bubble phase pressure gradient can be obtained and compared to theory and numerical simulations. The presence of bounding walls further complicates the experiments, since the detailed interactions of the bubbles with bounding walls is not well understood, especially in the presence of gravity, where the momentum and energy exchange depends on the inclination of the wall [3]

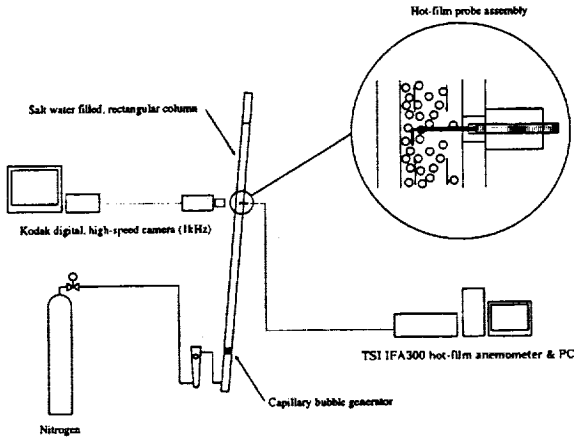

Figure 1: Schematic of the experimental apparatus for studying buoyancy driven shear flows of bubble suspensions.

In the experiment shown schematically in Figure (1), Nitrogen gas is introduced through an array of capillaries at the base of a tall, inclined channel filled with an aqueous electrolyte solution. The addition of an electrolyte (0.06 molL^{-1} $MgSO_4$) prevents bubble coalescence by the short range, repulsive, hydration forces that are present at the gas-liquid interface when bubbles come into close contact [2].

The rising bubbles generate a unidirectional shear flow, where the denser suspension at the lower surface of the channel falls, while the less dense suspension at the upper surface rises. The dimensions of the channel (2x0.2x0.02m) are such that the shear flow at the point of measurement is fully developed in the stream-wise direction, and uniform across the width. Furthermore, the gap width is large enough for continuum behavior to be observed, and small enough to maintain laminar flow at the highest shear rates (O(10s^{-1})). When the shear rate is too high, unsteady, large scale coherent structures form, which give rise to undesirable temporal fluctuations in the average velocity field.

The steady shear flow develops a bubble phase pressure gradient across the channel gap, which balances the buoyancy force driving bubbles toward the upper surface. A novel application of hot-film anemometry is

used to measure the resulting gas volume fraction profile. In this technique the bubble collision rate with the sensor is related to the gas volume fraction by knowing the collision surface area enveloping the sensor. Bubble collisions with the sensor are identified using an algorithm that exploits the characteristic curvature and slope of the hot-film anemometer signal when bubbles collide with the sensor. The collision surface area is obtained from high-speed photography, to measure the relative position of single bubbles colliding with the sensor, in conjunction with the signal from the hot-film anemometer. The root-mean-squared fluid velocity, which has contributions from the average fluid velocity and fluctuations, can be obtained from the hot-film anemometer signal. This requires calibrating the hot-film sensor at liquid velocities in the range 0-1ms^{-1}.

The characterization and calibration of the hot-film anemometer sensor will be discussed, as well as an algorithm for identifying bubble collisions, and hence determining the bubble collision rate and the root-mean-squared liquid velocity as a function of distance across the channel gap. These measurements will be compared with solutions of the averaged equations of motion, for a range of gas volume fractions and channel inclination angles. Observations of bubble interactions with the channel walls will be discussed, and how these guide the choice of appropriate boundary conditions for the solution of the averaged equations of motion.

Acknowledgments

This work is supported by NASA under grant NAG3-1853.

References

[1] S. Y. Kang, A. S. Sangani, H. K. Tsao, and D. L. Koch. Rheology of dense bubble suspensions. *Phys. Fluids*, 9:1540--1561, 1997.

[2] H. K. Tsao and D. L Koch. Collisions of slightly deformable, high Reynolds number bubbles with short-range repulsive forces. *Phys. Fluids*, 6:2591, 1994.

[3] H. K. Tsao and D. L Koch. Observations of high Reynolds number bubbles interacting with a rigid wall. *Phys. Fluids*, 9:44, 1997.

DIRECT NUMERICAL SIMULATION OF DROP BREAKUP IN ISOTROPIC TURBULENCE

Jerzy Blawzdziewicz
Vittorio Cristini
Michael Loewenberg

Department of Chemical Engineering
Yale University
New Haven, Connecticut 06520-8286

Lance R. Collins

Department of Chemical Engineering
Pennsylvania State University
College Park, Pennsylvania

Abstract

Deformation and breakup of a three-dimensional viscous drop in isotropic turbulence has been modeled by direct numerical simulation. A pseudospectral representation of the turbulent outer flow field is rigorously coupled to a detailed three-dimensional boundary integral description of the drop microphysics. The drop is assumed to be smaller than the Kolmogorov scale. Drop dynamics depend on the drop viscosity and capillary number.

Under the averaged flow conditions (viscosity ratio and capillary number), our simulations reveal widely variable behavior on different trajectories: on some trajectories drops become highly elongated without breaking while drops on other trajectories break at only modest length. Our results indicate that simplified models of drop dynamics are unreliable predictors of drop breakup in turbulence.

In weaker flows, our simulations show that drops break at modest length into two large daughter drops with only a small volume of satellite drops. In stronger flows, drops become highly elongated before breaking indicating that many satellites are produced.

Low-viscosity drops respond quickly to changes in the external flow and break shortly after experiencing a sufficiently strong fluctuation. Deformation of high-viscosity drops occurs on a time scale longer than the Kolmogorov time; thus larger energy dissipation rates are required for breakup.

Session 5C: Special Topics I

NON-COALESCENCE EFFECTS IN MICROGRAVITY

G. P. Neitzel[1], P. Dell'Aversana [2] and D. Castagnolo[2]

[1]School of Mechanical Engineering, Georgia Institute of Technology, Atlanta, GA 30332-0405 USA
paul.neitzel@me.gatech.edu
[2]Microgravity Advanced Research and Support Center, Via Communale Tavernola, 80144 Napoli, ITALY.

ABSTRACT

Forced non-coalescence between two bodies of the same liquid may be achieved by a variety of means, all of which provide relative tangential motion of the adjacent free-surfaces. This motion serves to provide a lubricating film of the surrounding gas to the gap which prevents the liquid surfaces from coming into contact. One means of forcing non-coalescence is to use thermocapillarity to drive the lubricating film by having the liquids at different temperatures. This paper will examine a number of scenarios of non-coalescence behavior, both qualitatively and quantitatively, and describe some envisioned applications of the phenomenon which may have relevance in both microgravity and terrestrial environments.

COLLIDE: MICROGRAVITY EXPERIMENT ON COLLISIONS IN PLANETARY RINGS AND PROTOPLANETARY DISKS

J. E. Colwell[1], M. Taylor[2], L. Lininger[3], B. Arbetter[1],and A. Sikorski[1], [1]Laboratory for Atmospheric and Space Physics, University of Colorado, Boulder CO 80309-0392, USA, [2]STScI, 3700 San Martin Dr., Baltimore MD 21218, USA, [3]Lockheed Martin Missiles and Space, 1111 Lockheed Martin Way, Sunnyvale CA 94089, USA.

Dust is ubiquitous in the solar system. Surfaces of asteroids, planetary satellites and planetary ring particles are coated with dust generated by the hypervelocity bombardment of micrometeoroids. In planetary rings and in the early stages of planetesimal accretion in the protoplanetary nebula, interparticle collisions occur at low relative velocities. Planetary ring particles are on nearly circular orbits with low inclinations, and collision velocities are set by Keplerian shear and small perturbations in orbits induced by nearby moons. This results in collision velocities on the order of 1 cm/s. The dust released by these interparticle collisions has been observed by the Voyager 1 and 2 spacecrafts in the ring systems of each of the giant planets. Because the dust particles generally have short lifetimes (<100 years), production of dust from interparticle collisions is an ongoing process.

In some planetary ring systems, and in some circumstellar disks, only the dust component of the particle size distribution is observable. The dust thus acts as a tracer of the more massive particles in the disk. Understanding the collisional release of dust in low energy collisions is therefore necessary to link dust observations to the large particle dynamics. The partitioning of energy in low energy collisions between dust-covered low-surface-gravity particles will influence the dynamical evolution of these collisionally evolved systems, and whether collisions are accretional or erosional. This has important implications for the early stages of planetesimal accretion.

The Collisions Into Dust Experiment (COLLIDE) is the first microgravity experiment to study the partitioning of energy into dust ejecta in very low velocity impacts. Although not exactly duplicating the conditions that exist in a collision between planetary ring particles, COLLIDE will provide the first information on the amount, speed, and direction of dust particles ejected from a deep regolith when impacted at low velocities. This data will make a natural extension of the existing set of ground-based laboratory data on high velocity impacts into powders. It will also provide a guide for further microgravity investigations into these types of collisions.

COLLIDE is a Get Away Special payload for the Space Shuttle (STS) and had its first flight on STS-90, launched April 17, 1998. The experiment consists of six independent impact chambers to allow six different sets of impact parameters to be used during one flight (Table 1). Each impact chamber is self-contained, with a target tray of simulated planetary regolith (loose grains or debris on a planetary, asteroidal, or satellite surface), lighting, and a launcher mechanism. Because the ejecta is dispersed by the impact, each chamber can be used only once per flight.

The data consist of videotape records of each impact taken by consumer grade digital video camcorders. Illumination is provided by 20 high-intensity light emitting diodes in each impact chamber, and the teflon sphere projectiles are launched by springs designed to provide impact speeds between 1 and 100 cm/s. The ensemble of many impact experiments will allow us to express fundamental quantities, such as ejecta mass, as a function of non-dimensional scaling parameters. These will then be compared to the existing set of data on high-energy impacts from ground-based experiments.

Table 1. COLLIDE Impact Parameters

IBS	Velocity (cm/s)	Impactor Radius (cm)	Dust Depth (cm)
1	100.0	.95	1.9
2	1.05	.48	0.95
3	1.05	.48	1.9
4	21.5	.48	1.9
5	4.64	.48	1.9
6	100.0	.48	1.9

The data obtained by COLLIDE can only be obtained in a microgravity environment. The energy imparted to the target regolith in the low-velocity impacts studied here is insufficient to overcome Earth's gravity and allow ejecta properties such as velocity distributions to be measured. Because of the relatively long time scale for the slowest impacts, extended periods of microgravity are necessary. The time for each impact experiment in COLLIDE ranges from 30 s to 180 s, and the total duration of the experiment is 27 minutes.

COLLIDE was designed and built primarily by students at the Laboratory for Atmospheric and Space Physics at the University of Colorado. The time from initial design to flight was less than 2 years. The experiment is powered by 18 alkaline D cells and uses an Intel 80C51GB microcontroller. Each impact takes place in sequence to minimize power draw and prevent vibrations from one experiment interfering with another. The Get Away Special canister was evacuated and sealed prior to launch at a pressure approximately 0.0001 atmospheres to minimize gas-particle interactions between the ejecta and the ambient atmosphere. Two camcorders were in separate, sealed containers with air to prevent outgassing of lubricants. Each

camcorder views three impact chambers with a line of sight parallel to the plane of the target surface.

A baroswitch which activated on ascent of STS-90 through 50,000 feet closed the COLLIDE power circuit. This began a 24 hour timing circuit in COLLIDE, and the first impact was scheduled to occur 24 hours after launch. Astronaut initiation of the experiment occurred at 27.9 hours after launch, after the nominal end of the built-in timer. The Space Shuttle orbiter Columbia landed on May 3, 1998, and COLLIDE was removed from the flight canister on May 18, 1998. Initial results from the first flight of COLLIDE will be presented.

WEAKLY NONLINEAR DESCRIPTION OF PARAMETRIC INSTABILITIES IN VIBRATING FLOWS

E. Knobloch, Department of Physics, University of California, Berkeley CA 94720, USA, knobloch@physics.berkeley.edu, J. M. Vega, E.T.S.I. Aeronauticos, Universidad Politecnica de Madrid, 28040 Madrid, Spain, vega@fmetsia.upm.es

This project focuses on the effects of weak dissipation on vibrational flows in microgravity and in particular on (a) the generation of mean flows through viscous effects and their reaction on the flows themselves, and (b) the effects of finite group velocity and dispersion on dynamics in large domains. The basic mechanism responsible for the generation of such flows is nonlinear and was identified by Schlichting [12] and Longuet-Higgins [8]. However, only recently has it become possible to describe such flows self-consistently in terms of amplitude equations for the parametrically excited waves coupled to a mean flow equation. The derivation of these equations is nontrivial because the limit of zero viscosity is singular. This project focuses on various aspects of this singular problem (i.e., the limit $C \equiv \nu(gh^3)^{-1/2} \ll 1$) in the weakly nonlinear regime. A number of distinct cases is identified depending on the values of the Bond number $B \equiv \rho g h^2/\sigma$, the size of the nonlinear terms, distance above threshold and the length scales of interest. The theory provides a quantitative explanation of a number of experiments on the vibration modes of liquid bridges and related experiments on parametric excitation of capillary waves in containers of both small and large aspect ratio. The following is a summary of results obtained thus far.

Surface-wave damping in a brimful circular cylinder by C. Martel, J.A. Nicolas and J.M. Vega [10]: Following Higuera et al [5] and Martel and Knobloch [9] the damping rate for gravity-capillary waves in a brimful circular cylinder was computed to $O(C)$. These calculations required the computation of the contributions from the bulk and viscous boundary layers to this order. The theoretical damping rate agrees with the measured rate [4] to within typically 5% (26% in the worst case), a substantial improvement over the $O(C^{1/2})$ result of Henderson and Miles [4]. The calculation lends us confidence that we have correctly identified the major source of discrepancy between existing theory and experiment and that we know how to correct the theory, at least in cases in which surface contamination and contact angle dynamics can be ignored. The boundary layer calculations are at the heart of this resolution: even though $C^{1/2} \ll 1$ (specifically $C = O(10^{-4})$ for typical experiments using water) this is not small enough for the leading order asymptotics to give a quantitatively correct approximation to the damping rate (in contrast to the situation for the eigenfrequencies). The calculation has triggered a new experimental effort to measure damping rates of gravity-capillary waves in finite domains by M. Schatz and forms the basis for future nonlinear studies of such waves in cylinders.

Chaotic oscillations in a nearly inviscid axisymmetric capillary bridge at $2:1$ resonance, by F.J. Mancebo, J.A. Nicolas and J.M. Vega (Phys. Fluids, in press): This paper considers a liquid bridge in microgravity supported between two disks vibrating at two frequencies close to $2:1$ resonance. Under appropriate conditions this vibration excites the corresponding natural vibration modes (assumed axisymmetric) and these interact nonlinearly. In the nearly inviscid limit $C \ll 1$ this interaction is described by a pair of amplitude equations (autonomous odes) whose structure depends on the parity of the modes. Both quadratic and cubic nonlinearities arise depending on aspect ratio. The calculation of these terms requires the computation of the contributions from the Stokes boundary layers at the disks, the interface boundary layer, the two corner tori near the edge of the disks and from the bulk. The results are used to make a number of predictions about the sub- and superharmonic response of a liquid bridge subjected to this type of excitation under experimentally relevant conditions, and the ensuing chaotic oscillations.

Quasi-steady vortical structures in vertically vibrating soap films by J.M. Vega, F.J. Higuera and P.D. Weidman (JFM, in press): A theory accounting for the steady vortical flows observed in vertically vibrated soap films [1] is developed. These flows are shown to be the result of oscillatory tangential and normal stresses on the film from the surrounding air. These force a non-oscillatory deflection of the film and tangential motion of the liquid. A non-oscillatory volume force dominates when the excitation frequency is close to the eigenfrequency of a natural Marangoni mode of the film. Sample vortex patterns are computed and compared with experiment.

Compressional modes in parametrically driven Faraday waves in an annulus by C.

Martel, E. Knobloch and J.M. Vega (in progress): Experiments by Douady et al [2] on parametrically driven water waves in an annulus ($C = 4.4\,10^{-4}$, $B = 8.9$) reveal the presence of a secondary instability of a uniform pattern of standing waves (SW) in the form of an oscillatory *compression* mode. This bifurcation is to be interpreted as a (pitchfork) bifurcation with eigenvector that breaks the reflection symmetry of the SW. At sufficiently small amplitude the SW dynamics are dominated by advection at the group velocity and the experiment is described by *nonlocal* amplitude equations [6]. Because of the relatively high SW wavenumber (wavelength $\approx$ 1cm) the coefficients can be deduced from [3]. We show that with periodic boundary conditions (appropriate to an annular cell) such a mode is expected to be present for the experimental parameter values and explore its dynamics beyond threshold. The resulting theory applies in the regime where the dynamics are dominated by advection at the group velocity. In this preliminary theory mean flows are ignored. Viscosity-driven mean flows will be included in a more refined treatment that is under way. A related investigation of the Faraday problem with exact or broken D_4 symmetry is motivated by the experiments of Simonelli and Gollub [13] who found no time-dependence in a square container beyond phase-locked standing waves, in contrast to a slightly non-square container in which they observed periodic and chaotic bursts very close to onset. We anticipate an explanation of this behavior along the lines advanced below for the presence of bursts. The real parts of the necessary cubic coefficients are being calculated to leading order in $O(C)$ and viscosity-generated mean flows have yet to be included. The resulting theory should provide the first quantitative description of this interesting phenomenon.

Bursts by J. Moehlis and E. Knobloch (PRL, in press): Under appropriate conditions the competition between nearly degenerate Hopf modes with odd and even parity results in dramatic bursts very near the onset of primary instability. This behavior sets in as a secondary instability and involves global connections to infinite amplitude states, and arises in two-dimensional systems of large but finite aspect ratio undergoing an oscillatory instability, or in systems with nearly square symmetry, as discussed by Landsberg and Knobloch [7]. The mechanism identified is natural in these systems and appears to be responsible for the regular or irregular excursions of large dynamic range observed in many systems near onset of primary instability.

Dynamics of parametrically modulated dissipative systems in an annulus by E. Knobloch, C. Martel, J. Moehlis and J.M. Vega (in progress): Dynamics of parametrically modulated dissipative systems undergoing a symmetry-breaking Hopf bifurcation on a line are explored in full generality, with particular emphasis on the case in which either standing waves or travelling waves are subcritical [11]. In closely related equations (see above) this regime can lead to bursting. The possible dynamical regimes involving spatially uniform states have been identified, including standing waves and nonsymmetric mixed modes phase-locked to the drive and interactions between them. Instabilities due to spatially inhomogeneous perturbations leading to compression-like states have been described and lead to a number of novel spatially inhomogeneous states.

References

[1] M. Airiau, DEA Report, Ecole Normale Superieure, Paris, 1986; V.O. Afenchenko, A.B. Ezersky, S.V. Kiyashko, M.I. Rabinovich and P.D. Weidman, Phys. Fluids, in press.

[2] S. Douady, S. Fauve and O. Thual, Europhys. Lett. 10, 309 (1989).

[3] P.L. Hansen and P. Alstrom, J. Fluid Mech. 351, 301 (1997).

[4] D.M. Henderson and J.W. Miles, J. Fluid Mech. 213, 95 (1990).

[5] M. Higuera, J.A. Nicolas and J.M. Vega, Phys. Fluids 6, 438 (1994).

[6] E. Knobloch and J. De Luca, Nonlinearity 3, 575 (1990), C. Alvarez Pereira and J.M. Vega, Euro. Jnl. of Appl. Math. 3, 55 (1992).

[7] A.S. Landsberg and E. Knobloch, Phys. Rev. E 53, 3579 (1996).

[8] M.S. Longuet-Higgins, Phil. Trans. R. Soc. London A 245, 535 (1953).

[9] C. Martel and E. Knobloch, Phys. Rev. E 56, 5544 (1997).

[10] C. Martel, J.A. Nicolas and J.M. Vega, J. Fluid Mech. 360, 213 (1998).

[11] H. Riecke, J.D. Crawford and E. Knobloch, in NATO ASI Series B 237, 61 (1991).

[12] H. Schlichting, Z. Phys. 33, 327 (1932).

[13] F. Simonelli and J.P. Gollub, J. Fluid Mech. 199, 471 (1989).

Session 6A: Phase Change IV: Boiling

PRESSURE-RADIATION FORCES ON VAPOR BUBBLES

V. Harik, Y. Hao, H.N. Oğuz, A. Prosperetti, Department of Mechanical Engineering, The Johns Hopkins University, Baltimore MD 21218, prosperetti@jhu.edu

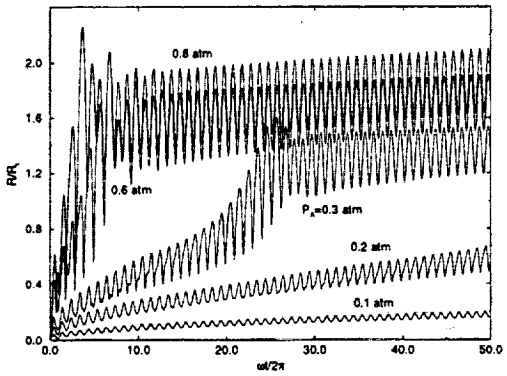

Figure 1: Radius versus time for vapor bubbles in saturated water at 1 atm and 1 kHz for various acoustic pressure amplitudes. The radius is normalized by the linear resonant radius $R_{res} = 2.71$ mm.

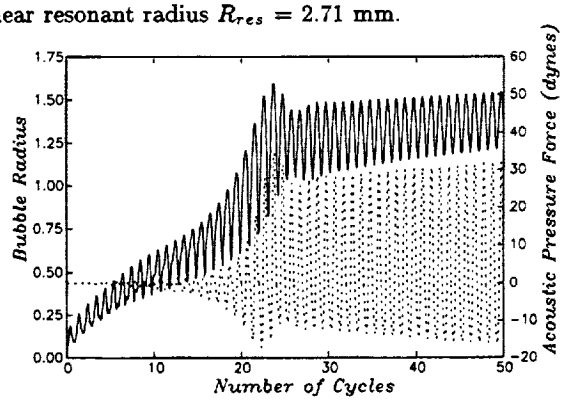

Figure 2: The solid line (left vertical scale) is the radius versus time for a vapor bubble in saturated water at 1 atm and 1 kHz for an acoustic pressure amplitude of 0.3 atm. The radius is normalized by the linear resonant radius $R_{res} = 2.71$ mm. The dashed line (right vertical scale) shows the corresponding instantaneous force.

In a microgravity environment the absence of buoyancy prevents vapor bubbles from moving away from a boiling surface. This circumstance negatively affects boiling heat transfer and promotes an early transition to the highly inefficient film boiling regime. Acoustic pressure radiation (or Bjerknes) forces provide a possible alternative to buoyancy as a means for bubble removal. The purpose of this work is to examine theoretically this possibility.

The first step is the study of the forced pulsations of a vapor bubble in a sound field. A mathematical model has been developed consisting of the Keller equation, describing the radial pulsations of a bubble in a slightly compressible liquid, and of the energy equations in the liquid and in the gas. For the latter, advantage is taken of the fact that the pressure in the bubble can be assumed to a good approximation to be spatially uniform. This assumption justifies the neglect of the vapor momentum equation and enables the vapor continuity and energy equations to be combined to give a single non-linear partial differential equation for the vapor temperature. The spatial dependence of the partial differential equations is treated numerically by a Chebyshev-based collocation method and the resulting system of ordinary differential equations is then integrated in time. Some typical results for vapor bubbles in water at 100 °C and a frequency of 1 kHz are shown in Fig. 1 for various acoustic pressure amplitudes P_A. The results are normalized by the linear resonant radius that has a value of 2.71 mm in this example.

The first feature that stands out from these results is the relatively rapid growth of the average radius of the bubble. This is a manifestation of the phenomenon of rectified heat transfer, which is the analogue of rectified diffusion of mass for gas bubbles. The sound field "pumps" heat into the bubble due to the alternating stretching and compressing of the thermal boundary layer and of the bubble surface. The growth is relatively

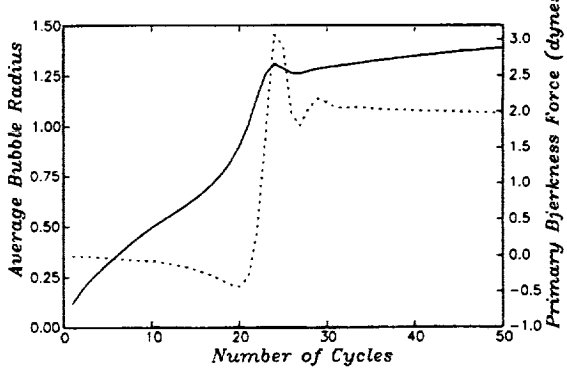

Figure 3: Bubble radius (solid line) and pressure-radiation force (dashed line) averaged over each cycle for the case of Fig. 2.

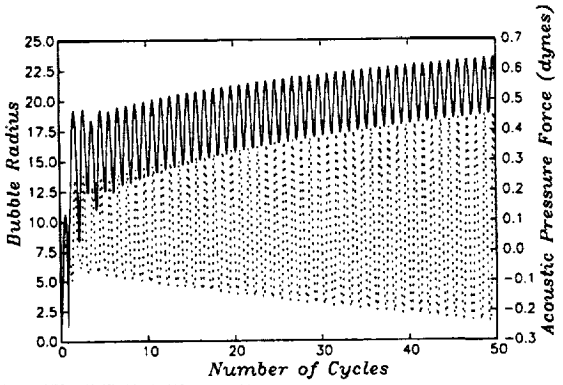

Figure 4: The solid line (left vertical scale) is the radius versus time for a vapor bubble in saturated water at 1 atm and 20 kHz for an acoustic pressure amplitude of 0.6 atm. The radius is normalized by the linear resonant radius $R_{res} = 10$ μm. The dashed line (right vertical scale) shows the corresponding instantaneous force.

rapid up to the resonant radius, after which it slows down considerably although it is never zero. The response in the vicinity of the resonant radius is particularly strong, but clear traces of the nonlinear resonances at lower radii can also be detected in the figure.

With the assumption that the pressure field surrounding the bubble varies slowly over the bubble surface, the net pressure force acting on the bubble can be approximated as

$$F \simeq -V \nabla p(x_B, t) = -V \nabla P_A - V \nabla p_2 , \qquad (1)$$

where $V = V(t)$ is the instantaneous bubble volume, P_A is the acoustic pressure field, and p_2 is the pressure field due to other bubble(s) in the neighborhood of the given bubble. We consider this contribution (responsible for the so-called *secondary Bjerknes force*) chiefly because the vapor bubbles of present concern grow near solid boundaries the effect of which, to a first approximation, can be represented by an "image" bubble that pulsates in phase with the real bubble. The average of the first term in the right-hand side of (1) over a cycle is the so-called primary Bjerknes force.

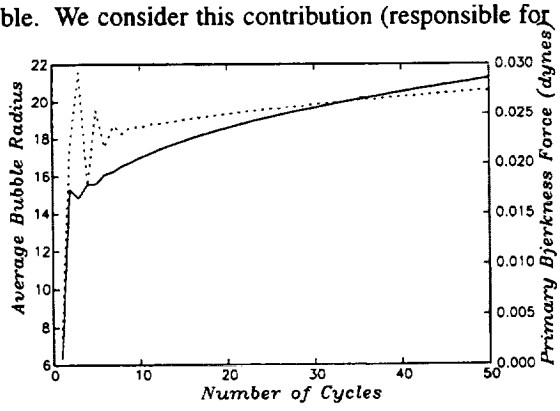

Figure 5: Bubble radius (solid line) and pressure-radiation force (dashed line) averaged over each cycle for the case of Fig. 4.

Figure 2 shows the instantaneous primary force (dashed line, right vertical scale) superimposed on the normalized bubble radius (solid line, left vertical scale) as a function of time for the case with $P_A = 0.3$ atm of Fig. 1. To generate this figure we have assumed a spatial distribution of the pressure given by

$$P_A(x) = P_S \cos kz , \qquad (2)$$

where P_S is amplitude of the wave and k the wave number. The bubble is positioned at $z = 2$ mm, so that $kz = 0.0084$ rad. The amplitude of oscillation of the force is proportional to the instantaneous volume and therefore it grows with the bubble mean radius. The time average value of the force, shown in Fig. 3 (dashed line, right vertical scale; the solid line to be read on the other scale is the mean radius), behaves however in a very different manner. It starts out negative, since the bubble is driven below its natural frequency, becomes more negative as the amplitude of oscillation grows with the bubble radius, and then abruptly changes sign as the radius goes through the resonant value. After a brief transient, one observes a steady decline in spite of the fact that, as shown by the solid line, the mean bubble radius keeps increasing. This behavior is a consequence of the fact that, as the radius moves further and further away from resonance, the oscillation amplitude of the bubble decreases. To have an intuitive feeling for the magnitude of the effect, note that the buoyancy force on a bubble with a radius equal to the resonant value, 2.71 mm, is about 82 dynes. Thus the acoustic effect is small, although it can be increased by placing the bubble at a greater distance from the pressure antinode where the pressure gradient is stronger.

Corresponding results for different parameter values are shown in Figs. 4 and 5. Here $P_S = 0.6$ atm and $\omega/2\pi = 20$ kHz. The liquid is saturated water at 1 atm and $R_{res} = 10$ μm. The pressure field is again given by (2) and the bubble is at 0.2 mm from the antinode. In this case the initial bubble radius is equal to the resonant value. As a consequence the amplitude of oscillation is large and the bubble grows very quickly. The Bjerknes force is always positive, i.e., directed away from the pressure antinode.

Condensation of Forced Convection Two-Phase Flow in a Miniature Tube

E. BEGG[1], A. FAGHRI[1], *1 Department of Mechanical Engineering, University of Connecticut, Storrs, CT 06269,* D. KRUSTALEV [2], *2 Thermocore, Inc.Lancaster, PA 17601*

Abstract

A physical and mathematical model of annular film condensation at the inlet of a miniature tube has been developed. In the model the liquid flow has been coupled with the vapor flow along the liquid-vapor interface through the interfacial temperature, heat flux, shear stress and pressure jump conditions due to surface tension effects. The model predicts the shape of the liquid-vapor interface along the condenser and leads to the conclusion that there is complete condensation at a certain distance from the condenser inlet. The numerical results show that complete condensation of the incoming vapor is possible at comparatively low heat loads and that this is a special case of a more general condensation regime with two-phase bubbly flow downstream of the initial annular film condensation region. Observations from the flow visualization experiment confirm the existence and qualitative features of annular film condensation leading to the complete condensation phenomenon in a small diameter ($d \leq 3.25$ mm) circular tube condenser.

ACOUSTIC STREAMING IN MICROGRAVITY: FLOW STABILITY AND HEAT TRANSFER ENHANCEMENT

E.H. Trinh , Jet Propulsion Laboratory, California Institute of Technology, MS 183-401, 4800 Oak Grove Drive, Pasadena CA 91109, Eugene.H.Trinh@jpl.nasa.gov

ABSTRACT

The active control of the rates of heat and mass transfer in non-isothermal systems is often a desired capability associated with many industrial and technological practices. In general, this is accomplished by varying the interfacial area and by inducing appropriate flow fields in the medium through which transport takes place. For example, the control of gas and melt flow rates, atomizing gas pressure, initial melt temperature, and host medium conductivity are used to change the quenching rate in gas atomization processes of powder metallurgy . Thus, even for Earth-bound activities for which natural convection is often important, the control of flow fields in the vicinity of the contact interfaces is of significant practical value.

In a low gravity environment, the drastic reduction of natural buoyancy will make the contribution from any externally imposed flow field even more important. For example, heat transfer processes involving change of phase (such as boiling) are drastically affected by the elimination of buoyancy-driven removal of vapor bubbles. In the absence of artificially induced flows, heat or mass transfer in Microgravity is expected to be dominated by radiation, conduction, or diffusion processes. Acoustic streaming-induced convective flows have also been shown to substantially enhance heat and mass transfer, even under the full action of the Earth gravitational field. A detailed understanding of this effect is not yet available, however, because natural convection interferes with accurate heat and mass transport measurements under most experimental conditions found in Earth-based laboratories. The exception might be found at very high acoustic pressure at which stage the second order streaming flow becomes turbulent and theoretical analysis is even more complicated. We are carrying out a ground-based research program to experimentally and theoretically examine both the configuration and stability of acoustically induced streaming flows in order to advance the understanding of the physical mechanisms responsible for their generation, and to develop a predictive model for the observed enhancement in the rates of heat and mass exchange.

In this paper, we describe some of the results obtained during the first phase of the experimental investigation of the characteristics and effects of ultrasonically-induced streaming flows in resonant cavities in both gaseous as well as liquid media. We concentrate on systems involving single particles dispersed in a continuous fluid host medium. Heat and mass are exchanged between the disperse and continuous phase, and the degree to which such interaction can be enhanced by acoustically-induced convection is the primary subject of interest.

High intensity sound waves induce steady-state fluid flow (streaming flow) because of viscous dissipation and through their interaction with boundaries. The characteristic velocity associated with this steady motion is proportional to the square of the time-varying acoustic velocity (or pressure), and the streaming flow regime can vary between slow and laminar to highly chaotic and turbulent. The associated impact on transport processes can therefore be tailored to the specific system requirements. In this research we are not only interested in understanding and controlling streaming flow parameters by changing global acoustic and dimensional variables, but also in the local flows resulting from acoustically-induced motion of isolated fluid particles.

Acoustic streaming can be used effectively to influence the evolution of systems involving a continuous liquid medium and a dispersion of gas or liquid particles by imposing global flows, but also through the excitation of surface motion on the fluid particles themselves. We have found that significant flow around isolated gas bubbles can be generated by inducing short-wavelength capillary waves on the bubble surfaces. Such localized flow fields can effectively enhance mass transport within even dilute bubble suspensions since they extend to several bubble diameters. Similarly, the induction of large-amplitude shape oscillations on bubbles and drops leads to the generation of vigorous circulation in a region extending several particle diameters. We have specifically measured a manifold increase in the rate of gas dissolution into the host liquid by exciting either capillary waves and shape oscillations.

For droplets of liquid suspended in a gaseous medium, we have found that acoustic streaming greatly influences the rate of mass exchange, and can be used to tightly control the rate of growth or evaporation, thus effectively enhancing natural buoyancy in 1-G and replacing it in low-gravity. In addition, controlled variations of the acoustic parameters can be used to induce droplet rotation along various axes.

We have thus demonstrated that acoustic methods can lead to the control of the local environment of a suspension of a large number of discrete fluid particles and to a substantial enhancement in the transport rate of dispersions and suspensions of fluid particles in a continuous fluid environment. This finely controlled action would not only replace the action of gravity, but would provide additional versatility and effectiveness.

Session 6B: Special Topics II

(Extended Abstract)

Extensional Rheometry of Polymer Solutions and the Uniaxial Elongation of Viscoelastic Filaments

Gareth H. McKinley, Stephen H. Spiegelberg, Shelley L. Anna & Minwu Yao[2]
Department of Mechanical Engineering, M.I.T., Cambridge MA 02139, USA
[2]Ohio Aerospace Institute, Brookpark, OH 44132, USA

The uniaxial extensional viscosity is a fundamental material property of a fluid which characterizes the resistance of the material to stretching deformations. For a viscoelastic fluid such as a polymer melt or solution, this material property is a function of both the rate of stretching (i.e. 'strain-rate') and the total deformation (i.e. the 'true strain') imposed. The resulting material property is of great importance in governing the dynamics and stability of polymer processing operations such as fiber-spinning and injection molding, yet it is notoriously difficult to measure this material function due to the difficulty in eliminating shearing effects arising as a consequence of the 'no-slip' boundary condition at all solid-liquid surfaces. Filament stretching rheometers provide one of the few ways of unambiguously measuring the transient elongational response of 'mobile' polymer solutions that are viscous but not rigid enough to test in the extensiometers commonly employed for extremely viscous melts. As the magnitude of the gravitational body force acting on the fluid filament is decreased, the lower bound on the zero-shear-rate viscosity of the fluid that can be used in the device is progressively decreased. However, even in a microgravity environment, the deformable nature of the free-surface of the test fluid and the no-slip boundary conditions pinning the liquid bridge to the rigid endplates preclude generation of truly homogeneous kinematics in a filament stretching device, and it is essential to combine experimental measurements with computational rheometry in order to understand the dynamical characteristics of the apparatus.

In the present paper we investigate the transient extensional stress growth in a concentrated solution of high molecular weight monodisperse polystyrene. The solution has been well characterized in steady and transient shear flows and the viscometric properties are representative of a broad class of physically-entangled melts and solutions. The evolution in the transient Trouton ratio measured experimentally at different deformation rates is compared with numerical computations and with theoretical predictions for ideal homogeneous uniaxial elongation. Finite

element simulations of the filament stretching device with single-mode and multi-mode viscoelastic models demonstrate quantitative agreement between the predicted and observed increases in the extensional viscosity with Hencky strain. The computed Trouton ratio is also in good agreement with theoretical expectations for ideal homogeneous uniaxial extension, despite the strongly nonhomogeneous viscoelastic necking of the fluid column observed during elongation in the filament stretching device.

Following the cessation of elongation, numerical simulations predict an interesting and complex evolution in the kinematics of the fluid filament. Initially, the tensile stresses in the column relax in the nonlinear form predicted theoretically, indicating that filament stretching devices can be used to monitor transient extensional stress relaxation, provided that the evolution history of both the tensile force at the end-plate and the filament radius at the mid-plane are carefully measured. However, at longer times after cessation of stretching, the local extension rate at the axial mid-plane begins to increase rapidly, leading to a 'necking failure' that is greatly accelerated compared to that expected in a corresponding Newtonian filament. The calculations show that this unstable necking is *not* driven by the surface tension but by the viscoelasticity of the fluid, and is coupled with significant elastic recoil of the strained material near the end-plates. The rate of necking in the column is sensitive to the functional form of the transient extensional viscosity predicted by the constitutive model; in particular the magnitude and the rate of strain-hardening that occurs during uniaxial elongation. Even if a non-Newtonian fluid exhibits some strain-hardening, this can be insufficient to stabilize the contraction in the filament radius as material elements stretch. Viscoelastic effects result in a localized rate of thinning that is enhanced beyond that of a strain-independent Newtonian filament and the elongated fluid thread appears to break in a finite time. This phenomena can also be simply and accurately described by an appropriate set of coupled one-dimensional thin filament equations that use the finite element computations to provide a suitable initial condition for the distribution of the polymeric stresses in the filament.

This qualitative difference between weakly strain-hardening polymer melts and strongly strain-hardening elastic fluids (such as very dilute polymer solutions that are well-modeled by Oldroyd-B or FENE-P dumbbell constitutive models) can be understood in terms of a modified Considère analysis commonly employed for describing necking in tensile tests of solid polymer samples. The dynamics of the filament failure are intimately connected to the transient uniaxial elongational stress growth of the polymeric material and are manifested in common everyday life and also in industrial processing operations through heuristic concepts such as 'spinnability' and 'tackiness'.

FLOW-INDUCED BIREFRINGENCE MEASUREMENT SYSTEM USING DUAL-CRYSTAL TRANSVERSE ELECTRO-OPTIC MODULATOR FOR MICROGRAVITY FLUID PHYSICS APPLICATIONS

Jeffrey R. Mackey, NYMA, Inc. NASA Lewis Group
2001 Aerospace Parkway, Brook Park, Ohio 44142, jmackey@lerc.nasa.gov

ABSTRACT

We have developed a new instrument that can measure fast transient birefringence and polymer chain orientation angle in complex fluids. The instrument uses a dual-crystal transverse electro-optic modulator with the second crystal's modulation voltage applied 180° out of phase from that of the first crystal. In this manner, the second crystal compensates for the intrinsic static birefringence of the first crystal, *and* it doubles the modulation depth. By incorporating a transverse electro-optic modulator with two lithium-niobate ($LiNbO_3$) crystals oriented orthogonal to each other with a custom-designed optical system, we have produced a very small, robust instrument capable of fast transient retardation measurements. By measuring the sample thickness or optical path length through the sample, we can calculate the transient birefringence. This system can also measure dichroism.

We have compared the calibration results and retardation and orientation angle measurements of this instrument with those of a photoelastic modulator (PEM) based system using a quarter wave plate and a high-precision 1/16-wave plate to simulate a birefringent sample. Transient birefringence measurements on the order of 10^{-9} can be measured using either modulator.

Session 6C: Convective Instability

Long-Wavelength Rupturing Instability in Surface-Tension-Driven Benard Convection

J. B. Swift[1], Stephen J. Van Hook[1], Ricardo Becerril[1], W. D. McCormick[1], H. L. Swinney[1], [1] Center for Nonlinear Dynamics and Dept. of Physics, The University of Texas, Austin, Texas 78712, USA.
svanhook@chaos.ph.utexas.edu., Michael F. Schatz[2], [2] Georgia Institute of Technology, Atlanta, Georgia 30332.
schatz@ranch.physics.gatech.edu.

A liquid layer with a free upper surface and heated from below is subject to thermocapillary-induced convective instabilities. We use very thin liquid layers (~ 0.01 cm) to significantly reduce buoyancy effects and simulate Marangoni convection in microgravity. We observe thermocapillary-driven convection in two qualitatively different modes --- short-wavelength "Benard" hexagonal convection cells and a long-wavelength interfacial rupturing mode. We focus on the long-wavelength mode and present experimental observations and theoretical analyses of the long-wavelength instability. Depending on the depths and thermal conducitivities of the liquid and the gas above it, the interface can rupture downwards and form a "dry spot" or rupture upwards and form a "high spot". Linear stability theory gives good agreement to the experimental measurements of onset as long as sidewall effects are taken into account. Nonlinear theory correctly predicts the subcritical nature of the bifurcation and the selection between dry spot and high spots.

PLIF Flow Visualization of Incompressible Richtmyer-Meshkov Instability

C.E. Niederhaus[1] and J.W. Jacobs[2],
Department of Aerospace and Mechanical Engineering
University of Arizona
Tucson, AZ 85721
[1]email: niederha@u.arizona.edu
[2]email: jacobs@ame.arizona.edu

Richtmyer-Meshkov (RM) instability occurs when two fluids of different densities are impulsively accelerated normal to their nearly planar interface. It is one of the most fundamental of fluid instabilities and is of importance in fields ranging from astrophysics to material processing. Because RM instabilities are normally carried out in shock tubes using gases, where the generation of a sharp well controlled interface is difficult, there is a scarcity of well visualized experimental results. The experiments presented here utilize a novel technique which avoids many of the experimental difficulties that have previously limited the study of RM instability. In this system, the instability is generated by bouncing a thin rectangular tank containing two liquids off of a fixed spring. Planar Laser Induced Fluorescence (PLIF) is utilized to visualize the instability, providing very clear views of the interface far into the nonlinear regime.

ABSOLUTE AND CONVECTIVE INSTABILITY OF A LIQUID JET

S. P. Lin,[1] M. Hudman[2] and J. N. Chen[3], [1,2,3]Clarkson University, Potsdam, NY 13699.

ABSTRACT

The existence of absolute instability in a liquid jet has been predicted for some time (ref. 1-5). The disturbance grows in time and propagates both upstream and downstream in an absolutely unstable liquid jet. An image of absolute instability has been captureda at the NASA 2.2 second drop tower, and is reported here. The transition from convective to absolute instability is observed experimentally. The experimental results are compared with the theoretical predictions on the transition Weber number as functions of the Reynolds number. The role of interfacial shear relative to all other relevant forces which cause the onset of jet breakup had not been quantitatively elucidated before (ref. 6), and is explained here.

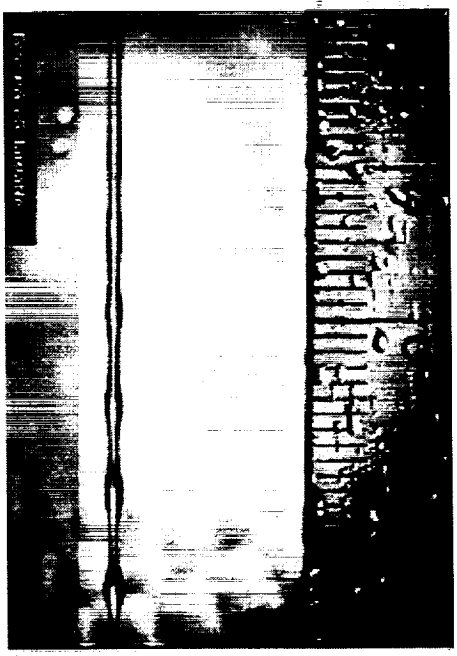

Left: A convectively unstable liquid jet. ($We = 100$, $Re = 160$)

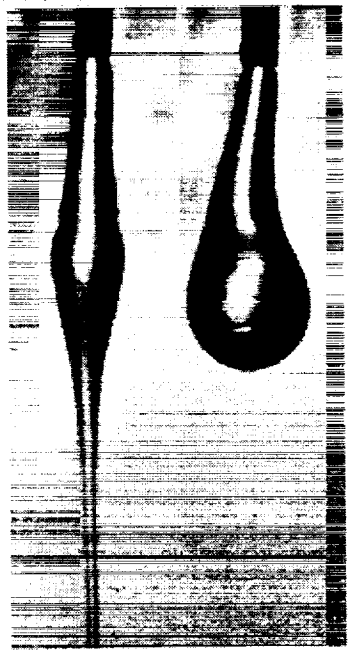

Right: An absolutely unstable liquid jet 0.2 seconds after the drop and 0.4 seconds after the drop. (We=0.349, Re=0.082)

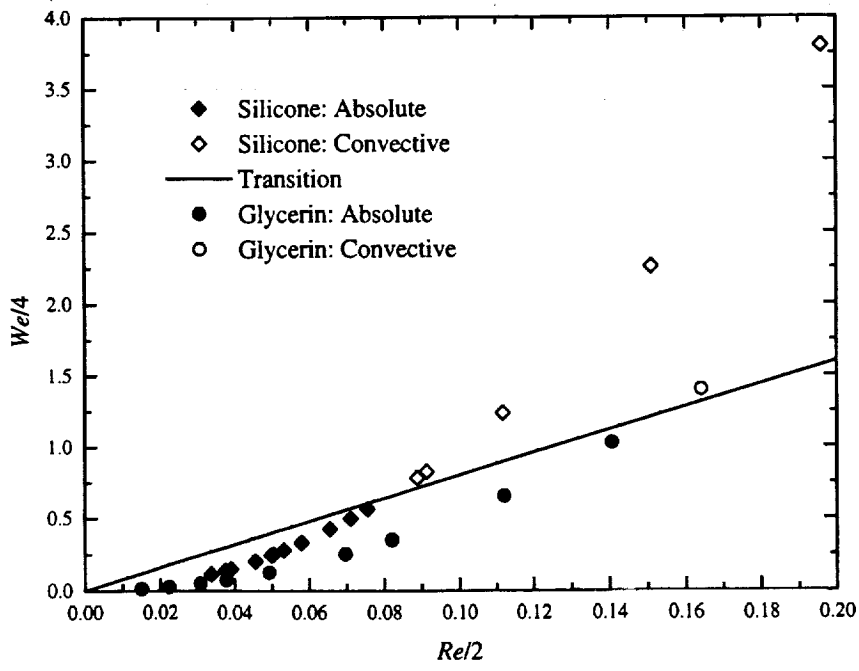

Right: Transition from absolute to convective instability.

Session 7A: Bubbles and Drops

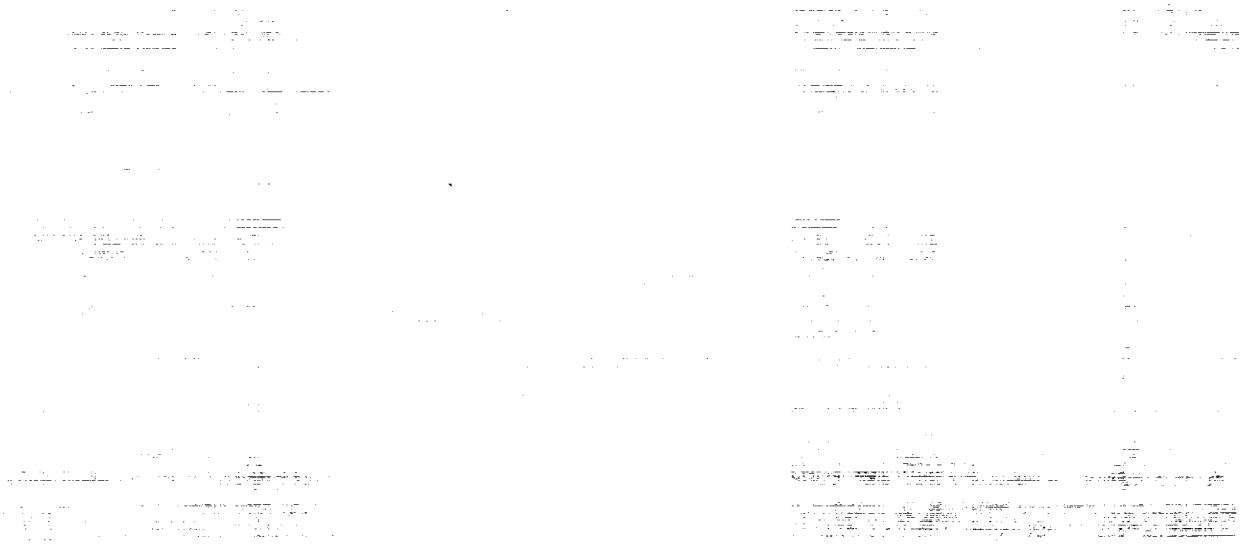

DROP EJECTION FROM AN OSCILLATING ROD

E. D. Wilkes, O. A. Basaran, School of Chemical Engineering, Purdue University, West Lafayette IN 47906, USA, obasaran@ecn.purdue.edu

The dynamics of a drop of a Newtonian liquid that is pendant from or sessile on a solid rod that is forced to undergo time-periodic oscillations along its axis is studied theoretically. The free boundary problem governing the time evolution of the shape of the drop and the flow field inside it is solved by a method of lines using a finite element algorithm incorporating an adaptive mesh. When the forcing amplitude is small, the drop approaches a limit cycle at large times and undergoes steady oscillations thereafter. However, drop breakup is the consequence if the forcing amplitude exceeds a critical value. Over a wide range of amplitudes above this critical value, drop ejection from the rod occurs during the second oscillation period from the commencement of rod motion. Remarkably, the shape of the interface at breakup and the volume of the primary drop formed are insensitive to changes in forcing amplitude. The interface shape at times close to and at breakup is a multi-valued function of distance measured along the rod axis and hence cannot be described by recently popularized one-dimensional approximations. The computations show that drop ejection occurs without the formation of a long neck. Therefore, this method of drop formation holds promise of preventing formation of undesirable satellite droplets.

NUMERICAL MODELING OF THREE-DIMENSIONAL FLUID FLOW WITH PHASE CHANGE

Asghar Esmaeeli, Vedat Arpacı, Department of Mechanical Engineering and Applied Mechanics, The University of Michigan, Ann Arbor, Michigan

ABSTRACT

We present a numerical method to compute phase change dynamics of three-dimensional deformable bubbles. The full Navier-Stokes and energy equations are solved for both phases by a front tracking/finite difference technique. The fluid boundary is explicitly tracked by discrete points that are connected by triangular elements to form a front that is used to keep the stratification of material properties sharp and to calculate the interfacial source terms. Two simulations are presented to show robustness of the method in handling complex phase boundaries. In the first case, growth of a vapor bubble in zero gravity is studied where large volume increase of the bubble is managed by adaptively increasing the front resolution. In the second case, growth of a bubble under high gravity is studied where indentation at the rear of the bubble results in a region of large curvature which challenges the front tracking in three dimensions.

Experimental Trajectories of Two Drops in Planar Extensional Flow

D.C. Tretheway and L.G. Leal, Department of Chemical Engineering
University of California Santa Barbara, Santa Barbara, CA 93106

Introduction

The coalescence and breakup of drops immersed in an immiscible suspending fluid plays an integral role in many industrial, biological, and natural processes such as liquid-liquid extraction and rain drop formation and growth. While breakup involves only a single drop in the suspending fluid, coalescence requires two drops to collide and remain together for a sufficient amount of time for film drainage to occur. Thus, the coalescence probability which incorporates the collision rate and the interaction time depends directly on the hydrodynamic interaction between the two drops. Wang, Zinchenko, and Davis (JFM **249**, 227-239) extended the theoretical rigid sphere work of Batchelor and Green (JFM **56**, 375-400) by investigating the hydrodynamic interaction between two spherical drops subjected to a linear flow field. By calculating the trajectories of two spherical drops, the effects of hydrodynamic interactions on the collision efficiencies and thus coalescence probability of two spherical drops were examined. While these theoretical results for spheres provide insight into the collision process, few drops in an actual systems are spherical. As a result, more recent theoretical and computational work with the boundary integral formulation has studied the interaction of deformable drops. Lowenberg and Hinch (JFM **338**, 299-315) studied the collision of two deformable drops in a shear flow while Zinchenko, Rother, and Davis (Phys. Fluids **9**, 1493-1511) have studied the bouyancy drive interaction of deformable drops. While theoretical work continues to advance, experimental studies with which to confirm the theoretical calculations are quite limited. Zhang, Davis and Ruth (JFM **249**, 227-239) have examined the bouyancy driven interaction between two nearly spherical drops, with results that agree with theoretical calculations for spheres. Guido and Simeone (JFM **357**, 1-20) studied the binary collision of two drops in shear flow. The results showed good agreement with the numerical simulations of Lowenberg and Hinch, (JFM **338**, 299-315) but a direct comparison with spherical theory was not provided.

Since it is cumbersome, at best, to combine boundary integral calculations with trajectory calculations for large-scale systems with many drops, a key issue in developing a theoretical basis for design in mixing and dispersion applications, is to determine conditions where theoretical calculations for spherical drops provide a sufficiently accurate representation of the collision process. In this work, we map the experimental trajectories of two deformable drops in 2-d extensional flow and compare the experimental results with theoretical calculations for spherical drops. We examine the effects deformation has on the interaction of two drops and the necessity of incorportating deformation into theoretical calculations which estimate the collision rates, the collision efficiencies, and the interaction times of two drops.

Experiment

The trajectories of two drops are mapped in the four roll mill, an experimental apparatus which has been used extensively in the study of drop deformation and breakup. Two equal sized drops (approx. 3mm in diameter) are formed in the same plane by injecting a single drop into the four roll mill and subjecting the drop to an extensional flow at a shear rate which exceeds the critical shear rate for drop breakup. After the drop has extended past its critical deformation the flow is stopped and the drop breaks by the end pinching mechanism. Any satellite drops which form during breakup are removed from the device without disrupting the two primary drops. The two drops are then adjusted to the desired initial positions and the motors are engaged to produce the desired flow field. The experimental drop positions are recorded by taking 35mm photos of the moving drops at known times and then analyzing the negatives to obtain their positions.

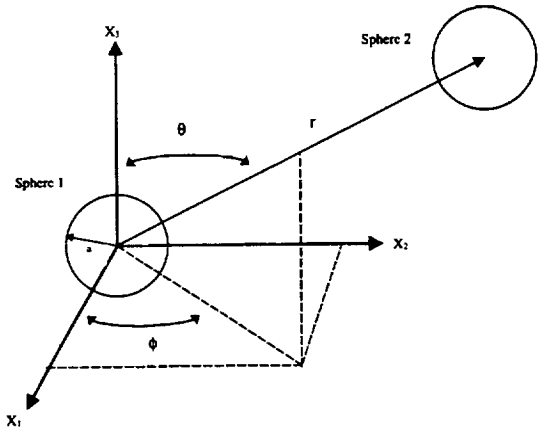

Figure 1. Schematic of the coordinate system used for the trajectory equations.

The experimental drop trajectories are compared with the theoretical calculations in the relative coordinate system shown in Figure 1. The separation between the drops, s (s = r/a), and the in plane orientation angle, ϕ, are calculated from measured positions of the drops. The out of plane orientation angle, θ, is constant at $\pi/2$. The theoretical trajectories are calculated from the relative velocity equation for two spherical drops in a linear flow field. If the separation between the

drops is sufficiently small, an ad hoc modification to the numerical solution of the relative velocity equation is included to keep the spherical drops separated in the compressional quadrant of the flow. The modification is equivalent to forcing the spherical drops to remain barely touching until they rotate into the extensional quadrant of the flow.

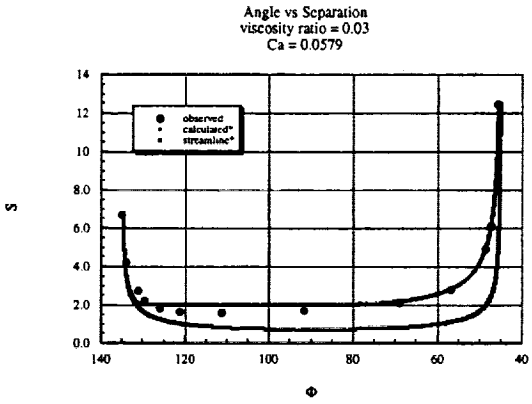

Figure 2. A typical relative trajectory for two deformed drops. $D_f = 0.136$

Conclusions

By comparing the experimental results with the theory for spherical drops modified as described above, a number of conclusions can be drawn. First, the spherical theory accurately predicts the approach and exit trajectories of two drops even for drops with a substantial degree of flow induced deformation. As a result, the spherical theory should provide an adequate estimate of the collision efficiencies for both spherical and deformed drops. Second, for drops which do not come into close approach (the drops interact but remain sufficiently separated that no thin film forms), the spherical theory accurately predicts the symmetric trajectories and captures the increased hydrodynamic interactions for higher viscosity ratios, regardless of the flow induced deformation. Third, for spherical or deformed drops, the spherical theory with the ad hoc modification provides a reasonable estimate of the maximum interaction time of two drops in close approach (i.e. the drops form a thin film as they approach). Fourth, for drops in close approach, the trajectory curves are asymmetric and irreversible with a minimum separation which corresponds to the minor axis of the deformed drops and is less than the minimum separation of two spheres (s=2).

Figure 2 partially illustrates the above conclusions. It shows a typical relative trajectory of two drops with a flow induced deformation of 0.136 (Talyor's deformation parameter). From Figure 2 it is apparent that the trajectory curve is not symmetric about 90°, the minimum separation is less than the minimum separation of two spheres (s=2), the spherical theory accurately predicts the approach (from 135° towards 90° until s=2) and exit (from 90° towards 45° after s>2) trajectories, and the interaction is irreversible.

GROUND-BASED STUDIES OF THERMOCAPILLARY FLOWS IN LEVITATED LASER-HEATED DROPS

S.S. Sadhal[1], H. Zhao[1], and Eugene H. Trinh[2]
[1]Department of Mechanical and Aerospace Engineering, University of Southern California, Los Angeles, CA 90089–1453, USA, sadhal@usc.edu
[2]Jet Propulsion Laboratory 183–401, 4800 Oak Grove, Pasadena, CA 91109, USA, Eugene.H.Trinh@jpl.nasa.gov

In this investigation theoretical and experimental studies on the fluid-flow phenomena together with the thermal effects on drops levitated in acoustic and/or electrostatic fields are being carried out. The experimentation in 1-G requires a strong acoustic field and consequently, there is significant interference with other thermal-fluid effects. While most of the work has been directed towards particles in strong acoustic fields to overcome gravity, some results for microgravity have been obtained. A Glovebox experiment for the MSL-1 Mission has also been tied in with this investigation. One of the primary objectives of the space experiment is to evaluate the acoustic stability criteria in microgravity. In addition, an understanding of the residual internal flows within a quasi-isothermal drop, induced by a positioning ultrasonic field at various power levels, is required.

The analytical effort has been focused largely on the study of fundamental fluid flow around particles in acoustic fields. Several new and interesting analytical results have been obtained for levitated particles. Investigations have been carried out for a liquid drop at the velocity antinode of a standing wave, a solid particle at the velocity node, and a particle in an intermediate position.

It is well known that for a particle at the velocity antinode there exists steady streaming around the particle, and adjacent to the particle a thin recirculating layer has been predicted. For a particle at the velocity node, such a layer has a different behavior, in that, it covers the spherical particle only partially. The streamlines for in this Stokes layer are not closed but instead merge with the outer streaming. The situation of a solid particle at the velocity node has been extended to the case of a liquid drop by allowing tangential velocity and stress continuity. This has led to an interesting prediction that the recirculation the adjacent layer ceases when a relationship between the frequency ω and some of the thermophysical parameters exceeds a certain value. This cessation of recirculation is not fully understood but some explanations have been put forward. For the case of a liquid drop positioned between a node and the antinode, similar behavior for the recirculating layer is observed. When the recirculation does not exist, vortices are predicted at the upstream side of the drop with respect to the streaming flow, as shown in Figure 1. This has, in fact, been observed with levitated drops as shown in Figure 2.

An experiment for the Glovebox flight investigation took place during the MSL-1 Mission in early July 1997. This work was initiated to assess the capability for ultrasonic positioning in microgravity, and for drop internal flow measurement. A compact ultrasonic positioner was designed and integrated with laser diode illumination in order to experimentally demonstrate the rotation control of freely suspended drops in low gravity and to obtain preliminary flow field measurements for isothermal droplets. The initial goal of performing preliminary measurement on spot-heated droplets was not realized due to a combination of safety and Glovebox facility constraints.

The important findings from the flight investigations include the identification of the ultrasonic parameters which affect the ability to control the particle position in a microgravity environment. In addition, measurement of the residual rotation rate were carried out, and indicate a residual steady rotation of about 0.1 rps with the acoustic power required to counteract the Shuttle attitude control firings. The first accurate data for drop deformation as a function of acoustic pressure were obtained for a sample located at the pressure minimum plane in the ultrasonic standing wave. All ground-based data are for a drop away from the pressure nodal plane because of gravity. Based on these preliminary assessments, the current apparatus is deemed effective for the accurate positioning of drops in air in an actual microgravity environment.

The development of the apparatus for the reflight of the IFFD (Internal Flow in a Free Drop) investigation is well under way. A sting heater consisting of a thermistor mounted on a stainless steel rod and held on a micropositioner stage will be used to provide local heating for a free drop with a maximum temperature rise of 20°C. The tip of the heater will be placed in the proximity of a drop in order to provide differential heating. The internal flows recorded through the mo-

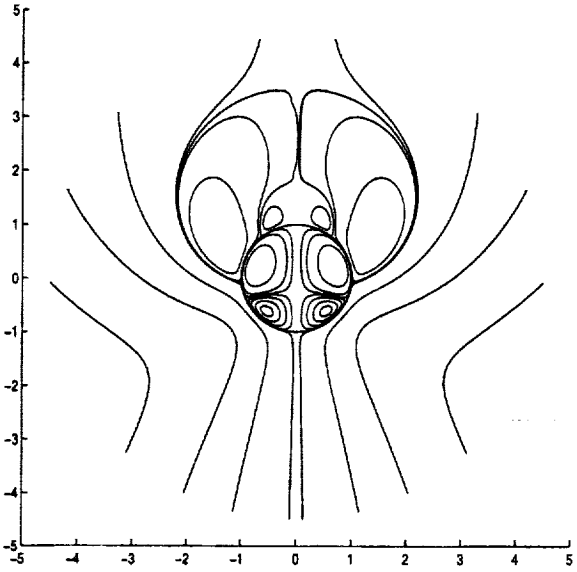

Figure 1: Theoretical prediction of streaming flow past a liquid drop between the node and the antinode. The outer streaming is in the downward direction.

Figure 2: Visualization of flow around an acoustically levitated particle showing an upstream-side vortex.

tion of suspended tracer particles within the drop will be compared with those generated when the drop is in direct contact with the heater tip. Ground-based tests have shown that the heater tip can be safely moved to within 2 mm of a 4 mm diameter levitated drop without perturbing it. The effects of acoustic streaming will also be investigated for a sting-held drop by comparing the internal flows for different acoustic power levels.

For ground-based studies, a previously-described apparatus has been used to record the motion of fluorescent tracer particles suspended in the drop liquid. The scattered light is gathered along two orthogonal views using holographic notch filters to block the elastically scattered light from the drop surface. The liquid used was an aqueous mixture of glycerin and silicone oil (Polydimethylsiloxanes) and a focused CO_2 laser was used to spot-heat the levitated drop. The results show that although it was possible to accurately measure the internal flows of isothermal drops, the combination of Earth-based ultrasonic levitation and spot heating induces an uncontrolled torque which drives a random rotational motion of the drops. With electrostatic levitation, however, this problem has been eliminated. Preliminary observations have been carried out with electrostatically levitated charged drops in 1-G with focused CO_2 laser heating from the side. The quantitative characterization of the resulting complicated buoyancy and thermocapillary-induced flows require a three-dimensional analysis of the flow field.

Thermocapillary flows coupled to natural buoyancy-driven convection have been observed for electrostatically levitated droplets using spot heating from a focused CO_2 laser directed to the right side of the drop. The current spot size is about 300 μm and the levitated drops have diameters between 3 and 5 mm. The predicted vortical motion could be observed, although the flow pattern is very asymmetric due to the gravitational bias. Radiant input power is controlled by varying the duty cycle of the laser. Further measurements will be taken using a smaller (100 μm laser spot size).

Acknowledgements

The investigators are very grateful for the support of this work under Grant No.: NAG3-1842 from the Microgravity Fluid Physics Program of the National Aeronautics and Space Administration.

THERMOCAPILLARY MIGRATION AND INTERACTIONS OF BUBBLES AND DROPS

R. Shankar Subramanian, Clarkson University, Potsdam, New York 13699-5705,
R. Balasubramaniam, NCMR, NASA Lewis Research Center, Cleveland, Ohio 44135,
G. Wozniak, Freiberg University of Mining and Technology, D-09596 Freiberg, Germany and
P.H. Hadland, Aker Offshore Partner AS, P.O. Box 589, 4001 Stavanger, Norway

ABSTRACT

Experiments were performed aboard the LMS mission of the Space Shuttle in summer 1996 in the BDPU on isolated air bubbles and Fluorinert FC-75 drops as well as on interacting bubbles/drops migrating in a temperature gradient in a Dow-Corning DC-200 series silicone oil of nominal viscosity 10 centistokes. The data, recorded in the form of videotape images as well as cine images in selected runs, have been analyzed. The behavior of the isolated objects is consistent with earlier observations made aboard the IML-2 mission while the range of Reynolds and Marangoni numbers has been extended substantially over that in the IML-2 experiments. Large bubbles were found to be slightly deformed to an oblate shape while no deformation could be detected in the case of similarly large drops. Results on interacting drops and bubbles display interesting and unanticipated features. In some experiments, drops are found to follow a three-dimensional trajectory. In others, trailing drops and bubbles are found to move off the axis of the cell when migrating behind a leading drop or bubble which moves along the axis. In this type of run, if the trailing drop is sufficiently large, it is found to pass the leading drop. Finally, behavior similar to that observed in IML-2, namely that a small leading drop slows the movement of a larger trailing drop moving along the cell axis, was observed as well.

Session 7B: Liquid Bridges

STABILITY LIMITS AND DYNAMICS OF NONAXISYMMETRIC LIQUID BRIDGES.

J. Iwan D. Alexander[1], Lev A. Slobozhanin[2], Andrew H. Resnick[2], Jean-Francois Ramus[2] and Sylvie. Delafontaine[2]

[1]National Center for Microgravity Research and Department of Mechanical and Aerospace Engineering, Case Western Reserve University, Cleveland, OH 441106; [2]Center for Microgravity and Materials Research, University of Alabama in Huntsville, Huntsville, AL 35899

Abstract

Liquid bridges have been the focus of numerous theoretical and experimental research since the early work by Plateau more than a century ago [1]. More recently, motivated by interest in their physical behavior and their occurrence in a variety of technological situations, liquid bridges have become the subjects of many experimental and theoretical investigations. Furthermore, opportunities to carry out experiments in the near weightless environment of a low-earth-orbit spacecraft have also led to a number of low-gravity experiments involving large liquid bridges (see, for example, Refs. [2,3]).

In this paper we present selected results from our theoretical and experimental work concerning the stability of nonaxisymmetric liquid bridges, isorotating axisymmetric bridges between equidimensional disks and bridges contained between unequal disks. Finally, we present results concerning the stability of axisymmetric equilibrium configurations for a capillary liquid partly contained in a closed circular cylinder.

The stability of two types of static nonaxisymmetric bridge configurations was considered. In both cases, the bridge was held between equidimensional coaxial disks. In the first example, gravity was taken to be oriented perpendicular to the axis through the supporting. The second example dealt with nonaxisymmetric bridges subject to axial acceleration. Both problems were solved numerically using the *Surface Evolver code* [4].

Stability of was examined as a function of slenderness, Λ (ratio of the disk separation to the mean diameter, $2r_0$, of the two support disks), and the relative volume, V (ratio of the actual liquid volume to the volume of a cylinder with a radius r_0). The location of the stability boundary for a given Bond number, B, was determined by fixing the slenderness, Λ , and minimizing the energy for some value of V. Outside the stability boundary, the bridges break before the energy is minimized. Inside the stability boundary, bridges maintain their integrity and reach a minimum energy configuration. Thus, we were able to employ a simple iterative search technique to find the approximate location of the boundary. For a given B and a fixed value of Λ that is less than the maximum stable slenderness, Λ_{max}, there exists a maximum and minimum stable relative volume. The maximum volume stability limit tends to infinity as $\Lambda \to 0$. For any given (lateral) B, the minimum volume stability limit becomes indistinguishable from the zero B limit when Λ becomes sufficiently small.

In related work carried out in collaboration with Prof. J. Meseguer and Dr. F. Zayas of the Universidad Politecnica de Madrid, we have also examined results of an asymptotic analysis of the stability limits for lateral gravity. The results show that, at least close to the reference configuration ($\Lambda \sim\pi$, $v\sim 0$, $B_a\sim 0$, $B_l\sim 0$) there is a self-similar solution for the stability limits, the behavior being the same regardless of the slenderness or volume. The maximum stable slenderness, Λ_{max}, of a liquid bridge between equal disks, and a nearly cylindrical volume, when subjected to both axial (B_a) and lateral (B_l) Bond numbers becomes

$$b_l = (1 - (b_a)^{2/3})^{1/2}, \qquad (1)$$

where

$$b_a = (3/2)^2 \lambda^{-3/2} B_a, \text{ and } b_l = (\pi/2)\lambda^{-1/2} B_l, \qquad (2)$$

are the reduced axial and lateral Bond numbers and $\lambda = 1 - \Lambda_{max}/\pi + v/2$, where $v = V - 1$. Numerical results obtained using *Surface Evolver* [4] were found to be in good agreement with Eq. (1).

For axisymmetric bridges subject to axial gravity it is known that along most of the maximum volume stability limit axisymmetric bridges are unstable to nonaxisymmetric perturbations. We examined the bifurcation of solutions for a weightless liquid bridge in the neighborhood of this stability boundary. Depending on the system parameters, loss of stability with respect to nonaxisymmetric perturbations resulted in either a jump or a continuous transition to stable nonaxisymmetric shapes. The value of the slenderness at which a change in the type of transition occurred was found to be $\Lambda_s = 0.4946$. Results from an experimental investigation [6] based on a neutral buoyancy technique agree with this prediction.

For bridges between coaxial disks and subject to axial gravity, little is known about the stability of nonaxisymmetric configurations beyond the maximum (axisymmetric) volume limit. We examined the stability of these bridges using *Surface Evolver* for $B = 0.1$ and 2. We found that the maximum volume segment of the stability limit follows the same trend as for lateral gravity.

The stability of axisymmetric equilibrium states of an isorotating liquid bridge between equidimensional

circular disks in a constant axial gravity field was also considered [5]. Emphasis was given to bridges satisfying two types of constraint typical of the floating zone method for materials purification and single crystal growth. First we considered the constraint $V = 1$. For this case, the critical values of Λ and of the surface slopes (β_1, β_2) at both disks were determined for a wide range of B and Weber (W) numbers. The second constraint is that the surface slope β_1 at one of the disks is prescribed. The chosen values were 90° and 75° and correspond to extremes in growth angle values encountered in floating zone crystal growth. For this case, the dependencies of critical Λ and V values on B and W have been calculated. In addition, both axial gravity directions were considered separately and the values of the slope angle, β_2, at the other disk were also analyzed for critical states.

The solution of the stability problem for any axisymmetric isorotating liquid bridge between equal disks is discussed in detail using the case for $B = W = 0.1$ as an example. In particular, the relationship between the general boundary of the stability region and the stability of bridges subject to the constraints outlined above is examined.

The stability of an axisymmetric liquid bridge between unequal circular disks in an axial gravity field was examined for all possible values of the liquid volume and disk separation. The parameter defining the disk inequality is K, the ratio between the radii of the smaller and larger disks. Wide ranges of B and K were considered. Emphasis was given to previously unexplored parts of the stability boundaries. In particular, we examined the maximum volume stability limit for bridges of arbitrary Λ and the minimum volume stability limit for small Λ. The maximum volume limit was found to have two distinct properties: large values of the critical relative volume at small Λ, and the possibility that stability is lost to axisymmetric perturbations at small K. For a given set of K, the maximum value of B beyond which stability is no longer possible for any combination of V and Λ was determined. In addition, the maximum value of the actual liquid volume of a stable bridge that can be held between given disks for all possible disk separations was obtained for fixed B. It was found that this volume decreases as K decreases and (depending on the sign of B) tends to the critical volume of a sessile or pendant drop attached to the larger disk. Experimental results [6] are in good agreement with our theoretical results.

Finally, we present results concerning the stability of axisymmetric equilibrium configurations of a capillary liquid in a circular cylindrical container with planar ends that are orthogonal to a cylindrical wall. The liquid either is subject to an axial gravity field or is under zero-gravity conditions. We consider *doubly connected* free surfaces that bound an annular region occupied by the gas. This study was motivated by the problem of partly contained melts in low gravity solidification experiments. Preliminary results prove that a free surface with one of contact lines on one of the cylinder's planar ends and the other on a lateral wall is always unstable if the wetting angle, α, lies in the range $0 \le \alpha \le 90°$. The stability regions for such a configuration have been constructed in the plane "α - V", (here $V = v_g/r_0^3$ is the relative gas volume) for set values of the B in the interval $-10 \le B \le 60$. It has been established that the stability region is connected if $B > B_0$ or $B < B_1$ ($-1.69 > B_0 > -1.70$ and $-1.79 > B_1 > -1.80$). If $B_1 < B < B_0$, the stability region consists of two disconnected parts. It is also shown that a doubly connected free surface with both contact lines on a cylindrical wall may exist only under zero-gravity conditions. Further analysis revealed that only unduloidal free surfaces with profiles that contain inflection points may be stable to nonaxisymmetric perturbations. Such a free surface may be stable to arbitrary perturbations if $\alpha > 121°$. For a given $121° < \alpha < 180°$, a minimum stability limit of the relative gas volume and a maximum stability limit have been determined. Two special liquid bridge configurations were also analyzed. One with a free surface pinned to edges of both end plates of a cylinder and the other with one part of the free surface pinned to edges of a cylinder's planar end and the other to a solid rod contained within the cylinder. This problem is connected with a new technique for "contactless" directional crystallization in low gravity. We analyzed the stability conditions for the first configuration at $B = 0$ and $B = 0.05$, and arbitrary values of other parameters (the wetting angles, aspect ratio and the liquid relative volume). Similar results have been obtained for the second configuration.

References

[1] J. Plateau, "Statique expérimentale et théoretique des liquides" (Gautier–Villars, Paris, 1873).

[2] D. Langbein, in Materials Science in Space, Eds. B. Feuerbacher, H. Hamacher and R. Naumann (Springer, Berlin, 1987) 401.

[3] I. Martinez, J. M. Haynes, and D. Langbein, in Fluid Sciences and Materials Sciences in Space, ed. H. Walter, (Springer Verlag, Berlin, 1987) 53.

[4] K. Brakke, Exper. Math. **1** (1992) 141.

[5] L. A. Slobozhanin and J. I. D. Alexander, Phys. Fluids **9** (1997) 1880.

[6] A. H. Resnick, Ph.D. Thesis, The University of Alabama in Huntsville, 1997.

RADIATION AND MAXWELL STRESS STABILIZATION OF LIQUID BRIDGES

M. J. Marr-Lyon, D. B. Thiessen, F. J. Blonigen, P. L. Marston, Department of Physics, Washington State University, Pullman, WA 99164-2814; marston@wsu.edu

ABSTRACT

A fluid configuration unique to the zero-gravity environment is the liquid cylinder surrounded by air or vacuum. The stability of a liquid cylinder which bridges two solid cylinders may have implications for various low-gravity fluid management situations. It is well known that a cylindrical liquid bridge in zero gravity becomes unstable and breaks when the length of the cylinder exceeds its circumference. The ratio of length to diameter of a cylindrical liquid bridge is defined as the slenderness, $S = L/2R$, and the stability limit $S = \pi$ is known as the Rayleigh–Plateau (RP) limit. A stable cylindrical liquid bridge has many modes of oscillation corresponding to different volume-conservative surface deformations. The lowest-frequency mode, known as the (2,0) mode, is the first to become unstable when the slenderness exceeds π. The (2,0) mode is an axisymmetric surface deformation in which one end of the bridge becomes fat and the other end thin. At the point of instability the deformation grows until the thin end of the bridge breaks. The stabilization schemes explored in this work are based on counteracting the growth of this surface deformation by applying a surface stress distribution which either preferentially pushes radially inward on the fat part of the bridge or pulls radially outward on the thin part. Both acoustic radiation stress [Marr-Lyon et. al., J. Fluid Mech. **351**, 345-357 (1997)] and the Maxwell stress [Marston et al., Bull. Am. Phys. Soc. **42**, 2122 (1997)] have been used to stabilize liquid bridges in this work. Both passive and active acoustic stabilization schemes as well as an active electrostatic method have been explored.

Considering only the (2,0) mode, liquid bridge dynamics are equivalent to the dynamics of a damped harmonic oscillator in which the amplitude of the (2,0) mode corresponds to the oscillator's displacement. The (2,0) mode surface deformation has an associated change in surface area which provides a restoring force proportional to the (2,0) mode amplitude. The effective spring constant for this restoring force is proportional to $[(\pi/S)^2 - 1]$. Thus the natural spring constant becomes negative when $S > \pi$ which results in instability. An externally applied stress distribution which couples into the (2,0) mode can act as an additional effective force on the oscillator mass. If this external force is applied in proportion to the amplitude of the (2,0) mode deformation with the appropriate gain, the effective spring constant can be made positive for $S > \pi$ thus allowing for longer stable bridges. Active feedback stabilization involves measuring the (2,0) mode amplitude and then altering the stress distribution on the bridge in proportion. For the case of passive acoustic stabilization an additional restoring force from acoustic radiation stress naturally arises from the interation between the bridge shape and the sound field.

Laboratory experiments: Active acoustic stabilization was first demonstrated by us in ground-based Plateau tank experiments for a silicone-oil bridge in a water bath [Marr-Lyon et. al., J. Fluid Mech. **351**, 345–357 (1997)]. Acoustic radiation stresses on the bridge could be spatially redistributed very rapidly in response to bridge deformation by simply changing the drive frequency of a specially designed asymmetric acoustic transducer. Stabilization was accomplished to a slenderness of 4.3. Active acoustic stabilization for a liquid bridge in air under low gravity conditions requires different technology from that used in the Plateau tank. Preliminary tests have been conducted on two acoustic transducer systems for rapidly redistributing the acoustic radiation stress on a bridge in air. Coupling into the (2,0) mode has been demonstrated for a soap-film bridge under normal gravity conditions. An important consideration for active stabilization of a bridge in air is the feedback delay. Feedback delay, which depends substantially on the Q of the transducer resonance, results in reduced bridge stability. A low-Q transducer therefore is expected to be advantageous.

We also stabilized an electrically conducting bridge in a Plateau tank by actively controlling Maxwell electrostatic stresses. Two ring electrodes which are concentric with the bridge are positioned near the ends of the bridge in an insulating liquid. The diameter and spacing of the electrodes are chosen in such a way that the stress distribution couples strongly into the (2,0) mode of the bridge when a voltage is applied to one of the electrodes. When one end of the bridge begins to thin, a voltage is applied to the electrode on that end which attracts the bridge liquid, thus counteracting the tendency to thin and break. Stabilization has

been accomplished for a bridge of slenderness 4.3 by this method.

KC-135 based experiments: A liquid bridge in air is predicted to be stabilized when positioned at a pressure node in an acoustic standing wave with the bridge axis perpendicular to the sound propagation direction [Marston, J. Acoust. Soc. Am. **97**, 3377 (1995)]. The stabilization is a passive result of the interaction of the sound field with the bridge. The radius of the bridge supports and the frequency of the sound field are chosen such that the radiation stresses cause the regions of smaller local radius to be expanded and regions of larger local radius to be squeezed, thus counteracting the growth of the (2,0) mode. Passive stabilization was demonstrated by us in low gravity for a liquid bridge in air during parabolic flights aboard NASA's KC-135 aircraft. A bridge mixture of glycerol and water with a viscosity of 20 cS supported between cylindrical tips of radius 2.16 mm was stabilized to a slenderness of 3.5 in a 21 kHz acoustic standing wave. The bridge broke immediately when the acoustic standing wave was turned off.

This research was supported by NASA grant NAG3-1918.

STABILITY OF SHAPES HELD BY SURFACE TENSION AND SUBJECTED TO FLOW

Yi-Ju Chen, ESAM, Northwestern University, Evanston, IL 60208, USA, chen@arnold.esam.nwu.edu, Nathaniel D. Robinson and Paul H. Steen, Chemical Engineering, Cornell University, Ithaca, NY, USA, steen@cheme.cornell.edu

A liquid/gas or liquid/liquid interface is shaped by surface tension whenever surface area is large relative to volume (small physical length) or when gravity is reduced relative to the surface force (small capillary length). The stability of such an interface is important to a variety of earth-based applications, to float-zone experiments in a space shuttle and to successful liquid management in a space laboratory, more generally.

Results of three problems are summarized in this contribution. Each involves the fundamental capillary instability of an interfacial bridge and is an extension of previous work. The first two problems concern equilibrium shapes of liquid bridges near the stability boundary corresponding to maximum length (Plateau-Rayleigh limit). For the first, a previously formulated nonlinear theory to account for imposed gravity and interfacial shear disturbances in an isothermal environment [1,2] is quantitatively tested in experiment. For the second problem, the liquid bridge is subjected to a shear that models the effect of a thermocapillary flow generated by a ring heater in a liquid encapsulated float-zone configuration[3]. In the absence of gravity, this symmetric perturbation can stabilize the bridge to lengths on the order of 30% beyond the Plateau-Rayleigh (PR) limit, which is on the order of heretofore unexplained shuttle observations. The third problem considers the dynamics of collapse and pinchoff of a film bridge (no gravity) --- what happens in the absence of stabilization. Here we summarize experimental efforts to measure the self-similar cone-and-crater structure predicted by a previous theory[4].

1. CHEN, Y-J & STEEN, PH 1994 Influence of flow on Interface Shape Stability *Proc. 14th IMACS World Conf.*, Atlanta, GA, July, pp.629-32.

2. CHEN, Y-J 1997 Stability and breakup of capillary surfaces of revolution: liquid and film bridges. PhD dissertation, Cornell University.

3. CHEN, Y-J & STEEN, PH 1996 Influence of thermocapillary flow on capillary stability: Long float-zones in low gravity. *Proc. 3rd Microgravity Fluid Physics Conf.*, Cleveland OH, 13-15 June, pp.481-3.

4. CHEN, Y-J & STEEN, PH 1997 Dynamics of inviscid capillary breakup:collapse and pinchoff of a film bridge. *J. Fluid Mech.* **341**, pp. 245-267.

ELECTROHYDRODYNAMIC STABILITY OF A LIQUID BRIDGE - THE 'ALEX' EXPERIMENT

C. L. Burcham[1], S. Sankaran[2], & D. A. Saville[3] [1,3]Department of Chemical Engineering, Princeton University, Princeton, NJ, [2]NASA Lewis Research Center, Cleveland OH, [3]dsaville@morticia.princeton.edu

ABSTRACT

To provide insight into the roles of electrical forces, experiments on the stability of a liquid bridge were carried out during the 1996 Life And Microgravity Science Mission on the space shuttle *Columbia.* In terrestrial laboratories a Plateau configuration (where the bridge is surrounded by a matched density liquid) is necessary to avoid deformation due to buoyancy. This complicates the electrical boundary conditions, since charge is transported across the liquid-liquid interface. In the microgravity environment, a cylindrical bridge can be deployed in a gas which considerably simplifies the boundary condition. Nevertheless, to provide a tie-in to terrestrial experiments, two-phase experiments were carried out. The agreement with previous work was excellent. Then several experiments were conducted with a bridge deployed in a dielectric gas, SF_6. In experiments with steady fields, it was found that the bridge was less stable than predicted by a linearized stability analysis using the Taylor-Melcher leaky dielectric model.

ABSTRACT: DYNAMIC MODELING OF MICROGRAVITY FLOW

J. U. Brackbill[1], Damir Juric[1], David Torres[1], Elizabeth Kallman[2], [1]Theoretical Division, Los Alamos National Laboratory, Los Alamos, NM 87545, jub@lanl.gov, [2]Mechanical Engineering, UC Berkeley, Berkeley CA 94720

The absence of gravity and buoyancy in microgravity flow imposes new requirements on numerical models of fluid flow. Forces that are small in terrestrial flow, such as surface tension, are dominant in the absence of gravity, even on large spatial scales. Forces that are large in terrestrial flows, such as buoyancy, are absent in the absence of gravity. Thus, surface tension is important under almost all circumstances in microgravity flow, and must be done accurately and economically. The lack of buoyancy changes the physics of boiling and combustion, and requires the development of new approaches to modeling such flows.

Here we consider the numerical aspects of modeling microgravity flows. We revisit the continuum surface force model for use in interface capturing methods, with special emphasis on how one can compute accurately equilibrium or near equilibrium flows. We also review recent work on film boiling and solidification, using an interface tracking method.

The continuum surface force (CSF) model was developed to model surface pressures occurring at transient fluid interfaces with arbitrary and time-dependent topology [1]. CSF confines the contributions of the surface tension force to a small portion of the computation mesh in the neighborhood of the interface. This poses a challenge in formulating sufficiently accurate finite difference expressions [1]. Errors sometimes manifest themselves as parasitic currents that persist even when there should be equilibrium. A dimensional analysis shows that the maximum velocity around a bubble of radius R is given by $u_{max} = K\sigma/\eta$, where K is some constant. Numerical experiments verify this law with $K \approx 10^{-2}$. [2]

As a remedy, we present a projection method in which equilibrium corresponds to achievement of constant values of a pressure like variable. The numerical errors are much reduced, and the only added complexity is the need to solve an additional elliptic equation.

Where $\vec{F}_s$ accounts for surface tension forces, one can decompose $\vec{F}_s/\rho$ into a solenoidal part ($\nabla\vec{\lambda}$) and an irrotational part divided by density

$$\frac{1}{\rho}\vec{F}_s = \nabla\vec{\lambda} + \frac{\nabla\phi}{\rho}. \qquad (1)$$

Such a decomposition is admissible if one considers an arbitrary interface between two inviscid, incompressible fluids initially at rest.

In order to enforce the zero divergence of $\vec{u}$ in the original formulation with regards to the surface tension force, the equation $\nabla \cdot \frac{1}{\rho^n}\nabla(\mathcal{L})^{-1} = 1$, where $\mathcal{L}$ is the discrete pressure Poisson operator, must be enforced on the discrete level. This requires that a pressure Poisson equation be solved with infinite precision. In order to enforce the zero divergence of $\vec{u}$ with regards to the surface tension force in the new formulation, $\nabla \cdot \nabla = 0$ must be enforced on the discrete level. This can be enforced on a rectilinear grid with many discretizations.

Thus, the new method with the decomposition differs from the original method by allowing one to achieve a force balance between surface tension and pressure on the discrete level.

The improved CSF formulation is illustrated by several standard problems. In one of these, we investigate the reduction in parasitic flow with the projection method. In a calculation on a 4040 mesh of an initially circular cylinder, any flow is an error. However, the flow with FLIP is much reduced by the new formulation. The magnitude of the flow corresponds to $K \approx 6.10^{-4}$, compared with $K \approx 10^{-2}$ reported by Lafaurie et al. [2].

Our theoretical and numerical studies of interfacial flows in microgravity have also focused on exploring some of the more poorly understood physical phenomena that arise in single and multicomponent systems when fluid flow, interface dynamics and phase change are fully coupled. To accomplish this coupling we have continued to extend the capabilities of a finite difference/front tracking method developed in [3]. In its most general form the method uses a single set of conservation equations for all the phases involved. The phase boundary is treated as an imbedded interface by adding to these transport equations the appropriate source terms for surface tension, interphase mass transfer, jumps in material properties and rejection/absorption of latent heat and solute. These source terms are in the form of delta functions localized at the interface and are selected in such a way as to satisfy the correct jump conditions across the phase boundary.

We begin by specifying the constant material properties for each phase. The bulk phases are incompressible but we allow for volume expansion or shrinkage at the phase interface due to the density change upon phase transition. Equations for the material property fields can be written for the entire domain using an indicator

function, $I(\vec{x},t)$, which , for example, has the value 1 in the solid phase and 0 in the liquid phase. I is similar to the color function used in the CSF method or the phase-field variable in the phase field method. However here, as will be shown below, we determine I from the known position of the tracked interface rather than use it to determine the position of the interface. The values of the material property fields at every location are given by $b(\vec{x},t) = b_1 + (b_2 - b_1)\, I(\vec{x},t)$, where the subscripts 1 and 2 refer to the two phases. b represents density, ρ, viscosity, μ, specific heat, c, thermal conductivity, K, or chemical diffusivity, D.

We find $I(\vec{x},t)$ by solving a Poisson equation where the right hand side is a function only of the known interface position at time t. The interface is advected in a Lagrangian fashion by integrating

$$(d\vec{x}_i/dt)\cdot\hat{n} = \vec{V}\cdot\hat{n} \qquad (2)$$

where $\vec{V}$ is the interface velocity vector. We assume that the tangential components of the interface velocity, $\vec{V}$, and material velocity, $\vec{u}$, at the interface are equal, *i.e.* no slip at the interface.

Away from the interface the single field formulation reduces to the customary mass, momentum, thermal energy and solute transport equations for each of the bulk phases while integration of these equations across the interface incorporates the correct mass, momentum and energy balances across the interface.

The formulation is completed by a thermodynamic constraint on the interface temperature, $T_i = T(\vec{x}_i)$, that must be satisfied at the phase boundary. The simplest choice is to assume that $T_i = T_{sat}$ or if considering a dilute multicomponent solution $T_i = T_{sat} - m\tilde{C}_i$, where m is the slope of the liquid or vapor line in a phase equilibrium diagram, and $\tilde{C}_i$ is the interface solute concentration. In reality the interface temperature is a much more complicated function and we use a more complete form derived in [3].

The equations of motion along along with the interface temperature constraint are solved iteratively for the correct normal interface velocity, $\vec{V}\cdot\hat{n}$, that will satisfy the interface temperature constraint. For the spatial discretization, we use the MAC method with a staggered grid. A first order, phase change projection algorithm is used for the time integration. In explicit front tracking, the phase interface is represented discretely by Lagrangian markers connected to form a front which lies within and moves through the stationary Eulerian grid. As the front moves and deforms, interface points are added, deleted and reconnected as necessary throughout the calculation. Thus the interface can exhibit arbitrarily complex interface deformations and topology changes. Information from integral source terms are passed between the moving Lagrangian interface and the stationary Eulerian mesh using the immersed boundary technique. With this technique, the sharp interface is approximated by a smooth distribution function that is used to distribute the sources at the interface over mesh points nearest the interface. Thus the front is given a finite thickness on the order of the mesh size to provide stability and smoothness with no numerical diffusion since this thickness remains constant for all time.

We demonstrate the capabilities of front-tracking for phase change problems with two-dimensional calculations of film boiling and alloy solidification.

References

[1] J. U. Brackbill, D. B. Kothe, and C. Zemach, "A Continuum Method for Modeling Surface Tension, *J. Comput. Phys.*, Vol. 100, 335 (1992).

[2] B. Lafaurie, V. Nardone, R. Scardovelli, S. Zaleski and G. Zanetti, "Modeling Merging and Fragmentation in Multiphase Flows with SURFER," *J. Comput. Phys.*, Vol. 113, 134 (1994).

[3] D. Juric and G. Tryggvason, "Computations of Boiling Flows," *Int. J. Multiphase Flow*, in press.

Session 7C: Interfacial Phenomena III

Fluid/Solid Boundary Conditions in Non-Isothermal Systems

PI: DANIEL E. ROSNER, NASA-MSAD Grant No. NAG 3-1951

Yale University, Department of Chemical Engineering
High Temperature Chemical Reaction Engineering (HTCRE-) Laboratory
New Haven, CT 06520-8286 USA

In a short paper (*Phys. Fluids A* **1** (11) 1761-1763 (1989)) the *PI* pointed out for the first time that vapor-filled nonisothermal crystal growth ampoules operating in micro-gravity will experience convection *driven* by both "wall-induced thermal creep" as well as thermal stresses (in the bulk vapor). But, as emphasized in our subsequent review of thermally-induced *particle phoresis* (Rosner *et.al.*, 1992) these "thermal creep" boundary condition (BC-) phenomena also determine the readily observed migration rates ("phoresis") of suspended "small" solid particles in suspension. This led us to the idea (Topic 1, below) that careful phoresis measurements in a suitably designed microgravity environment (to preclude complications such as 'sedimentation' or 'bouyant rise' for particles large enough both to sustain large temperature differences and avoid appreciable Brownian motion) could be used to obtain unambiguous information about the nature of the tangential momentum transfer boundary condition (*cf.* Eq.1 below) over a broad range of Newtonian fluid densities. This would be especially interesting since present *theoretical* methods are really valid only in the low density ("ideal"-) gas limit. As noted below, we recently carried out numerical simulations of the "low-density" Boltzmann equation which not only clarified the wall ("creep") BC, but also thermal stress (non-Newton-Stokes-) effects *within* such crystal-growth ampoule flows . However, to clarify the nature of the BC transition from the Enskog-Chapman regime to the technologically important but theoretically less tractable case of *liquid-like densities* (including supercritical polyatomic vapors) it is inevitable that high-quality *experimental* data for carefully selected fluid/solid interfaces will be required. The best environment for obtaining these data appears to be the *microgravity* environment, as spelled out in Topic 1 below.

Previous theoretical work on "thermal creep" at fluid/solid interfaces (going back to J.C. Maxwell[1879]) has been understandably focused on "structureless", single component *low density gas* motion adjacent to a non-isothermal smooth flat solid surface, usually exploiting an approximate (*eg.* linearized) model of the Boltzmann equation and a "diffuse reflection" molecule/surface interaction model. However, since many applications are multi-dimensional and involve non-dilute mixtures of disparate mass polyatomic molecules, frequently well outside of the domain of "ideal" gas behavior, many generalizations are urgently needed to understand and ultimately predict such flows, whether in micro-gravity or in ground-based laboratories. Progress has been slow, in part because of the absence of reliable *experimental data* on the dimensionless thermal creep (or wall *'slip') coefficient* , C_{tc} , appearing in the relevant tangential momentum BC:

$$(v_{t,w})_{tc} = C_{tc} \cdot n \cdot (\cdot \ln T_{fluid,w} / \cdot x). \qquad (1)$$

Here $(v_{t,w})_{tc}$ is the thermal creep contribution to the *tangential* component (x-direction) of the fluid *velocity* relative to the solid surface, n is the momentum diffusivity ("kinematic viscosity", m/r) of the fluid, and $T_{fluid,w}$ is the *fluid* temperature evaluated at the fluid/solid interface.

In the present paper we consider, sequentially, our current thinking and recent advances in each the following areas:

1. The Design of photophoretic "space race" experiments to extract the thermal creep coefficient C_{tc}

2. Thermophoresis of isolated solid spheres and aggregates in gases

3. Solid sphere thermophoresis in Newtonian liquids and dense vapors

4. Thermophoresis of small immiscible liquid droplets: Thermal creep contribution

5. Applications of Direct Simulation Monte Carlo (DSMC) Methods, including extensions to dense, hard-sphere fluids (ie. non-negligible molecular volume fraction $(p/6)\bullet n s^3$

In our view, the ultimate goal of this line of research is a rational molecular-level theory which predicts the dependence of C_{tc} on relevant dimensionless parameters describing the way fluid molecules interact with the solid surface, and how they interact among themselves (see, *eg.*, Rosner and Papadopoulos,1996). Accordingly, micro-gravity based data (Topic 1) will be an important step forward.

Relevant Results: Yale/HTCRE Laboratory Research Group

Castillo, J.L., Mackowski, D.W. and Rosner, D.E.(1990), "Photophoretic Contribution to Transport of Absorbing Particles Across Combustion Gas Boundary Layers", *Prog. Energy Comb. Sci.* (ACS Symposium Special Issue: **Deposition**) **16**, 253-260

Castillo, J.L., Rosner, D.E. and Kumar, M.(1998), "Thermophoresis of Small Liquid Droplets in Gases", (in prep)

Filippov, A.V. and D.E. Rosner,(1998) "Energy Transfer Between Aerosol Particles and Gas at High Temperature Ratios in the Transition Regime"; DSMC-based results submitted for Edinburgh *International Aerosol Conference*, September, 1998; Prepared for submission to *Int. J. Heat Mass Transfer* May

Filippov, A.V. , D.E. Rosner, Xing, Y. McEnally, C.S., Long, M.B. and Schaeffer, A.M.(1998) "Comparison Between Detailed LII Method and TEM Analysis for Ultrafine Soot Particles in Flames", *27th Comb. Symposium*, Boulder CO; Poster# W5G05

Garcia-Ybarra, P., and Rosner, D.E., (1989), "Thermophoretic Properties of Non-spherical Particles and Large Molecules", *AIChE J.*, **35**(5) 139-147

Garcia-Ybarra, P., and Castillo, J.L.(1997), " Mass Transfer Dominated by Thermal Diffusion in Laminar Boundary Layers", *J. Fluid Mechs.* **336**, 379-409

Gomez, A. and Rosner, D.E.(1993),"Thermophoretic Effects on Particles in Counterflow Laminar Diffusion Flames", *Comb. Sci. Tech.* **89**, 335-362

Mackowski , D.W. (1989), "Photophoresis of Aerosol Particles in the Free-molecular and Slip-Flow Regimes" *Int. J. Heat Mass Transfer* **32** (5) 843-854

Mackowski , D.W. and Papadopoulos, D.W.(1997), " Comparison of Burnett and DSMC Predictions of Pressure Distributions and Normal Stress in One-Dimensional Non-isothermal Gases", *Phys. Fluids A (Fluid Dynamics)* (submitted)

Papadopoulos, D.H. and Rosner, D.E., (1995), "Enclosure Gas Flows Driven by Non-isothermal Walls" *Physics Fluids A (Fluid Dynamics)* , **7** (11) 2535-2537

Papadopoulos, D.H. and Rosner, D.E.(1996), "Direct Simulation of Concentration Creep in a Binary Gas-Filled Enclosure", *Phys Fluids* **8** (11) 3179-3193

Papadopoulos, D.H. and Rosner, D.E.(1996), "Internal Flows Driven by Kinetic Boundary Layers", Paper B3, *20th Int. Sympos. on Rarefied Gas Dynamics* , C. Shen, ed., Beijing, China, August; pp. 143-148.

Papadopoulos, D.H. (1996), **Internal Flows Induced by Kinetic Boundary Layer Phenomena** , PhD Dissertation, Yale University Graduate School, Department of Chemical Engineering, November

Rosner, D.E.(1980),"Thermal (Soret-)Diffusion Effects on Interfacial Mass Transfer Rates",*PCH*(Pergamon)**1**, 159-185

Rosner, DE.,(1986), **Transport Processes in Chemically Reacting Flow Systems**, Butterworth- Heinemann (Stoneham MA) (3d Printing, 1990; 2d ed. in preparation)

Rosner, D.E. (1989), "Side-wall gas 'Creep' and Thermal Stress Convection' in Microgravity Experiments on Film Growth by Vapor Transport ", *Physics Fluids A (Fluid Dynamics)* , **1** (11) 1761-1763

Rosner, D.E., Garcia-Ybarra , P. and Mackowski, D.W.(1991), "Size and Structure-Insensitivity of the Thermophoretic Transport of Aggregated 'Soot' Particles in Gases", *Comb. Sci. Tech.* **80** 87-101

Rosner, D.E., Mackowski, D.W., Tassopoulos, M., Castillo, J.L., and Garcia-Ybarra, P. (1992)," Effects of Heat Transfer on the Dynamics and Transport of Small Particles Suspended in Gases", *I/EC-Research* (ACS), **31** (3) 760-769(1992))

Rosner, D.E., *et.al.*(1998), "Soot Morphology- and High Pressure Effects on Thermophoretically-Dominated Deposition Rates", *27th Comb. Symposium*, Boulder CO; Poster # W5G-11

Rosner, D.E. and Khalil, Y.(1998) " Particle Morphology and Knudsen Transition Effects on Thermophoretically-Dominated Total Mass Deposition Rates From 'Coagulation-Aged' Aerosol Populations", *J. Aerosol Sci.* (submitted)

Rosner, D.E. and Papadopoulos, D.(1996)) , "Jump, Creep and Slip Boundary Conditions at Non-Equilibrium Gas/Solid Interfaces"(Invited paper, E. Ruckenstein Birthday Issue) *I/EC-Research* (ACS),**35** (9) 3210-3222

Tandon, P., and Rosner, D.E.(1995), "Translational Brownian Diffusion Coefficient of Large (Multi-particle) Suspended Aggregates", *Ind Eng Chem-Res* (ACS)**34** 3265-3277; and *AIChE J.*,**40**(7) 1167-1182 (1994)

4th NASA Microgravity Fluid Physics & Transport Phenom. Conf. Aug.12-14,1998; Cleveland OH

A SYMMETRY BREAKING EXPERIMENT ABOARD MIR AND THE STABILITY OF ROTATING LIQUID FILMS

P. Concus, University of California, Berkeley CA 94720-3840, USA, concus@math.berkeley.edu,
R. Finn, Stanford University, Stanford, CA 94305-2125, USA, finn@gauss.stanford.edu,
D. Gomes, Instituto Superior Técnico, Lisbon, Portugal and University of California, Berkeley CA 94720-3840, USA, dgomes@math.berkeley.edu,
J. McCuan, Mathematical Sciences Research Institute, Berkeley, CA 94720-5070, USA, john@msri.org,
M. Weislogel, NASA Lewis Research Center, Cleveland, OH 44135, USA, mark.weislogel@lerc.nasa.gov

We discuss results for two parts of our study on the behavior of liquids under low-gravity conditions. The first concerns the Interface Configuration Experiment (ICE) aboard the Space Station Mir on the Mir-21/ NASA-2 mission. The experiment investigates fluid interfaces in certain "exotic" containers in a low-gravity environment. These containers are rotationally symmetric and have the property that for given contact angle and liquid volume, a continuum of distinct rotationally symmetric equilibrium configurations can appear, all of which have the same mechanical energy. These symmetric equilibrium configurations are however unstable, in that deformations that are not rotationally symmetric can be shown mathematically to yield configurations with lower energy. On an earlier Space Shuttle mission it was found experimentally, in confirmation of mathematical results, that the stable configuration that formed was not rotationally symmetric. In the Mir mission there formed as well a second, distinct locally stable non-rotationally-symmetric configuration, as predicted by numerical computations; the two configurations possessed different dynamic characteristics. This intriguing phenomenon of asymmetric local energy minimizers in a symmetric container can occur even if conditions for an exotic container are not completely satisfied.

The second investigation concerns the behavior of slowly rotating liquids in a low-gravity environment. For many liquids the classical Young-Laplace-Gauss formulation for equilibrium capillary free surfaces gives reliable information concerning the shape and stability of free-surface interfaces. Our investigation concerns the behavior of a case of a highly wetting liquid partly filling a container, for which straightforward application of the classical theory may not hold, as under certain conditions "super-wetting" liquid films can form covering the container's inner surface. A configuration of particular interest is that of a highly wetting liquid partly filling the annular region in a closed circular cylindrical container with concentric rod; the entire configuration is to be kept rotating at a uniform speed in such a manner as to maintain the center of mass on the axis of symmetry. This configuration has been proposed as a space-orbiting cryogenic cooling device for the STEP and Gravity Probe-B Relativity Mission studies. In a 1-g experimental study, which attempted to minimize the relative effects of gravity (by using small physical dimensions and large rotation speeds), it was found that a liquid film that formed on the rod became unstable. Liquid was "pumped" continually into the film from the bulk of the liquid, with liquid departing from the film sporadically in blobs. Equilibrium never was achieved. A subsequent mathematical study, based on a classical formulation enhanced to include a van der Waals potential of adhesion, gave critical film thickness and length criteria for the model problem of a film of uniform thickness on a cylindrical rod. Numerical experiments based on the enhanced formulation were then carried out for the actual container geometry for low-gravity. It was found, over a broad range of parameters, that the liquid films that form on the central rod are always sufficiently thin so as to remain stable, never becoming thick enough to satisfy the mathematical criteria for instability. Thus, the experimentally observed instability must derive from other factors. It is not known presently if an experiment conducted in microgravity, free of the scaling and complications inherent in a 1-g experiment simulation, would exhibit the instability.

CRTICAL VELOCITIES IN OPEN CAPILLARY FLOWS

Michael E. Dreyer, Uwe Rosendahl, Hans J. Rath
Center of Applied Space Technology and Microgravity (ZARM)
University of Bremen, D-28354 Bremen, Germany dreyer@zarm.uni-bremden.de

Within the compensated or reduced gravity environment of an orbiting spacecraft, the hydrostatic pressure vanished and surface tension forces become dominant. This leads to a different design of all fluid containing devices due to the fact that a preferential orientation of the liquid bulk ceases to exist. So called surface tension tanks (STT) are used since several decades in a spacecrafts and satellites to transport and position propellant and to ensure bubble free supply of the engines. Capillary vanes are an important part of the propellant management device (PMD) of a STT. Capillary vanes consist of a more or less complicated metal sheet located near the tank wall to induce small radii of curvature of the free surface which leads to a liquid pressure below ambient pressure. Presently the vanes create an open flow path from the bulk of the propellant to a reservoir. The reservoir supplies gas free propellant to the thrusters, whenever outflow is demanded. The detailed knowledge of stability limits and flow rates in open capillary vanes is an important criterion for an efficient design of propellant management devices (PMD) in surface tension tanks. For future surface tension tanks the reservoir shall be omitted and the thrusters supplies directly by the vanes. To guarantee gas free propellant supply the limits of flow rates in capillary vanes have to be known.

We consider the flow of liquid along a capillary vane as shown in Fig. 1. The vane consists of two parallel plates of distance a, breadth b and length l, and a flow in direction of the vane axis is assumed. The flow path s is bounded at the sides by free surfaces, whose radii of curvature correspond to the pressure drop at the surface. If a constant volume flux Q is applied, the inner pressure of the liquid and the curvature of the free surface change in flow direction.

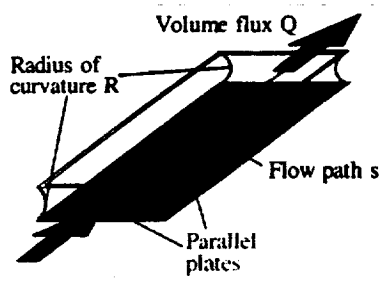

Figure 1: Model of a capillary vane consisting of two parallel plates. The flow through the vane along the vane axis s leads to a decreasing radius of curvature.

For the analysis we follow the steady state approach given by Jaekle[1] with a refinement for the pressure losses. This leads to a non-linear ordinary differential equation which reads in non-dimensional form

$$\frac{dR^*}{ds^*} = \frac{\frac{Oh}{8}\frac{A^{*2}}{Q^*}\left\{k_{pf} + k_{pe}e^{-\frac{s^*}{s_0^*}}\right\}}{\frac{dA^*}{dR^*} - \frac{A^{*3}}{Q^{*2}R^{*2}}} \qquad (1)$$

with $R^* = 2R/a$, $s^* = s/a$, $A^* = A/ab$, $Q^* = Q/\sqrt{2\sigma ab^2/\rho}$, $k_{pf} = 96$, $k_{pe} = 268$, $s_0^* = Q^*/125\ OhA^*$ (Surface tension is denoted with σ, density with ρ, and the dynamic viscosity with μ). The non-dimensional parameters are the OHNESORGE number $Oh = \mu/\sqrt{2a\rho\sigma}$, and the gap ratio $\Lambda = a/b$ in the non-dimensional form of $A = f(R)$

$$A^* = 1 - \frac{\Lambda}{2}\left[R^{*2} arc\sin\frac{1}{R^*} - \sqrt{R^{*2} - 1}\right] \cdot \qquad (2)$$

Eq. (1) must be solved with boundary conditions for the

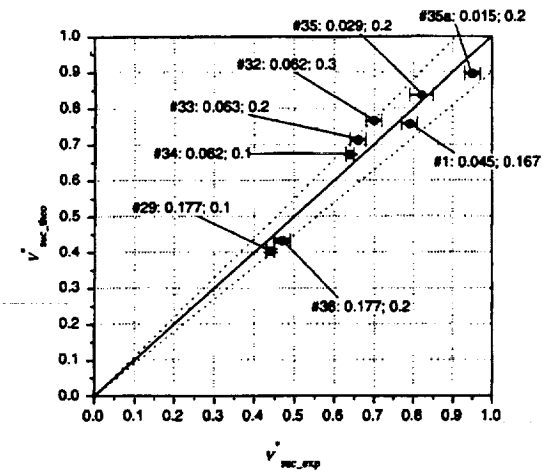

Figure 2: Comparison of experimental and theoretically predicted data for the maximum dimensionless velocity between parallel plates. The labels refer to the data set number (see Tab. 1), the dimensional-less length of the capillary l^*, and the gap ratio Λ, respectively. The dotted lines mark the ±10% deviation from the identity.

radius of curvature R. The entrance radius $R(s = 0)$ can be calculated following the analysis given by Dreyer et al.[2] taking into account the pressure losses in the reservoir and at the entrance of the vane. The outlet radius of curvature cannot decrease below the minimal radius $R(s = l) = a/2$.

As a solution of Eq. (1) we expect a relation $Q^* = f(\mathrm{Oh}, \Lambda, l^*)$ with the non-dimensional length $l^* = \mathrm{Oh}\, l/a$ which is an appropriate form of the capillary rise height discussed in Dreyer et al.[3]

The aim of the experiments was to determine the critical volume flux through a capillary vane, consisting of two parallel plates. To eliminate the gravity effects and to establish a liquid path between the parallel plates by means of the surface tension only, the experiments were performed under microgravity conditions using the Drop Tower Bremen (4.74 s experiment time, residual acceleration less than 10^{-5} g_0, with g_0 gravity acceleration on earth).

The results are depicted in non-dimensional form

Table 1: Non-dimensional parameters for the drop tower experiments.

#	Λ [-]	Oh [-]	l^* [-]
1	0.167	0.00238	0.045
29	0.1	0.0047	0.177
32	0.3	0.00197	0.062
33	0.2	0.00197	0.063
34	0.1	0.00197	0062
35	0.2	0.00152	0.029
35a	0.2	0.00152	0.015
36	0.2	0.00472	0.177

in Fig. 2 where the critical volume flux achieved from the experiment $Q_{\mathrm{crit}}^{\mathrm{theo}}$ and computed from Eq. (1) $Q_{\mathrm{crit}}^{\mathrm{theo}}$ are scaled by

$$v_{\mathrm{suc}}^* = Q/A_m v_c \sqrt{1-\Lambda}, \qquad (3)$$

with $A_m = ab - \pi a^2/8$.

The theory is able to predict the maximum forced flow in capillary vanes with a good accuracy of ±10% for a wide range of the non-dimensional parameter Ohnesorge number Oh, gap ratio Λ, and capillary length l^*. Both regions where viscous friction force as well as convective forces are dominating the flow were covered. Due to the assumption of stationary flow and neglect of the second radius of curvature, deviations between calculated and measured interface shapes occur at the inlet and outlet sections.

REFERENCES

1. Jaekle, D.E., Propellant Management Device Conceptual Design and Analysis: Vanes, AIAA-91-2172, 27th Joint Propulsion Conference, June 24-26, Sacramento, CA (1991).

2. Dreyer, M., Delgado, A., Rath, J.-J., Fluid Motion in Capillary Vanes under Reduced Gravity, Microgravity Science and Technology V/4, 203 (1993).

3. Dreyer, M., Delgado, A., Rath, J.-J., Capillary Rise of Liquid between Parallel Plates under Microgravity, J. Colloid Interf. Sci. 163, 158-168 (1994).

Thermoacoustic Effects at a Solid-Fluid Boundary

A. Gopinath[1], [1]Department of Mechanical Engineering, Naval Postgraduate School, Monterey CA 93943, USA, gopinath@nps.navy.mil

In Study I, the problem of thermoacoustic streaming in a plane parallel resonant channel, representative of the stack in a thermoacoustic engine, has been developed in a general dimensionless form. The utility of such a formulation and its wide ranging applicability to different solid--fluid combinations is demonstrated by which a consistent account of all the energy--exchange mechanisms can be made. Certain (wide-gap, thick-wall) simplifications are initially made to arrive at more manageable forms of the time--averaged temperature distributions of interest in both the fluid gap, and the channel walls. These simplifications clarify the origin of the thermoacoustic effect and provide a description of the responsible physical mechanisms based on which the validity of the "bucket-brigade" model is examined. The unexpected role of a little-known second-order thermal expansion coefficient is pointed out. It is shown that the conjugate wall--fluid coupling is crucial in yielding the large time-averaged axial temperature gradients that can be induced in the channel. In particular, the heat transfer rates at the ends of the channel are found to play an important role in determining the magnitude of these time-averaged gradients. The more general and practically useful case of arbitrary channel gap widths is also treated and it is found that for ideal gas working fluids there is an optimum channel gap width for which the axial thermal stratification in the channel is maximized. A comparison of the predictions from this study with available experimental data shows very good agreement. A more detailed report of this work may be found in the full-length paper by Gopinath *et al.* (A. Gopinath, N. L. Tait, & S. L. Garrett, "Thermoacoustic streaming in a resonant channel: The time-averaged temperature distribution," *J. Acoust. Soc. Am.* **103**, 1388--1405 (1998)).

In Study II, experimental work has been conducted in air to measure the convective heat transfer rates from a cylinder in a strong zero-mean oscillatory flow. The cylinder is representative of a heat exchanger tube, while the flow is representative of the strong acoustic fields in a thermoacoustic engine. The flow is low-amplitude in nature, i. e. acoustic particle displacement amplitudes are small on the scale of the characteristic body dimension. The geometry under consideration is a cylinder which is representative of a heat exchanger tube. For the low amplitude cases treated, acoustic streaming is the dominant heat transport mechanism and is replaced by small scale vortex shedding when this flow becomes unstable. A large amount of data was gathered that confirmed the square-root dependence of the Nusselt number on the streaming Reynolds number, R_s, in the laminar regime of operation, and a suitable correlation has been developed which agrees well with earlier theoretical predictions. Additional data for larger values of R_s indicates a stronger power-law dependence and is indicative of the unstable vortex shedding regime of the oscillatory flow. It may be noted that the actual magnitude of the relevant Reynolds number, R_s, involved is of $O(10^2 - 10^3)$ and can be considerably smaller than the values commonly encountered in conventional mean flows which may typically lie in the range $O(10^4 - 10^7)$. Nonetheless, as the values of the Nusselt number for these oscillatory flows indicate, the magnitudes of the heat transfer coefficients themselves are very much comparable in magnitude to those encountered in conventional mean flows, thus indicating the potential for significant convective heat transfer rates despite the zero-mean nature of the driving acoustic flow. Such correlations could be of utility in the design of heat exchangers for thermoacoustic engines. Suggestions have been made to extend these correlations for gases with lower Prandtl numbers that are likely to be used in such engines. A more detailed report of this work may be found in the full-length paper by Gopinath & Harder (A. Gopinath & D. H. Harder, "An experimental study of heat transfer from a cylinder in low-amplitude oscillatory flows," *submitted Int. J. Heat Mass Transfer* (1998)).

DAMPING OF DROP OSCILLATIONS BY SURFACTANTS AND SURFACE VISCOSITY

Brian M. Rush, Ali Nadim, Dept. Aero. and Mech. Engr., Boston University, Boston, MA 02215 USA

Abstract

The roles played by surfactants and interfacial rheology on damping the shape oscillations of liquid drops are analyzed for the case of axisymmetric shape oscillations of a nearly spherical liquid drop surrounded by another fluid in the absence of gravity. Both fluids are taken to be viscous, although the Reynolds number associated with the shape oscillations is assumed large enough that deviations from inviscid flow are only present in thin Stokes boundary layers near the no-slip interface. Also, an insoluble surfactant is assumed to be present at the interface and surface tension is taken to be a linearly decreasing function of local surfactant concentration. This surfactant layer is further assumed to behave as a two-dimensional Newtonian fluid layer characterized by surface shear and dilatational viscosities.

Under these conditions, several sources can be identified for mechanical dissipation and the ultimate damping of the shape oscillations of the drop. These include viscous effects associated with the bulk fluids that appear in two distinct forms: one associated with the oscillatory viscous boundary layers which form near the interface between the drop and surrounding fluid, and the other associated with the flows far from the interface which resemble potential flow although they dissipate energy through weak viscous action. Surfactants and surface rheology additionally contribute to dissipation in other ways. The surface shear and dilatational viscosities dissipate energy within the interface in much the same way as the viscous dissipation in the three-dimensional bulk fluids just mentioned. Moreover, as various parts of the interface locally increase or decrease in area during shape oscillations, the concentration of surfactants locally decreases or increases. This leads to gradients in surfactant concentration on the interface where the process of gradient diffusion of surfactants within the interface, itself an irreversible process, leads to energy dissipation. Also, the Marangoni flow resulting from this non-uniformity in surface tension contributes to viscous damping.

This paper outlines the derivation of a general mechanical energy equation for such a system. It contains dissipation terms accounting for each of the mechanisms described above. The energy equation is applied to a slightly perturbed axisymmetric drop oscillating in a low-density surrounding fluid to derive an approximate ordinary differential equation (resembling that of a damped harmonic oscillator) which describes the time evolution of pure shape modes.

In parallel to the analytical treatment, the implementation of a boundary integral method for potential (i.e. inviscid) flow is presented for the case of a two-dimensional drop oscillating in vacuum. The effect of a constant surface dilatational viscosity is included in the computations by combining the tangential and normal components of the dynamic boundary condition into a single equivalent expression. This expression, combined with Bernoulli's equation for the pressure, the kinematic boundary condition and the regularized Fredholm integral equation of the second kind representing Laplace's equation for potential flow, produces a coupled set of nonlinear equations that allow the time evolution of the drop's shape to be followed. Surface dilatational viscosity is shown to have a damping effect on the free oscillations of the drop.

Conference Schedule

Fourth Microgravity Fluid Physics & Transport Phenomena Conference
Cleveland, Ohio

Tuesday, August 11, 1998

2-5 PM	Tour of NASA Lewis (advance reservation required). Buses leaving from Sheraton.
5-7 PM	Registration and cash bar: Sheraton City Centre Hotel (Grand Ballroom Lobby)

Wednesday, August 12, 1998

7:30 AM	Registration: Sheraton City Centre Hotel (Grand Ballroom Lobby)
8:30	Opening Plenary Session (Grand Ballroom) Chair: Jack Salzman, Chief, Microgravity Science Division, NASA Lewis Research Center
8:30	Welcome: Martin P. Kress, Deputy Director, NASA Lewis Research Center
8:45	Overview of NASA's Life & Microgravity Sciences and Applications Program Dr. Arnauld E. Nicogossian, M.D., NASA Associate Administrator, Life & Microgravity Sciences and Applications
9:15	Keynote: Dr. John-David Bartoe, Manager, Research, International Space Station Program, NASA Johnson Space Center
10:15	Conference Objectives: Dr. Simon Ostrach, Director, National Center for Microgravity Research on Fluids and Combustion
10:30	Break
10:45	NASA Research Announcement - Fluid Physics & Transport Phenomena Discipline: Dr. Brad Carpenter, Lead Enterprise Scientist, Microgravity Research Division, Office of Life & Microgravity Science and Applications, NASA Headquarters
11:05	Fluid Physics & Transport Phenomena Research Thrusts: Dr. G. Paul Neitzel, Georgia Institute of Technology/Chairman, Microgravity Fluid Physics and Transport Phenomena Discipline Working Group
11:25	Fluid Physics Research on the International Space Station Planned Utilization of ISS US Fluids and Combustion Facility ESA Fluids Science Module NASDA Fluid Physics Facility
12:00 noon	Lunch
1:30 PM	Parallel Sessions 1A-C
3:10	Break
3:40	Parallel Sessions 2A-C
5:40	Free time

Thursday, August 13, 1998

8:00 AM	Thursday Plenary Session: Chair: Dr. David Weitz ,University of Pennsylvania (Grand Ballroom) Plenary Lecturer: Dr. Dudley Saville, Princeton University: Electrohydrodynamics & Electrokinetics: Moving Fluids & Particles with Electric Fields
8:40	Featured Speakers: Dr. Paul Chaikin and Dr. William Russel, Princeton University: The Dynamics Of Disorder-Order Transitions In Hard Sphere Colloidal Dispersions
9:20	Break
9:30	Parallel Sessions 3A-C
10:50	Break
11:15	Parallel Sessions 4A-C
12:35 PM	Lunch
2:00	Exposition: New Principal Investigators & Diagnostics Exhibits(Grand Ballroom)
6:15	Shuttle service to Great Lakes Science Center - Lolly the Trolley
6:30	Cash bar
7:30	OMNIMAX® Movie: Mission to Mir
8:15	Dinner
9:30	Shuttle service to Sheraton City Centre Hotel

Friday, August 14, 1998

8:00 AM	Friday Plenary Session: Chair: Dr. Iwan Alexander, Senior Scientist (Fluids), National Center for Microgravity Research on Fluids and Combustion/Case Western Reserve University (Grand Ballroom) Plenary Lecturer: Dr. Ronald Probstein, Massachusetts Institute of Technology: Micro-scale and Meso-scale Effects on Macroscopic Fluid Dynamics
8:40	Featured Speaker: Dr. Stein Sture, University of Colorado: Mechanics of Granular Materials at Low Effective Stresses
9:10	Dr. Robert Rhome, Director, Microgravity Research Division, Office of Life and Microgravity Sciences and Applications, NASA Headquarters: Microgravity Research Program and Human Exploration and Development of Space
9:40	Break
9:55	Parallel Sessions 5A-C
10:55	Break
11:25	Parallel Sessions 6A-C
12:25 PM	Luncheon: Speaker: Dr. Norman Thagard, M.D., Professor and Bernard F. Sliger Eminent Scholar Chair, Florida A&M University/Florida State University College of Engineering, NASA Astronaut (retired)
2:00	Parallel Sessions 7A-C
3:40	Adjourn

Tuesday, August 11, 1998

2:00-5:00 P.M. Tour of NASA Lewis Research Center

5:00-7:00 P.M. Registration and Cash Bar
Sheraton City Centre Hotel
(Grand Ballroom Lobby)

Wednesday, August 12, 1998
Morning

7:30 A.M.	Registration: Sheraton City Centre Hotel (Grand Ballroom Lobby)
8:30-12:00 noon	Opening Plenary (Grand Ballroom) Chair: Jack Salzman, Chief, Microgravity Science Division, NASA Lewis Research Center
8:30	Welcome: Martin P. Kress, Deputy Director, NASA Lewis Research Center
8:45	Overview of NASA's Life & Microgravity Sciences and Applications Program Dr. Arnauld E. Nicogossian, M.D., NASA Associate Administrator, Life & Microgravity Sciences and Applications
9:15	Keynote: Dr. John-David Bartoe, Manager, Research, International Space Station Program, NASA Johnson Space Center
10:15	Conference Objectives Dr. Simon Ostrach, Director, National Center for Microgravity Research on Fluids and Combustion
10:30	Break
10:45	NASA Research Announcement - Fluid Physics & Transport Phenomena Discipline Dr. Brad Carpenter, Lead Enterprise Scientist, Microgravity Research Division, Office of Life & Microgravity Science and Applications, NASA Headquarters
11:05	Fluid Physics & Transport Phenomena Research Thrusts Dr. G. Paul Neitzel, Georgia Institute of Technology Chairman, Microgravity Fluid Physics & Transport Phenomena Discipline Working Group
11:25	Fluid Physics Research on the International Space Station Planned Utilization of ISS US Fluids and Combustion Facility ESA Fluids Science Module NASDA Fluid Physics Facility
12:00 noon	Lunch

Wednesday Afternoon

Parallel Sessions 1A-1C

1:30-3:10 P.M.

DOLDER-HASSLER ROOM
Multiphase Flow I
Session Chair: Hasan Oguz, Johns Hopkins University

1:30
Mark McCready, University of Notre Dame: Mechanism of Atomization in a Two Layer Couette Flow

1:50
Vermuri Balakotaiah, University of Houston: Studies on Normal & Microgravity Annular Two-Phase Flows

2:10
Davood Abdollahian, S. Levi, Inc.: Experimental And Analytical Study Of Two-Phase Flow In Microgravity

2:30
Edward Keshock, Cleveland State University: Measurement of Two-Phase Flow Characteristics Under Microgravity Conditions

2:50
Simon Ostrach, NCMR/Case Western Reserve University: Industrial Processes Affected by Gravity

RITZ ROOM
Electric And Magnetic Effects
Session Chair: Robert Davis, University of Colorado at Boulder

1:30
John Hart/Daniel Ohlsen, University of Colorado at Boulder: Waves In Radial Gravity Using Magnetic Fluids

1:50
George Bankoff, Northwestern University: Control Of Flowing Liquid Films By Electrostatic Fields In Space

2:10
Robert Davis, University of Colorado at Boulder: Cell And Particle Interactions And Aggregation During Electrophoretic Motion

2:30
Boyd Edwards, West Virginia University: Magnetic Control of Convection In Electrically Nonconducting Fluids

2:50
Robert Kusner, NASA Lewis Research Center: Electric Field Induced Interfacial Instabilities

GRAND BALLROOM
G-Jitter And Stochastic Flow
Session Chair: Iwan Alexander, NCMR/Case Western Reserve University

1:30
Jorge Vinals, Florida State University: Fluid Physics In A Fluctuating Acceleration Environment

1:50
George Homsy, Stanford University: Thermocapillary Flows with Low-Frequency g-Jitter

2:10
Michael Schatz, University of Texas at Austin: Ground-Based Experiments On Vibrational Thermal Convection

2:30
Seth Putterman, University of California at Los Angeles: Diffusing Light Photography of Containerless Ripple Turbulence

2:50
Eric Shaqfeh, Stanford University: Drop Breakup In Fixed Bed Flows As Model Stochastic Flow Fields

3:10-3:40 P.M. Break

Wednesday Afternoon

Parallel Sessions 2A-2C

3:40-5:40 P.M

DOLDER-HASSLER
Multiphase Flow II
Session Chair: Mark McCready, University of Notre Dame

3:40
Yasuhiro Kamotani, Case Western Reserve University: Bubble Generation In A Flowing Liquid Medium And Resulting 2-Phase Flow In Microgravity

4:00
Hasan Oguz, Johns Hopkins University: Production Of Gas Bubbles In Reduced-G Environments

4:20
Luis Bernal, University of Michigan: Vortex Droplet Formation by a Vortex Ring in Microgravity

4:40
Chris Rogers, Tufts University: Decoupling The Role Of Inertia And Gravity On Particle Dispersion

5:00
Mohammad Kassemi, NCMR: Bubble Dynamics On A Heated Surface

5:20
Sanjoy Banerjee, University of California at Santa Barbara: A Three-Dimensional Level Set Method for Direct Simulation Of Two-Phase Flows in Variable Gravity Environments

RITZ
Colloids
Session Chair: Paul Chaikin, Princeton University

3:40
Douglas Durian, University of California at Los Angeles: Shear-Induced Melting Of Aqueous Foams

4:00
Jing Liu, California State University at Long Beach: Dynamics of Single Chains of Suspended Ferrofluid Particles

4:20
Alice Gast, Stanford University: Chain Dynamics in Magnetorheological Suspensions

4:40
David Weitz, University of Pennsylvania: Physics of Colloids in Space

5:00
Penger Tong, Oklahoma State University: Analogies Between Colloidal Sedimentation and Turbulent Convection at High Prandtl Numbers

5:20
Noel Clark, University of Colorado Structure, Hydrodynamics, And Phase Transitions Of Freely Suspended Liquid Crystals

GRAND BALLROOM
Interfacial Phenomena I
Session Chair: Dan Rosner, Yale University

3:40
Enrique Ramé/Stephen Garoff, NCMR/Carnegie Mellon University: The Influence of Thin Films on the Hydrodymanics Near Moving Contact Lines

4:00
Leonard Schwartz, University of Delaware: Direct Numerical Simulation of Wetting and Spreading Behavior on Heterogeneous and Roughened Substrates

4:20
Ziyuan Liu/Marc Perlin, University of Michigan: On The Boundary Conditions At An Oscillating Contact Line

4:40
Seth Lichter, Northwestern University: The Micromechanics Of The Moving Contact Line

5:00
Ain Sonin, Massachusetts Institute of Technology: Dynamics Of The Molten Contact Line

5:20
Jayanth Banavar/Joel Koplik, Pennsylvania State University/ City College of the City University of New York: Effective Forces Between Colloidal Particles

Wednesday Evening
Free Time

Thursday, August 13, 1998
Morning

8:00 A.M. Thursday Plenary
Chair: Dr. David Weitz, University of Pennsylvania
(Grand Ballroom)

Plenary Lecturer:
Electrohydrodynamics & Electrokinetics: Moving Fluids & Particles with Electric Fields
Dr. Dudley Saville, Princeton University

Featured Speakers:
The Dynamics Of Disorder-Order Transitions In Hard Sphere Colloidal Dispersions
Dr. Paul Chaikin and Dr. William Russel/Princeton University

9:20 A.M. Break

Parallel Sessions 3A-3C
9:30-10:50 A.M.

GRAND BALLROOM
Phase Change I-Boiling
Session Chair:
Andrea Prosperetti,
Johns Hopkins University

9:30
Peter Wayner, Jr., Rensselaer Polytechnic Institute: Constrained Vapor Bubble

9:50
Kevin Hallinan, University of Dayton: Comments on the Operation of Capillary Pumped Loops In Low Gravity

10:10
Herman Merte, University of Michigan: A Study Of Nucleate Boiling With Forced Convection

10:30
Cila Herman, Johns Hopkins University: Experimental Investigation Of Pool Boiling Heat Transfer Enhancement In Microgravity In The Presence Of E Fields

DOLDER-HASSLER
Near Critical Point Flows
Session Chair: Joe Goddard, University of California at San Diego

9:30
Robert Berg, National Institute of Standards and Technology: Critical Viscosity Of Xenon: Surprises and Scientific Results

9:50
John Hegseth, University of New Orleans: Growth And Morphology Of Phase Separating Supercritical Fluids (GMSF), Boiling in Subcritical Fluids, and Critical Fluctuations

10:10
John Hegseth, University of New Orleans: A Compressible Geophysical Flow Experiment

10:30
Eric Kaler, University of Delaware: Phase Separation Kinetics in IsoPycnic Mixtures of H2O/CO2/Ethoxylated Alcohol Surfactants

RITZ
Interfacial Phenomena II
Session Chair: Joel Koplik, City College of the City University of New York

9:30
James Maher, University of Pittsburgh: The Dissolution of an Interface Between Miscible Liquids

9:50
Daniel Mackowski, Auburn University: Investigation Of Thermal Stress Convection In Nonisothermal Gases Under Microgravity Conditions

10:10
E. James Davis, University of Washington: Phoretic Forces

10:30
Kathleen Stebe, Johns Hopkins University: Surfactants on a Droplet in an Extensional Flow: Stresses Created by Monolayer-Forming Surfactants

10:50 A.M. Break

Thursday Morning

Parallel Sessions 4A-4C

11:15 A.M.-12:35 P.M.

GRAND BALLROOM
Phase Change II: Solidification
Session Chair: Ain Sonin, Massachusetts Institute of Technology

11:15
Sam Coriell, National Institute for Standards and Technology: Interface Morphology During Crystal Growth: Effects Of Anisotropy And Fluid Flow

11:35
Stephen Davis, Northwestern University: Directional Solidification of a Binary Alloy into a Cellular Convection Flow: Localized Morphologies

11:55
Dino Megaridis, University of Illinois at Chicago: Fluid Dynamics And Solidification Of Molten Solder Droplets Impacting On A Substrate

12:15
Saleh Tanveer, Ohio State University: Two-Dimensional Dendritic Crystal Growth for Weak Undercooling

RITZ
Granular Media
Session Chair: Ashok Sangani, Syracuse University

11:15
James Jenkins, Cornell University: Particle Segregation in Collisional Shearing Flows

11:35
Joe Goddard, University of California at San Diego: Material Instabilities In Particulate Systems

11:55
Robert Behringer, Duke University: Gravity and Granular Materials

12:15
Masami Nakagawa, Colorado School of Mines: MRI Measurements And Granular Dynamics Simulation Of Segregation Of Granular Mixtures

DOLDER-HASSLER
Thermocapillary Flows I
Session Chair: Y . Kamotani, Case Western Reserve University

11:15
Simon Ostrach, NCMR/Case Western Reserve University: Surface Tension Driven Convection Experiment -2

11:35
Hossein Haj-Hariri, University of Virginia: Thermally-Driven Interfacial Flows In Multi-Layered Fluid Structures

11:55
Robert Kelly, University of California at Los Angeles: Studies In Thermocapillary Convection Of The Marangoni-Benard Type

12:15
Sindo Kou, University of Wisconsin: Thermocapillary Convection in a Low Pr Material Under Simulated Reduced Gravity

12:35 - 2:00 P.M. Lunch

Thursday Afternoon

Exposition

2:00-5:00 P.M.

Grand Ballroom

Poster	Presenter/Affiliation
Phase Diagrams of Electric-Field Induced Aggregation In Conducting Colloids	Andreas Acrivos, City College of the City University of New York
Ultrasonic Thermal Field Imaging of Opaque Fluids	C. David Andereck, Ohio State University
A Novel Acousto-Electric Levitator for Studies of Drop and Particle Clusters and Arrays	Robert E. Apfel, Yale University
Fluid Physics of Foam Evolution and Flow	Hassan Aref, University of Illinois at Urbana-Champaign
Inertial Effects in Suspension Dynamics	John F. Brady, California Institute of Technology
Marangoni Effects on Near-Bubble Microscale Transport During Boiling of Binary Fluid Mixtures	Van P. Carey, University of California at Berkeley
Dynamics of Dust in Photoelectron Layers Near Surfaces in Space	Joshua E. Colwell, University of Colorado at Boulder
Scaling of Multiphase Flow Regimes and Interfacial Behavior at Microgravity	Christopher J. Crowley, Creare, Inc.
Thermocapillary-Induced Phase Separation with Coalescence	Robert H. Davis, University of Colorado
Simulation of Rotating Thermal Convection and Comparison With Space-Laboratory Experiments	Anil Deane, University of Maryland
Attenuation of Gas Turbulence by a Nearly Stationary Dispersion of Fine Particles	John K. Eaton, Stanford University
A Dust Aggregation and Concentration System (DACS) for the Microgravity Space Environment	Frank J. Giovane, Naval Research Laboratory
Plasma Dust Crystallization	John A. Goree, University of Iowa
Determination of the Accommodation Coefficient Using Vapor/Gas Bubble Dynamics in an Acoustic Field	Nail Gumerov, Dynaflow, Inc.
Engineering of Novel Biocolloidal Suspensions	Daniel A. Hammer, University of Pennsylvania
Sonoluminescence in Space: the Critical Role of Buoyancy in Stability and Emission Mechanisms	R. Glynn Holt, Boston University
Rheology of Foam Near the Order-Disorder Phase Transition	R. Glynn Holt, Boston University
Fluid Flow in an Evaporating Droplet	Ronald G. Larson, University of Michigan
Studies of Gas - Particle Interactions in a Microgravity Flow Cell	Michel Y. Louge, Cornell University
Microgravity Experiments to Evaluate Electrostatic Forces in Controlling Cohesion and Adhesion of Granular Materials	John R. Marshall, SETI/NASA Ames Research Center
Single Bubble Sonoluminescence in Low Gravity and Optical Radiation Pressure Positioning of the Bubble	Philip Marston, Washington State University
An Interferometric Investigation of Contact Line Dynamics in Spreading Polymer Melts and Solutions	Gareth H. McKinley, Massachusetts Institute of Technology
Numerical Simulation of Parametric Instability in Two and Three-Dimensional Fluid Interfaces	Constantine Pozrikidis, University of California at San Diego
Complex Dynamics in Marangoni Convection with Rotation	Hermann Riecke, Northwestern University

Poster	Presenter/Affiliation
The Effect of Surface Induced Flows on Bubble and Particle Integration	Paul J. Sides, Carnegie Mellon University
Modeling of Transport Processes in a Solid Oxide Electrolyzer Generating Oxygen on Mars	K.R. Sridhar, University of Arizona
Computations of Boiling in Microgravity	Gretar Tryggvason, University of Michigan
Entropic Surface Crystals and Crystal Binary Growth in Binary Hard-Sphere Colloids	Arjun G. Yodh, University of Pennsylvania
Enhanced Boiling on Micro-Configured Composite Surfaces Under Microgravity Conditions	Nengli Zhang, Ohio Aerospace Institute
The Small-Scale Structure of Turbulence	Gregory Zimmerli, National Center for Microgravity Research on Fluids and Combustion
Paramagnetic Liquid Bridge in a Gravity-Compensating Magnetic Field	Charles Rosenblatt, Case Western Reserve University

Exhibits

Throughout Conference Meeting Area

Note: Exhibits Are Available Throughout the Duration of the Conference

Exhibit Title	Presenter
Compact Fiber Optic Probes for Static and Dynamic Light Scattering and Biomedical Applications	R. Ansari National Center for Microgravity Research on Fluids and Combustion NCMR
Compact Laser Light Scattering Multiangle Apparatus	R. Ansari National Center for Microgravity Research on Fluids and Combustion NCMR
On-line particle sizing in fluids under flow	R. Ansari National Center for Microgravity Research on Fluids and Combustion NCMR
Fluids Integrated Rack	R. Corban NASA Lewis Research Center
Acceleration Measurement Discipline	R. DeLombard NASA Lewis Research Center
Optical Tweezers	D. Griffin NASA Lewis Research Center
ERE	N. Hall NASA Lewis Research Center
Laser Light Scattering with Multiple Scattering Suppression	W. Meyer National Center for Microgravity Research on Fluids and Combustion
Surface Light Scattering	W. Meyer National Center for Microgravity Research on Fluids and Combustion
CDOT	W. Meyer, National Center for Microgravity Research on Fluids and Combustion
National Center for Microgravity Research On Fluids and Combustion	A. Heyward, National Center for Microgravity Research on Fluids and Combustion
Laser Feedback Interferometry	B. Ovryn National Center for Microgravity Research on Fluids and Combustion
Common-Path Interferometry for Fluid Measurements	N. Rashidnia National Center for Microgravity Research on Fluids and Combustion
MSD K-12 Education Program	M. Rogers National Center for Microgravity Research on Fluids and Combustion
Optical Microscopy of Colloids	R. Rogers NASA Lewis Research Center LeRC
International Space Station Telescience	K. Schubert NASA Lewis Research Center
Mechanics of Granular Materials	S. Sture, University of Colorado
Astrotech Space Operations	M. Windsor, Astrotech Burkhardt Franke, Daimler-Benz Aerospace, Bremen, Germany
Microgravity Program Performance Goals	D. Woodard, Marshall Space Flight Center
Microgravity Principal Investigator Locations	D. Woodard, Marshall Space Flight Center
Slowly Rotating Optical Breadboard	G. Zimmerli National Center for Microgravity Research on Fluids and Combustion

Thursday Evening

5:00 P.M.: Free time

6:15 P.M.: Shuttle service begins to Great Lakes Science Center (Lolly the Trolley)

6:30 P.M.: Cash Bar, Great Lakes Science Center

7:30 P.M.: OMNIMAX® Movie: Mission to Mir, Great Lakes Science Center

8:15 P.M.: Dinner, Great Lakes Science Center

9:45-10:30 P.M.: Shuttle service return to Sheraton City Centre Hotel

Friday, August 14, 1998
Morning

8:00 A.M. Friday Plenary
Chair: Dr. Iwan Alexander, Senior Scientist, National Center for Microgravity Research On Fluids and Combustion/Case Western Reserve University
(Grand Ballroom)

Plenary Lecturer:
8:00-8:40 A.M.
Micro-scale and Meso-scale Effects on Macroscopic Fluid Dynamics
Dr. Ronald Probstein, Massachusetts Institute of Technology

Featured Speaker:
8:40-9:10 A.M.
Mechanics Of Granular Materials at Low Effective Stresses
Dr. Stein Sture, University of Colorado

9:10-9:40 A.M.
Microgravity Research Program and Human Exploration and Development of Space
Dr. Robert Rhome, Director, Microgravity Science Division, Office of Life and Microgravity Sciences and Applications, NASA Headquarters

9:40 -9:55 A.M. Break

Friday Morning, 1998

Parallel Sessions 5A-5C

9:55-10:55 A.M.

DOLDER-HASSLER
Phase Change III: Boiling
Chair: Peter Wayner
Rensselaer Polytechnic Institute

9:55
Vijay Dhir, University of California at Los Angeles: Investigation Of Nucleate Boiling Mechanisms Under Microgravity Conditions

10:15
Jungho Kim, University of Denver: Boiling Heat Transfer Measurements on Highly Conductive Surfaces Using Microscale Heater and Temperature Arrays

10:35
Marc Smith, Georgia Institute of Technology: Vibration-Induced Droplet Atomization

GRAND BALLROOM
Suspensions
Session Chair: Alice Gast, Stanford University

9:55
S. E. Elghobashi, University of California at Irvine: Effects Of Gravity On Sheared Turbulence Laden With Bubbles And Droplets

10:15
R.J. Hill/A. Sangani
Cornell University/Syracuse University: Buoyancy Driven Shear Flows of Bubble Suspensions

10:35
Michael Loewenberg, Yale University: Direct Numerical Simulation of Drop Breakup in Isotropic Turbulence

RITZ
Special Topics I
Session Chair: Gareth McKinley, Massachusetts Institute of Technology

9:55
Paul Neitzel, Georgia Institute of Technology: Non-Coalescence Effects In Microgravity

10:15
Josh Colwell, University of Colorado at Boulder: Collide: Microgravity Experiment on Collisions in Planetary Rings and Protoplanetary Disks

10:35
Edgar Knobloch, University of California at Berkeley: Weakly Nonlinear Description of Parametric Instabilities in Vibrating Flows

10:55 A.M. Break

Friday Morning

Parallel Sessions 6A-6C

11:25 A.M.- 12:25 P.M.

DOLDER-HASSLER
Phase Change IV: Boiling
Session Chair: Vijay Dhir, University of California at Los Angeles

11:25
Andrea Prosperetti, Johns Hopkins University: Pressure Radiation Forces on Vapor Bubbles

11:45
Amir Faghri, University of Connecticut: Condensation Of Forced Convection Two-Phase Flow in a Miniature Tube

12:05
Eugene Trinh, Jet Propulsion Laboratory: Acoustic Shearing In Microgravity: Flow Stability And Heat Transfer Enhancement

RITZ
Special Topics II
Session Chair: Eric Shaqfeh, Stanford University

11:25
Gareth McKinley, Massachusetts Institute of Technology: Extensional Rheometry of Polymer Solutions and the Uniaxial Elongation of Viscoelastic Filaments

11:45
Jeff Mackey, NYMA, Inc.: Flow-Induced Birefringence Measurement System Using Dual-Crystal Transverse Electro-Optic Modulator for Microgravity Fluid Physics Applications

12:05
Ben Ovryn, NCMR: Phase Shifted Laser Feedback Interference Microscopy: Applications to Fluid Physics Phenomena

GRAND BALLROOM
Convective Instability
Session Chair: Hossein Haj-Hariri, University of Virginia

11:25
J.B. Swift/H. Swinney, University of Texas at Austin: Long Wavelength Rupturing Instability in Surface-Tension-Driven Benard Convection

11:45
Jeffrey Jacobs, University of Arizona: PLIF Flow Visualization of Incompressible Richtmeyer-Meshokov Instability

12:05
Sung Lin, Clarkson University: Absolute And Convective Instability Of A Liquid Jet

12:35 - 2:00 P.M. Lunch

Luncheon Speaker: Dr. Norman Thagard, M.D., Professor & Bernard F. Sliger Eminent Scholar Chair, FAMU/FSU College of Engineering, and NASA Astronaut (retired)

Friday Afternoon

Parallel Sessions 7A-7C
2:00 P.M.- 3:40 P.M.

RITZ
Bubbles and Drops
Session Chair: Luis Bernal, University of Michigan

2:00
Osman Basaran, Purdue University: Drop Ejection from an Oscillating Rod

2:20
A. Esmaeeli/V. Arpaci/An-Ti Chai, University of Michigan/NASA Lewis Research Center: Numerical Modeling of Three-Dimensional Fluid Flow with Phase Change

2:40
L.G. Leal, University of California at Santa Barbara: The Breakup and Coalescence of Gas Bubbles Driven by the Velocity Gradients of Non-Uniform Flow

3:00
Eugene Trinh/Satwindar Sadhal, Jet Propulsion Laboratory/University of Southern California: Ground-Based Studies Of Thermocapillary Flows In Levitated Laser-Heated Drops

3:20
R. Balasubramaniam, NCMR: Thermocapillary Migration and Interactions Of Bubbles And Drops

GRAND BALLROOM
Liquid Bridges
Session Chair: Mike Schatz, University of Texas at Austin

2:00
Iwan Alexander, NCMR/Case Western Reserve University: Stability Limits And Dynamics Of Nonaxisymmetric Liquid Bridges

2:20
Philip Marston, Washington State University: Radiation and Maxwell Stress Stabilization Of Liquid Bridges

2:40
Paul Steen, Cornell University: Stability Of Shapes Held By Surface Tension And Subjected To Flow

3:00
Dudley Saville, Princeton University: Electrohydrodynamic Stability of a Liquid Bridge

3:20
Jeremiah Brackbill, Los Alamos National Laboratory: Dynamic Modelling Of Microgravity Flow

DOLDER-HASSLER
Interfacial Phenomena III
Session Chair: Kathleen Stebe, Johns Hopkins University

2:00
Daniel Rosner, Yale University: Fluid/Solid Boundary Conditions in Nonisothermal Systems

2:20
Paul Concus, University of California at Berkeley: A Symmetry Breaking Experiment Aboard Mir and the Stability of Rotating Liquid Films

2:40
Michael Dreyer/Hans Rath, University of Bremen: Critical Velocities In Open Capillary Flows

3:00
Ashok Gopinath, Naval Postgraduate School: Thermoacoustic Effects At A Solid-Fluid Boundary

3:20
Ali Nadim, Boston University: Damping of Drop Oscillations by Surfactants

3:40 P.M. Adjourn

Thank you for your participation in
the 4th Microgravity Fluid Physics and Transport Phenomena Conference

AUTHOR INDEX

*Abstract not available

REPORT DOCUMENTATION PAGE

Form Approved
OMB No. 0704-0188

1. AGENCY USE ONLY (*Leave blank*)	2. REPORT DATE	3. REPORT TYPE AND DATES COVERED
	March 1999	Conference Publication

4. TITLE AND SUBTITLE

Proceedings of the Fourth Microgravity Fluid Physics and Transport Phenomena Conference

5. FUNDING NUMBERS

WU-962-24-00-00

6. AUTHOR(S)

Bhim S.Singh, editor

7. PERFORMING ORGANIZATION NAME(S) AND ADDRESS(ES)

National Aeronautics and Space Administration
Glenn Research Center
Cleveland, Ohio 44135-3191

8. PERFORMING ORGANIZATION REPORT NUMBER

E-11280

9. SPONSORING/MONITORING AGENCY NAME(S) AND ADDRESS(ES)

National Aeronautics and Space Administration
Washington, DC 20546-0001

10. SPONSORING/MONITORING AGENCY REPORT NUMBER

NASA CP—1999-208526

11. SUPPLEMENTARY NOTES

Proceedings (abstract book and CD-ROM) of a conference held at and sponsored by the NASA Office of Life and Microgravity Science & Applications, NASA Glenn Research Center, Cleveland, Ohio, August 12-14, 1998. Responsible person, Bhim S. Singh, organization code 6712, (216) 433-5396.

12a. DISTRIBUTION/AVAILABILITY STATEMENT

Unclassified - Unlimited
Subject Category: 34 Distribution: Nonstandard

This publication is available from the NASA Center for AeroSpace Information, (301) 621-0390.

12b. DISTRIBUTION CODE

13. ABSTRACT ***(Maximum 200 words)***

This conference presents information to the scientific community on research results, future directions, and research opportunities in microgravity fluid physics and transport phenomena within NASA's microgravity research program. The conference theme is "The International Space Station." Plenary sessions provide an overview of the Microgravity Fluid Physics Program, the International Space Station and the opportunities ISS presents to fluid physics and transport phenomena researchers, and the process by which researchers may become involved in NASA's program, including information about the NASA Research Announcement in this area. Two plenary lectures present promising areas of research in electrohydrodynamics/electrokinetics in the movement of particles and in micro- and meso-scale effects on macroscopic fluid dynamics. Featured speakers in plenary sessions present results of recent flight experiments not heretofore presented. The conference publication consists of a book of abstracts and the full Proceedings of the 4th Microgravity Fluid Physics and Transport Phenomena Conference on CD-ROM, containing full papers presented at the conference. 90 papers are presented in 21 technical sessions, and a special exposition session presents 32 posters describing the work of principal investigators new to NASA's program in this discipline. 88 papers and 25 posters are presented in their entirety on the CD-ROM.

14. SUBJECT TERMS

Solidification; Convective instability; Granular media; Thermocapillary flow; Microgravity fluid physics; Multiphase flow; Electric/magnetic effects; G-jitter/stochastic flow; Colloids; Interfacial phenomena; Drops; Phase change; Boiling; Critical point; Suspensions; Convection; Bubbles; Liquid bridges

15. NUMBER OF PAGES

230

16. PRICE CODE

A11

17. SECURITY CLASSIFICATION OF REPORT	18. SECURITY CLASSIFICATION OF THIS PAGE	19. SECURITY CLASSIFICATION OF ABSTRACT	20. LIMITATION OF ABSTRACT
Unclassified	Unclassified	Unclassified	